THE PETROGRAPHY, DIAGENESIS AND ENVIRONMENTS OF DEPOSITION OF THE ARADEIBA FORMATION IN THE UNITY AND TALIH FIELDS, ABU GABRA BASIN, SUDAN

By

AZHARI A. ABDALLA

Bachelor of Science (Honors) in Geology
Faculty of Science
University of Khartoum
Khartoum, Sudan
1980

Submitted to the Faculty of the
Graduate College of the
Oklahoma State University
in partial fulfillment of
the requirements for
the Degree of
MASTER OF SCIENCE
May, 1990

THE PETROGRAPHY, DIAGENESIS AND ENVIRONMENTS OF DEPOSITION OF THE ARADEIBA FORMATION IN THE UNITY AND TALIH FIELDS, ABU GABRA BASIN, SUDAN

Thesis Approved:

Zuhair al-Hajeb
Thesis Adviser

Gary J. Stewart

John N. Hilton

Norman N. Durham
Dean of the Graduate College

ACKNOWLEDGEMENTS

This study would not have been possible without the invaluable input of several individuals to whom I am deeply indebted and sincerely grateful. Dr. Zuhair Al-Shaieb, my thesis advisor, provided me with academic guidance, crucial advice and tremendous support and encouragement all along. Dr. Gary Stewart, who served as a member of my thesis committee, kindly examined and discussed my maps and cross-sections and brought my attention to some necessary additions. He also revised my manuscript. Dr. John Shelton, who also served as a member of my committee read my draft and a special "Thank you" is extended to him for traveling to O.S.U. Campus to attend my thesis defense.

Chevron Oil Company and the Ministry of Energy of Sudan are deeply thanked for allowing me the data and the study materials.

I am also very thankful to Mr. Abdel Zahir M. Abdel Zahir, G.P.C.'s Exploration Director, who talked to Chevron, on my behalf, and gave this study the first breath of life. He also contributed tremendous effort to resolve the financial difficulties I experienced while doing this study. I should also express my great appreciation to the restless efforts devoted by Messrs Isam A. Abdalla and Imad

A. Abdalla to help solve my financial problems in the Ministry of Energy of Sudan.

Most of all, I do thank God for giving me the health, the ability and making all this come to light.

TABLE OF CONTENTS

Chapter Page

LIST OF TABLES

LIST OF PLATES

LIST OF FIGURES

Figure Page

CHAPTER I

INTRODUCTION

General Statement

The Republic of Sudan, covering an area of approximately one million square miles (967,498 sq. m.) in northeast Africa, has a rather complex geology. The complexity becomes even more serious when we consider the difficulties associated with geological research in Sudan, such as accessibility, climate severity, and, in most cases, lack of adequate financial support. Nevertheless, a good deal of geological investigations, mostly unpublished, has been accomplished by the Department of Geology and Mineral Resources, the Department of Geology in the University of Khartoum, and other public and private efforts. However, much of the geological information available before the 1970's was based on surfacial geological surveys. Some information about the subsurface geology, especially of the interior region of the country, was obtained from shallow drillings for irrigation and drinking water.

During the oil boom of the last decade, several international oil companies were actively involved in the search for hydrocarbons along the Sudanese portion of the Continental Shelf of the Red Sea. A wealth of geological knowledge was generated which contributed to a better understanding of the subsurface nature of the Continental Shelf of the Sudanese Red Sea.

Discouraging results forced most of the oil companies to call off their investigations in Sudan, since the Red Sea was considered the only worthwhile potential target for hydrocarbon accumulation. However, Chevron Oil Company, guided by results from broad satellite studies on rift basins in Kenya and Chad, decided to shift attention to the interior regions of Sudan in the western and southcentral parts. Chevron announced its first oil discovery from its second well drilled in 1978. Many discoveries followed, and the company drilled successive deep wells which triggered the beginning of extensive subsurface geological investigations in the interior regions of Sudan. The deep drilling coupled with seismic investigations suggested the presence of sedimentary rock sequences of some 35,000 feet, in an area which, is thought to be the site of shallow intracratonic sags.

It is hoped that, this study will contribute additional valuable data to the knowledge about the subsurface geology of the Sudan.

The Aradeiba Formation, the subject of this investigation, is of Upper Cretaceous (Turonian ?) age and is the first stratigraphic member of the Darfur Group. Oil production is evident in both the Unity and Talih fields from the main sand members (A, B, & C) of the Aradeiba Formation.

Objectives

The main objectives of this investigation are:

1. to conduct a detailed petrographic study of the three sand members of the Aradeiba Formation;

2. to investigate the diagenetic processes and products and their role on the reservoir quality. Also to construct a paragenetic sequence of the diagenetic cements for the Aradeiba Formation;

3. to determine the porosity types of the reservoir rocks.

4. to characterize the environment of deposition of the Aradeiba Formation.

Location

The Aradeiba Formation (Upper Cretaceous) is encountered some 7000 feet deep in wells drilled in the Unity and Talih oil fields. These fields are located in the southeastern portion of the Abu Gabra Basin in southcentral Sudan (Figure 1).

Methods of Investigation

To accomplish the goals of this study, the following methods were utilized together with an extensive literature review.

Core Samples

Detailed petrologic investigations of nine cores were carried out. A total core interval of 175.95 feet recovered from Unity No. 2, Unity No. 8, Unity No. 9, Unity No. 11 and Talih No. 2 wells was studied (Figure 2). A petrologic log was prepared for each core displaying the depth, rock type, sedimentary structures, etc. (See Chapter IV).

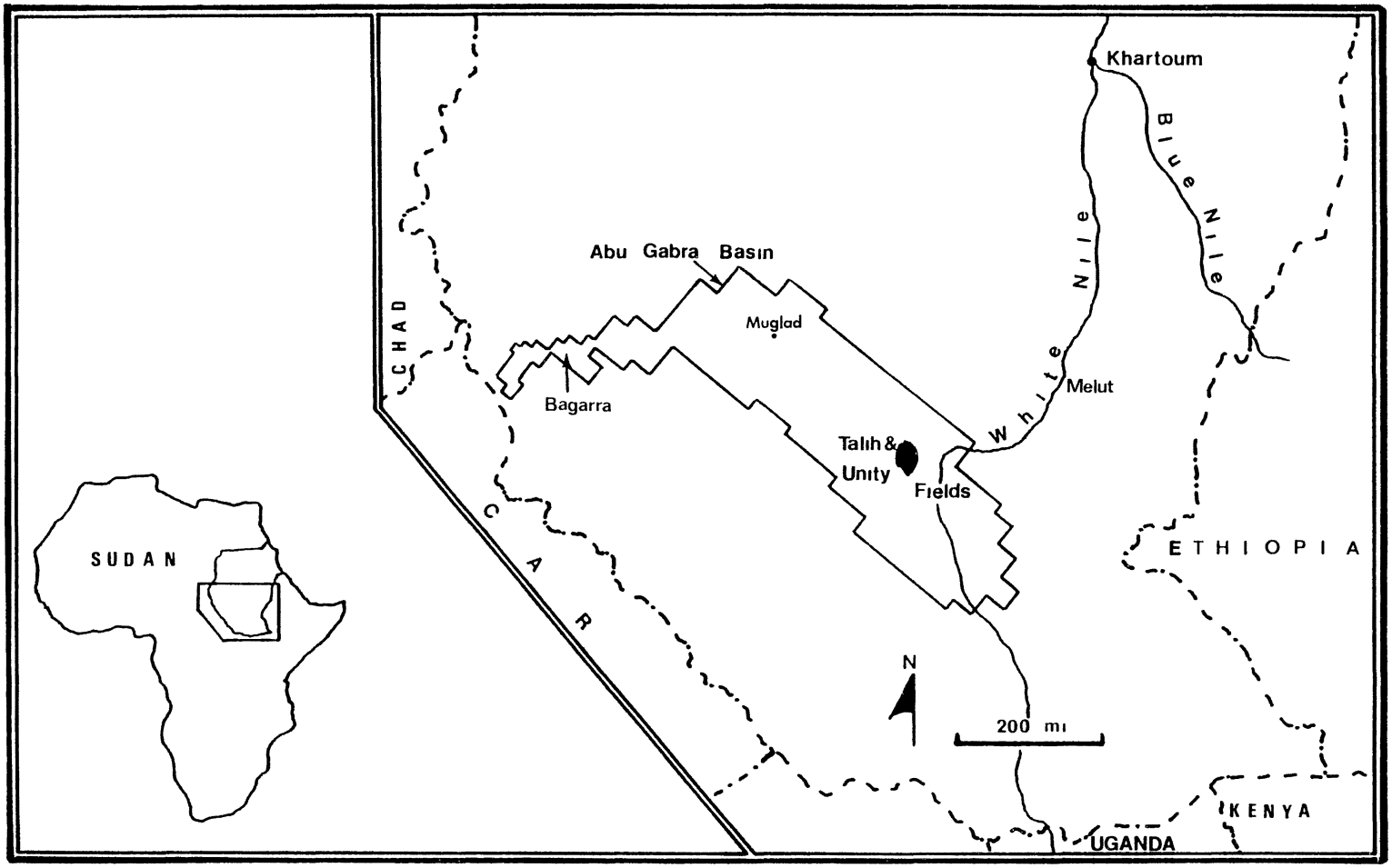

Figure 1. Location Map of the Study Area.

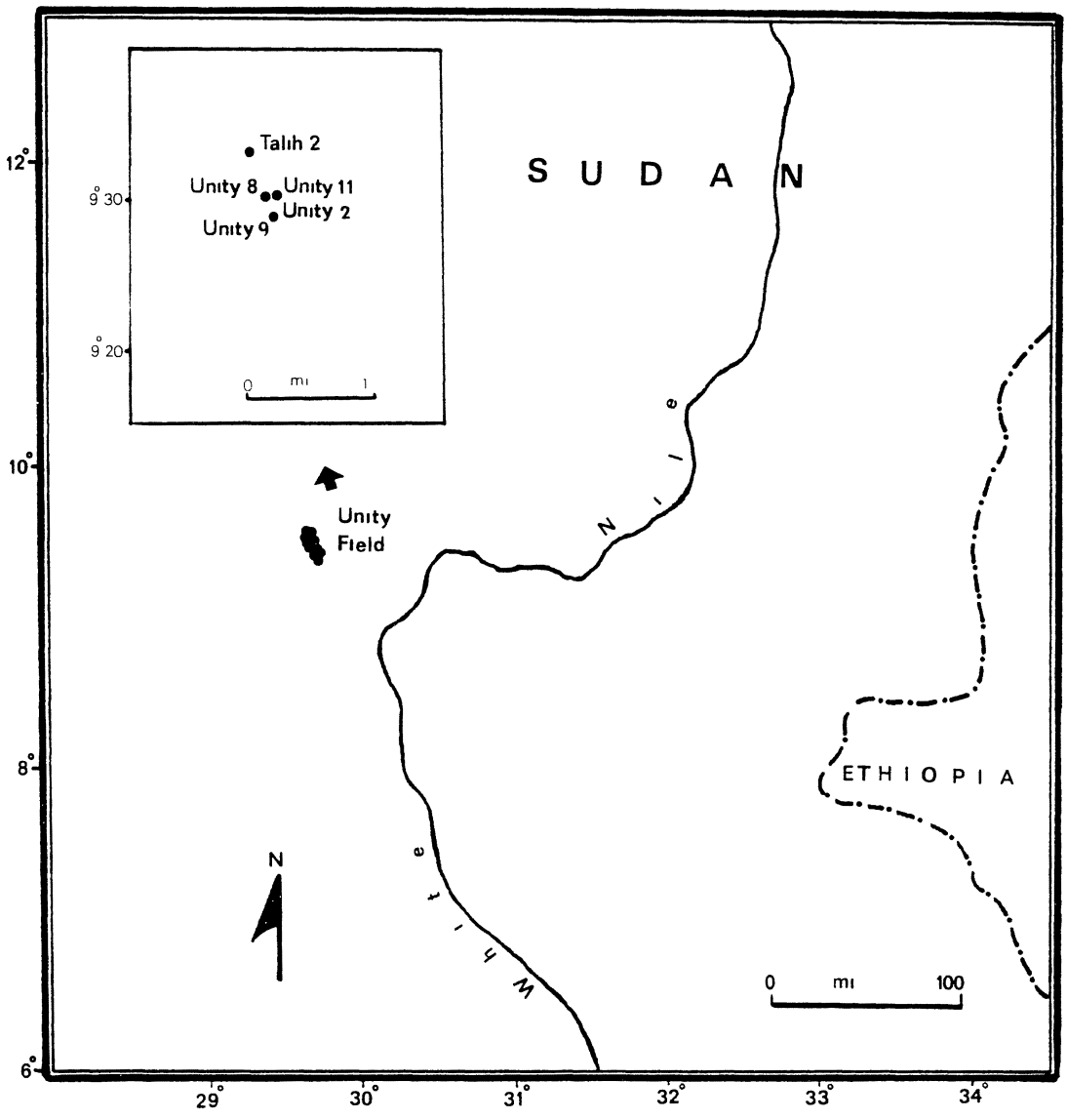

Figure 2. A Map showing the Locations of the Wells from which Core Samples were studied.

Thin Section

Forty thin sections prepared from the core samples were thoroughly studied under the petrographic microscope. The thin sections were stained with blue epoxy and sodium cobaltinitrite solutions to help identify porosity and potassium feldspars respectively. Quantitative modal analysis of the mineral constituents was conducted (See Appendix A).

X-Ray Diffraction

Eight sandstone and two claystone samples were analyzed by X-Ray Diffraction. Bulk, natural, glycolated and heated runs were conducted for identification of various clay minerals. (See Appendix B).

Cross-Sections and Subsurface Maps

Electrical-log data from wells of the Unity and Talih fields was used to construct cross-sections and thickness maps of the Aradeiba Formation, to determine possible trends and depositional characters.

Previous Investigations

Before the Chevron drillings in the mid 1980's, geological attention was focused on areas with significant outcrops, mostly towards the eastern, western and southern borders of Sudan. The south central interior regions, including the study area, were viewed as stable cratonic areas generally characterized by shallow basement rocks. The remarkable lack of outcrops with any investigative value in the study area made it unlikely for geologists to acquire any substantial clues as to what the subsurface geology looked like underneath that region. After the discoveries of Chevron Oil Company and the accompanying investigations, including the drilling of eighty six wells and various geophysical techniques performed throughout the Abu Gabra basin, the significance of the sedimentary section of that region was realized. It is known that Chevron Oil Company has gathered a considerable amount of geological and geophysical information and conducted numerous research studies in the oil fields of the Abu Gabra basin. However, the company, still working to better evaluate the basin, is handling its findings with a great deal of confidentiality. A recently published paper, Schull, 1988, gives a general account of Chevron's operations on the various concession areas the Company

holds in Sudan. The paper also provides a useful summary of the geology, tectonics and stratigraphy of the Abu Gabra basin along with the other Chevron's basins in Sudan. This study is therefore the first that treats the Aradeiba Formation in such depth.

CHAPTER II

STRUCTURE

Introduction

The African Continent is known mostly to be a stable craton. However, it is marked by two active and rather extensive structural features. These are the East African Rift System along the eastern edge and the Central African Rift System running across the center of the continent (Figure 3).

The Abu Gabra basin is a rift sedimentary basin that occupies part of the eastern segment of the Central African Rift System. The basin also has most probably been influenced by the tectonic activities along the East African Rift System. At least, it is known that the final rifting phase in the basin started within the same time frame as the Red Sea began to open up; (Schull, 1988). Moreover Medani and Vail (1974), related the Post-Cretaceous faulting of the Nubian Sandstone in Sudan to the effect of the East African Rift System. This rift system received a great deal of geophysical investigations from various workers. The studies of the Central African Rift System, on the other hand, are rather localized. Even the idea of viewing this feature as an extensive rift system is

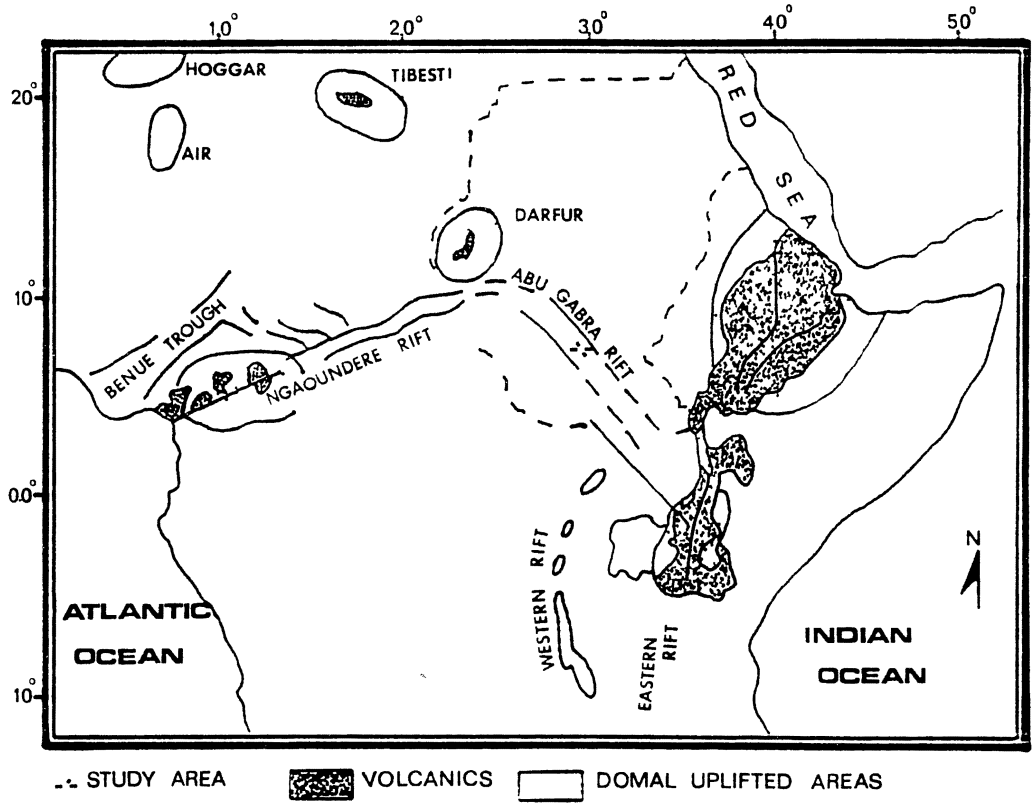

Figure 3. A Schematic Map of North and Central Africa showing the Western and Eastern Branches of the East African Rift and the segments of the Central African Rift. (After Browne and Fairhead, 1982.)

relatively new, introduced for the first time by Browne and Fairhead (1982).

In the writer's view, further efforts and geophysical investigations are worthwhile to study this system which seems to extend farther to the east through the basins of Melut and the Blue Nile. If that is the case, it is then most likely that the two systems are somehow interconnected.

In this chapter, a short account of the two rift systems is given together with the tectonic evolution of the Abu Gabra Basin and the structural style of the study area, the Unity Field.

The East African Rift System

The East African Rift System has two parallel branches along the eastern edge of the African Continent south to the Red Sea (Figure 3). A western branch known as the Gregory Rift, which is Late Miocene/Early Pliocene in age, and an eastern branch, which is believed to be of Late Pliocene age (Lowell and Genik, 1972). This system occupies most of the east African edge and extends through the Red Sea into the western edge of the Arabian Peninsula. According to Girdler et al. (1969), the Gregory Rift is

characterized by a region of axial volcanism and small scale faulting which is associated with a positive Bouger gravity anomaly. This anomaly is superimposed on a longer wavelength negative Bouger anomaly. These anomalies suggest the presence of a body of positive density contrast, the upper surface of which could be within one mile of the rift floor. It is likely, according to Girdler et al. (1969), that this is an intrusive zone of basaltic or gabbroic material which feeds the rift volcanoes. The presence of the intrusive material (possibly from the upper mantle) suggests that extreme crustal thinning has taken place, but as yet there is no crustal separation as in the Red Sea. The East African Rift System is actively creating an attenuated lithosphere under east Africa. That notion, according to Girdler et al. (1969), is backed with the following evidence:

1. the presence of normal faults and their increasing age with distance from the axis of the rift;

2. the presence and increasing age of volcanism from the rift axes; and

3. the interpretation of the associated smaller wave length positive Bouger anomaly along the axis of the eastern rift.

The nature of the faulting along the East African Rift System is mainly dip-slip with less strike-slip faults, which is also typical of the Abu Gabra basin and the study area as will be discussed later.

The Red Sea, through which the East AFrican Rift System continues, borders Sudan to the east. The evolution of the Red Sea is believed to have started in the Oligocene time with a phase of continental lithosphere arching, accompanied by normal faults across the crest. This arching is thought by Girdler et al. (1960) to have resulted from "a thermally activated volume increase attendant on convective upwelling in the asthenosphere." The continental lithosphere was then thinned due to lateral extension, perhaps caused by divergent convective flow in the asthenosphere (Nelson and Temple, 1972). A continuous phase of sea floor spreading then followed at a half-rate of 1 cm/y and the accumulative separation across the Red Sea is estimated to be 95-135 Km at the southern Red Sea.

The Central African Rift System

This rift system extends from Nigeria (west Africa) to Kenya (east Africa). The system began to develop in the Late Jurassic-Early Cretaceous during the breakup of Gondwanaland (Browne and Fairhead, 1983). Associated with

this rift system are several domal uplifts and related volcanism occur across the central and northern parts of the African continent at Air Hoggar, Tibesti, and Darfur (Figure 3). According to Browne and Fairhead (1983), these regions are linked by long wavelength negative Bouger gravity anomalies (Figure 4). The Darfur uplift, the WSW trending Ngaoundere rift (which extends from the Darfur region of west Sudan through the border regions of Central African Republic and Chad into Cameroon), and the SE trending Abu Gabra rift, which is located entirely within western and southern Sudan, represent the three arms of an incipient, intraplate triple junction (Browne and Fairhead, 1983).

The later two arms represent subsiding sedimentary rift structures. The Ngaoudere rift is a dextral shear zone of Late Pan-African origin, which can be traced, prior to the opening of the south Atlantic, as the Pernambuco fault lineament in Brazil (Browne and Fairhead, 1983). The segment of this shear zone that falls in Africa was reactivated in the Lower Cretaceous at the time of initial formation of the south Atlantic. The result of this reactivation was the development of deep, narrow fault-bounded sedimentary basins in Chad, Central African Republic and Sudan.

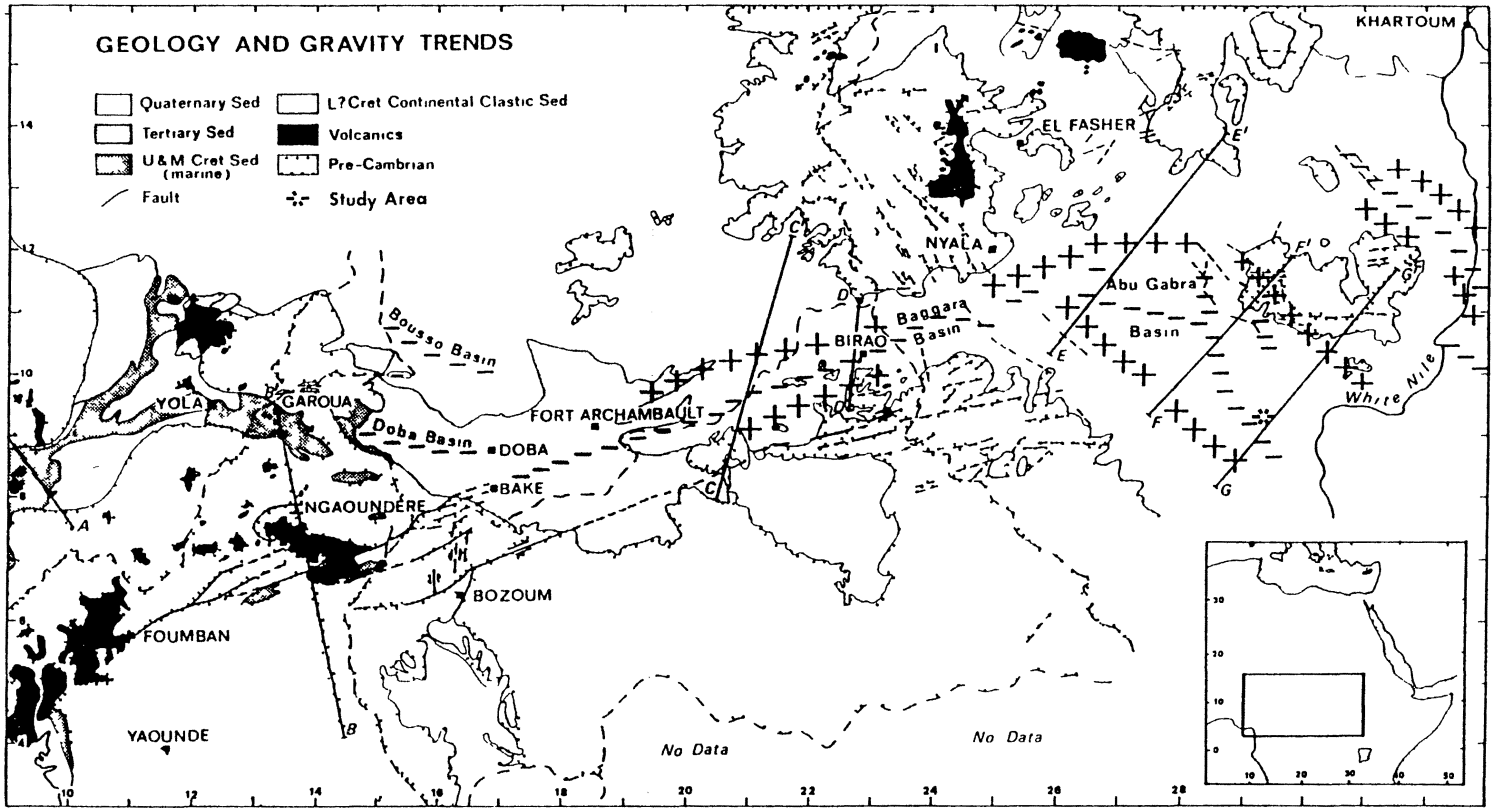

Figure 4. Generalized Geological Map of Central Africa showing the Bouguer Gravity Trends associated with the Abu Gabra Basin and the rest of the Central African Rift. (After Browne and Fairhead 1982)

According to Bott (1976), the Abu Gabra sedimentary basin is assumed to have formed due to crustal extension coupled with the failure of the upper part of the crust, being brittle, under tension caused by successive episodes of lystric normal faulting while the lower part has undergone ductile flow.

Tectonic Evolution of the Abu Gabra Basin

According to Schull, 1988, the Abu Gabra Basin and the other rift basins under Chevron concession in Sudan (Melut and the Blue Nile basins) have evolved through three tectonic phases, namely pre-rifting, rifting and sag phases (Figure 5).

Phase I (Pre-rifting)

This phase followed the Pan-African orogony (550 $\pm$ 100 MYBP), and it characterizes a period when the whole region was a site of sediment source to the adjacent subsiding areas during the Late Paleozoic and Early Mesozoic.

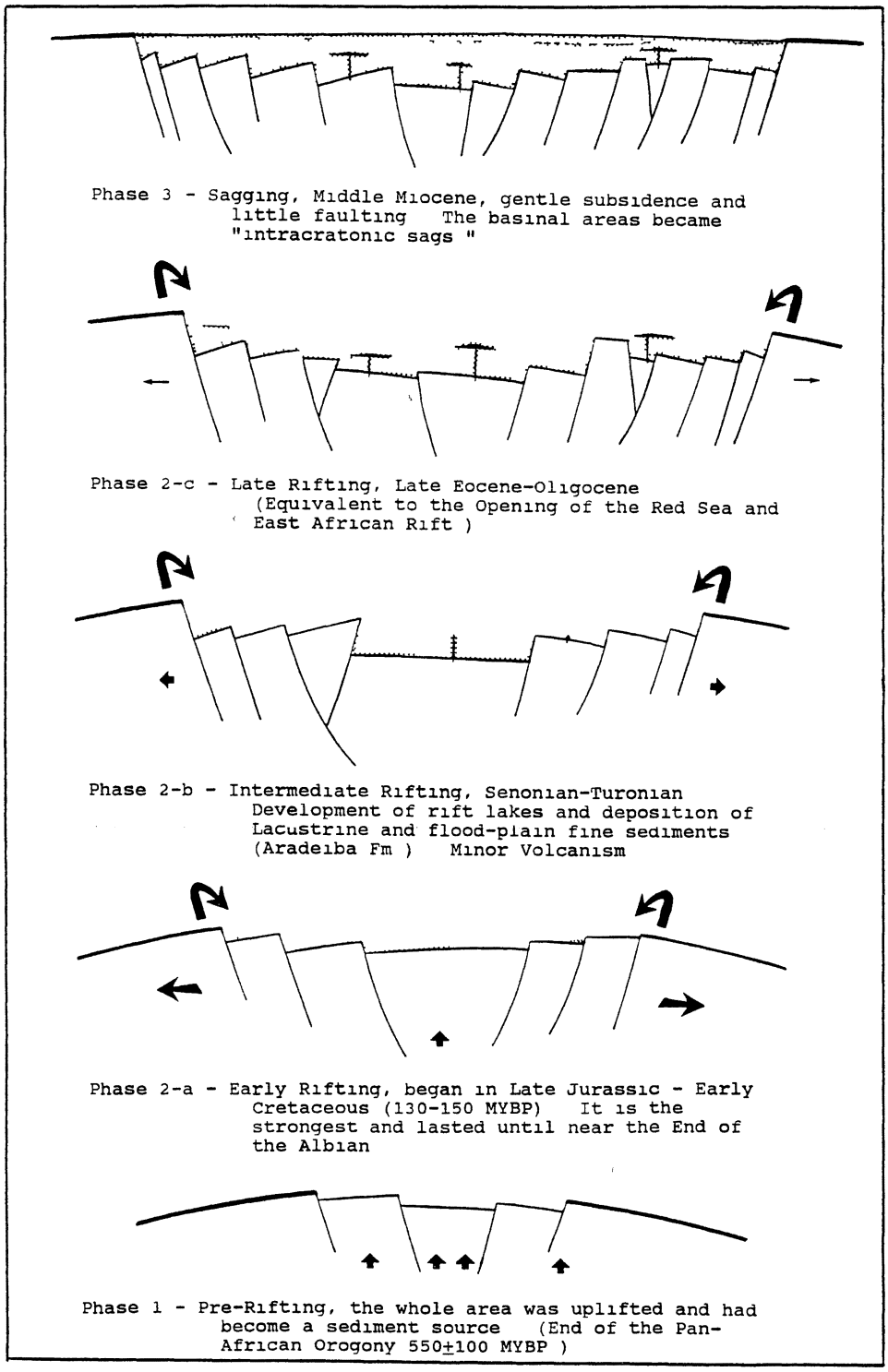

Figure 5. The Tectonic Evolution of the Abu Gabra Basin. (Based on Schull, 1988).

Phase II (Rifting)

Early Rifting. Evidence from sparse borehole control and seismic data indicate that rifting was initiated in Late Jurassic-Early Cretaceous (130-150 MYBP). During this sub-phase, the sediments of the Sharaf, Abu Gabra and finally Bentiu Formations were deposited. This phase was accompanied by listric normal faulting, which was responsible for the associated subsidence. It is concluded, according to Tom Shull (1988) from well and seismic data, that this early rifting was stronger than the succeeding ones and it lasted probably until near the end of the Albian.

Intermediate Rifting. The imprint of the intermediate rifting is clearly reflected on the stratigraphy of the basin by wide-spread deposition of lacustrine and fine flood-plain sediments. Unlike the first rifting, the intermediate sub-phase was accompanied by minor volcanism. A 300 ft. dolerite sill was drilled through in the Abu Gabra basin and was dated $\pm$ 82 MYBP. This segment of the rifting phase lasted through the Senonian-Turonian times and was terminated by the deposition of the sand-rich Amal formation (See Stratigraphy , Chapter 3).

Late Rifting. The last rifting began in the Late Eocene-Oligocene contemporaneous with the opening of the Red Sea. The sedimentation during this period was also characterized by thick extensive lacustrine and flood-plain deposits. Evidence from oil wells drilled in the Melut Basin indicated that this final rifting was accompanied by "thin Late Eocene basalt flows." (Schull, 1988)

Phase III (Sag Phase)

By the Middle Miocene the Abu Gabra Basin was well developed, and very little subsidence is evident thereafter. Minor volcanism took place during this period, represented by volcanic outcrops southeast of the town of Muglad (Figure 1) dated at 5.6 $\pm$ 0.6 and 2.7 $\pm$ 0.8 MYBP.

Structural Style of the Abu Gabra Basin and Unity Field

The dominant structural feature along the Abu Gabra Basin and the Unity field is the complex layout of normal and listric normal faults (Figures 6, 7, 8, 9 and 10). Considering the extensive rifting history of the basin, it is easy to understand the existance of the remarkably

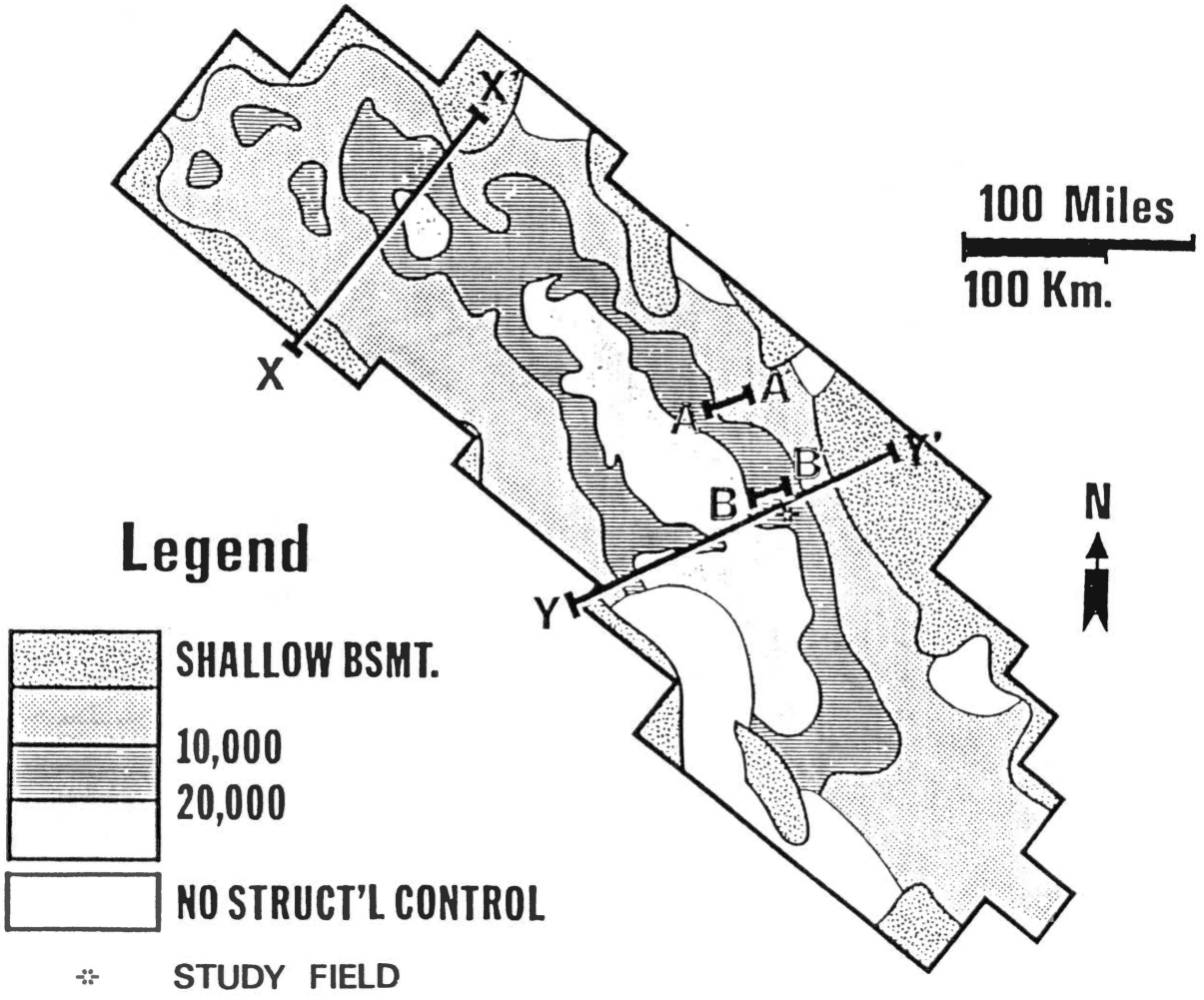

Figure 6. A Generalized Structure Map, Top Albian-Aptian Source Sequence, Abu Gabra Basin. (From Schull, 1988.)

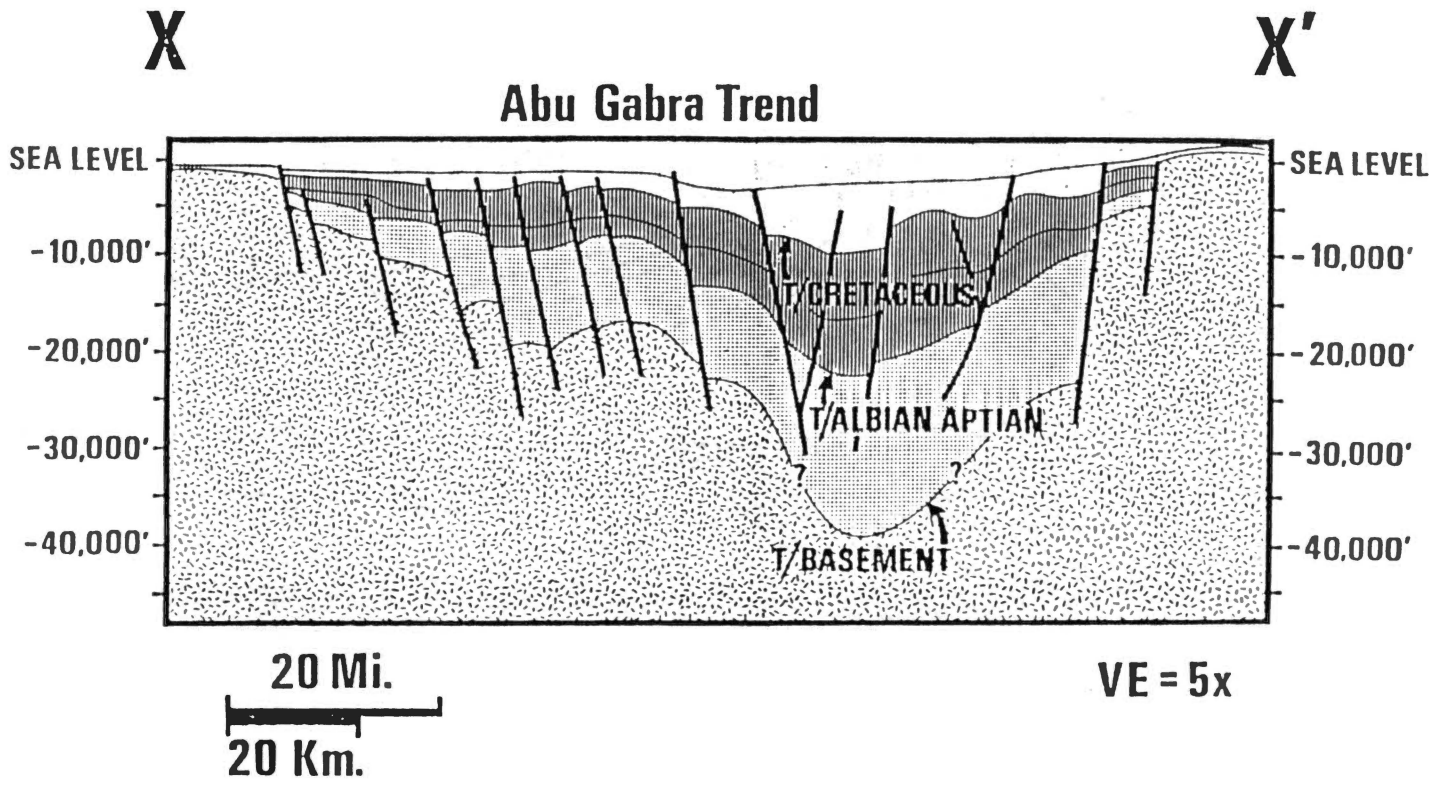

Figure 7. A Structural Profile x - x' (See Figure 6 for Location) across Northwestern Abu Gabra Basin. (From Schull, 1988.)

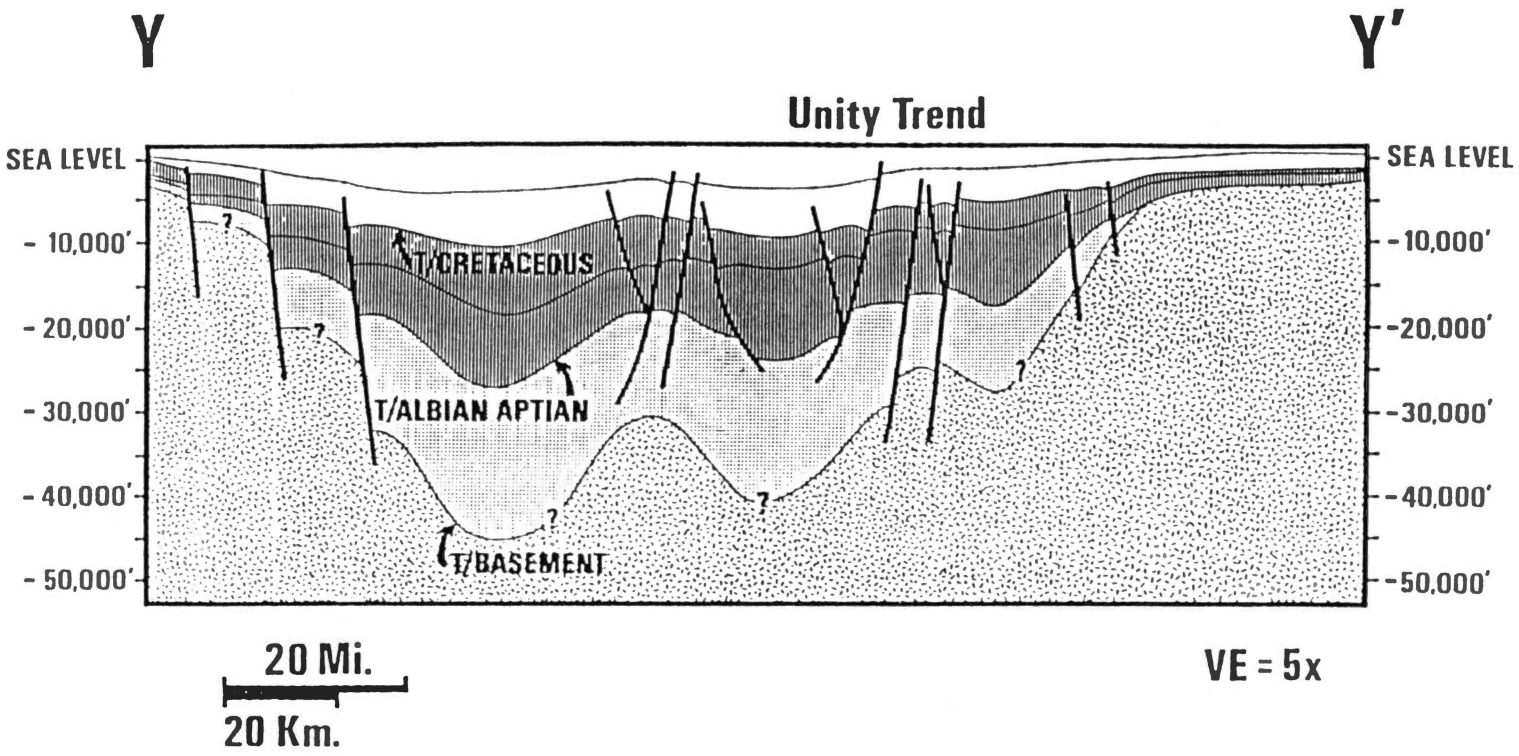

Figure 8. A Structural Profile Y - Y' (See Figure 6 for Location) running across the Study Area, the Unity Field. (From Schull, 1988.)

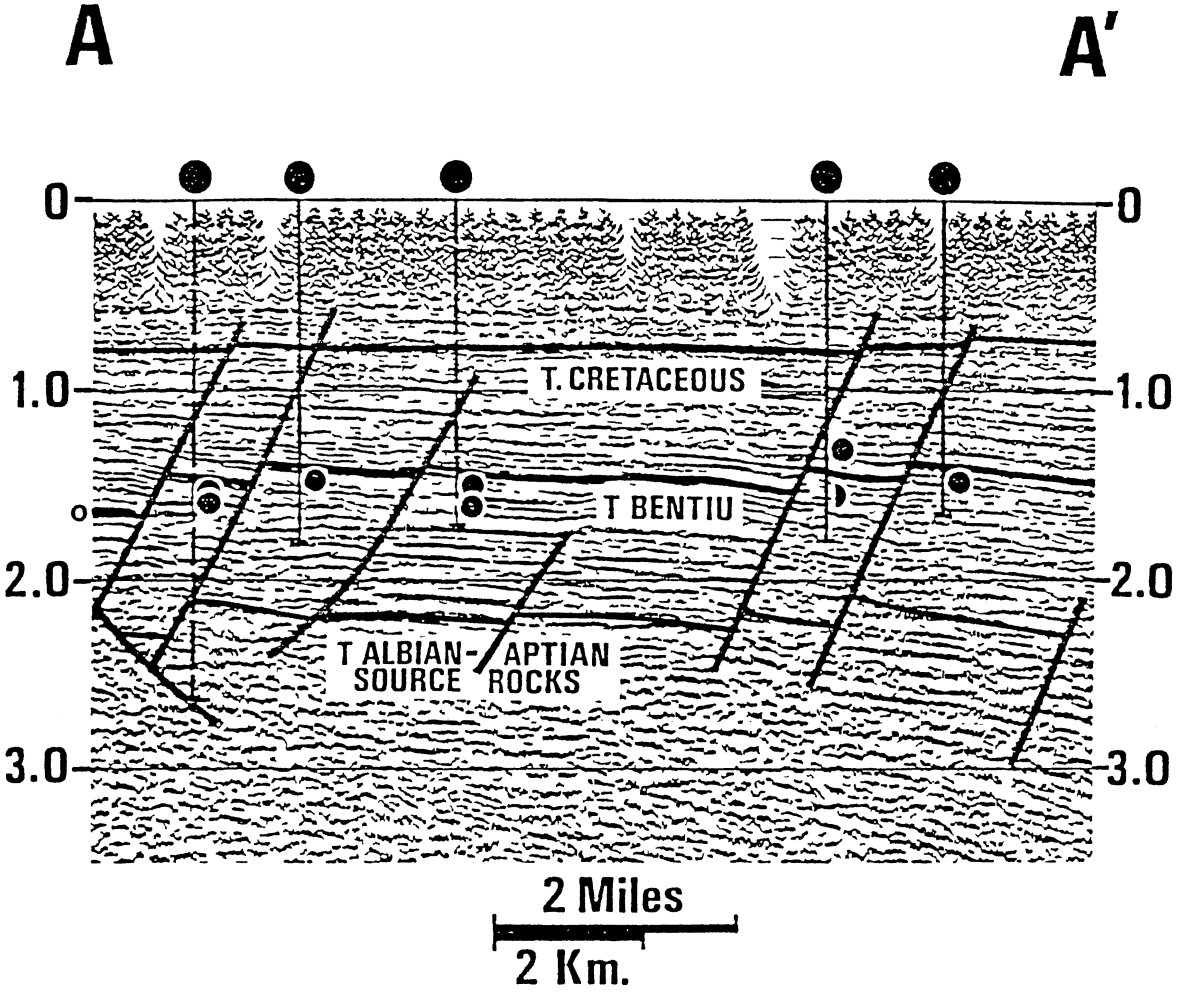

Figure 9. Time Migrated Seismic Section across Heglig Area (See Figure 6 for Location), Abu Gabra Basin. (From Schull, 1988.)

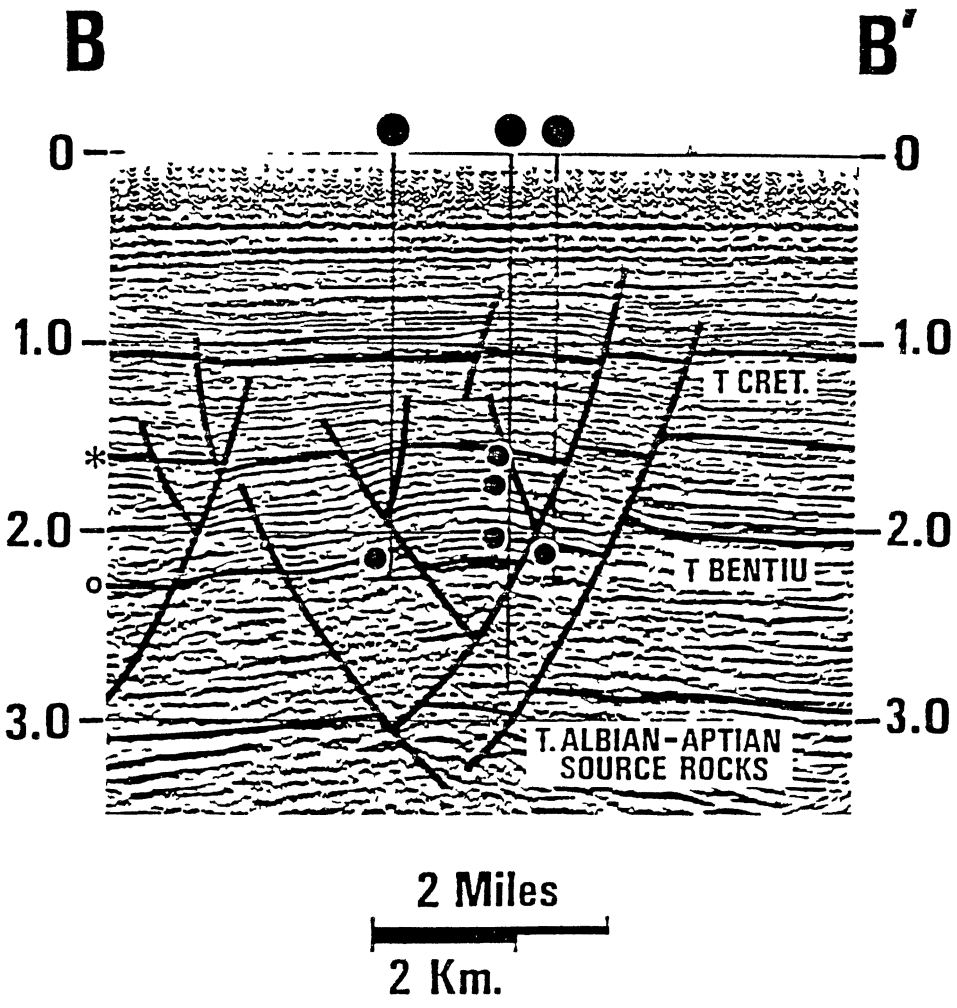

Figure 10. Time Migrated Seismic Section to the West of the Study Area (See Figure 6 for Location). Notice the complex layout of Normal and Normal Lystric Faults. (From Schull 1988.)

complex graben-horst features across the basin (Plates 1 and 2). According to Schull, 1988, the faults are predominantly oriented parallel or subparallel to the strike of the primary grabens and basin margins. The faults strike mainly at N40 - 50° W throughout the Abu Gabra Basin. However, older N-S trends also exist in the central and southern parts of the basin. Few transverse faults and ones those strike obliquely to the major trend also exist. It should be noted that, there is an outstanding variety in the vertical displacements, the geometry and growth history of these faults.

In the study area (Unity Field), the compaction of the rift sediments on the basement horsts seem to have resulted in drape-folding, which developed broad anticlinal structures. These structures were locally accentuated by extensive normal faulting. Accordingly, the associated structural hydrocarbon traps are extremely complex.

CHAPTER III

STRATIGRAPHY

Precambrian-Cambrian

The definition of the term "basement complex" given by Whiteman (1971), is adopted here to refer to rocks that underlie Paleozoic and Mesozoic rocks, and accepted to be predominantly Precambrian in age. These basement complex rocks are not reported to cropout anywhere within the study area, nor they have been reported to outcrop significantly within the entire Abu Gabra Basin. However, to the south, southwest and north of the basin, basement rocks occupy considerable areas (Figure 11). According to Whiteman (1971) due to the complexity in metamorphic grades and the lack of isotopic dates, there is no satisfactory comprehensive classification of the basement rocks in Sudan in general. That probably explains why almost all the basement complex rocks outcropping to the southwest and the south of the basin are mapped as undifferentiated. According to Whiteman (1971), the correlation of basement rocks cropping out to the south of the basin to those of Uganda and the Congo is more obvious than it is to the basement complex rocks north of the basin. The

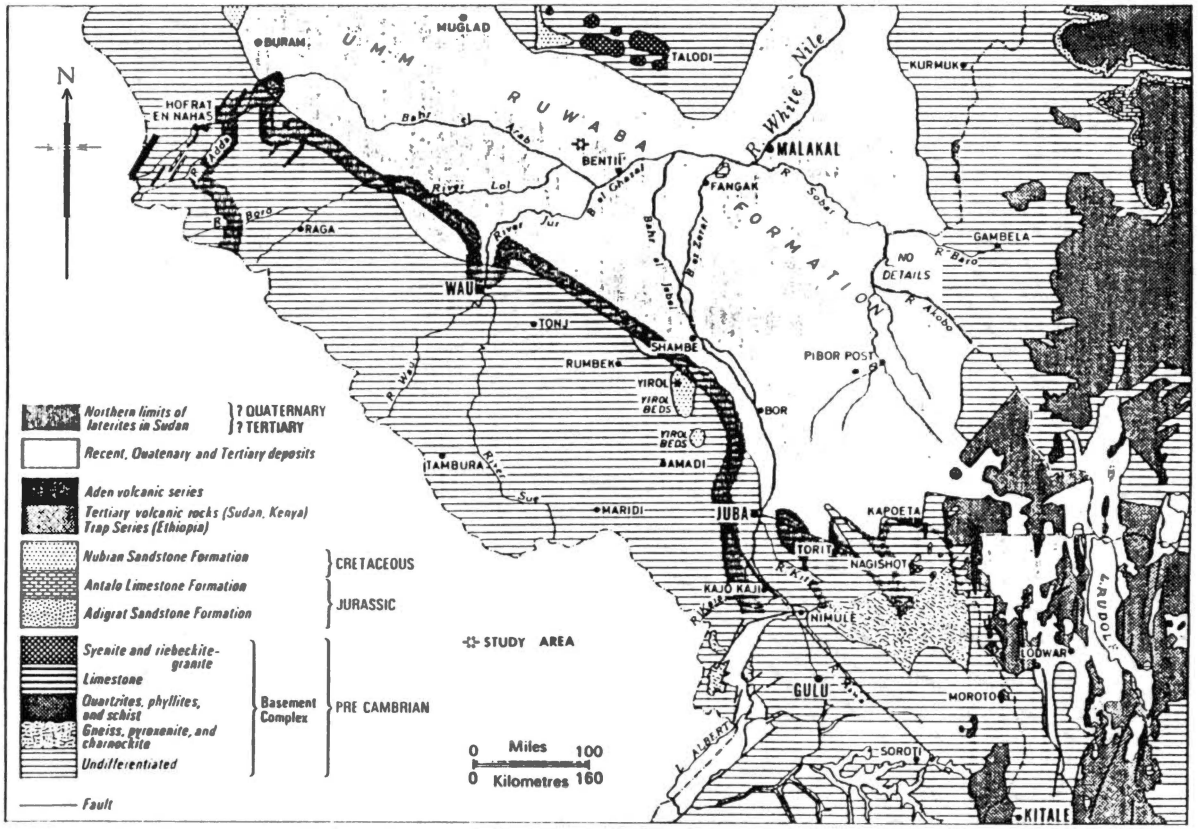

Figure 11. A Generalized Geologic Map of Southern Sudan and adjacent areas. Notice the crude Mapping of the Basement Complex Rocks. (From Whiteman, 1971.)

continuation of the Madi Quartzites of the West Nile Province of Uganda into southern Sudan along the course of the White Nile strengthens this correlation. In any case, very little geological work has been done in regard of describing the various rock types, their classification, or even the nature of their superposition. In general, the basement complex rocks to the south of the basin, according to Whiteman (1971), "consist of a group of granoblastic, foliated basic-to-acidic gneisses with hypersthene and feldspar, intruded into foliated paraschist and paragneisses." Andre (1948) studied the basement complex rocks of southern Sudan and identified the following rock groups:

Group 8: Charnockitic orthogneiss similar to the charnockitic rocks of nothern Uganda

Group 9: Foliated granites and granodiorites

Group 10: Feldspathoidal sodic syenites

He assigned Groups 8 and 9 to the Precambrian, whereas Group 10 was given a Cambrian to a possible post Paleozoic age. However, no order of superposition was mentioned.

To the north of the Abu Gabra Basin, northeast of the study area, the basement complex has been described by Rodis et al (1964) as being composed predominantly of granite, gneiss and schist with quartzites and crystalline

limestone. Immediately adjacent to the north edge of the Abu Gabra Basin (Talodi and Rashad areas, Figure 11), the basement complex rocks are described by Mansour and Samuel (1957) to reflect the following succession:

1. banded gneiss and schists, mainly hornblende - bearing occasionally interbedded with mıca-rich bands. The regional trend is predominantly north-northeast-south-southwest;

2. banded metasedimentary series ıncluding micaschists, graphitıc schists, slates, phyllıtes, quartzıtes and marbles;

3. foliated hornblende 'quasi-gneiss' of granitic to granodioritic composition; and

4. granites and syenites with the granites vary from fine to medium-grained to fine-grained biotitic varieties, (Whiteman, 1971).

At Hofrat En Nahas area (Figure 11) to the west of the basin, where ore deposits of maınly copper and, less importantly, uranium, have long been recorded, the basement complex is made of chlorıte schist, sericite schist, acid gneisses, amphibolites and talc schists.

In the subsurface along the Abu Gabra Basin, the basement complex has been reached in two of Chevron's wells. According to Tom Shull, 1988, the cored basement

samples from both wells consist of granodioritic gneiss that has been dated as ± 540 MYBP.

Paleozoic

The Paleozoic sediments of Libya extend to the south in Chad and to the east and southeast in Sudan through the Darfur and Kordofan regions directly west and northwest of the Abu Gabra Basin (Sanford, 1935). Whiteman (1971) states that Paleozoic sediments are likely to have a limited existence beneath the Nubian beds in northern Darfur, some 600 Km west and northwest of the study area. However, due to thickness considerations, he did not agree with the likelihood of Paleozoic sediments underlying the Nubian sandstone sediments in the Kordofan region, which is closer to the study area. This is further supported by the conclusion of Hottinger et al. (1959), that "the marine Paleozoic transgressions recorded in Libya did not reach the Sudan." Moreover from cross sections drawn by Whiteman (1971) and the Royal Dutch-Shell-BP (1959), the Paleozoic sediments of Libya are shown to pinch out drastically eastwards into the Sudan (Figure 12). It is also evident that Nubian beds rest directly on the basement complex rocks only few miles away to the south and east of the Paleozoic sediments of J. Uweinat in northwestern Sudan.

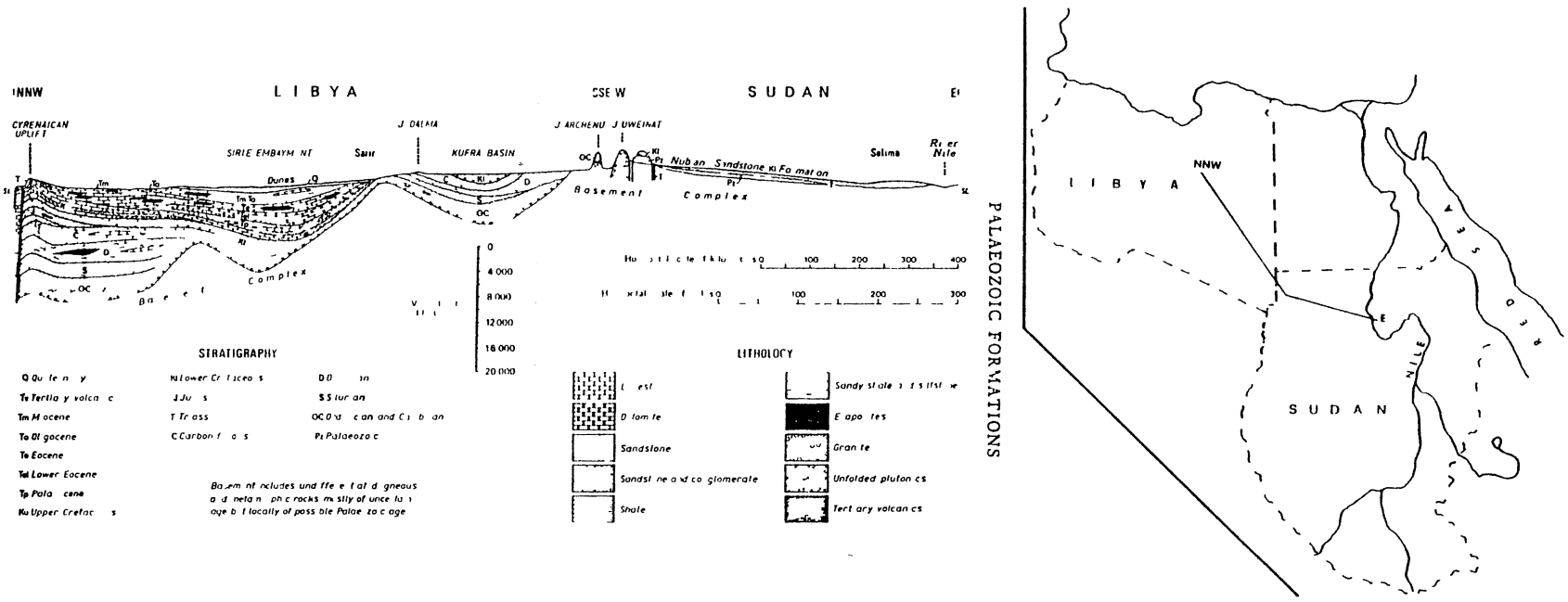

Figure 12. A Cross-section from Cyrenaica (Libya) to the Nile (Sudan) illustrating how Paleozoic Sediments drastically pinchout going East towards Sudan. (After Whiteman, 1971.)

Close to the northern edge of the Abu Gabra Basin a controversial formation crops out in southern Kordofan region known as the Nawa Formation. The controversy arises from uncertainty concerning its age and origin. The formation described by Whiteman (1971) to consist of:

> ...gently dipping sediments ranging from mudstones to arkosic grits; purple to green in color, abundantly micaceous, and containing up to 25 percent undecayed feldspar. Abundant fresh biotite, epidote, apatite, sphene and detrital cholorite, have been recognized in thin sections. Some of the mudstones are false bedded, and all the rocks are well compacted and, unmetamorphosed.

The maximum proved thickness of the Nawa Formation from water boreholes is recorded to be 443 ft. The presence of limestone in the Nawa Formation led Rodis et al. (1964) to consider the deposition of these sediments to have occurred in Late Paleozoic times in shallow seas developed in the region after a period of prolonged erosion during most of the Paleozoic. Whiteman (1971), however, tends to favor "a local and continental origin" for the Nawa Formation, with the acknowledgement that the limestone is likely to be of freshwater origin since no fossils were found.

Complying with the above discussion, the recent oil wells drilled by Chevron Company in the Abu Gabra Basin and the other basins, proved the absence of any sediments older

than Jurassic (Schull, 1988).

The poor presence, if not total absence, of Paleozoic sediments has long been a puzzle in northeast Africa (Sudan, Egypt, Ethiopia and even Saudi Arabia in the Arabian Peninsula). Speculations on this phenomenon include the idea that the whole region remained land during the Paleozoic. In his comprehensive summary and interpretation of Chevron exploration activities in Sudan, Schull, 1988 states: "From the Cambrian into the Mesozoic the agreement area was the location of an extensive continental platform." Other authors maintain that subsequent erosion wiped out the previously existing Paleozoic section. However, as for Sudan, the writer agrees mostly with the postulation given by Whiteman (1971) that due to inadequate geological investigations, Paleozoic sediments might have been misrepresented under the umbrella of "basement complex," which is yet to be thoroughly dated and classified.

Mesozoic

Introduction

The Mesozoic is represented by the most extensive and significant sedimentary section in Sudan, the Abu Gabra Basin, and the study area in particular. Its importance arises from the fact that it contains a vast number of the water aquifers and it also includes the most significant sedimentary sections proven as hydrocarbon source or reservoir rocks. The Nubian Sandstone sediments occupy the bulk of the Mesozoic system in Sudan, Egypt and Libya. However, the application of the term "Nubian Sandstone" seems to have a rather broad and vaguely defined context in each of the three countries. Discrepancies involving the age within the Mesozoic, the composition and the origin of the Nubian Sandstone, are very obvious. In Egypt, for instance, the term refers to those sediments of Turonian and Santonian age believed to be of fluvio-marine origin. In Libya, the Nubian Sandstone consists of a conglomeritic, coarse-grained sandstone with siltstone, and silty shale bands. The age of the Nubian Sandstone in Libya is recorded as Early Cretaceous (Klitzsch, 1963). However, reference to Jurassic plants at the lower part of the Nubian deposits has been made by Plauchut (in Klitzsch, 1963). In Sudan, the term "Nubian Sandstone Formation," as

it was used for surface geological surveys before the recent Chevron drillings, referred to:

> ...those bedded and usually flat-lying conglomerates, grits, sandstones, sandy mudstones and mudstones that rest unconformably on the basement complex and Paleozoic Sandstone Formations and are older than the Hudi Chert Formation (Early Tertiary) and the 'Early Tertiary' Lavas." (Whiteman, 1971).

From surface geology investigations coupled with information from shallow water-wells, the total thickness of the Nubian Sandstone sediments does not exceed a few hundred feet, 1000 feet of Nubian sediments were recorded in Sudan Geological Survey borehole number 1517, (Whiteman, 1972; Kheiralla, 1966). However, the oil wells drilled by Chevron Company in the Abu Gabra Basin together with seismostratigraphic interpretations indicate a thickness of 35,000 feet of Mesozoic and Cenozoic sediments (Schull, 1988), over 19,000 feet of which represented by Mesozoic sediments of the previously called Nubian Sandstone Formation. Aside from the thickness consideration, it is worth noting that a remarkable variation exists in the composition as well as the types and number of facies involved in the Nubian sediments. Moreover, the stratigraphic column established by Chevron (Figure 13) for

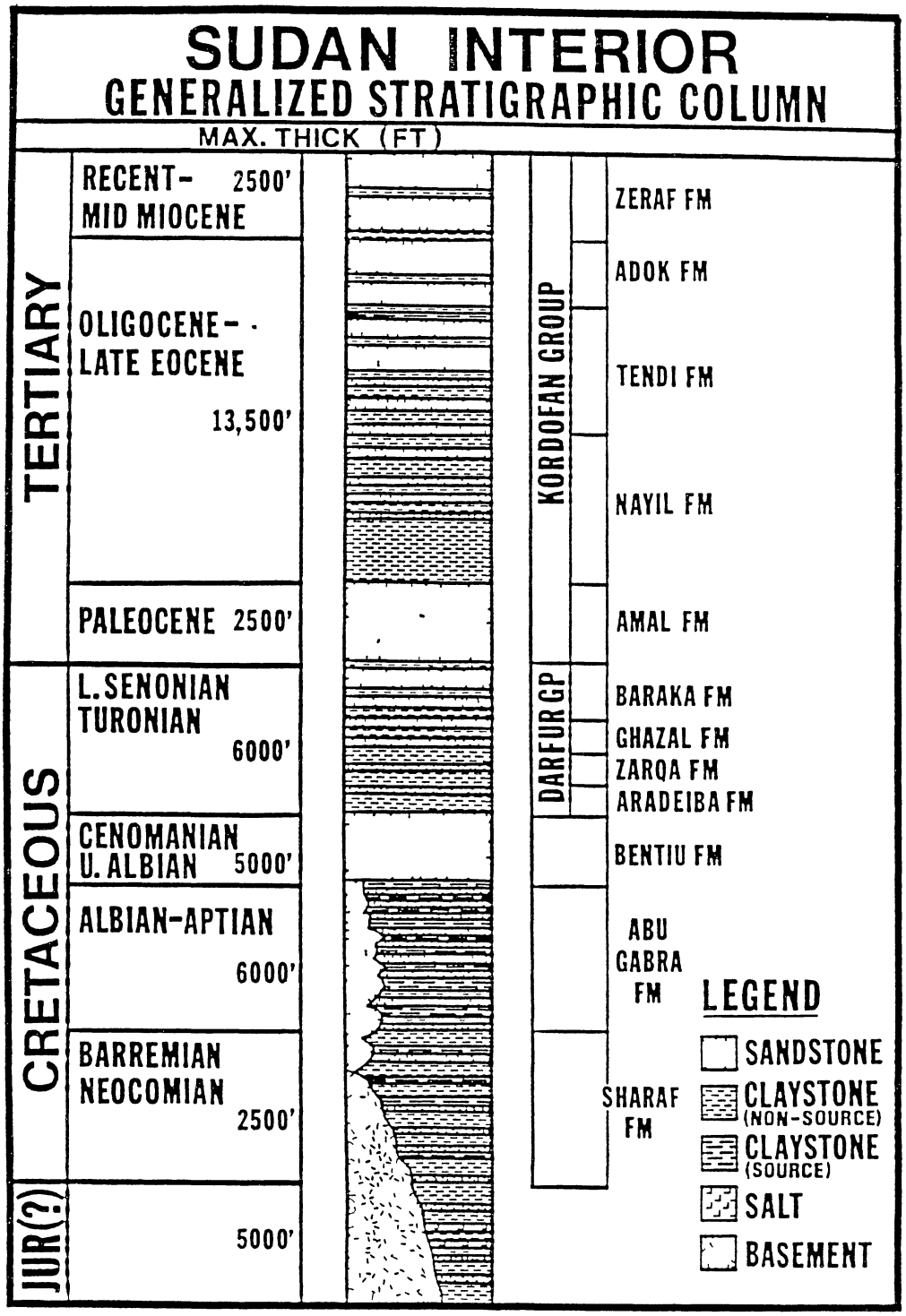

Figure 13. A Generalized Stratigraphic Column for the Abu Gabra Basin. (From Schull, 1988.)

the Abu Gabra Basin refers to one lithostratigraphic unit of Cretaceous age as a 'group', namely the Darfur Group. This group together with three other units recognized as formations, namely Sharaf, Abu Gabra and Bentiu, comprise the Cretaceous within the Abu Gabra Basin. With regard to the above mentioned points and the generally accepted notion that 'the Nubian Sandstone Formation in Egypt and northeast Africa refers to any Mesozoic sandstone of uncertain age,' I would like to state that the Nubian section is too extensive of a lithostratigraphic unit to be designated as just a formation. Accordingly, in this study it will be referred to as the Nubian Sandstone Supergroup.

The Nubian Sandstone Supergroup.

The oldest Mesozoic sediments penetrated within the Abu Gabra Basin are of Lower Cretaceous age (Barremian-Neocomian). However, Jurassic sediments of salts (halite), siltstones, and claystones are reported to have been drilled in the Blue Nile Basin some 400 miles northeast of the study area. According to Schull, 1988, the rifting and basin infilling associated with the Cretaceous-Early Tertiary resulted in two prominent depositional cycles, each is present as an upward coarsening sequence throughout

the basin. Sharaf, Abu Gabra, and Bentiu Formations represent the lower cycle, while the upper cycle includes the Darfur Group and the Early-Tertiary (Paleocene) Amal Formation.

The following stratigraphic account of the Cretaceous system is based on the valuable summary paper by Schull (1988) Lithologic descriptions of the Aradeiba Formation are based on the present study.

Barremian-Neocomian

Sharaf Formation

The sediments deposited during this time represent the early rift deposits of the Sharaf Formation. They consist of claystones, siltstones, and fine sandstones, which grade to coarse alluvial clastics toward the edges of the basin. The maximum penetration of the Sharaf Formation is 1200 feet at the northwest edge of the Abu Gabra Basin, and the formation is believed to thicken in the deepest troughs to the southwest. The environments of deposition are believed to be fluvial-floodplain and lacustrine.

Lower Albian-Aptian Abu

Gabra Formation

During this period, an extensive area of the basin was occupied by rift lakes. A thick section of lacustrine sediments have been deposited in the form of organic-rich claystones and shales with interbedded silts and fine grained sands. The maximum thickness of the Abu Gabra formation is estimated to be 6,000 feet, and it is interpreted to be the primary hydrocarbon source rock for the basin.

Cenomanian-Upper Albian

Bentiu Formation

The environments of deposition during this period were primarily alluvial and fluvial flood-plains of both braided and meandering streams. The subsequent deposits, predominantly thick sand sequences, serve as excellent reservoirs in Heglig field. The maximum thickness of the Bentiu Formation is 5,000 feet.

Senonian-Turonian

Darfur Group

This group includes the Aradeiba (subject of this study), Zarga, Ghazal, and Baraka Formations. During this

period, the deposited sediments were characterized by being generally fine-grained with some coarse-grained sections. The Aradeiba Formation is composed of at least three significant sandstone members (designated A, B and C, from top to bottom by Chevron Oil Company) separated by thick flood plain desposits of claystone (Aradeiba Claystone). The sand members are generally composed of shaley sandstone and fine to coarse snadstone beds. Sediments of subarkosic nature make the bulk of the sandstones of the Aradeiba Formation. In this study the Aradeiba claystone is classified into two facies F-G, gray to very dark gray in color and F-H with brown and reddish brown colors indicating subareal exposure.

Two cross-sections A-A' and B-B', and three thickness maps (one for each sandstone member) have been constructed to dilineate the extent and lateral variation in thickness of the three sand members (see plates 1 through 5, in pocket). However, it should be noted that, more well-data is needed to narrow down the possibilities of interpretation, especially towards the northern portion of the Unity Field. The cross-sections (plates 1 and 2) indicate that the Aradeiba Formation was deposited in a grabinal structure bounded by normal faults. On the upthrown flanks of the faults to the east and west, the

sandstone members undergo a noticeable thinning indicating the growth nature of these faults. Generally, the sandstones seem to diminish in thickness to the east and west, away from the axis of the northwesterly trending Unity Field. The Zarga Formation, like the Aradeiba Formation, is composed of claystones, shales, siltstones, and fine to medium-grained sandstones. The environments of deposition were basically "flood-plain and lacustrine." These fine sediments represent the initial deposits following the first rifting phase that ended with the deposition of the thick sands of Bentiu Formation. The observation that this lower portion of the Darfur Group is widespread throughout the entire basin reflects the influence of tectonics on the resultant sedimentation. In general, the Aradeiba and Zarga Formations act as a good seal rock considering that the vast thickness of fine sediments exist in that lower portion of the Darfur Group. Nevertheless, the moderately thick sand Channels (10-80 feet) act as essential reservoirs; for example, in the Aradeiba Formation in the Unity Field.

The sand content and the size of the sand grains noticeably increase toward the upper portion of the Darfur Group in Ghazal and Baraka Formations. The deposition of this unit took place mostly "in sand-rich fluvial and

alluvial fan environments, which prograded from the basin margins." The maximum thickness of this group is estimated to be 6000 feet.

Tertiary

Inference from shallow water-wells and surface geology investigations, before drilling for oil, led geologists Lawson (1927), Ball (1939), Andrew (1943), Andrew and Karkanis (1945), Berry and Whiteman (1968), and Whiteman (1972) to believe that the Tertiary is represented by sediments deposited in relatively shallow depressions along areas of the central and south central Sudan toward the Abu Gabra Basin. The deposits were named the Umm Ruaba Formation (after a small town in western Sudan) and described by Andrew (1943) to:

> ...consist of unconsolidated sands, sometimes gravelly, clayey sands and clays. The clays are mainly buff to grayish-white, or greenish-grey. In general the sediments are unsorted and feldspar and biotite are undecayed. Rapid facies changes are characteristics of the deposits.

An extensive surface cover of "heavy clays with kanker nodules" overlie much of the areas known to be underlain by the Umm Ruaba Formation. However on some areas the Umm

Ruaba Formation is overlain by the Pleistocene to recent Qoz sands; for instance, the northwestern portion of the Abu Gabra Basin around the town of Muglad. The Umm Ruaba Formation is believed to have been deposited under fluvial and lacustrine environments (Andrew and Karkanis, 1945). Whiteman (1971) postulates that the Umm Ruaba Formation was laid in standing waters and land deltas, and he adds that the thickness of the formation is at least 889 feet. It should be noted that the lack of diagnostic fossils makes it impossible to distinguish between the Tertiary and Quaternary sediments, therefore the Umm Ruaba Formation is generally considered as Tertiary-Pleistocene in age (Whiteman, 1971).

In the subsurface, the oil wells drilled by Chevron Oil Company provided overwhelming information about the Tertiary System, at least within the Abu Gabra Basin and the study area. According to Tom Shull, 1988, over 15,000 feet of Tertiary sediments have been evident from seismic and drilling data.

Paleocene: Amal Formation

This formation starts with a basal conglomerate to conglomeratic sandstone bed. Upwards, the Amal Formation

grades in to coarse and medium grained quartz arenites. Schull, 1988 states that this formation "represents high energy deposition in a regionally extensive alluvıal plain environment with coalescıng braided streams and alluvial fans."

Late Eocene-Middle Miocene:

Kordofan Group

The Kordofan Group includes Nayil, Tendi, Adok and Zeraf Formations. This group, which generally coarsens upwards, represents the second rifting cycle sediments. The lower formations, Nayil and Tendi, are mainly composed of fine grained sandstones, siltstones, and claystones, deposited in fluvial flood-plain and lacustrine environments. The sand-to-clay ratio ıncreases gradually upwards along the Korodofan Group and attains its maximum in the Adok and Zeraf Formations. The environments of deposition are interpreted to be exclusıvely braided rivers and alluvial fans.

Pleistocene-Recent

Qoz Deposits

These surface sand deposits are very extensive towards the northwestern portion of the Abu Gabra Basin. The name "Qoz" was originally intended by Edmonds (1942) to refer to the dune-like accumulations of sand in Kordofan Province (Figure 14). However, the term has been stretched to include the contemporaneous sheet-like recent sand deposits. The sands consist of well-rounded quartz grains of Nubian origin and vary in color from pale buff to deep red. The origin of these sand deposits is thought to be due to weathering of the Nubian Sandstone rocks (Edmonds, 1942).

The Clay Plains

These clay sheets are probably the most striking geomorphological feature of most of the Abu Gabra Basin. These extensive deposits cover the central and the southeastern parts of the basin, including the study area (FIgure 14). These sediments consist of 50 to 60% clay mixed with silt grains and very little coarse material, Whiteman (1971). These clayey soils are mostly alkaline,

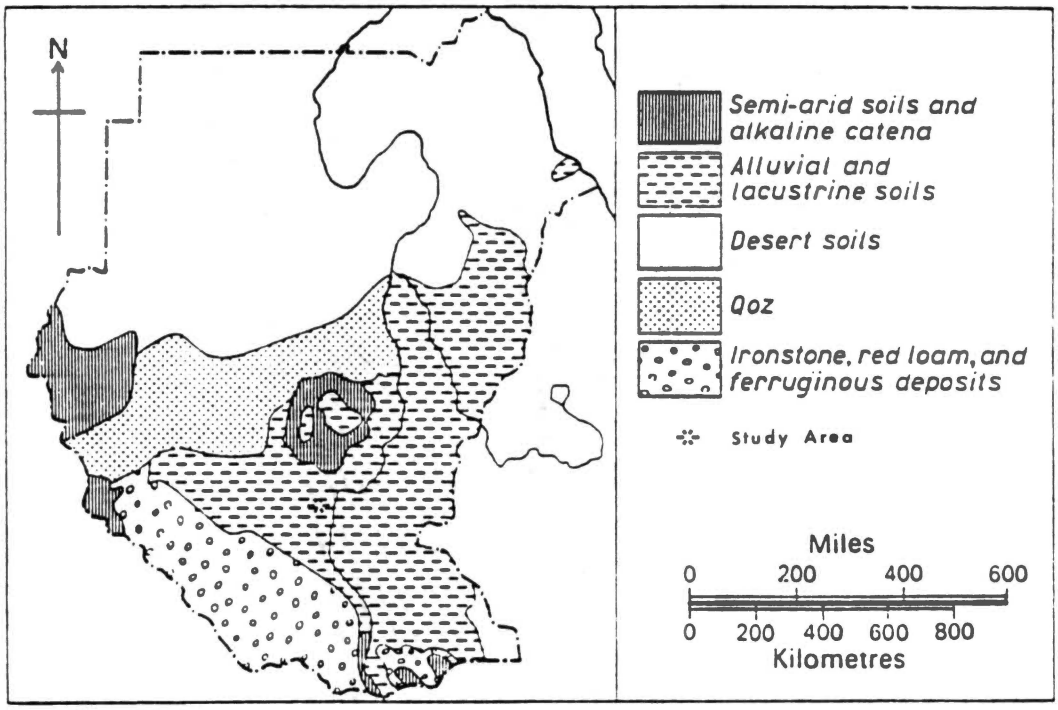

Figure 14. A Generalized Distribution Map of the Superficial Deposits and Soils of Pleistocene-Recent Age. (After Whiteman, 1971)

although humic soils exist in the Sudd region. Toward the southwestern border of the Abu Gabra Basin, these sheet clayey soils give way to iron-rich soils and laterites that extend across the Nile-Congo Divide.

The origin of the clayey soils is proposed by Grabham (1909) to be aeolian. He pointed out that these deposits are contemporaneous with the formation of the Qoz sediments.

CHAPTER IV

CORE AND LITHOTYPES DESCRIPTION

Introduction

This chapter consists of two parts. The first is a descriptive account of the cores covering the A, B and C sand members of the Aradeiba Formation. The total interval covered by the cores (Figures 15, 16, 17) is 198.45 feet sampled from five wells, namely Unity No. 2, Unity No. 8, Unity No. 9, Unity No. 11 and Talih No. 2 (Figure 2). In compliance with the confidentiality policy of Chevron Oil Company, only partial photographic coverage of the core samples was allowed.

In the second part, a detailed description of the eight recognized rock Lithotypes of the Aradeiba Formation is given. These Lithotypes were classified on the basis of variation in sedimentary structures and grain sizes as significant measures. The Lithotypes are named L-A through L-H.

Core Description

Well: Unity No. 2

Stratigraphic Unit: member A of Aradeiba Formation

Cored interval: 7890.5' - 7868' (Figure 18)

Figure 15. A Photograph of Parts of the Aradeiba (A) Core Samples from Unity No. 11 and Talih No. 2 Wells.

Figure 16. A Photograph of Parts of the Aradeiba (A) Core Samples from Unity No. 9 and Unity No. 11 Wells.

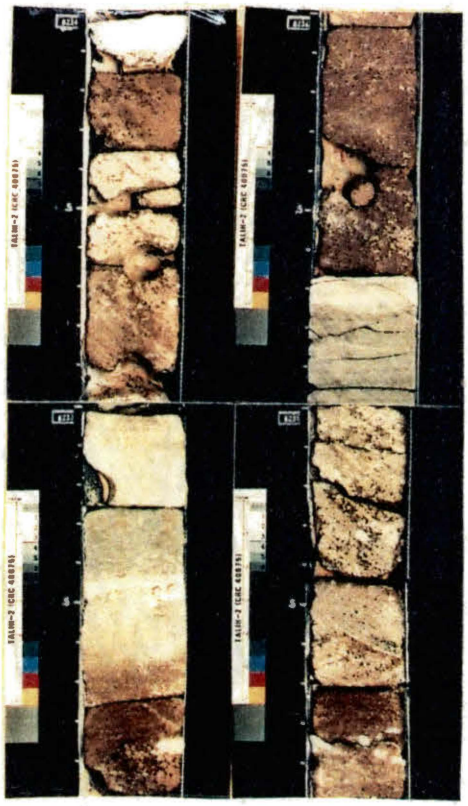

Figure 17. A Photograph of Parts of the Aradeiba (A) Core Samples from Talih No. 2.

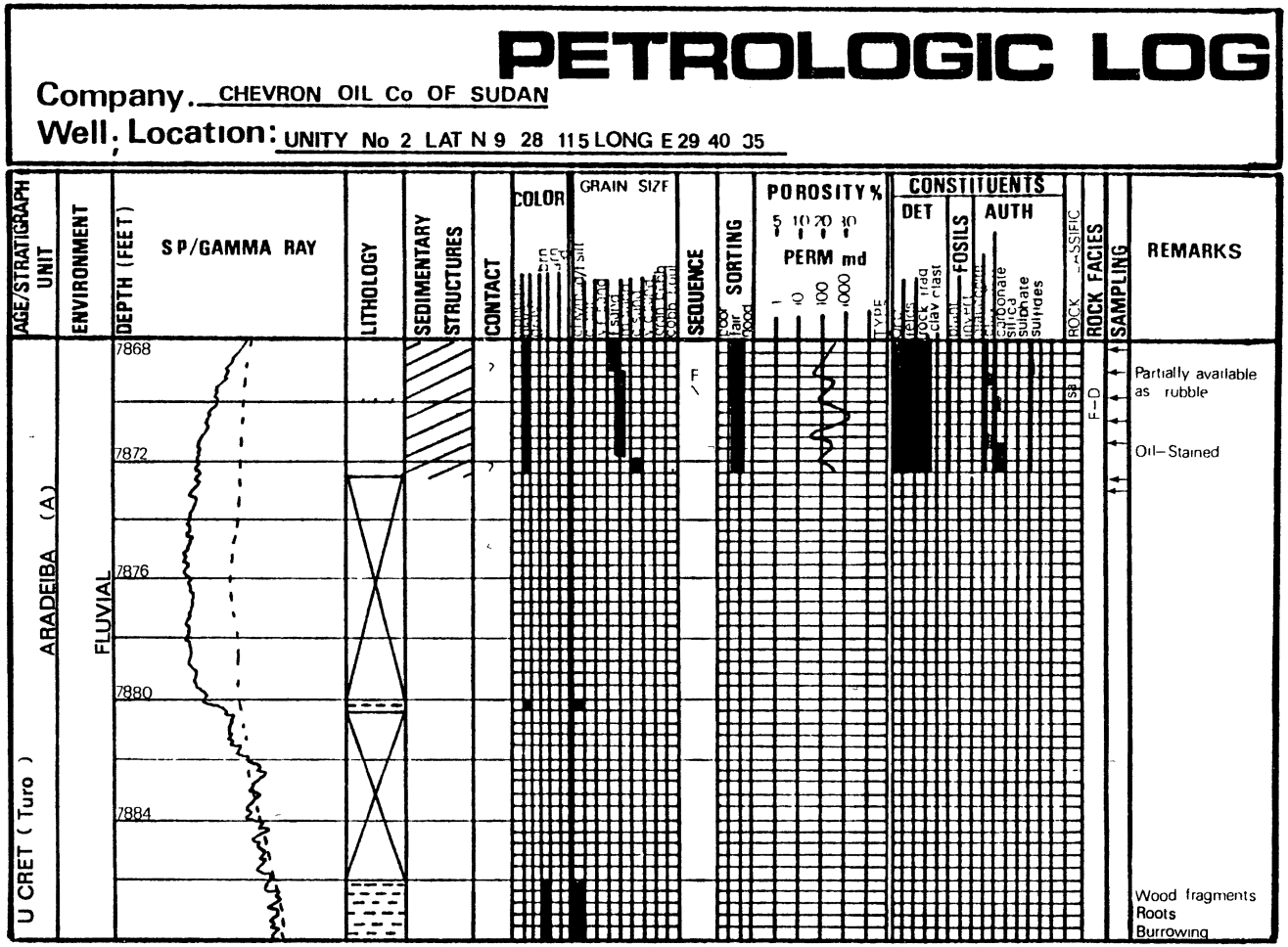

Figure 18. Petrolog of Aradeiba (A) Core, Unity No. 2.

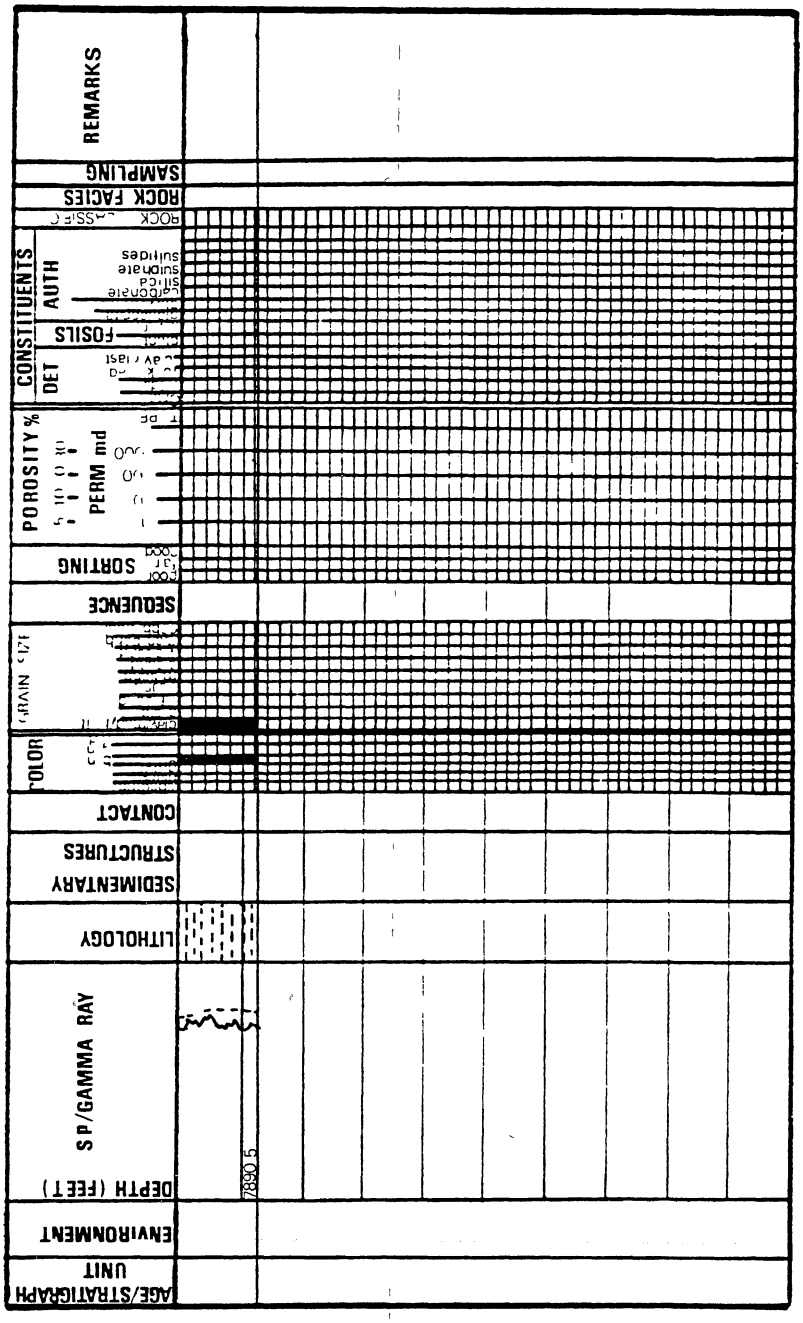

Figure 18. (Continued)

This core is composed of claystone and cross stratified sandstone.

The interval 7890.5' - 7886' consists of claystone, reddish brown, pinkish brown to dark pinkish brown in color. The uppermost portion of the core 7872.8 - 7868 is composed of coarse sandstone at the bottom grading to medium to fine grained sandstone at the top of the interval. The sandstones of this interval are moderately sorted and generally show a dark brown color due to oil staining. Planer cross bedding is the main sedimentary structure observed.

Well: Unity No. 8
Stratigraphic unit: member C of Aradeiba Formation
Cored interval: 7395.75' - 7368.1' (Figure 19)

The cored interval consists of silty claystone, claystone and sandstone. The interval 7395.7' - 7374.4' is composed of pinkish brown, greenish red and pinkish green claystone which is locally silty. The whole interval is recovered as rubble. The reddish color suggests a subareal exposure and period of oxidation. The upper portion of the core 7374.4' - 7368.1' consists of clean sandstone with tabular crossbedding and varies in grain size from medium at the bottom to very fine and rippled at the top.

Well: Unity No. 9

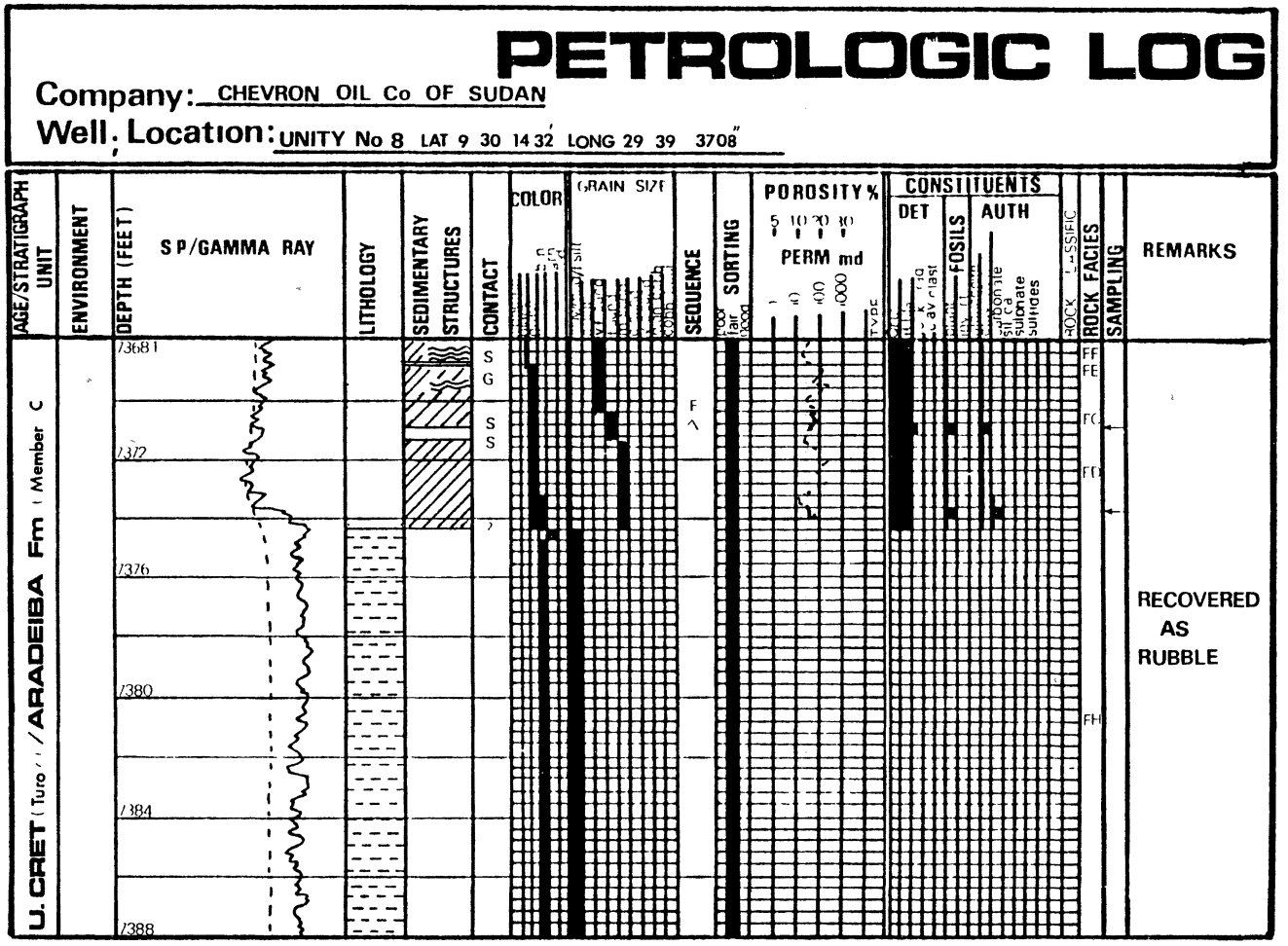

Figure 19. Petrolog of Aradeiba (C) Core, Unity No. 8.

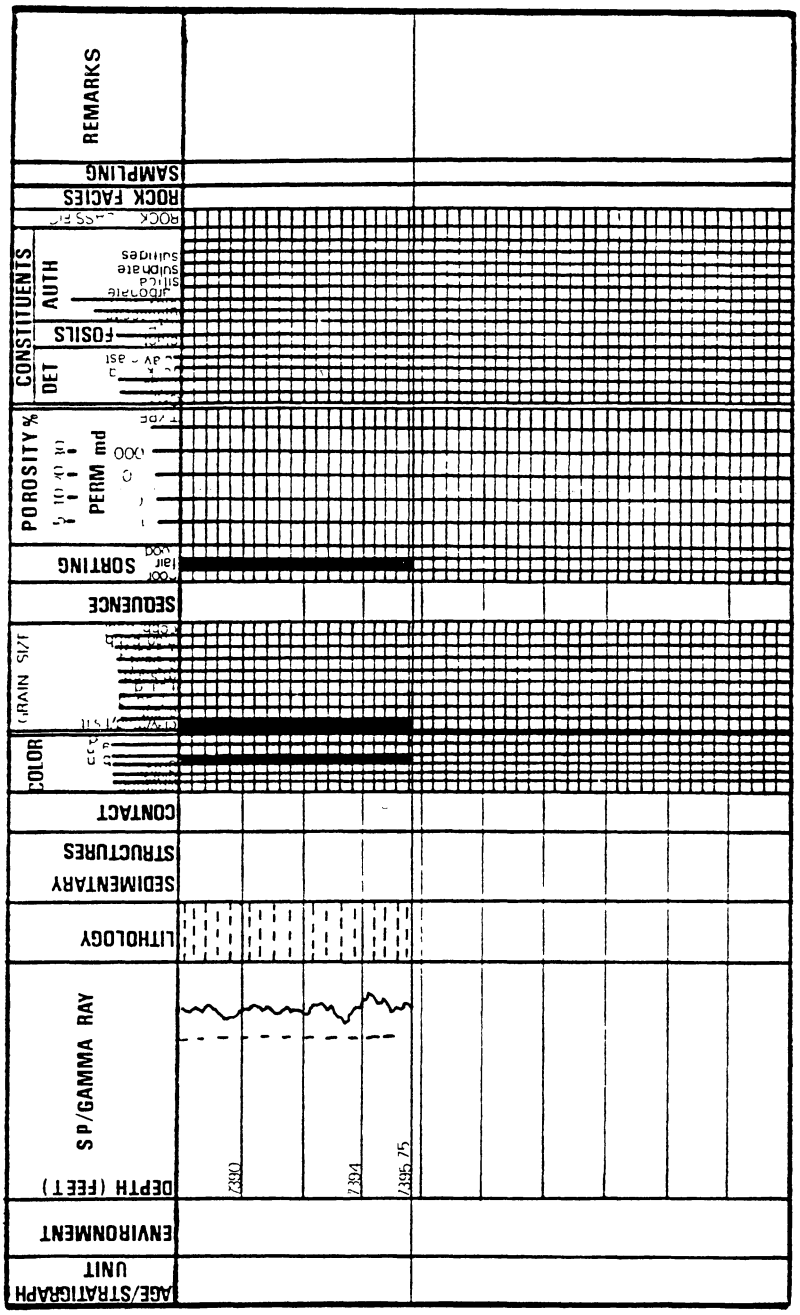

Figure 19. (Continued)

Stratigraphic unit: member C of Aradeiba Formation

Cored Interval: 8420.3' - 8393' (Figure 20)

The interval consists of silty claystone, shaley sandstone, claystone, sandstone, rip-up-clast conglomerate and interlaminated sandstone.

The bottom part from 8420.3' to 8416.2' consists of gray, greenish gray and dark gray silty claystone, micaceous and pyritic where silty. The interval 8416.2' - 8414.6' consists of very fine sandstone, locally laminated, locally interbedded with shale showing flaser bedding structures, locally silty, greenish gray, dark gray in color. This interval is succeeded by a thin bed (4 cm) of rip-up-clast conglomerate with elongate pinkish gray clay clasts. The following interval 8414.5' - 8410.6' consists of brownish gray to dark claystone, locally pinkish brown and locally silty (8413.4'). The interval 8410.6' - 8406.9' is composed of rippled sandstone, fine to very fine, greenish gray, light gray and whitish gray. Locally silty and locally with shaley bands. The interval 8406.9' - 8402.7' is made of kaolinitic sandstone, medium grained, light gray, white-spotted, dark brown where stained with oil and cross-bedded. The interval 8402.7' - 8399.4' consists of fine to very fine grained sandstone, gray and greenish gray in color, locally silty with faint cross-

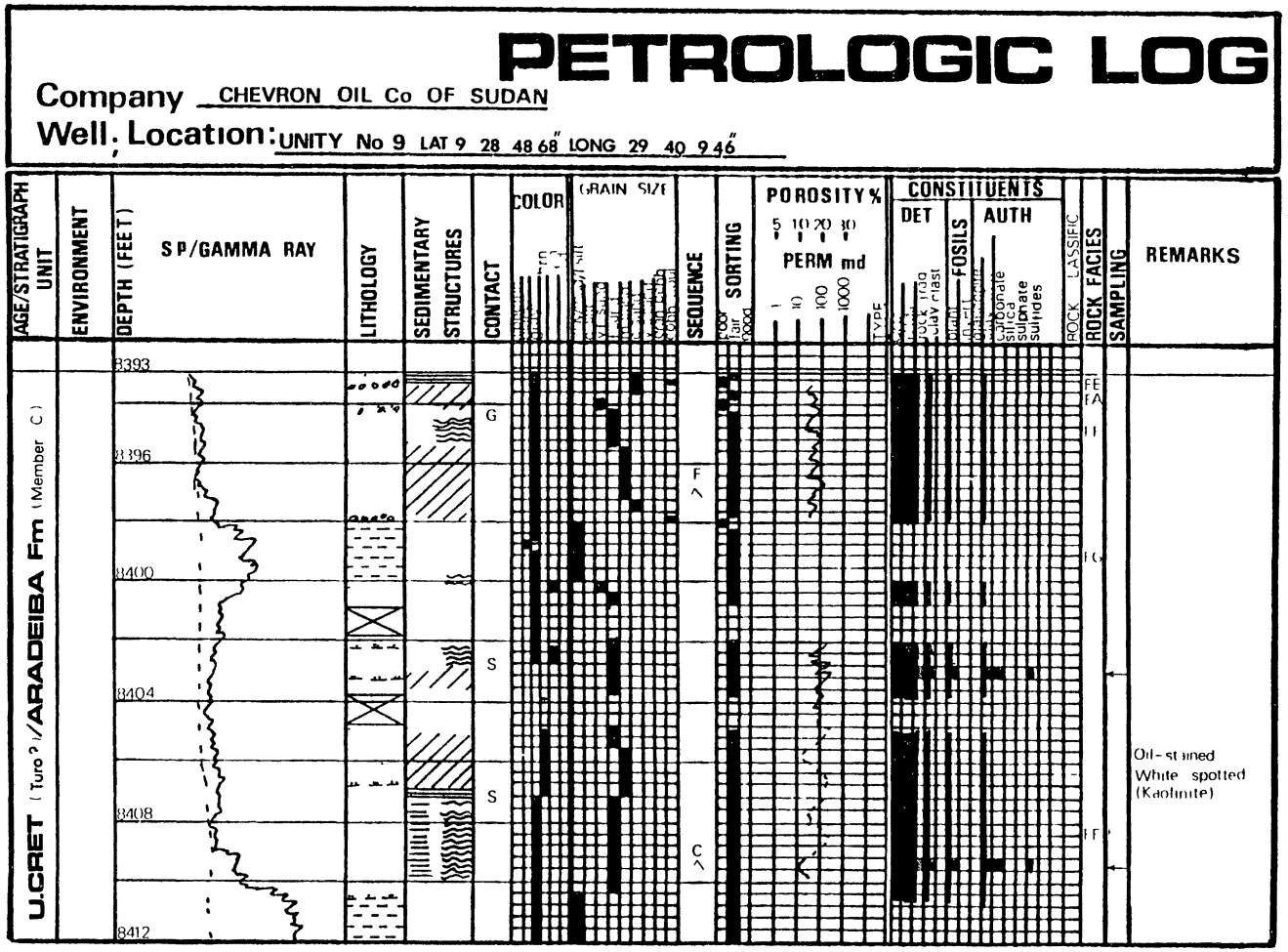

Figure 20. Petrolog of Aradeiba (C) Core, Unity No. 9.

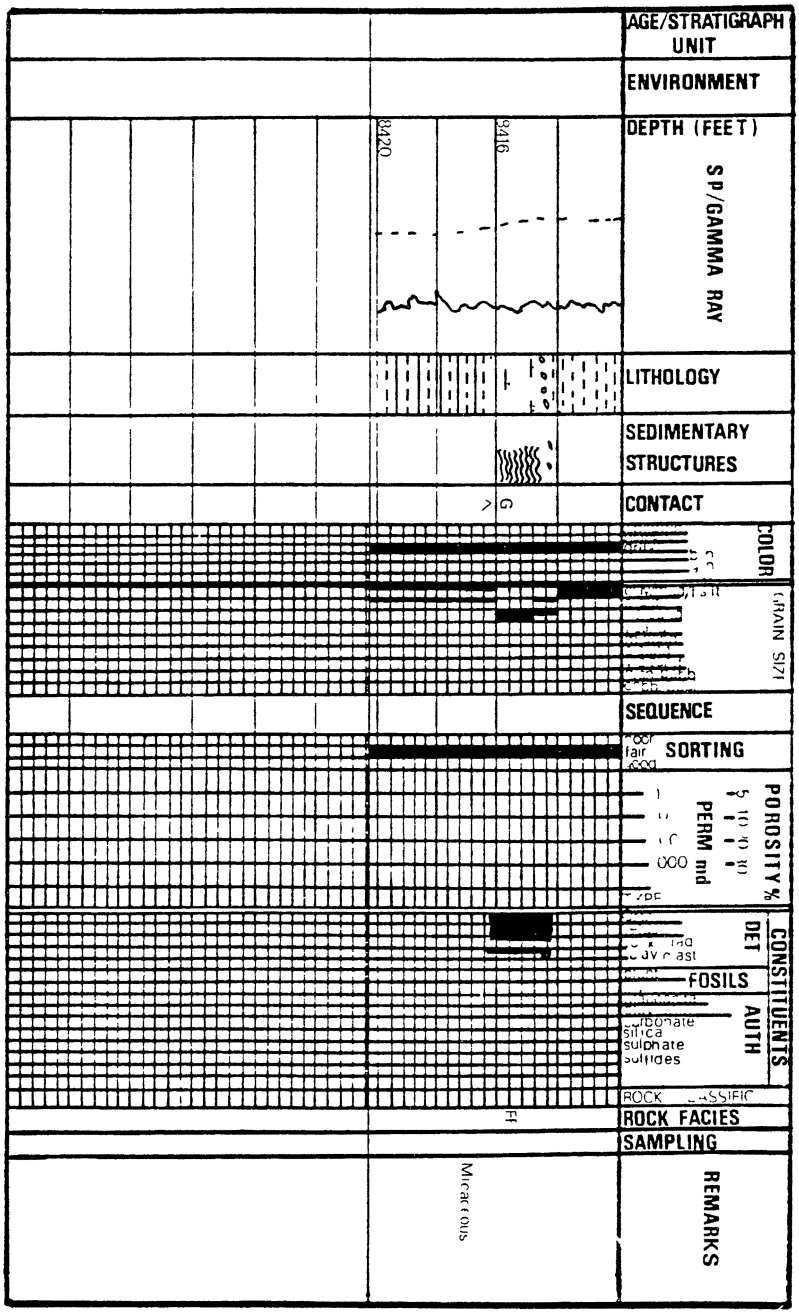

Figure 20. (Continued)

bedding and ripple mark structures. This interval gradually changes into a dark gray bed of claystone occupying the interval 8399.4' - 8398'.

The uppermost part of the core 8398' - 8393' consists of interbeds of cross-bedded sandstone, rippled sandstone and horizontally bedded sandstone with rip-up clast conglomerate at the base of the interval. The sandstone is medium grained, locally fine grained where rippled (8395.6' - 8394.4') locally interlaminated with gray, whitish gray and dark gray claystone.

Well: Unity No. 9

Stratigraphic unit: member B of Aradeiba Formation

Cored interval: 8243' - and 8234' (Figure 21)

This core is composed of sandstone, claystone and interlaminated sandstone. The interval 8243' - 8240' is composed of gray to whitish gray, fine to very fine grained, cross-bedded sandstone. The interval 8240' - 8237' consists of very dark gray carbonaceous claystone, locally silty, locally with black patches of organic material. The upper part of the core 8237' - 8234' consists of a silty sandstone interlaminated with claystone. The colors include gray, light gray and whitish brown. Wavy laminae and ripple marks are observed at 8235'.

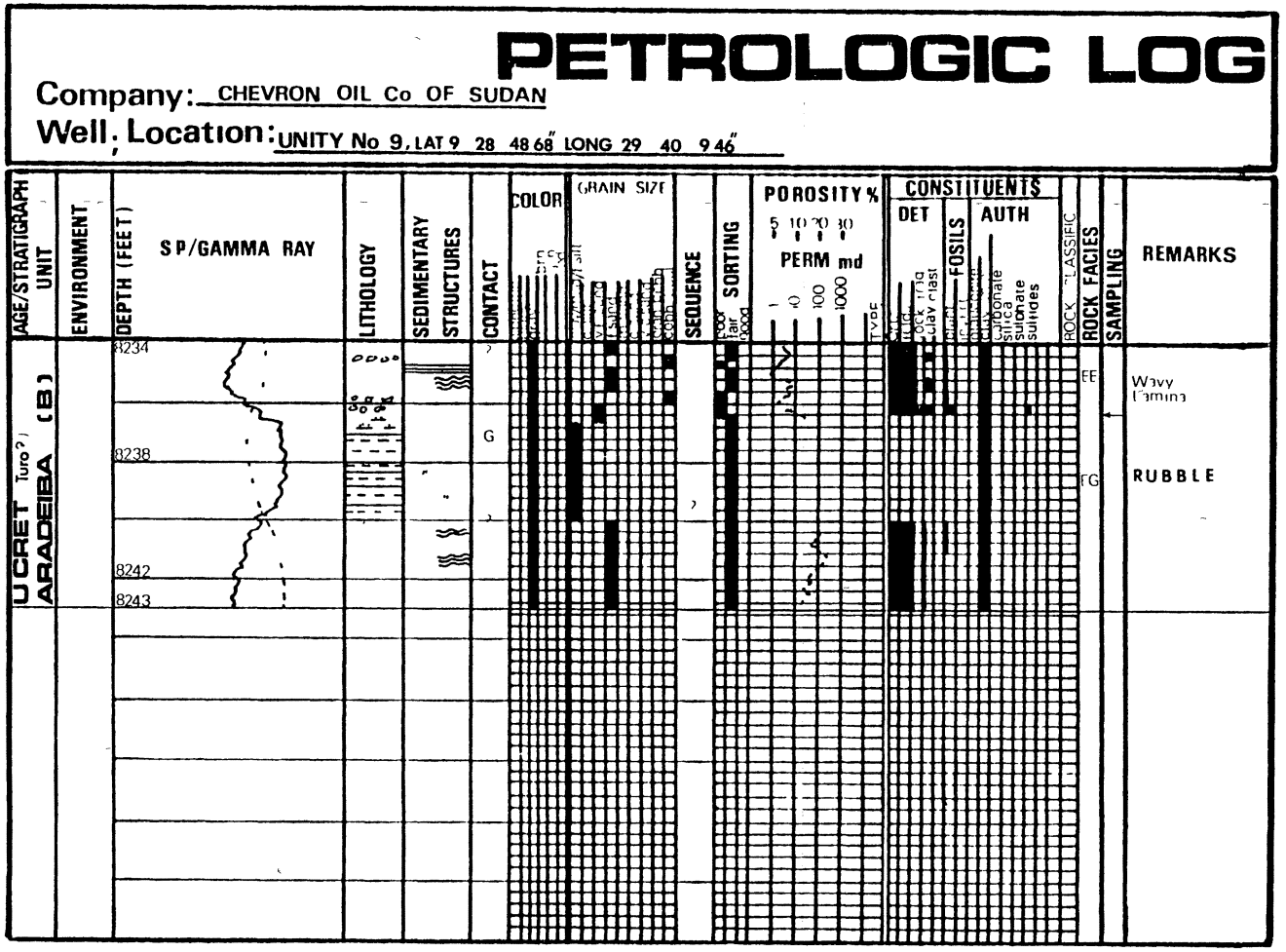

Figure 21. Petrolog of Aradeiba (B) Core, Unity No. 9.

Well: Unity No. 9

Stratigraphic unit: member A of Aradeiba Formation

Cored interval: 8037.25' - 8013' (Figure 22)

The rock constituents of this interval are claystone, interlaminated sandstone, shaley sandstone, conglomerate and sandstone.

The bottom part 8037.25' - 8033' consists of greenish gray to dark gray claystone, locally silty, kaolinitic where silty and the whole interval is recovered as rubble. The interval 8033' - 8024.6' consists of clean sandstone, cross-bedded, light gray, light brown, white spotted with kaolinite, dark brown where stained with oil and with medium grain size. The interval 8024.6' - 8023.2' is composed of a dark gray to dark brown rip-up clast conglomerate bed. The clay particles are elliptical in shape, vary between few mm and 4 cm in size and embodied in a ground mass of cross-bedded sandstone with white kaolinitic bands along the cross-bedding planes. The uppermost part 8023.2' - 8013' consists of a bed of medium to fine sandstone with laminae of shaley siltstone between 8017.3' and 8016.8'. In this interval, the sandstone is locally rippled and generally with planar cross-bedding, light gray in color and locally massive with wavy laminae.

Well: Unity No. 11

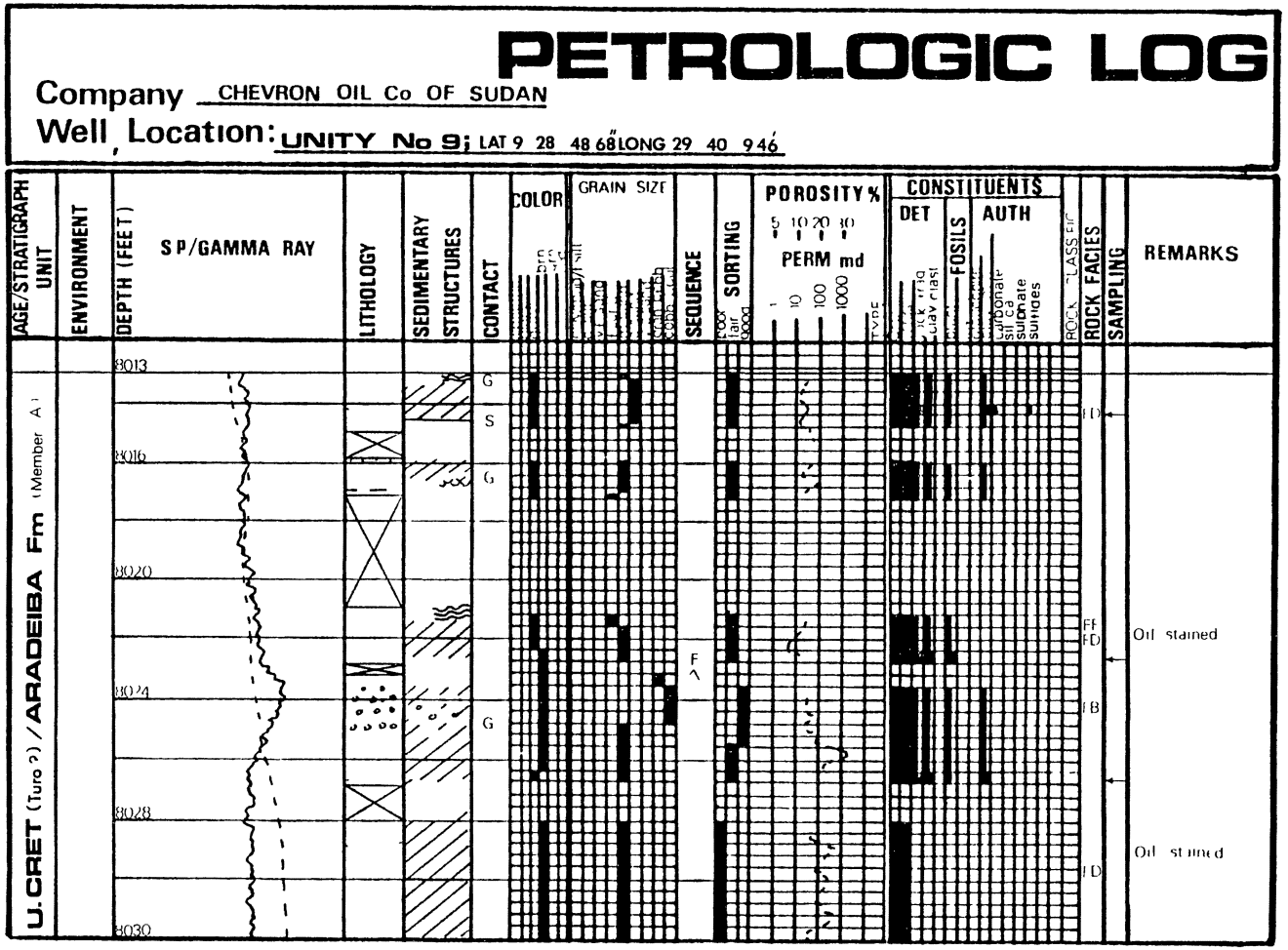

Figure 22. Petrolog of Aradeiba (A) Core, Unity No. 9.

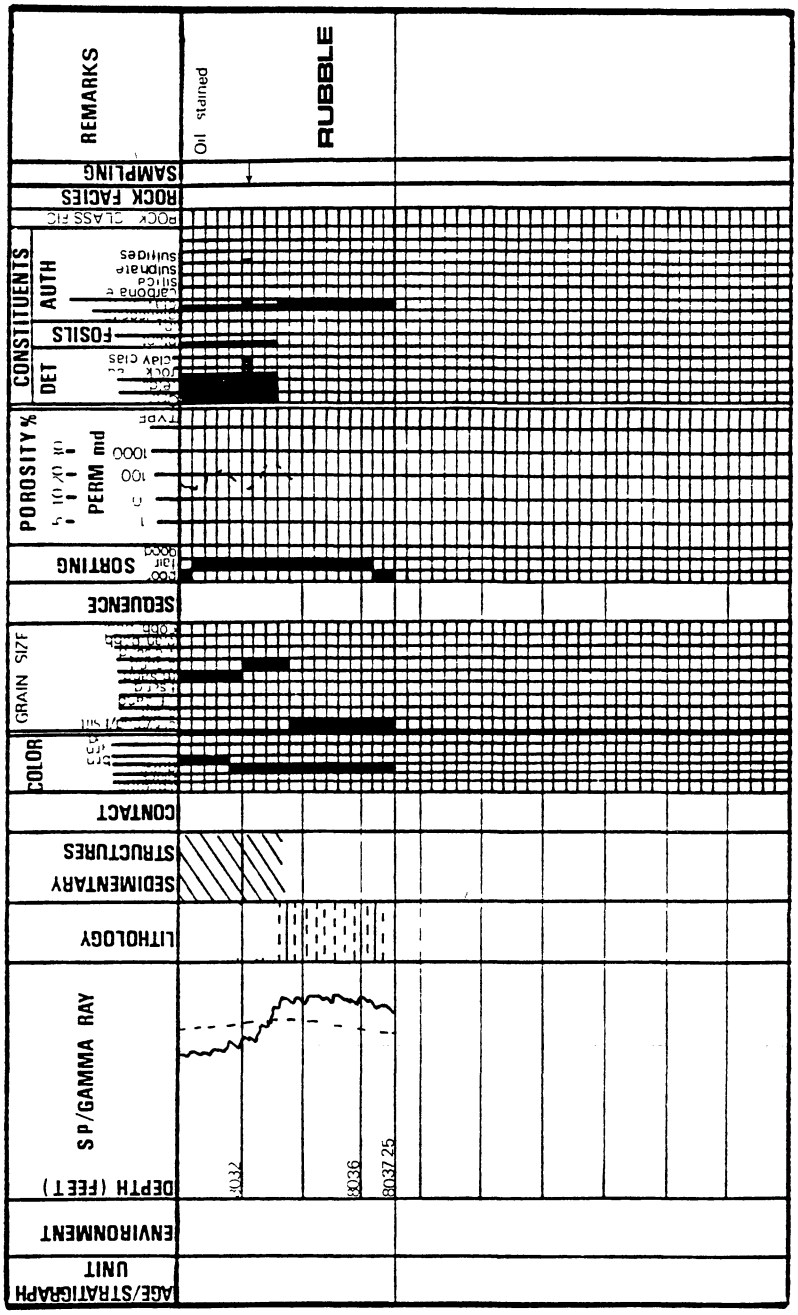

Figure 22. (Continued)

Stratigraphic unit: member C of Aradeiba Formation
Cored interval: 7496' - 7477.8' (Figure 23)

The cored interval consists predominantly of clean sandstone with occasional interbeds of rip-up clast conglomerate. The sandstone is black (where oil-stained), dark gray, gray, brown and greenish gray in color, medium to fine in grain size, cross-bedded except at the intervals 7494' - 9492.8' and 7492.8' - 7492' where it is massive and horizontally bedded respectively. The interval 7489' - 7487.6' contains elongated clay particles, randomly scattered throughout the sandstone. The size of the particles vary between few mm and 2.5 cm. Two thin beds of rip-up clast conglomerate made up of the same clay particles described above are found at 7489' and 7485.8'.

Well: Unity No. 11
Stratigraphic unit: member B of Aradeiba Formation
Cored interval: 7290.2' - 7267' (Figure 24).

The rock types making this interval are sandstone, siltstone, shaley sandstone, claystone and conglomerate. The interval between 7290.2' and 7287.5' consists of rippled sandstone, very fine, grading upwards into siltstone, light gray, and greenish gray in color. The interval 7287.5 - 7275.8' consists of pinkish brown, locally greenish gray, pinkish gray and dark gray

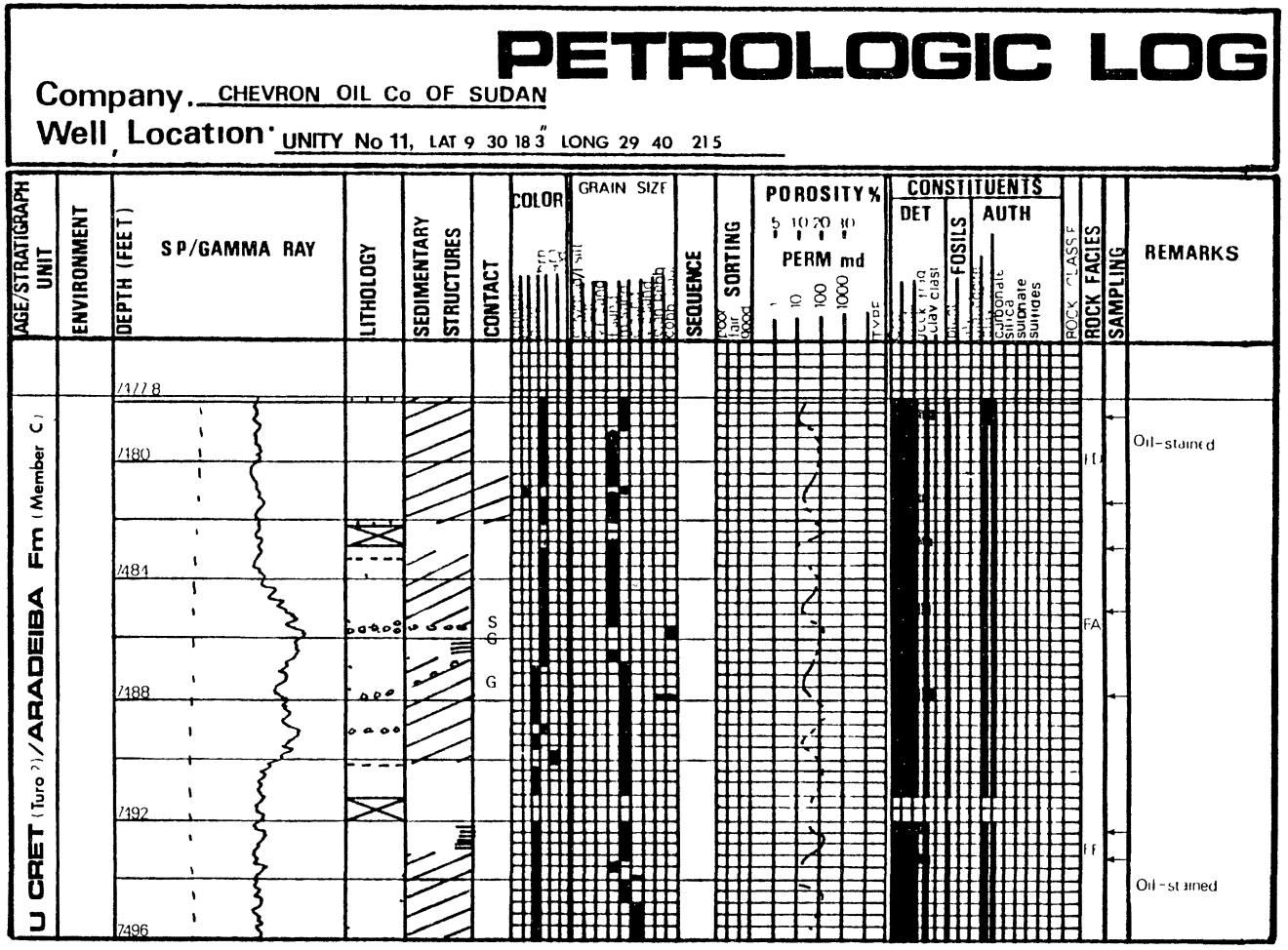

Figure 23. Petrolog of Aradeiba (C) Core, Unity No. 11.

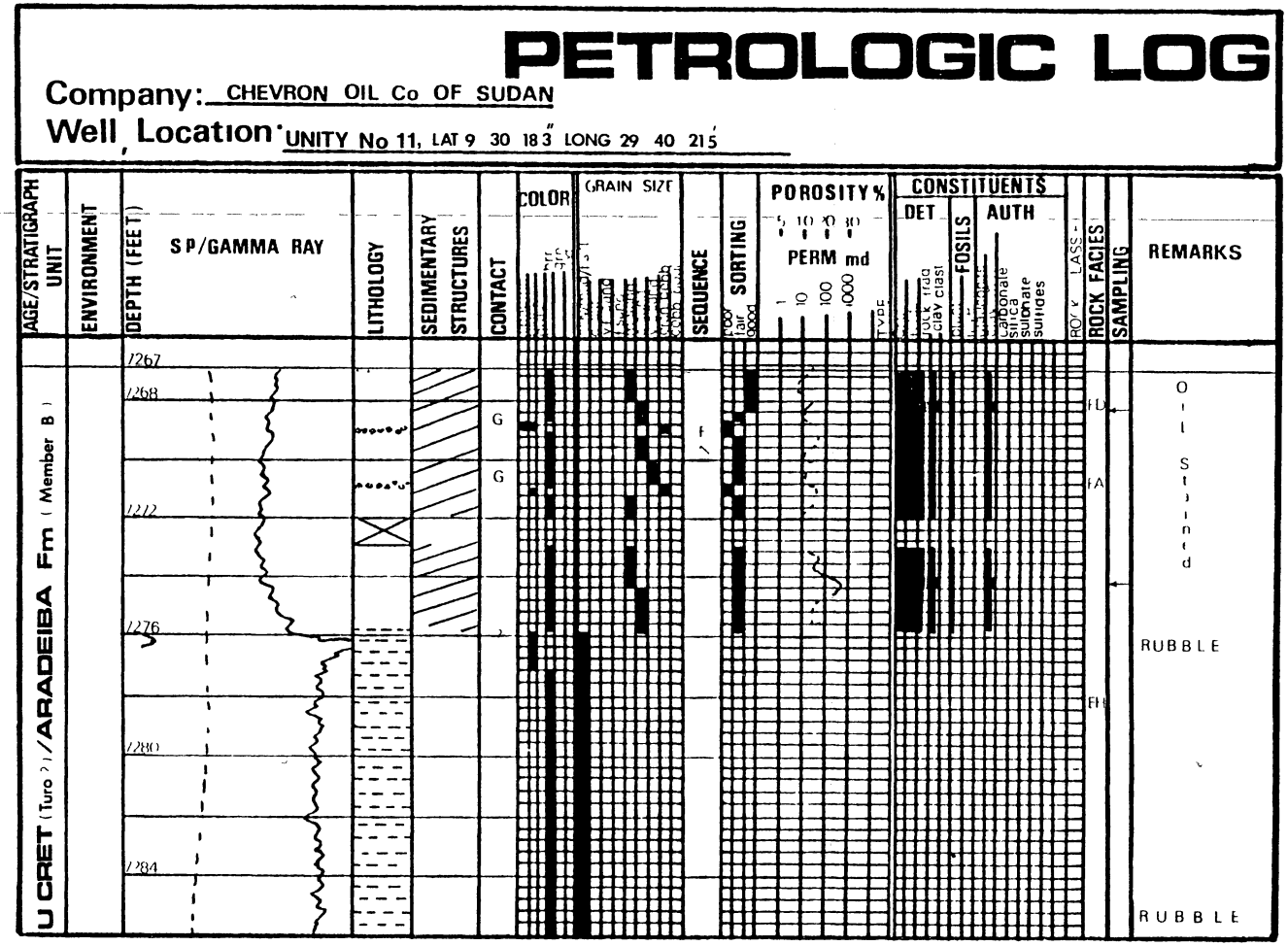

Figure 24. Petrolog of Aradeiba (B) Core, Unity No. 11.

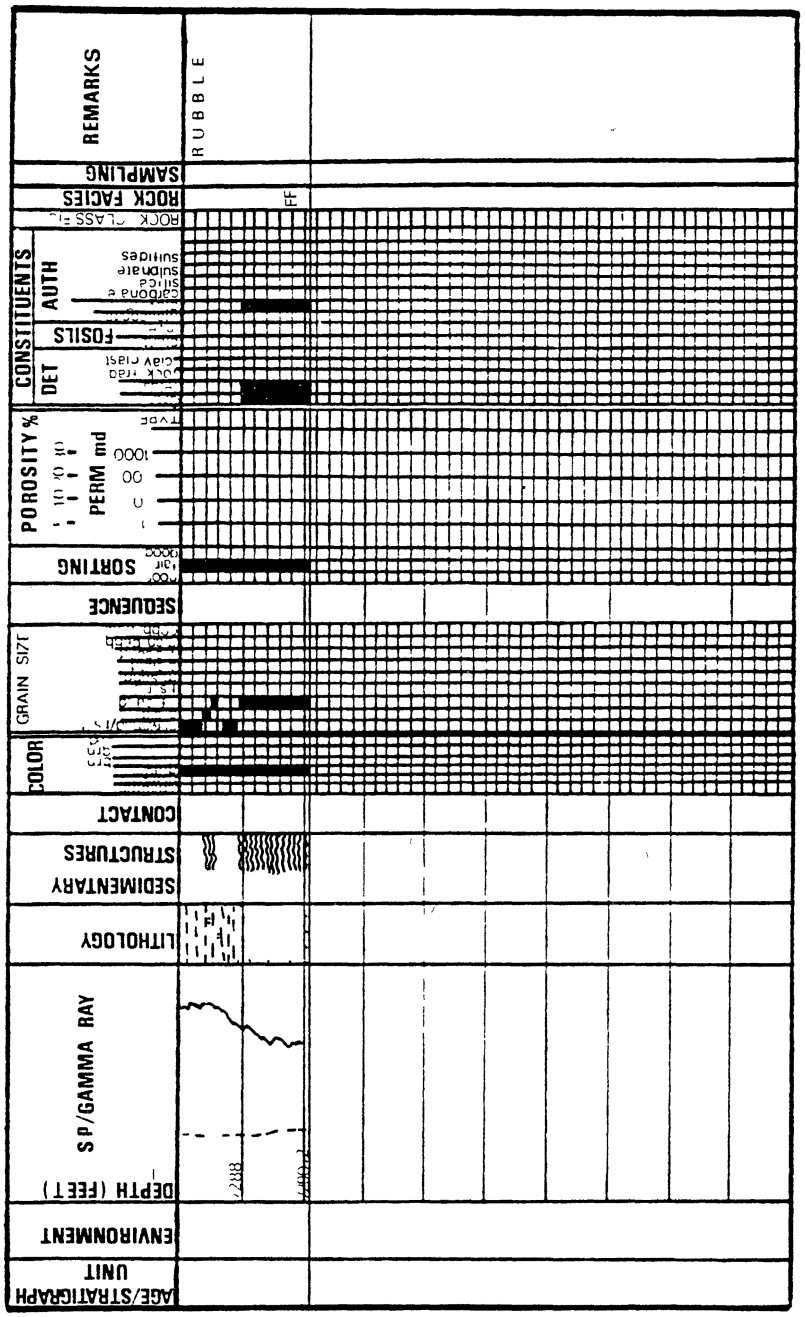

Figure 24. (Continued)

claystone. Locally silty, locally calcareous and the whole interval is recovered as rubble.

The uppermost part of the core 7275.8' - 7267' consists of clean sandstone, cross-bedded, locally massive, generally medium grained, locally very coarse and coarse gained. Two thin beds (2 to 3 cm thick) of rip-up-clast and quartz pebble conglomerate are observed at 7270.9' and 7369.3'. The shape of the quartz particles and the clay clasts is generally elliptical and their sizes vary between few mm and 2 cm.

Well: Unity No. 11
Stratigraphic unit: member A of Aradeiba Formation
Cored interval: 7080.65' - 7062' (Figure 25)

The cored interval of the Aradeiba A-member in this well consists of sandstone, silty claystone, interlaminated sandstone, and claystone.

The bottom part of the core (7080.65' - 7075') consists primarily of medium grained sandstone at the bottom grading to very fine sandstone at the top of the interval. The sedimentary structures include planar cross-bedding at the bottom (7080.65' - 7079.3'), horizontal bedding (7078.3' - 7078') and (7077.5' - 7076.4') and very small size ripple marks towards the top

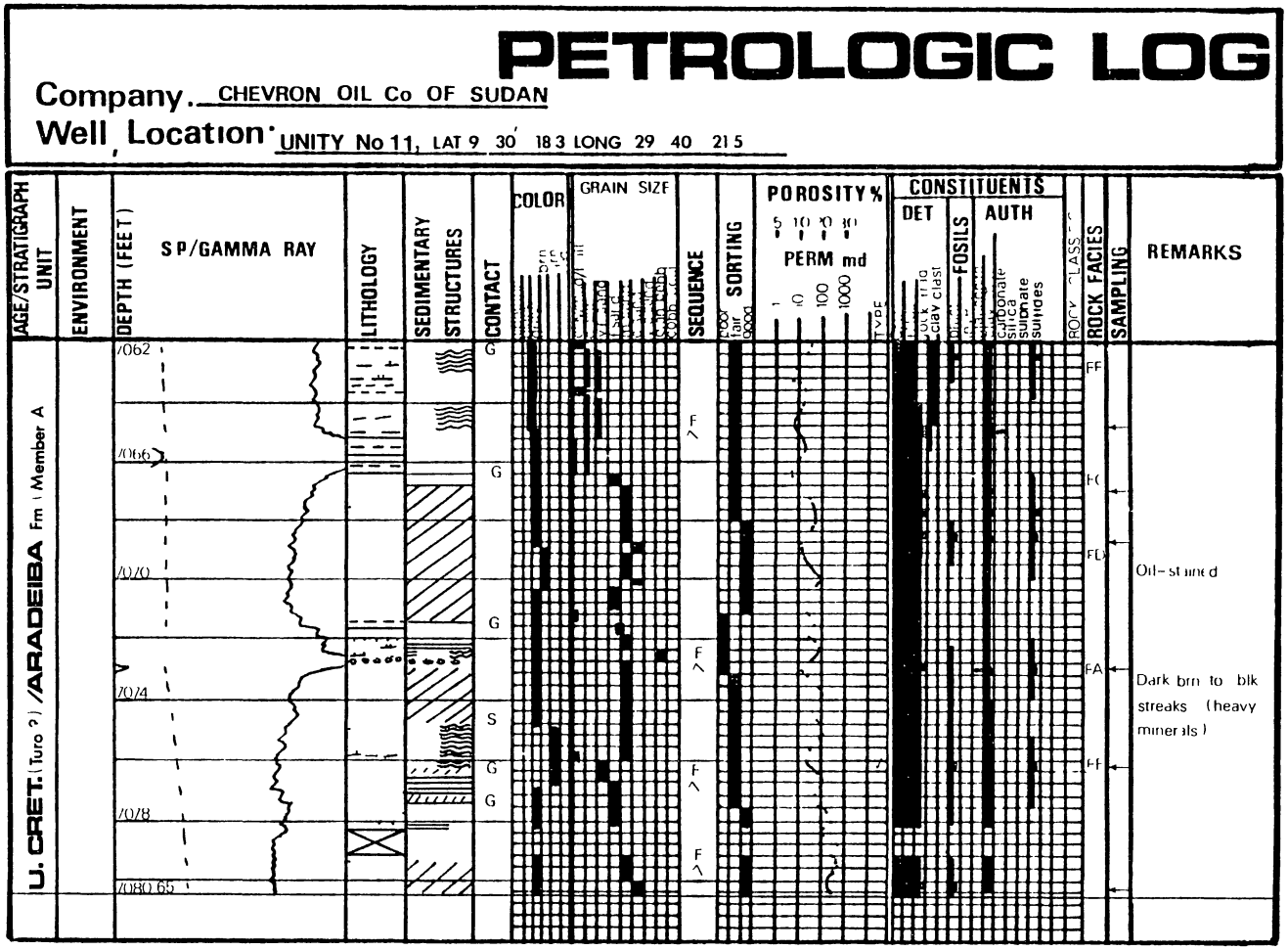

Figure 25. Petrolog of Aradeiba (A) Core, Unity No. 11.

of the interval. The sandstone is well to moderately sorted with gray, whitish gray and greenish gray colors. Very fine black streaks of heavy minerals are abundant at the bottom of the interval along the cross-bedding planes.

The interval 7075' - 7072.7' consists of coarse grained sandstone and grades upwards into medium and fine grained sandstone, cross-bedded, white brownish in color, locally with black and dark brown bands of heavy minerals. The uppermost interval of the core 7072.7' - 7062' consists of a conglomerate composed of elliptically shaped rip-up-clasts and quartz particles of size up to 2.5 cm. This bed is followed by an interval of cross-bedded sandstone, medium grained and interlaminated with shale. The interval 7071.8' - 7071.3' consists of a dark gray silty claystone that grades into very fine sandstone with occasional elongated rip-up-clasts. The interval 7071.3' - 7066.4' consists of sandstone varying in grain size from medium at the bottom to fine and very fine towards the top. Planar cross-bedding is the dominant sedimentary structure with some sections reflect massive and horizontal bedding structures. Oil staining is observed between 7070.3' and 7069.2'. The sandstone interval gradually changes into gray and dark gray siltstone, clayey siltstone and finally claystone towards the very top of the cored interval.

Well: Talih No. 2

Stratigraphic unit: member C of Aradeiba Formation

Cored interval: 8640' - 8627' (Figure 26)

The rock constituents of this interval of the Aradeiba C-member are claystone, conglomerate and sandstone. The bottom portion of the core 8640' - 8631.2' is made up mainly of pinkish brown claystone, locally light brown and greenish gray, locally slightly calcareous especially where greenish gray (8631.5'), and the entire interval is recovered as rubble. The uppermost part of the core 8631.2' - 8627' consists of cross-bedded sandstone, medium grained, light brown and gray in color, and generally well sorted. This interval is topped with a 6-cm thick bed of rip-up-clast conglomerate with elongated particles (a few mm to 3 cm in size) embodied in a ground mass of fine to very fine sandstone. The whole interval 8631.2' - 8627' reflects faint cross-bedding structures.

Well: Talih No. 2

Stratigraphic unit: member A of Aradeiba Formation

Cored interval: 8246' - 8228.1' (Figure 27)

This interval consists of conglomerate, sandstone, shaley sandstone and silty claystone. The interval 8246' - 8240.7' is composed predominantly of cross-bedded sandstone very coarse at the bottom changing into coarse, medium

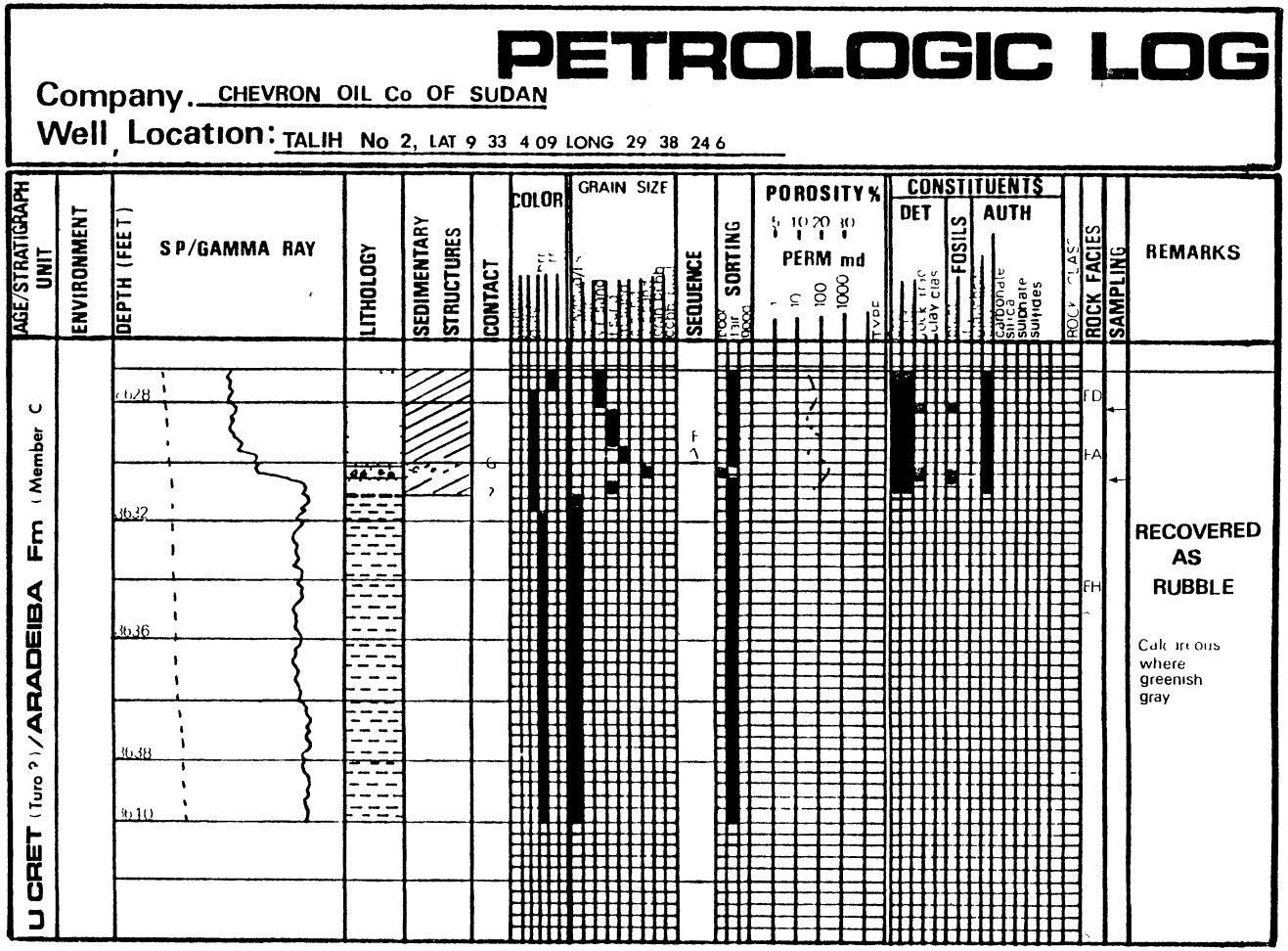

Figure 26. Petrolog of Aradeiba (C) Core, Talih No. 2.

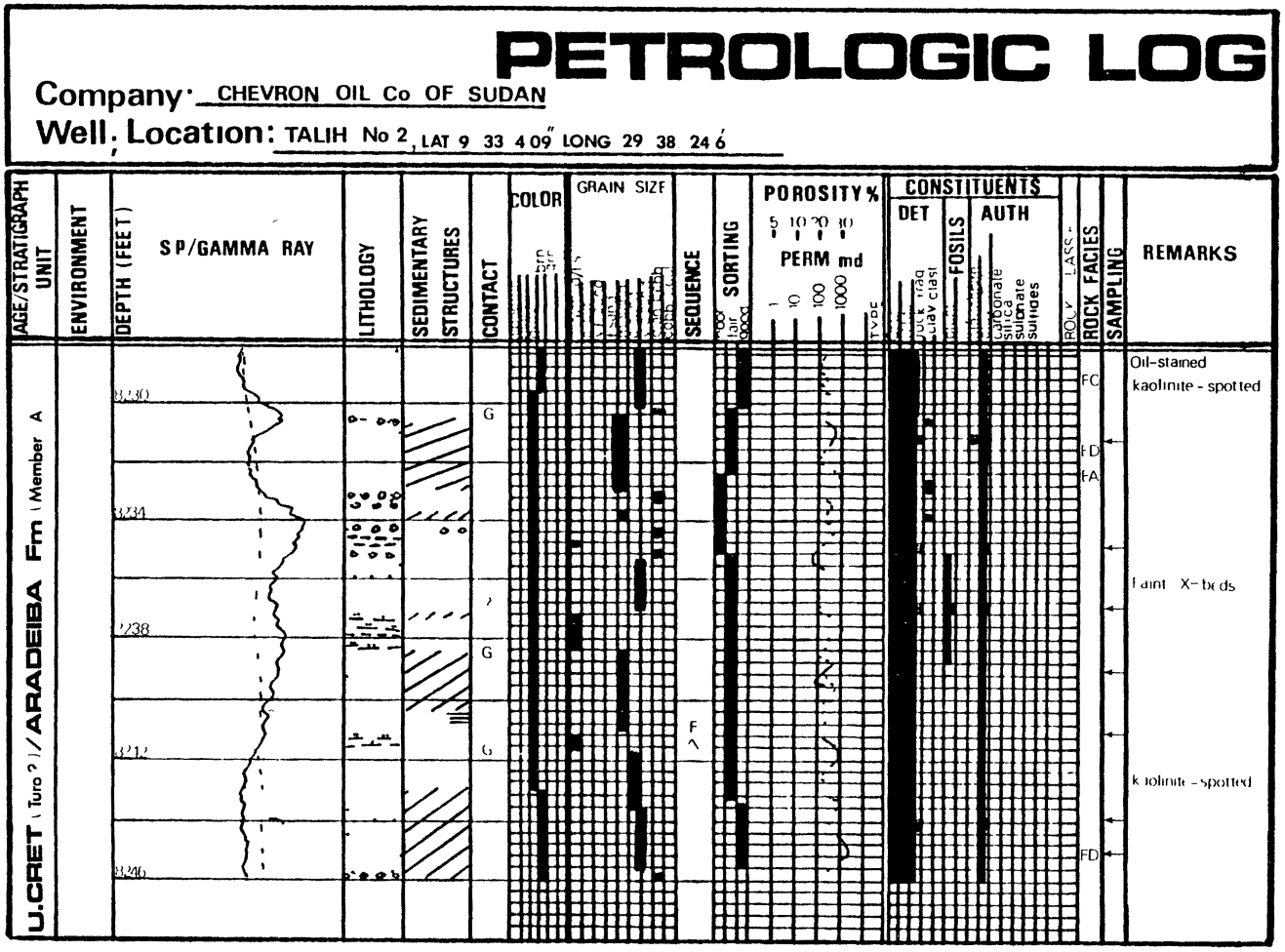

Figure 27. Petrolog of Aradeiba (A) Core, Talih No. 2.

grained upwards, and finally into a very fine shale interlaminated, horizontally bedded sandstone at the top. Colors include dark brown, (where stained with oil) whitish brown and gray. The cross-bedded sandstone is locally white-spotted due to abundance of kaolinite. The interval 8270.7' - 8237' consists mainly of medium grained kaolinitic sandstone that gradually grades into a silty claystone which changes upwards into a thin bed of dark gray claystone.

The rest of the cored interval 8237' - 8228.1' consists of medium grained, cross-bedded sandstone interbedded with thin (2-4 cm thick) beds of rip-up-clast conglomerate at 8234.4', 8233' and 9320.3'. The size of the clasts vary between a few mm and 3 cm with an elongate shape and generally oriented with the main direction of flow. The sandstone varies from very coarse, locally pebbly at the bottom to medium, kaolinitic at the middle part to very coarse, kaolinitic with faint plannar cross-bedding towards the top of the interval.

Lithotypes Description

The core samples of the Aradeiba Formation described above consist of eight different rock lithotypes. The sedimentary structures and the size of the grains are used as the prominent basis of classification with the variation

in color as a secondary measure especially in the claystones. The Lithotypes are named L-A through L-H. It should be noted that the energy level under which each lithotype was deposited is generally reflected by the grain size and the observed sedimentary structures. Therefore, an attempt is made here to describe the various lithotypes from bottom to top of a sequence..ls1

Lithotype L-A

Rip-Up-Clast Conglomerate (Figure 28). Gray, greenish gray to dark gray, locally with pinkish brown and pinkish gray mudstone clasts and rarely quartz particles. The size of the clasts vary from a few mm to 4 cm, elongated in shape, generally roughly stratified, locally massively deposited and embedded in a matrix of coarse to medium sandstone, very poorly sorted and locally pebbly. This facies is generally well cemented and locally very hard with calcareous cement. This facies is encountered mostly in the lower sand member C of the Aradeiba Formation.

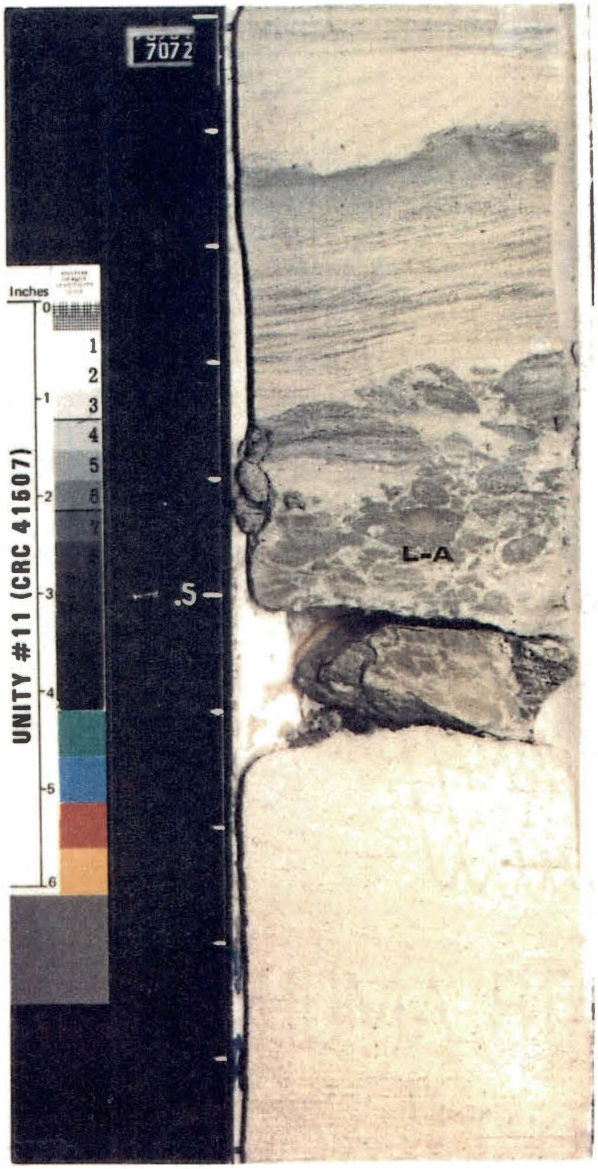

Figure 28. A Core Photograph showing Lithotype L-A.

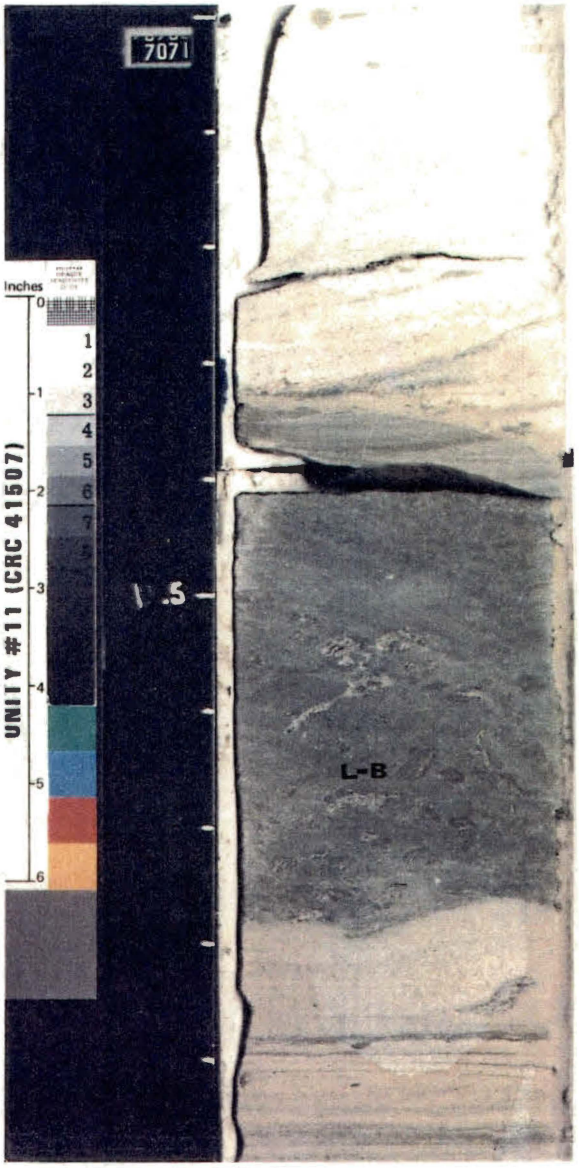

Figure 29. A Core Photograph showing Lithotype L-B.

Lithotype L-B

Sandstone with Mudstone Clasts (Figure 29). Light gray, greenish gray, light brown to dark brown, medium to fine sandstone. Elongated mudstone clasts are randomly scattered throughout, with pinkish gray to dark gray colors. The sandstone is fairly sorted, locally calcareous and locally exhibits faint plannar cross-bedding structures.

Lithotype L-C

Massive Sandstone (Figure 30, 31). This lithotype is composed of gray, greenish gray, dark gray and light brown massive sandstone, coarse to medium grained, locally fine, locally pebbly, fairly sorted to poorly sorted. It is encountered in all three members of the Aradeiba Formation.

Lithotype L-D

Cross-Bedded Sandstone (Figures 32, 33). Light gray, dark gray, brown to dark brown, greenish gray to yellowish gray, vary from medium to very fine in grain size, locally coarse and very coarse, poorly to moderately

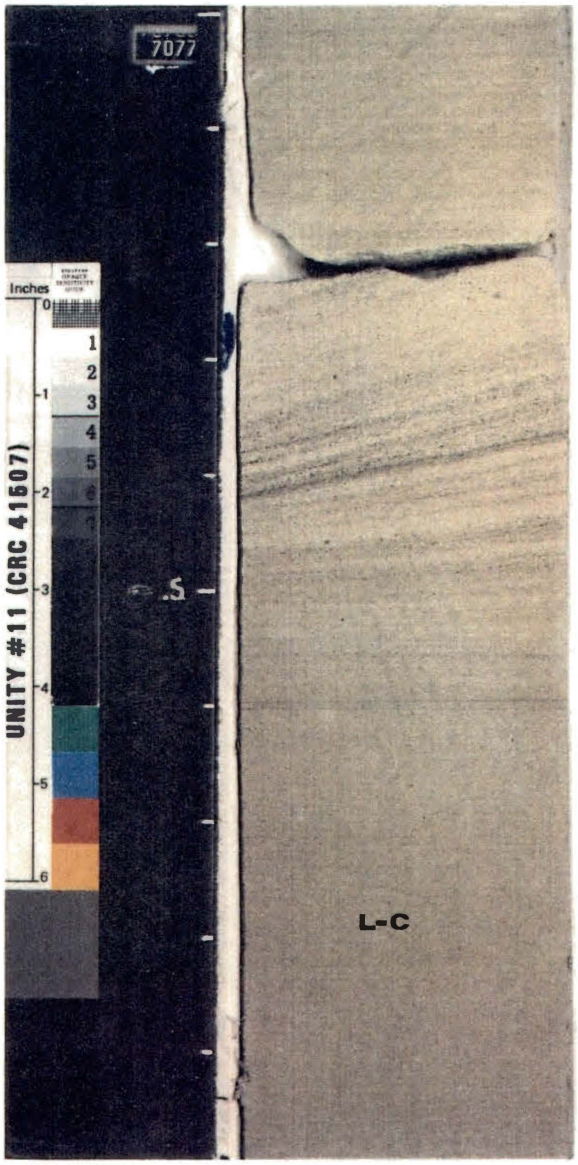

Figure 30. A Core Photograph showing the Massive Sandstone classified as Lithotype L-C.

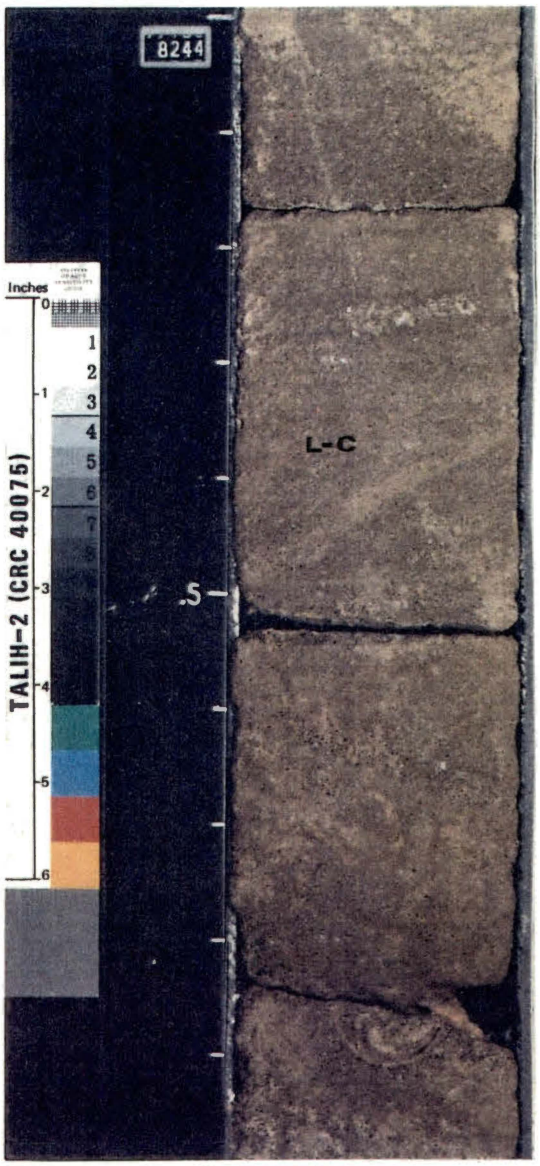

Figure 31. A Core Photograph showing Coarse to Medium Grained sample of Lithotype L-C.

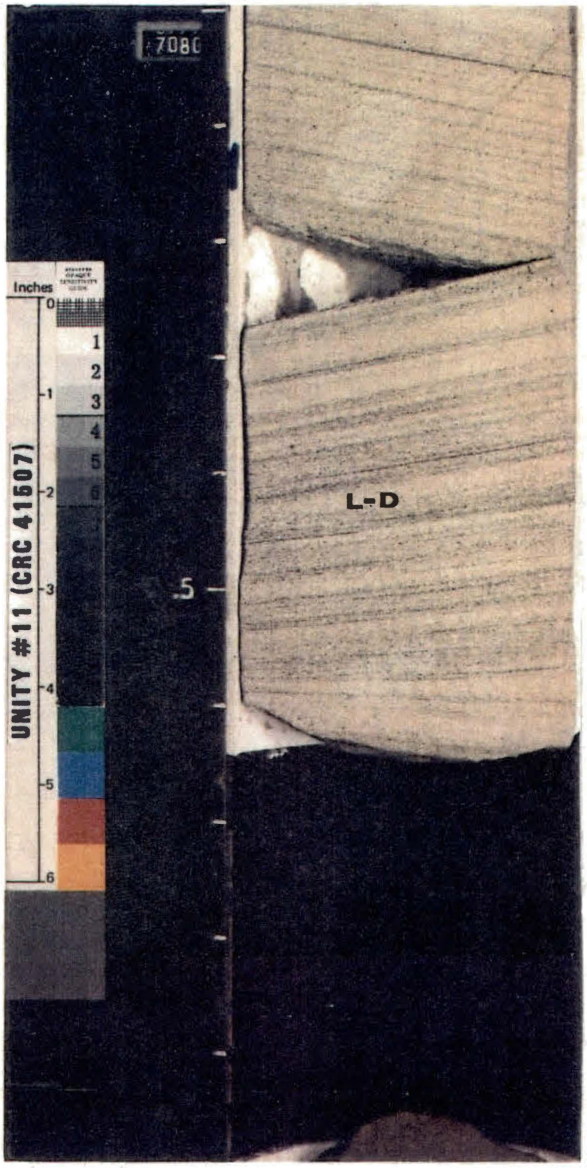

Figure 32. A Core Photograph the Low Angle Cross-stratification of Lithotype L-D.

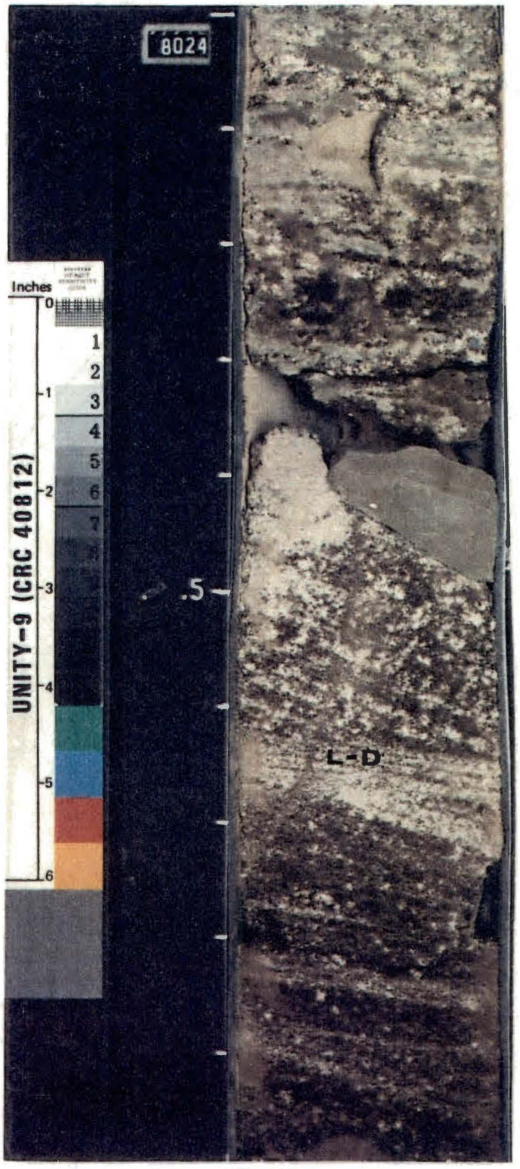

Figure 33. A Core Photograph showing Lithotype L-D with Kaolinitic Streaks.

sorted, planar cross-bedded with locally faint cross-bedding, locally kaolinitic with dark streaks of heavy minerals usually oriented with the cross-bedding planes, moderately cemented and locally calcareous.

Lithotype L-E

Horizontally Bedded Sandstone (Figure 34). Light gray, greenish gray, dark gray, light brown, fine and very fine grained. Occasionally medium, generally well sorted. Locally interlaminated and banded with streaks of heavy minerals, locally micaceous with calcareous cement.

Lithotype L-F

Rippled Sandstone (Figures 34, 35). Greenish gray, light to dark to very dark gray, generally fine grained, occasionally very fine, locally silty, locally shaley, fairly to poorly sorted with ripple mark structures, contains remnant fossil plants at random occurrences, locally micaceous and burrowed, locally bioturbated. The percentage of silt-size material is generally high in this lithotype.

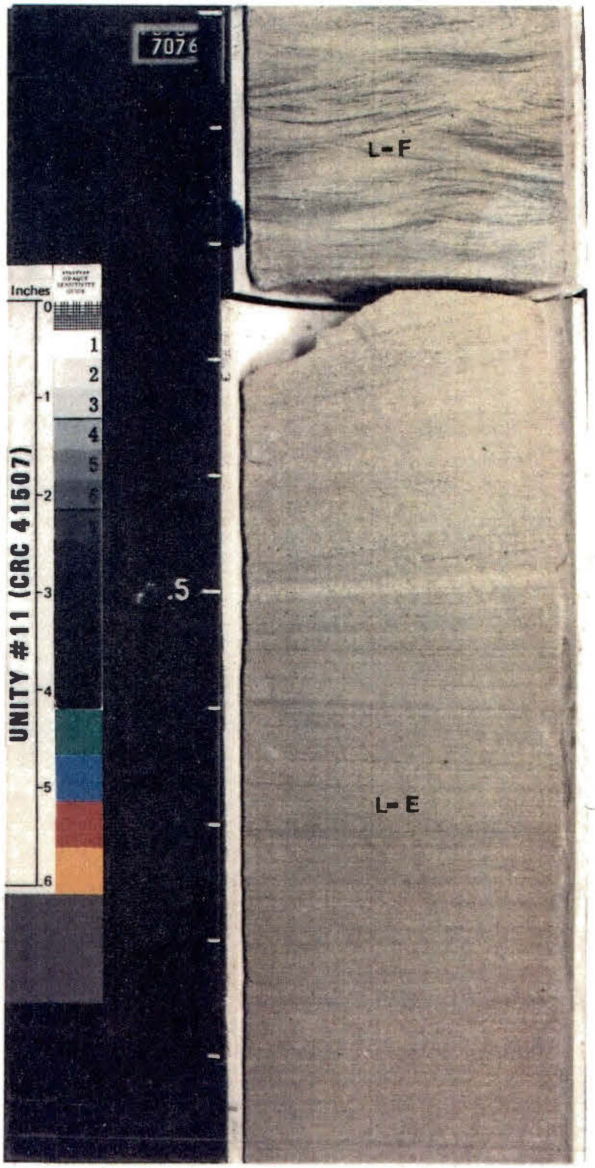

Figure 34. A Core Photograph showing Lithotype L-E and L-F.

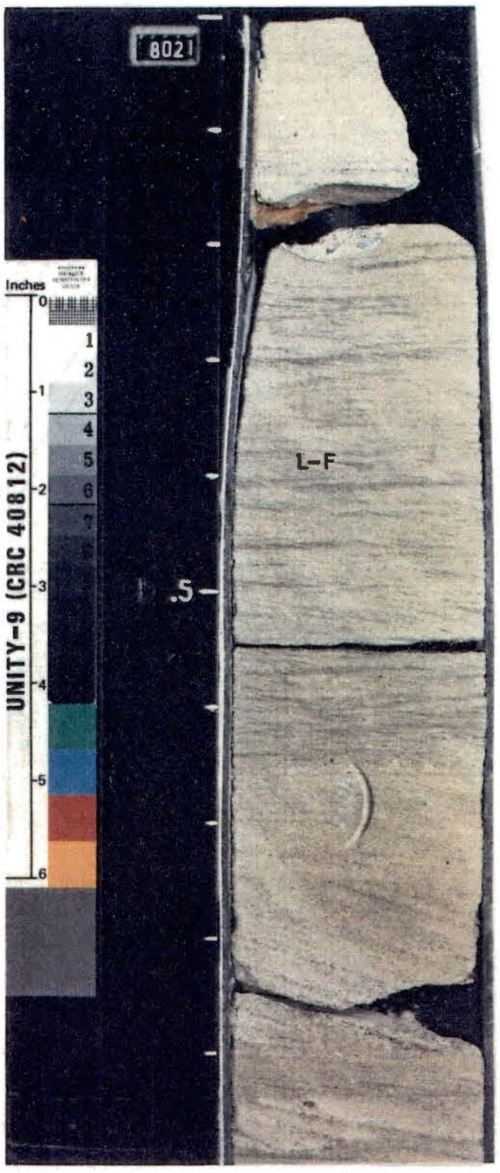

Figure 35. A Core Photograph showing Lithotype L-F.

Lithotype L-G

Claystone-G (Figure 36). Gray to very dark gray claystone, locally silty, locally with laminations of siltstone and very fine sandstone, generally bioturbated.

Lithotype L-H

Claystone-H. Pinkish, brown, reddish brown claystone, mostly silty and very rarely bioturbated.

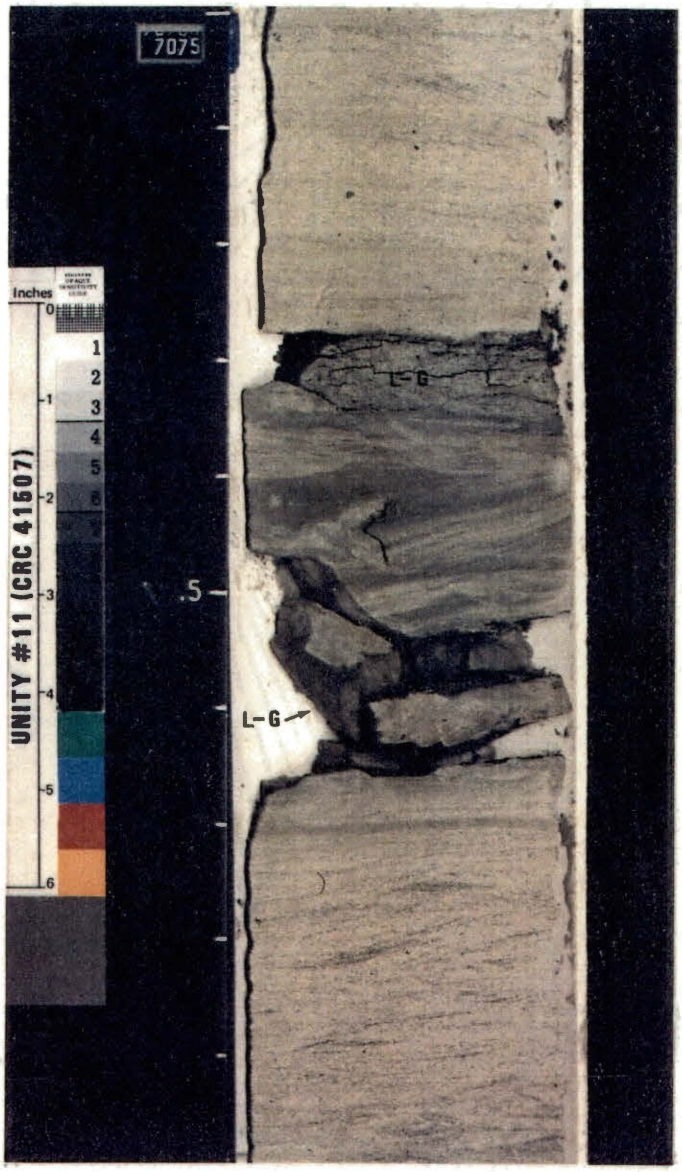

Figure 36. A Core Photograph showing Lithotype L-G.

CHAPTER V

PETROLOGY

Introduction

In this chapter a petrographic description of the constituent minerals of the Aradeiba sandstones is given. Table 1 shows the overall average compositional percentage of each mineral in the rocks of the Aradeiba Formation. Detailed accounts from point counts for each individual thin section are given in Appendix A. Ternary diagrams plotted for each sandstone member C, B and A, based on Quartz-Feldspar-Rock Fragments as end members are shown as Figures 37, 38 and 39. Eleven samples of the Aradeiba C-member plot as subarkose, one sample as arkose and two samples as lithic arkose. All the B-member samples plot as subarkose. Twenty of the thin sections from the A-member plot as subarkose, two samples fall in the arkose segment, and two samples in the lithic arkose domain of the Ternary diagram adopted from Folk's (1968) sandstone classification.

Table I. Net Averages of Constituent Minerals From all Thin Sections.

	ARADEIBA (C) AVG. (%)	ARADEIBA (B) AVG. (%)	ARADEIBA (A) AVG. (%)	NET AVG
DETRITAL CONSTITUENTS	76.40	72.00	67.10	71.80
Quartz	53.90	46.70	52.70	51.10
Monocrystalline	52.80	46.30	51.80	50.30
Polycrystalline	0.80	0.40	0.90	0.70
Feldspar	11.00	5.30	5.40	7.20
K-Feldspar	9.00	4.17	4.62	5.93
Plagioclase	2.00	1.13	0.78	1.30
Rock Fragments	3.80	4.70	2.92	3.80
Chert	0.30	0.30	0.02	0.20
Siltstone	0.40	0.67	0.70	0.59
Claystone	1.40	2.00	1.04	1.48
Metamorphic	1.70	1.73	1.16	1.53
Other Grains	2.70	1.67	3.56	2.60
Muscovite	0.40	0.17	0.52	0.36
Biotite	0.90	0.50	1.09	0.83
Garnet	0.50	0.17	0.92	0.53
Chlorite	0.10	0.20	0.12	0.14
Zircon	0.10	0.00	0.12	0.07
Tourmaline	0.10	0.18	0.32	0.20
Plant Material	0.60	0.50	0.47	0.50
Matrix	5.30	13.67	4.40	7.80
Clay Clasts	5.00	12.67	3.04	6.90
Chlorite	0.10	0.20	0.16	0.15
Silt	0.20	0.80	1.20	0.73
DIAGENETIC CONSTITUENTS	10.30	12.50	12.44	11.75
Cements	3.50	1.50	2.10	2.37
Silica	0.20	1.00	0.20	0.47
Feldspar	0.20	0.040	0.08	0.07
Calcite	3.10	0.30	1.08	1.49
Pyrite	0.10	0.16	0.64	0.30
Authegenic Clays	6.80	11.00	10.34	9.38
Kaolinite	3.40	8.67	4.04	5.37
Smectite	1.60	0.67	4.08	2.12
Illite	0.80	1.10	0.88	0.93
Chlorite	1.00	0.37	0.96	0.78
Porosity	12.30	15.50	17.70	15.17
Primary	6.10	12.50	10.90	9.80
Secondary	7.20	3.00	6.80	5.67

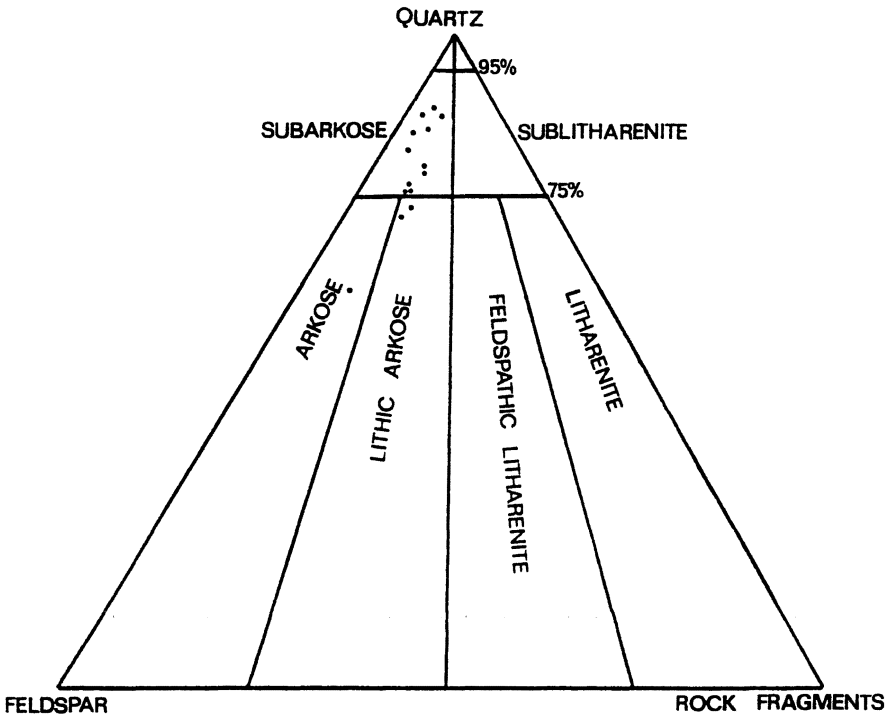

Figure 37. QRF Diagram Plot of Thin-section Compositions from all Core Samples of the Aradeiba Formation C-Member.

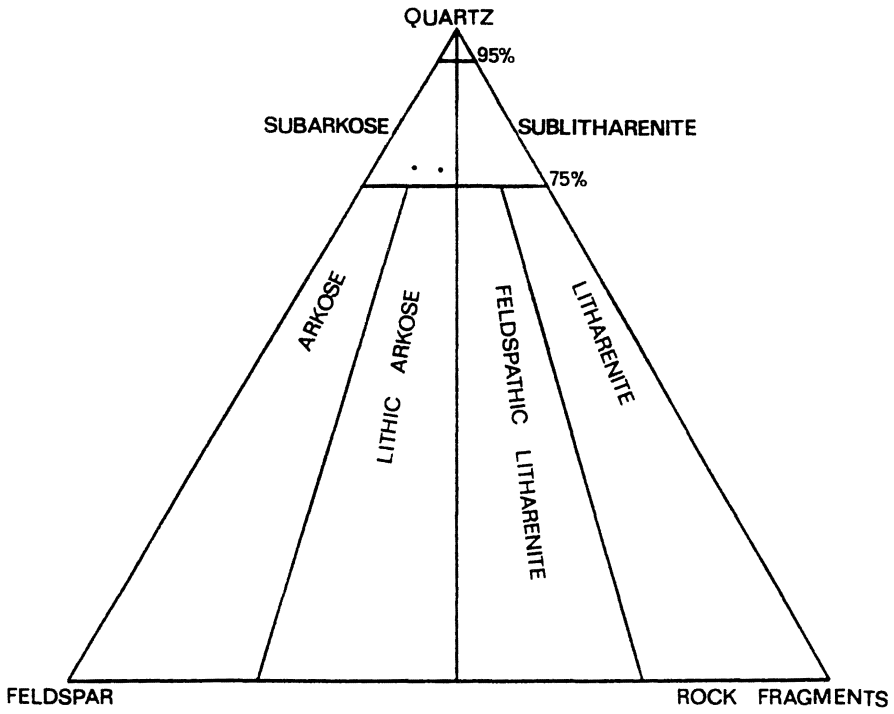

Figure 38. QRF Diagram Plot of Thin-section Composition from all Core Samples of the Aradeiba Formation B-Member.

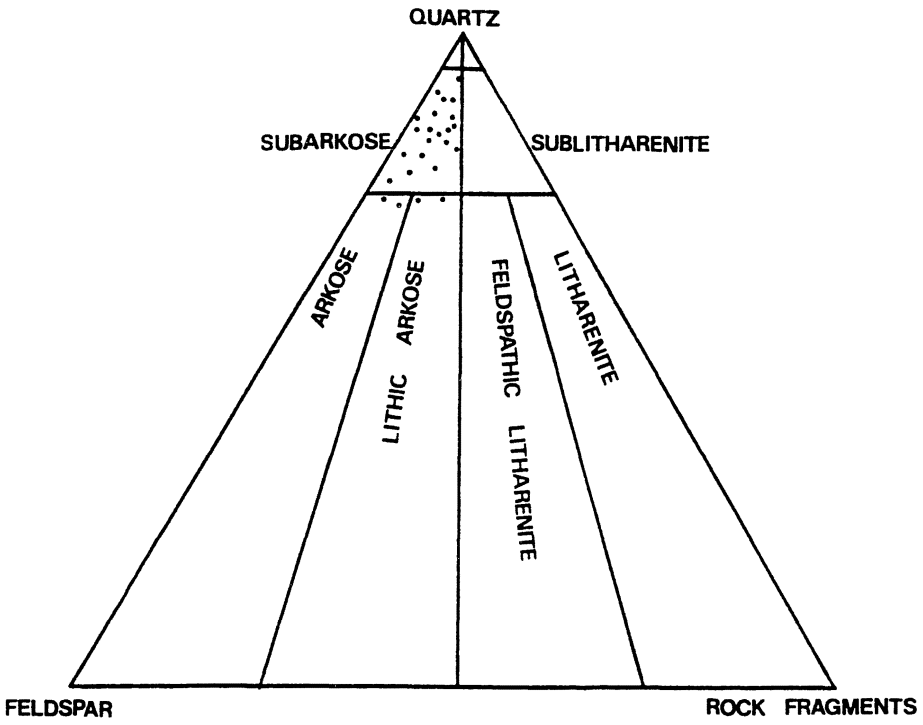

Figure 39. QRF Diagram Plot of Thin-section Composition from all Core Samples of the Aradeiba Formation A-Member.

Detrital Constituents

Quartz

Quartz is the dominant mineral constituent of the rocks of the Aradeiba Formation. Its compositional percentage ranges between 16% and 70% with an overall average of 51% for all the samples studied. However the percentages vary between 34% and 68% for the C-sandstone member averaging 54% as compared to 37% - 56%; 47% and 16%-70%; 53% for the B- and the A-sandstone members respectively. Monocrystalline grains constitute the predominant quartz type, generally with straight extinction with some varieties exhibiting strain-caused undulose extinction. The surfaces of the grains are specifically clean in the samples of the C-member as compared to those of the A-member, where individual samples contain quartz grains that show abundant vacules and inclusions. Polycrystalline quartz grains exist in trace to 2% amounts, often with distinct crenulated boundaries. Corrosion is very noticeable, especially in the C-sandstone samples giving the quartz grains a distinct crescent shape in most cases. The grain size varies from very coarse (1.9 mm) to very fine (0.065 mm)

with silt-sized grains (0.03 - 0.05 mm) composing the bulk of most samples specially in the upper members B and A. The shape of the grains is generally subangular to subrounded (Figure 40) with more roundness observed in the finer grains of the A-member samples.

Feldspar

The feldspars occur as a main constituent in all samples. However feldspar grains are more abundant in the sands of Aradeıba C with a range of 7% - 21% and an average of 11% compared to the B and A members with percentage ranges of 6% - 10%; 2% - 8% and averages of 5% and 5% respectively. The average feldspar compositional percentage for the Aradeiba Formation as a whole is 7%. Microcline (Figure 41), recognized by its cross-hatched twining and orthoclase (Figure 42)are the dominant alkali-feldspars. The microcline crystals are generally tabular with varyıng degrees of alteration to sericite and clay minerals. Plagioclase feldspars (Figure 43) reflecting the albite-twining are generally more altered, mostly with a cloudy appearance specifically in the sands of the Aradeiba C member. The alteration of the plagioclase feldspar ıs usually concentrated along

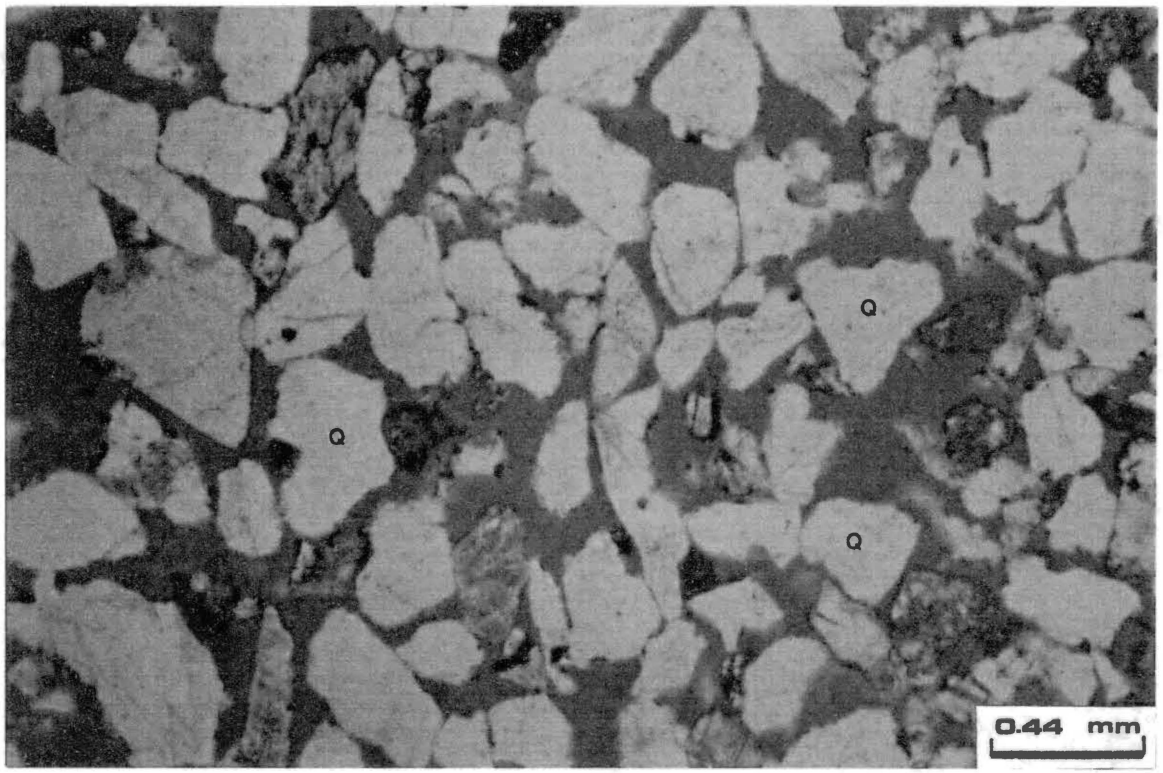

Figure 40. A Microphotograph showing Subangular to Subrounded Quartz Grains (Q); Plane Polarized.

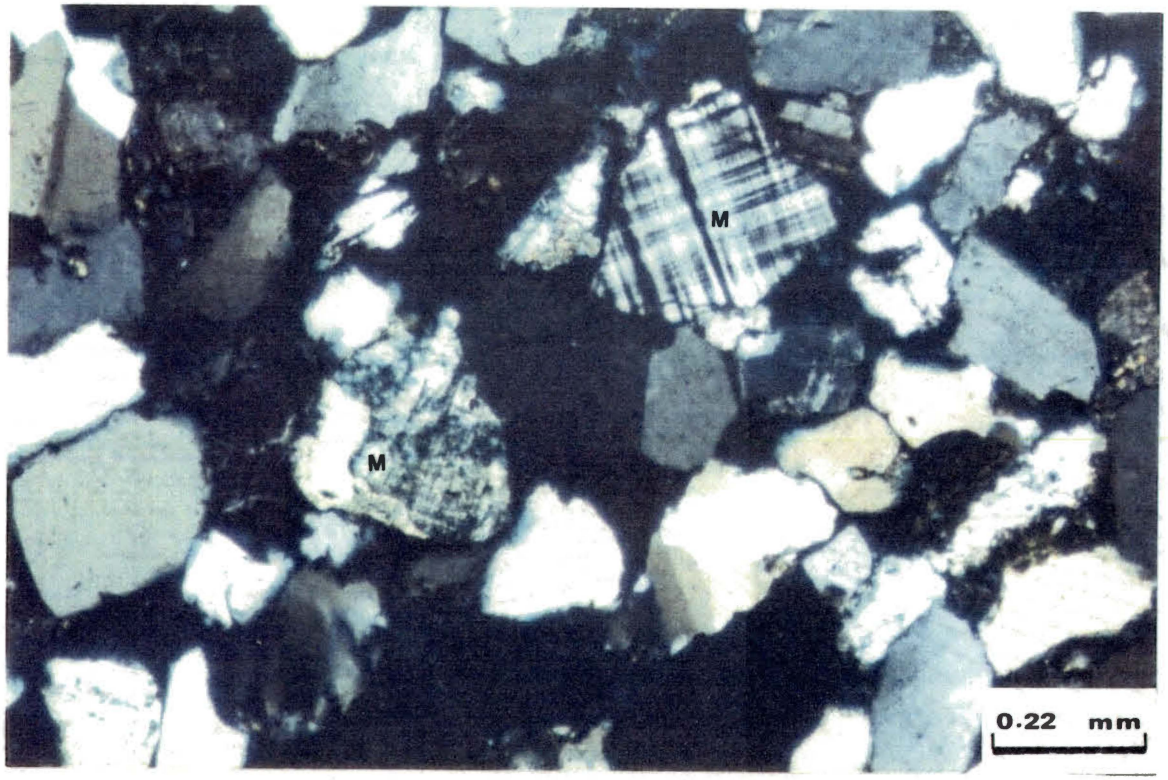

Figure 41. A Microphotograph showing Two Microcline (M) Grains, One is Altered and the Other One Reflects Typical Cross-hatched Twinning; Cross-polarized.

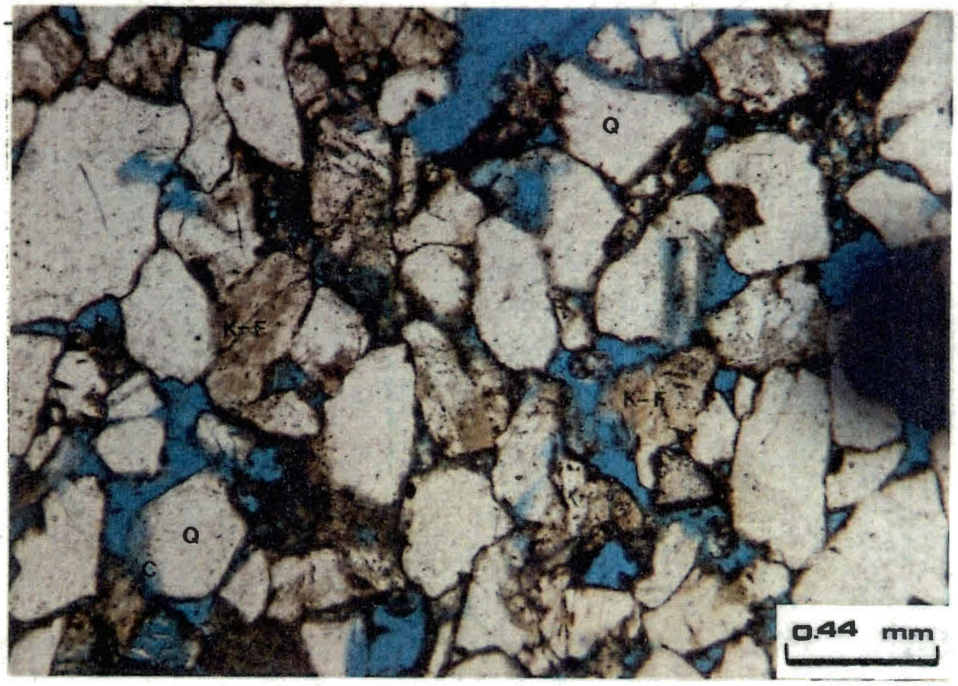

Figure 42. A Microphotograph showing several Grains of K-Feldspar (K-F) Stained Brownish by Sodium Cobaltinitrite. (Q) designates Quartz Grains, Notice the Corrosion (C); Plane Polarized.

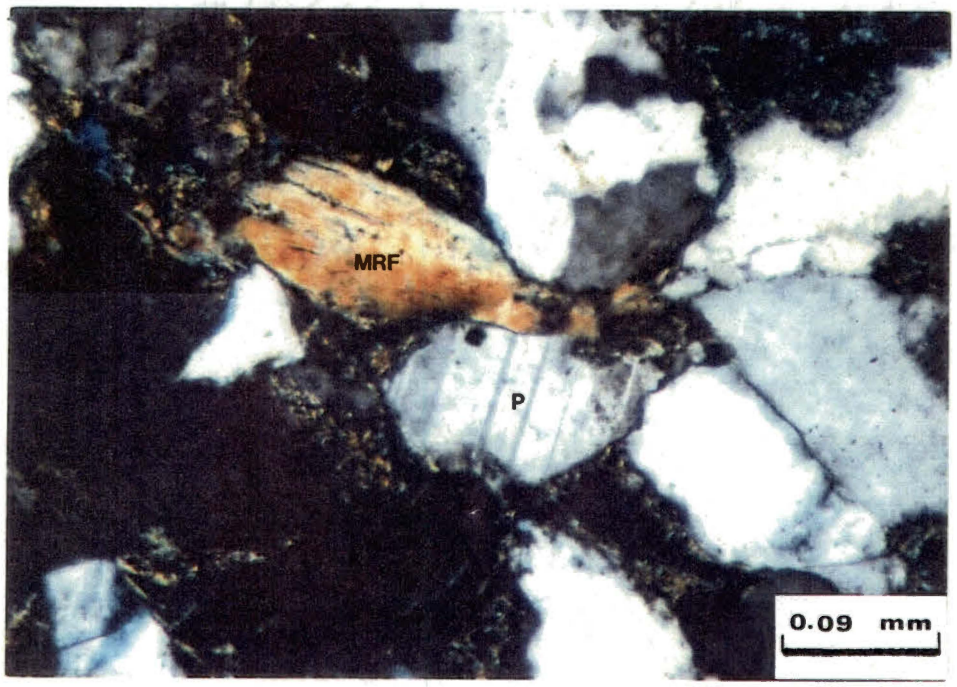

Figure 43. A Microphotograph showing a Plagioclase Grain (P) with the Characteristic Albite Twinning. (MRF): Metamorphic Rock Fragment; Cross-polarized.

individual twin lamelae or locally in the core of the grains. Partial and complete dissolution of the feldspar grains is common in all samples (Figure 44). The grain size varies from medium to very fine with the grains generally having subangular forms.

Rock Fragments

Two types of rock fragments were recognized, sedimentary and metamorphic. The former includes chert, siltstone and claystone. The metamorphic rock fragments include schist, high-birefringence gneiss with stretched quartz crystals and crenulated polycrystalline quartz particles. The percentage of rock fragments is observed to be uniform in the three sandstone members and it falls in the range of trace to 7% and averages 3.8% for the Aradeiba Formation in total.

a. Chert

It is present in trace amounts in the Aradeiba Formation. The chert fragments are composed of a very uniform microcrystalline quartz, generally reflecting low birefringence. The size of the fragments vary between medium and very fine, and they are mostly slightly elongated and sub-rounded in shape.

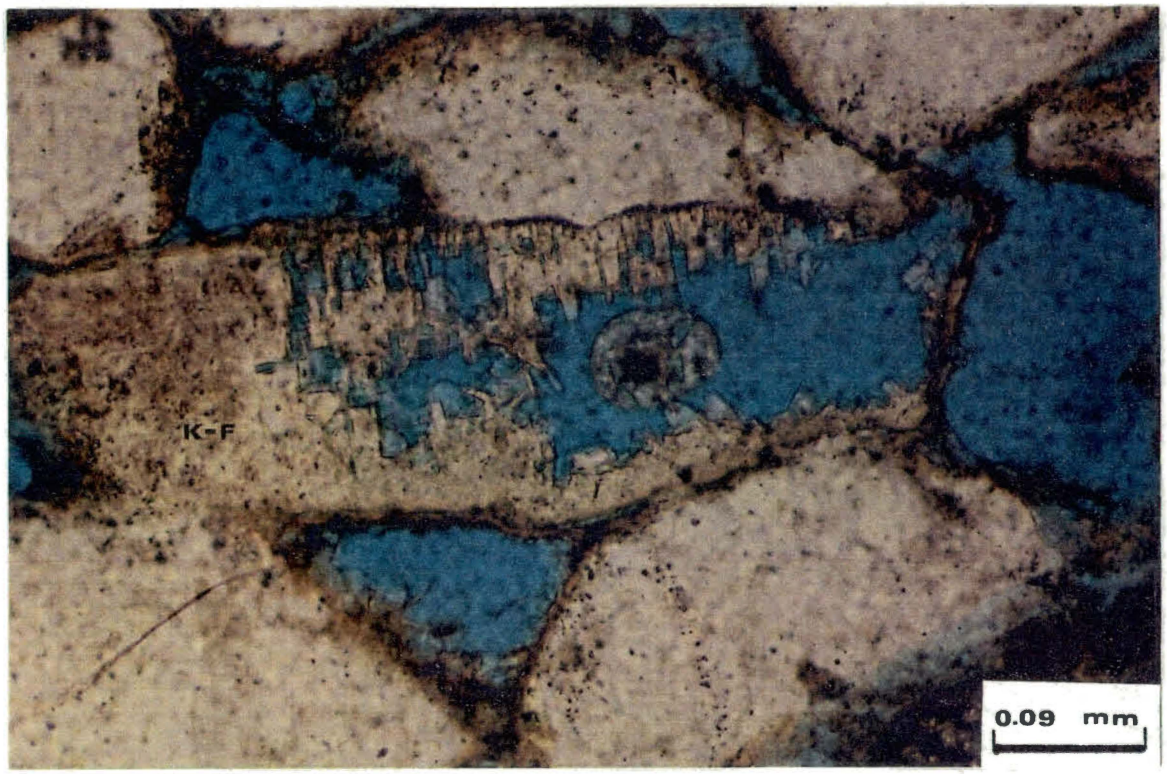

Figure 44. A Microphotograph from the Aradeiba C-Member illustrating Partial and Complete Dissolution of Feldspar (K-F) Grains; Plane Polarized.

b. Siltstone

Siltstone rock fragments generally occur in trace amounts and can make up to 1% in many samples. They occur as irregularly-shaped bodies that vary in size between 0.3 and 0.6 mm and mostly with angular to subangular forms. The fragments are composed of silt-sized quartz grains, generally embedded in a clayey matrix.

c. Claystone

These are the most abundant sedimentary rock fragments ranging in percentage between trace and 4% in the rocks of the Aradeiba Formation. The particles are generally deformed, locally squeezed between more brittle framework grains. The constituent clay minerals are particularly very finely crystalline with illite (high birefringent) as the dominant type.

d. Schist

Schist rock fragments exist in trace amounts in various samples. The fragments exhibit elongate shapes and usually deformed with strong crystal orientation. Muscovite is a dominant constituent in most occurrences, causing the particles to have a moderately high birefringence. (Figure 45).

e. Gneiss

These fragments are of larger sizes as compared to

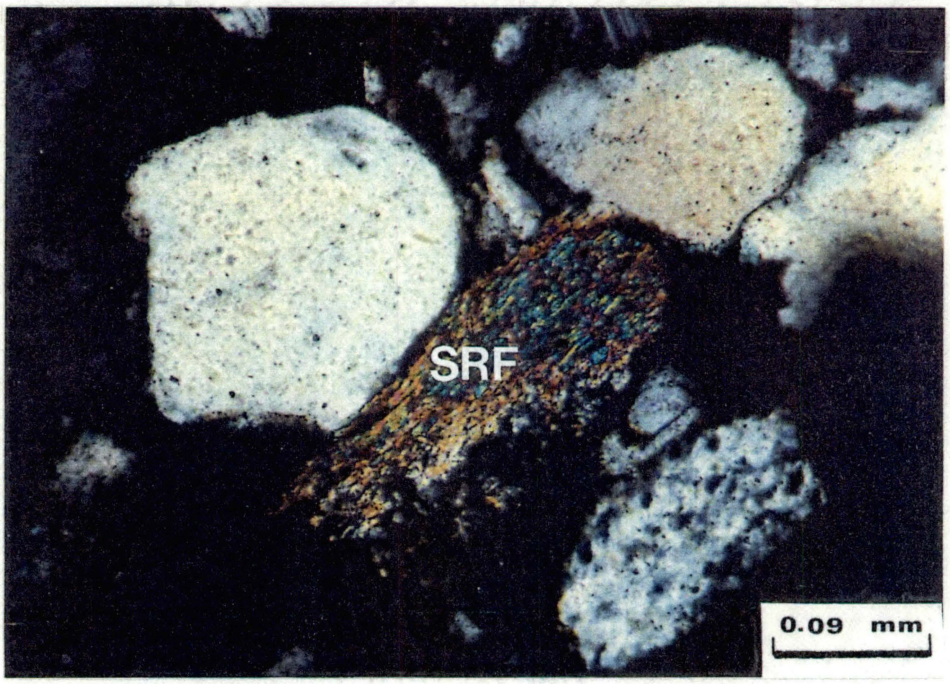

Figure 45. A Microphotograph showing a Schist Rock Fragment (SRF), the Interference Colors are caused by the Abundance of Muscovite; Cross Polarized.

the schist fragments and generally with subrounded and tabular shapes. They are composed mainly of "stretched", generally equant, uniformly-spread quartz crystals (Figure 46). The quartz crystals are often crenulate in shape and noticeably welded together. The gneiss fragments occur in trace amounts.

f. Metamorphic Quartz Fragments

Polycrystalline quartz fragments are classified here as rock fragments of metamorphic origin. There are two types, the first consist of numerous crenulate quartz crystals, highly sutured and welded together (Figure 47). The second type consists of normal quartz crystals in a polycrystalline fashion which is, in many cases, optically uniform. The size of the fragments vary considerably from a few mm to 2.0 cm.

Mica

Mica comprises trace to 6% and averages 1.2%, and is usually found as flakes or tablets with irregular outlines. The sizes of the micaceous flakes vary between 1.5 mm and 0.2 mm and average 0.3 mm. Both muscovite and biotite varieties are present (Figure 48). The biotite is generally intergrown with chlorite, showing strong

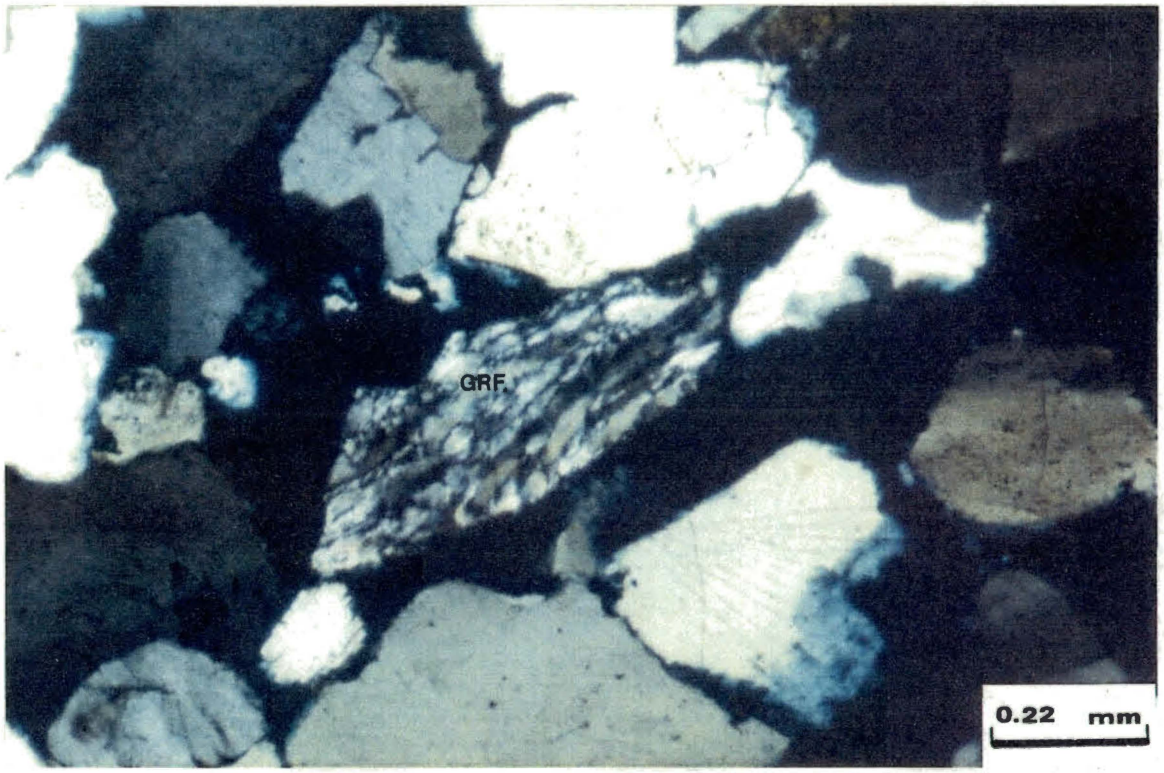

Figure 46. A Microphotograph showing a Gneiss Rock Fragment (GRF). Notice the Stretched Quartz Crystals; Cross Polarized.

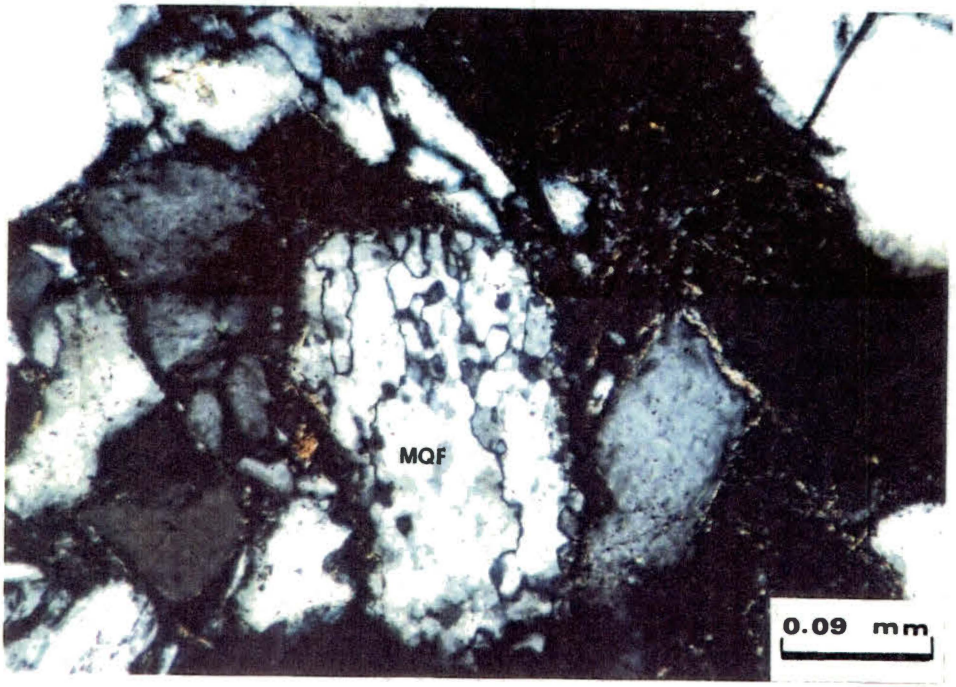

Figure 47. A Microphotograph showing a Metamorphic Quartz Fragment (MQF). The Quartz Crystals are Highly Sutured and Welded; Cross-polarized.

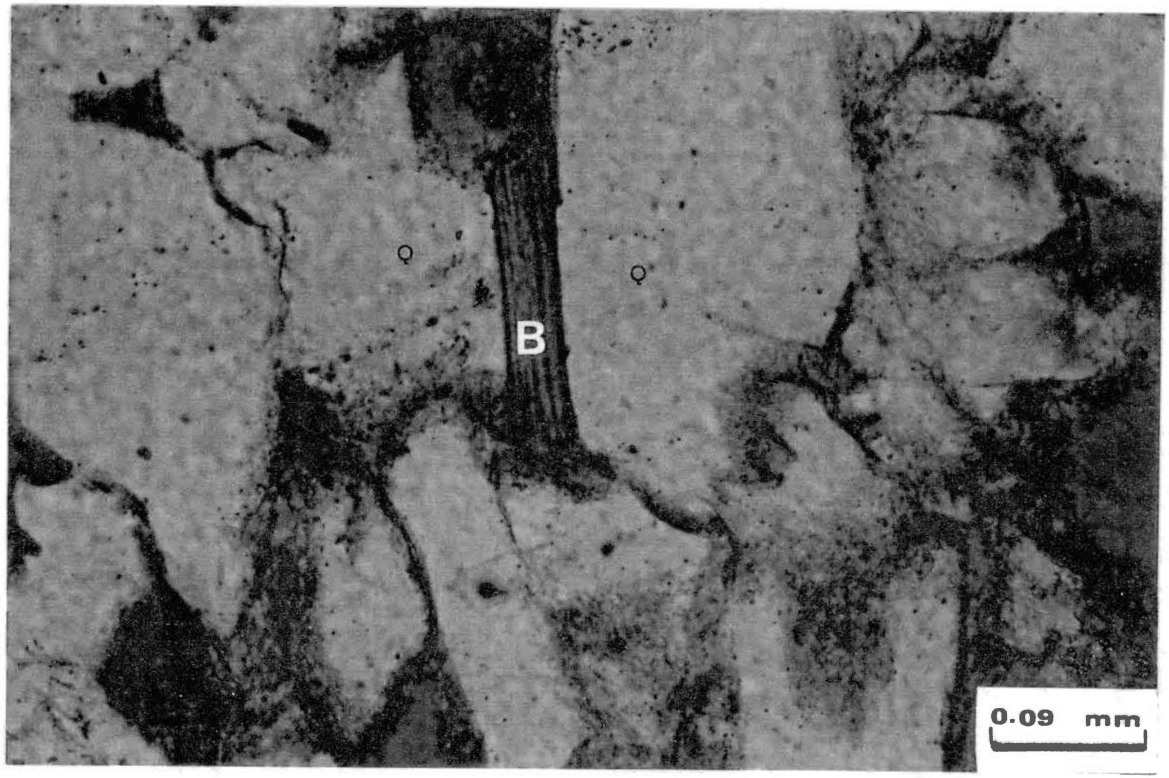

Figure 48. A Microphotograph showing an Illitized Biotite Grain (B) aligned between two Quartz Grains (Q); Plane Polarized.

pleochroism with greenish brown to dark brown colors. This variety is remarkably common in the fine sands of the Aradeiba A-member. The grains are generally bent and oriented due to compaction. Pale pleochroic halos are common where small grains of zircon are enclosed within the mica grains. Close to extinction a mottled appearance is very commonly observed, especially within the chloritized varieties, which are commonly squeezed in between more brittle grains of other detrital constituents.

Fossil Fragments

The only fossils found in the rocks of the Aradeiba Formation are generally trace amounts of plant material. These are present in every sample of the Aradeiba C-member with amounts of up to 1% in individual samples. Much less abundant, they have been recorded in the fine sands of the upper members.

Detrital Matrix

Illite and chlorite are the main constituent-clay minerals of the detrital clayey matrix in the sandstones of the Aradeiba Formation. The clayey matrix is commonly

abundant in the upper finer sands as compared to the C-sand member. Detrital matrix, composed of silt or mixed silt and clay is also observed, and in most cases uniformly spread throughout the samples of the A and B members. However, they are less common and exist in a patchy, localized fashion in the C-member samples. The percentage of the detrital matrix vary between trace and 35% for the sandstones of the Aradeıba Formation, with an overall average of 7.8%.

Heavy Minerals

Garnet ıs the most abundant mineral of this group. Its compositıonal percentage ranges between trace and 2.7% and the overall average is 0.53%. The garnet grains commonly appear as subhedral and less commonly as euhedral, with an average grain size of 0.3 mm. The remarkably high relief and the characteristic "pitted surface texture" are typically observed (Figure 49). Irregular fractures and inclusions are commonly seen in most of the grains. Isotropic garnet is the dominant type, but varieties with weak birefringence are not uncommon.

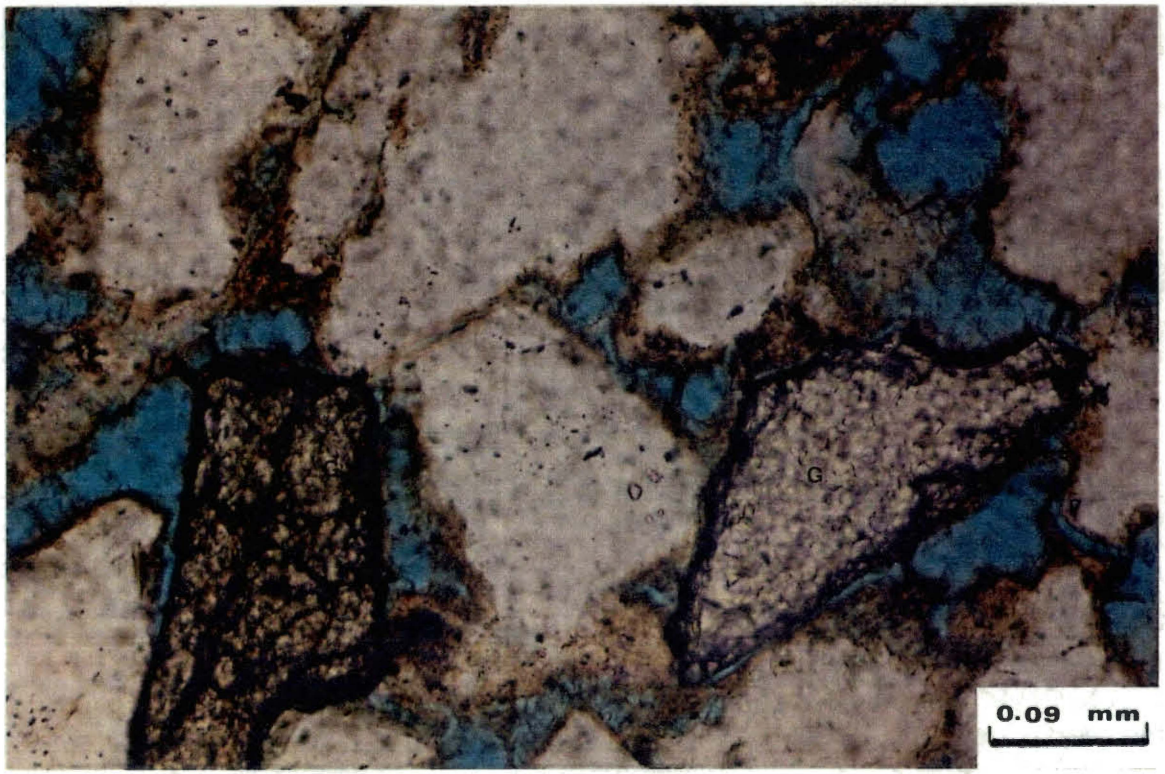

Figure 49. A Microphotograph showing two Grains of Garnet (G). Notice the high Relief and the "Pitted Surface Texture"; Plane Polarized.

Zircon commonly occur in rather small-sized crystals (0.1 mm in average) with very high relief and generally with euhedral to subhedral shapes. It also occurs as an inclusion in some of the micaceous flakes. It is observed only in trace amounts.

Tourmaline also exists in trace amounts observed as very tiny grains generally with rounded to subrounded shapes. The size of the grains range between 0.1 and 0.25 mm. The mineral is recognized by its high relief and pleochroism with colors varying from green to brown. It has been observed equally in all of the three sandstone members of the Aradeiba Formation.

Sphene has been spotted in one sample of the Aradeiba C-member.

Diagenetic Constituents

Silica

Only minute trace occurrences of quartz overgrowth have been observed in three samples of the C-sand member (Figure 50). The probable reasons for the absence of silica cementation will be discussed in depth in Chapter VII.

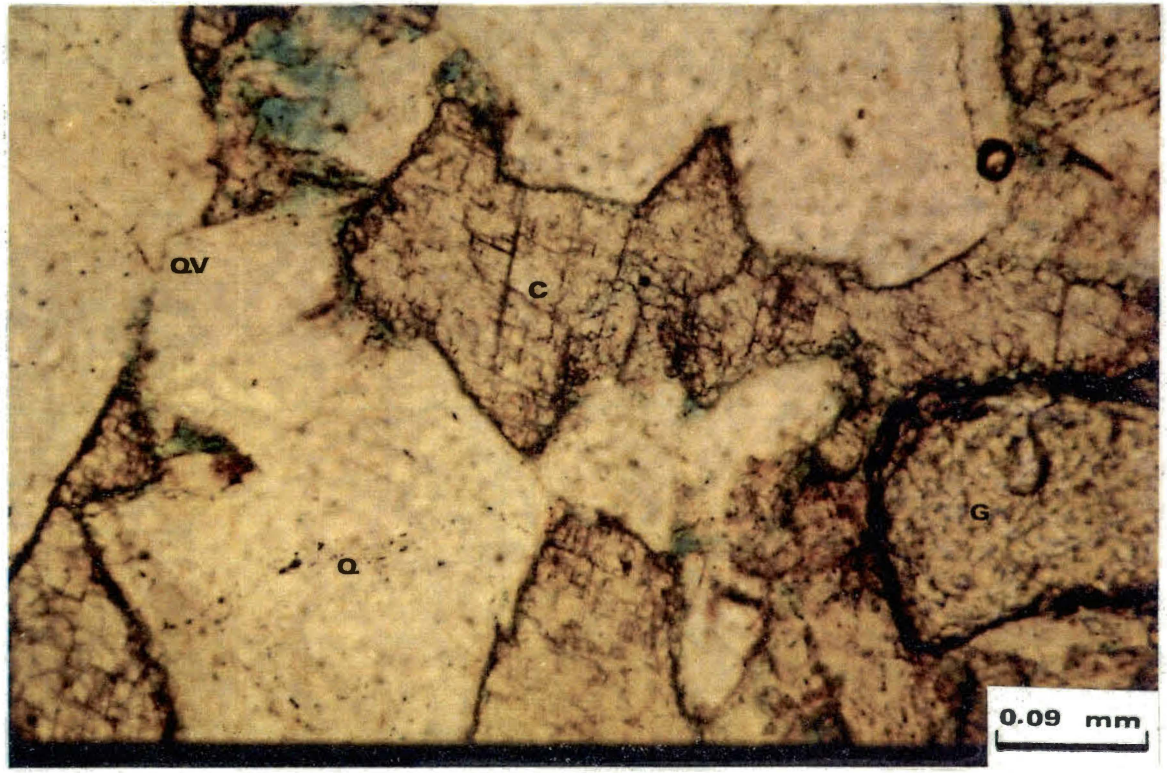

Figure 50. A Microphotograph showing Quartz Overgrowth (QV). Notice the Sharp Edge-Angles of the Diagenetic Overgrowth. Quartz Grains (Q); Calcite Cement (C); Garnet (G); Plane Polarized.

Carbonate Cement

Calcite (Figures 50, 51 and 52) is the only carbonate cement observed in the Aradeiba Formation. It constitutes a net compositional average of 1.5% reaching up to 2.4% in one individual thin section. The calcite is usually accompanied with high order interference colors and exhibits a patchy poikilotopic cement nature. Calcite twinkling (change in relief produced by rotating the polarizer through 90 degrees) is observed in many of the samples.

Feldspar

Feldspar overgrowth is extremely rare in the sandstones of the Aradeiba Formation. The only single obvious occurrence of feldspar overgrowth was observed in one sample produced from the C-member core. The host feldspar grains exhibiting overgrowth are partially altered with a clean unaltered tiny frame of feldspar cementation. The interlocking nature of the overgrowths with the original grains suggests its diagenetic origin.

Pyrite

Trace amounts of pyritic cement have been observed in the sandstones of the Aradeiba Formation. However, in

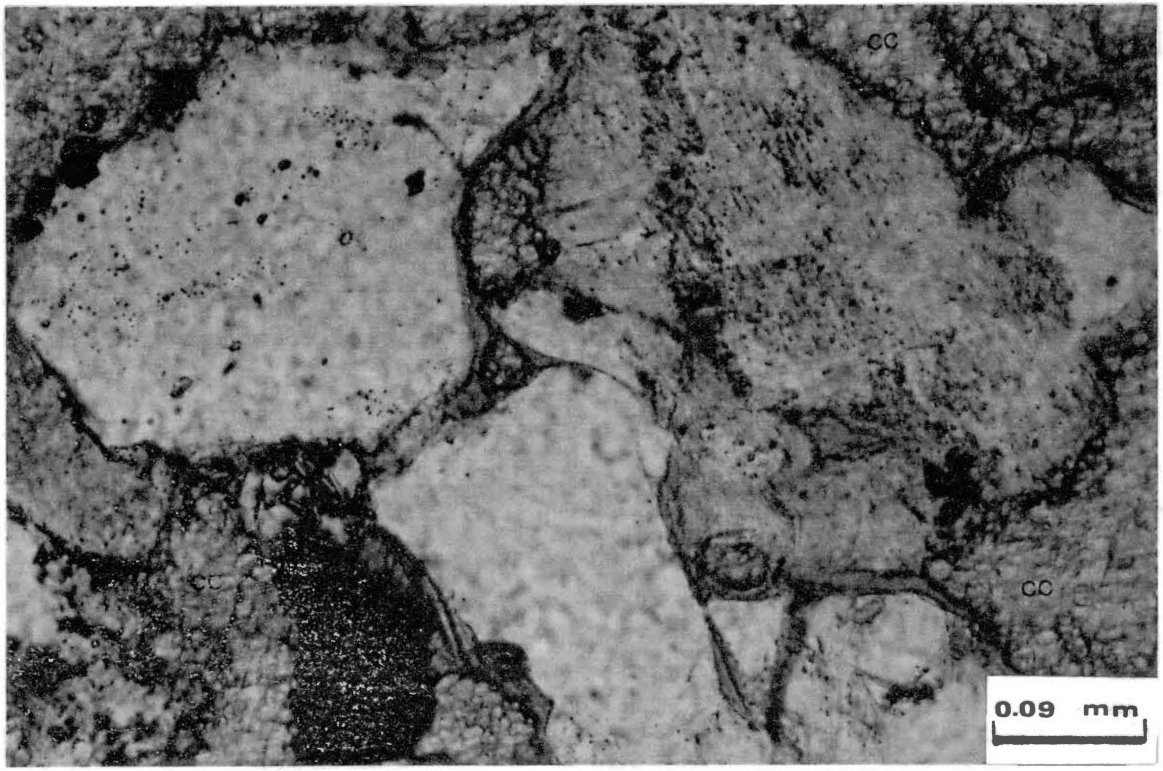

Figure 51. A Microphotograph showing Calcite Cement (CC); Plane Polarized.

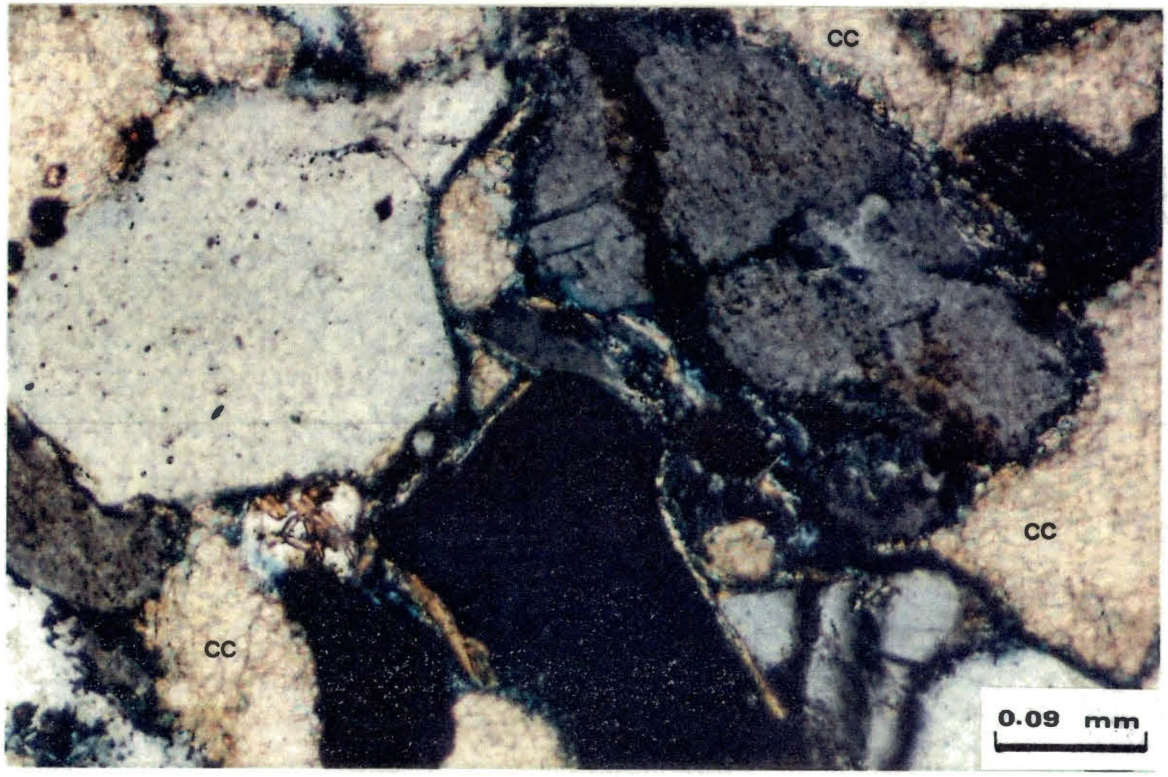

Figure 52. A Microphotograph same as Figure 51 with Crossed Polars.

two thin sections from the A-member percentages of 2% and 4% have been recorded. The pyrite cement is finely disseminated and locally occupying stylolites (Figure 53).

Clay Minerals

Clay minerals of diagenetic origin play a major role in the history and quality of the Aradeiba Formation rocks, in reference to both their amounts and diversity of occurrence. Kaolinite, smectite, illite and chlorite (both regular and 7-Å chlorite) are all present in varying amounts.

a. Kaolinite

It is the most abundantly observed clay mineral in the rocks of the Aradeiba Formation. Its overall average is 5.4%, however its compositional percentages vary between none and 23%. Kaolinite exists as a vermicular primary pore-filling material, occupying numerous pore spaces especially in the Aradeiba C-rocks (Figure 54). The kaolinite cement in these rocks is commonly characterized with a remarkably coarse crystal size and a worm-like structure, which indicates an in-situ formation (Figure 55).

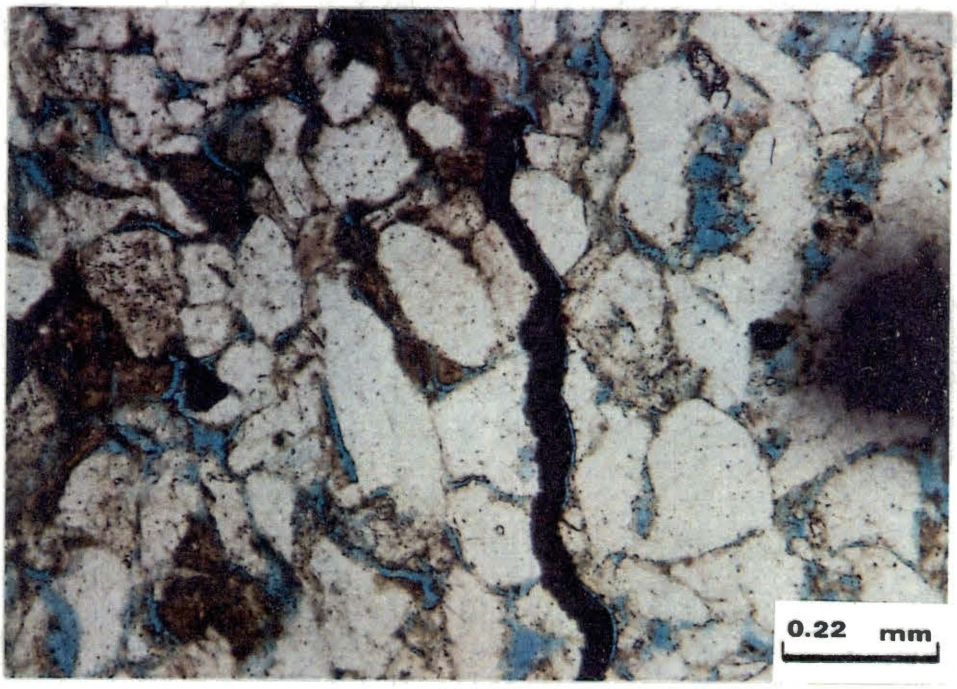

Figure 53. A Microphotograph showing Pyrite Cement Occupying a Stylolite; Plane Polarized.

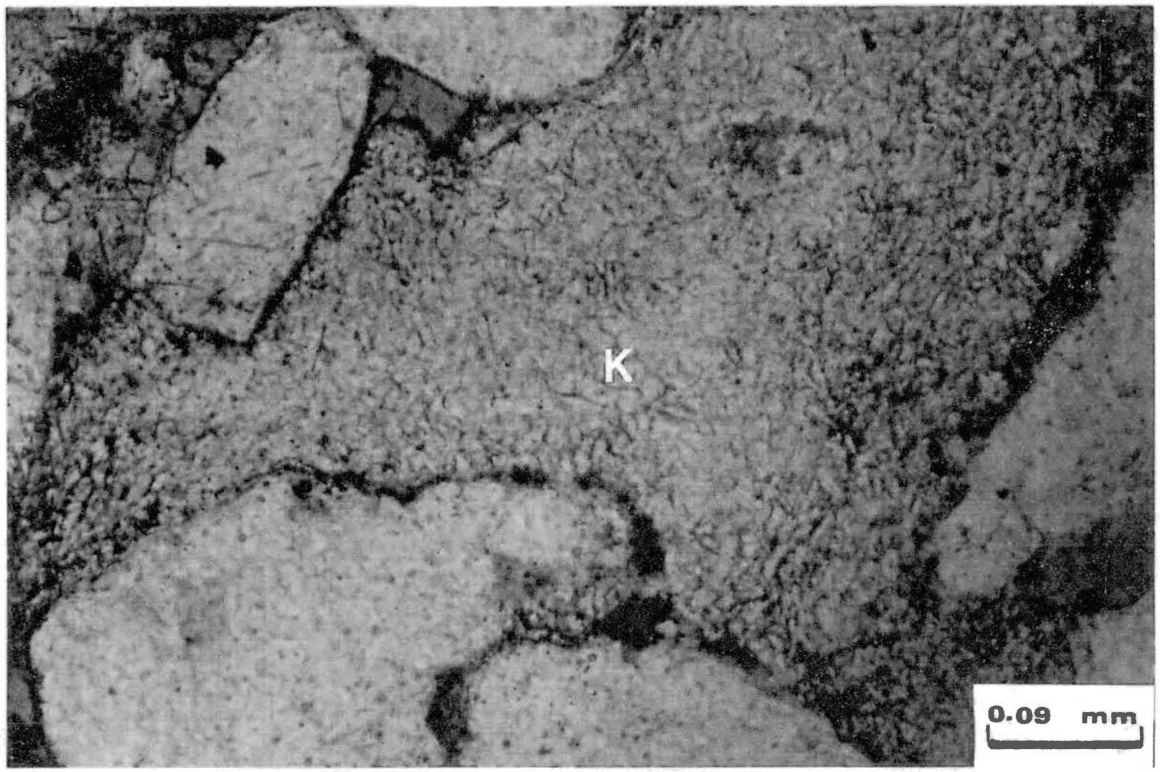

Figure 54. A Microphotograph showing Pore-Filling Kaolinite Cement (K); Plane Polarized.

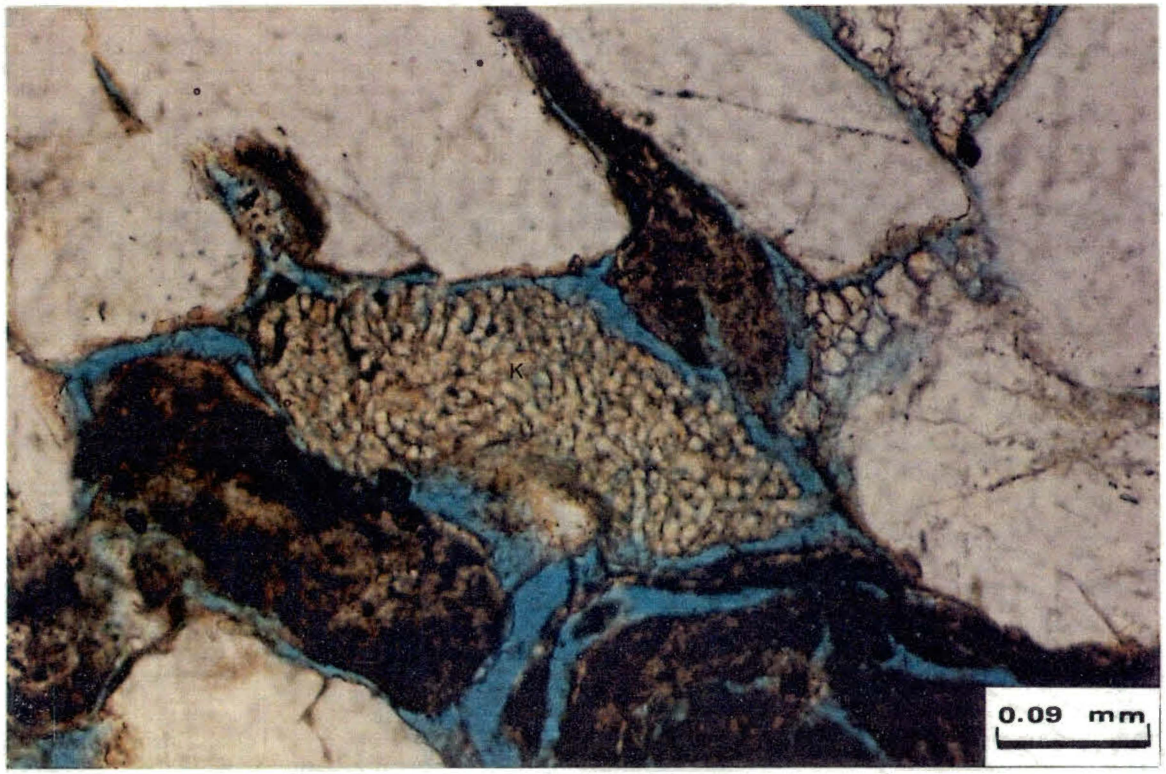

Figure 55. A Microphotograph showing the vermicular nature, the remarkable Coarse Crystal Size and the Worm-like Structure of the Kaolinite Cement (K); Plane Polarized.

b. Smectite

It has not been reliably possible to distinguish between smectite and illite under the petrographic microscope by reliance on differences in optical properties like birefringence, for instance. However core samples from the same (in most cases or varying very slightly) depths as the thin sections, were studied utilizing X-Ray diffraction techniques, and the distinction was made more readily. That made it easier to go back to the thin sections and obtain a scientific compositional percentage for each type of clay mineral.

The percentage of smectite varies from none to trace to 32% in the sandstones of the Aradeiba Formation. The overall average is 2.1%, with the A-member being the prominent host of relatively greater amounts of smectite compared to the B- and C- members respectively. Smectite occurs as a pore-filling cement and locally it bridges various pore-throats (Figure 56).

c. Illite

Illite also exists as a pore-filler and liner. Its compositional percentages range from none (especially in the C-member) to trace to 9% which was recorded in the finer sandstones of the A-sand. Its overall average

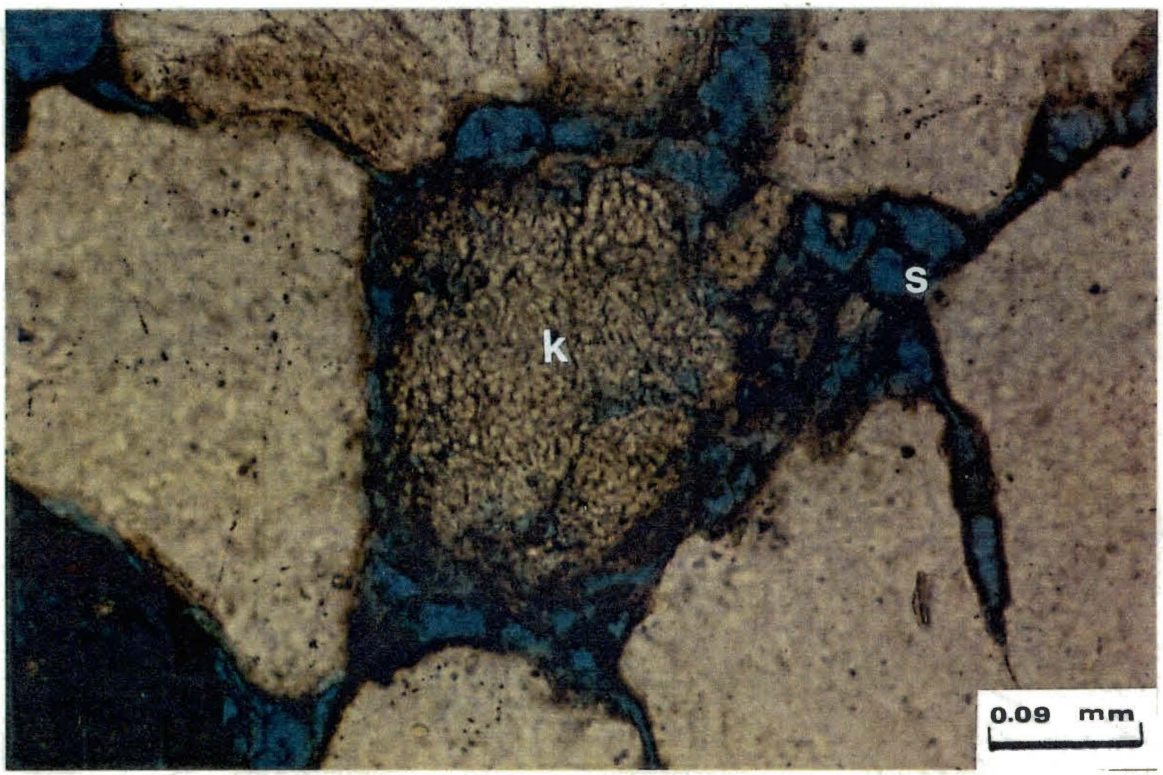

Figure 56. A Microphotograph showing Smectite Cement (S) Lining and bridging the Pores. The Cement in the Middle is Kaolinite (K); Plane Polarized.

composition is 0.93%.

d. Chlorite

It is the least abundant diagenetic clay mineral with an overall average of 0.78%. It is mostly absent in many samples and where it exists, it is found ın trace amounts. However one single occurrence amounted to 22.5% in a thin section from the A-member. Another sample was composed of 12% chlorite in the Aradeiba C-member. Chlorite occurs predominantly lınıng the pores and coating the framework grains. The mineral is lıght to medium green in color, with a pleochroic sıgnature from pale yellow to green and dark green. Anomalous interference colors are locally observed, but a low birefringence is almost typical. The chlorite typıcally shows "delicate projections" and its "face-to-edge" morphology is readily observed under high power magnification (Figure 57).

7- Å-Chlorite is also present in the Aradeiba Formatıon sandstones. This was detected usıng X-Ray diffraction (Figure 58 and Appendix B.).

Porosity

Both primary and secondary types of porosity have been observed in the rocks of the Aradeiba Formation. The

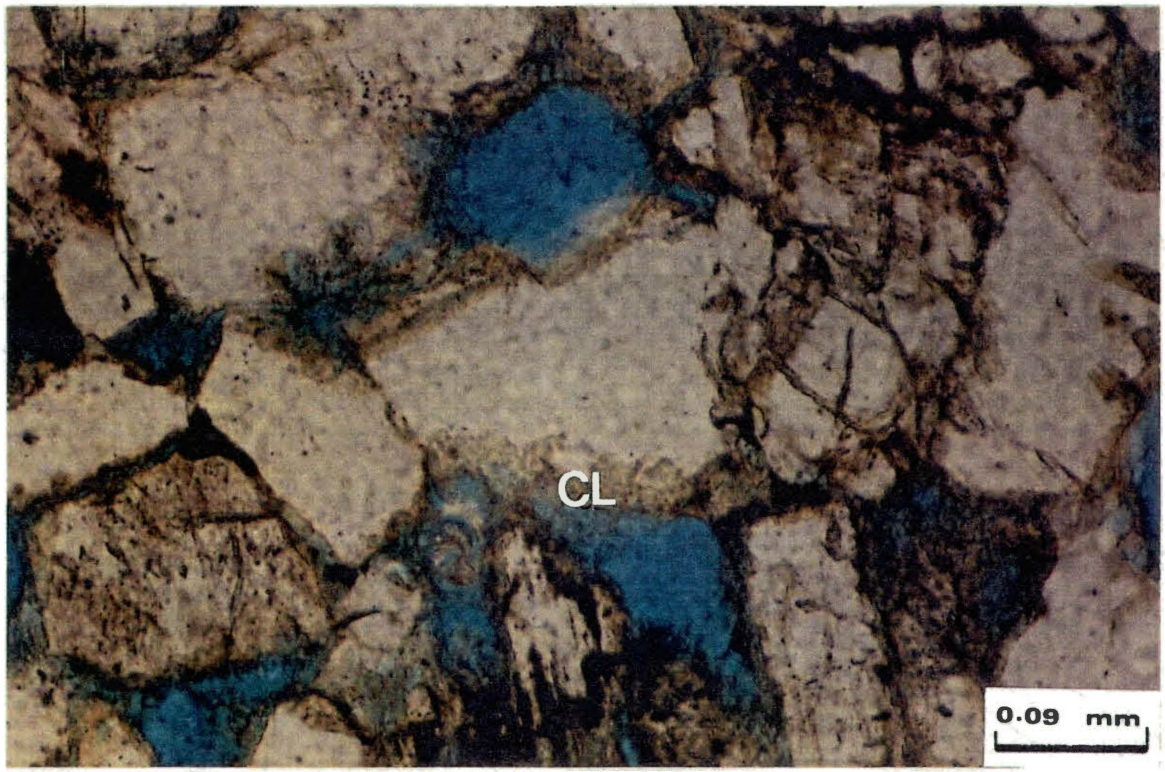

Figure 57. A Microphotograph showing Chlorite (CL) Lining the Pores. Notice the "Delicate Projections and Face-to-Edge Morphology; Plane Polarized.

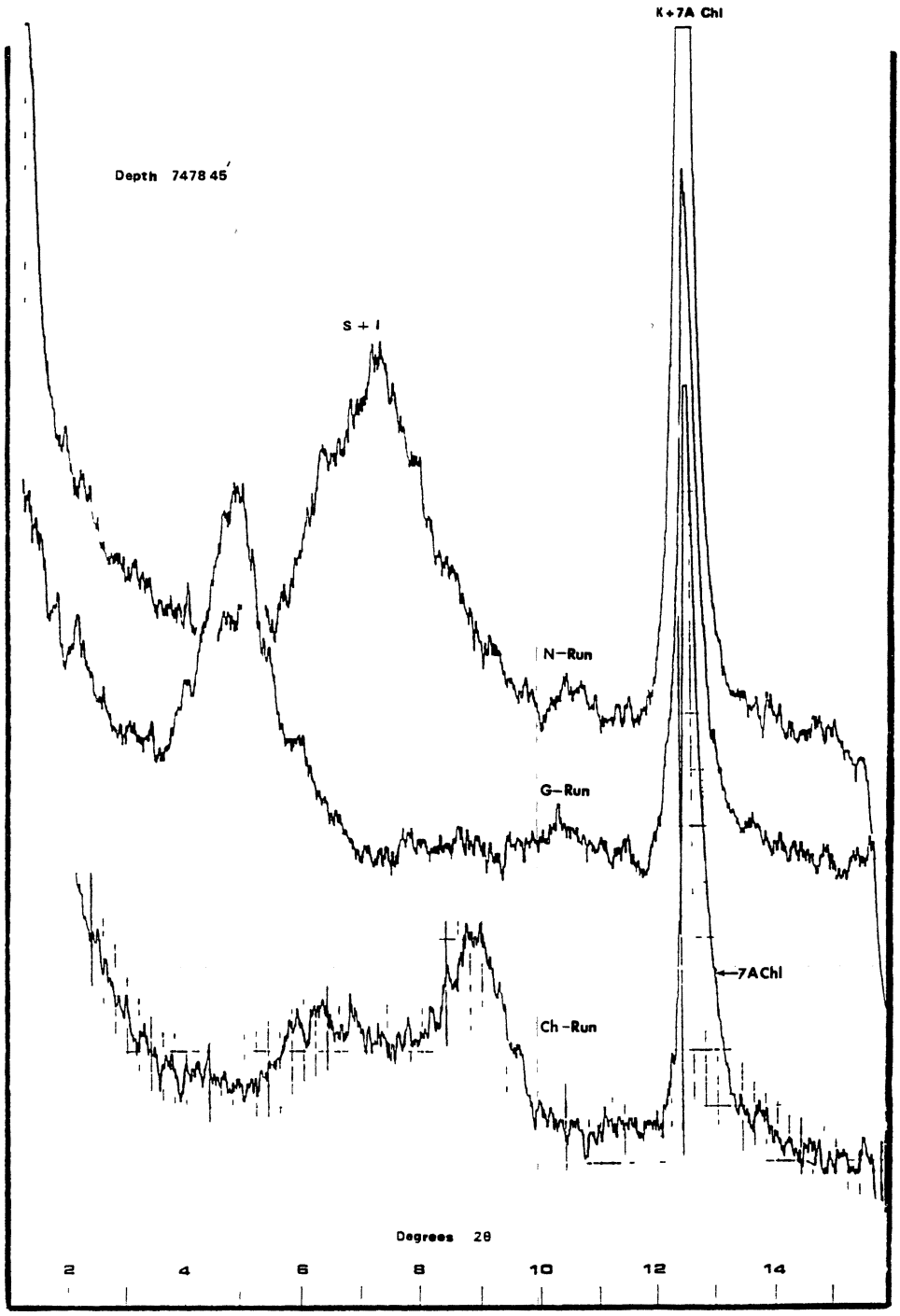

Figure 58. X-Ray Diffraction Peaks indicating the presence of 7Å Chlorite in the sandstones of the Aradeiba Formation.

A- and B-members show more pore spaces as compared to the sands of the C-member. The porosity percentage varies from trace to up to 32% with an overall average of 15%. The porosity will be discussed in greater depth in Chapter VII.

CHAPTER VI

PROVENANCE AND ENVIRONMENTS OF DEPOSITION

Introduction

A discussion of the provenance area and the dominant environments during the deposition of the Aradeiba Formation is presented in this chapter. The mostly medium to fine-grained sediments of the Aradeiba Formation are believed to have been deposited in channels and basin floodplains environments of meandering streams. This model is supported by several evidences as will be discussed through the chapter. The fine and very fine sandstones, siltstones and calcareous mudstones (mainly in the B and A members), with complex climbing-ripple structures could be interpreted as lacustrine deposits. However the lack of the typical "varvic nature" (Davis, 1983), the small amounts of carbonates and, less indicative, the lack of evaporites, combined with the strong stream-related features favor a fluvial interpretation. However a marginal lake environment is not an improbable possibility for those upper sediments of the Aradeiba Formation.

Provenance

It is well known that fluvial sediments inherit the mineralogy of their mother rocks (Cant, 1982). The terrigenous mineral combination of the rocks of the Aradeiba Formation includes quartz, K-feldspar, plagioclase, biotite muscovite, garnet and other heavy minerals. This mineral association points to a granitic or granodioritic source rocks (Davis, 1983). The remarkable abundance of garnet could be attributed to the presence of pegmatitic dikes in the source area. However the birefringent garnet grains (pyralspite) are related to metamorphic rock sources, mostly schist (Nesse, 1986). A metamorphic source is also indicated by the numerous rock fragments of metamorphic origin (Chapter V). These are namely, schist, gneiss and metamorphic polycrystalline quartz particles.

Rocks of the above mentioned description are available to the south, southwest and northwest of the study area (Chapter III). An attempt was made to study the angularity and the grain-size distribution in order to determine the direction or directions of sediment influx to subsequently pin point the source area more accurately. However the results were inconclusive, most probably,

because the available core samples were not specifically selected for that purpose and to achieve convincing results a more appropriate geographic distribution of samples is required. Nevertheless, it is appropriate from the sand thickness maps (plates 3 through 5) that sediments were introduced mostly from the south east into the study area.

Environments of Deposition

Mineralogy of Sediments

The Aradeiba Formation rocks are classified as subarkosic with a mineral association of quartz, K-Feldspar, plagioclase, muscovite, biotite, detrital chlorite, diagenetic clay minerals, calcite and pyrite cements and sedimentary and metamorphic rock fragments.

Texture

The grain sizes vary widely including clast-supported rip-up conglomerates with occasional quartz gravels, very coarse sands with scattered pebbles, medium to fine grained sediments, very fine sandstones and mottled siltstones, and thick intervals of claystones and shales.

The sorting also varies from well-sorted intervals to poorly-sorted. However the sediments are generally moderately sorted. The dominant shape of the grains is subangular to subrounded.

Sedimentary Structures

Several types of sedimentary structures representing both upper and lower-flow regimes are present in the core samples of the Aradeiba Formation (Chapter IV). Low angle cross-stratification, known as epsilon cross-stratification (Davis, 1983) is widely observed especially along the coarse and very coarse sections at sequence bases.

Horizontal lamination, indicating upper-flow regime and various types of ripple-cross-strata are also observed in the finer sediments. Thin beds of graded bedding are observed occasionally at the base of sequences. Several occurrences have been recorded where elongate-clast particles show imbrication structures.

Sequences

Figure 59 shows one of the typical fining-upward sequences recorded from the cores of the Aradeiba Formation. This phenomenon is attributed to the lateral migration of the stream belts which fine upward from lag

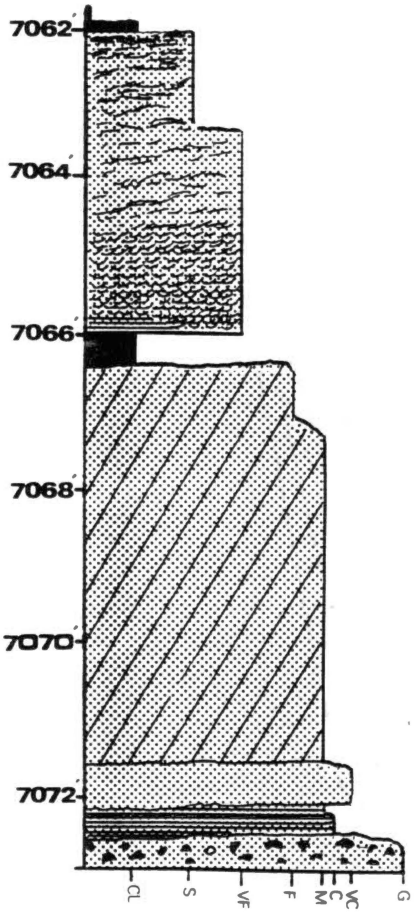

Figure 59. A Typical Fining-upward Sequence from the Aradeiba-A Member, Unity No. 11.

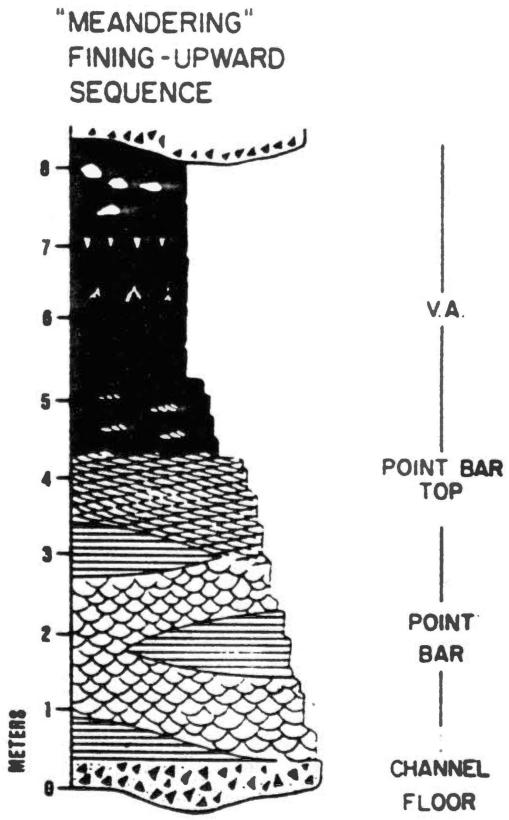

Figure 60. Classic fining-upward sequence deposited by lateral migration of a meandering river. (After Allen 1970).

gravel and intraclast conglomerate to sand to mud (Bernard et al., 1970 and Allen, 1970) (Figure 60).

Log Signature

Evidence from well logs (Gamma Ray and SP logs), indicate the typical bell-shape of stream channel deposits. Figure 61 is an example of bell-shaped SP curves generated by the presence of fining-upward sequences.

Fossils

With the exception of occasional fossil plant particles, no diagnostic fossils have been encountered from the studied samples.

Discussion and Conclusion

The sedimentary structures described above obviously indicate current-generated features. According to Davis (1983) the imbrication noticed on clast particles, typically provides an excellent orientation direction and their abundance indicates deposition in a fluvial environment. The epislon cross-stratification is attributed to the "ridge and swale" type of relief that develops as the point bars migrate in the meandering

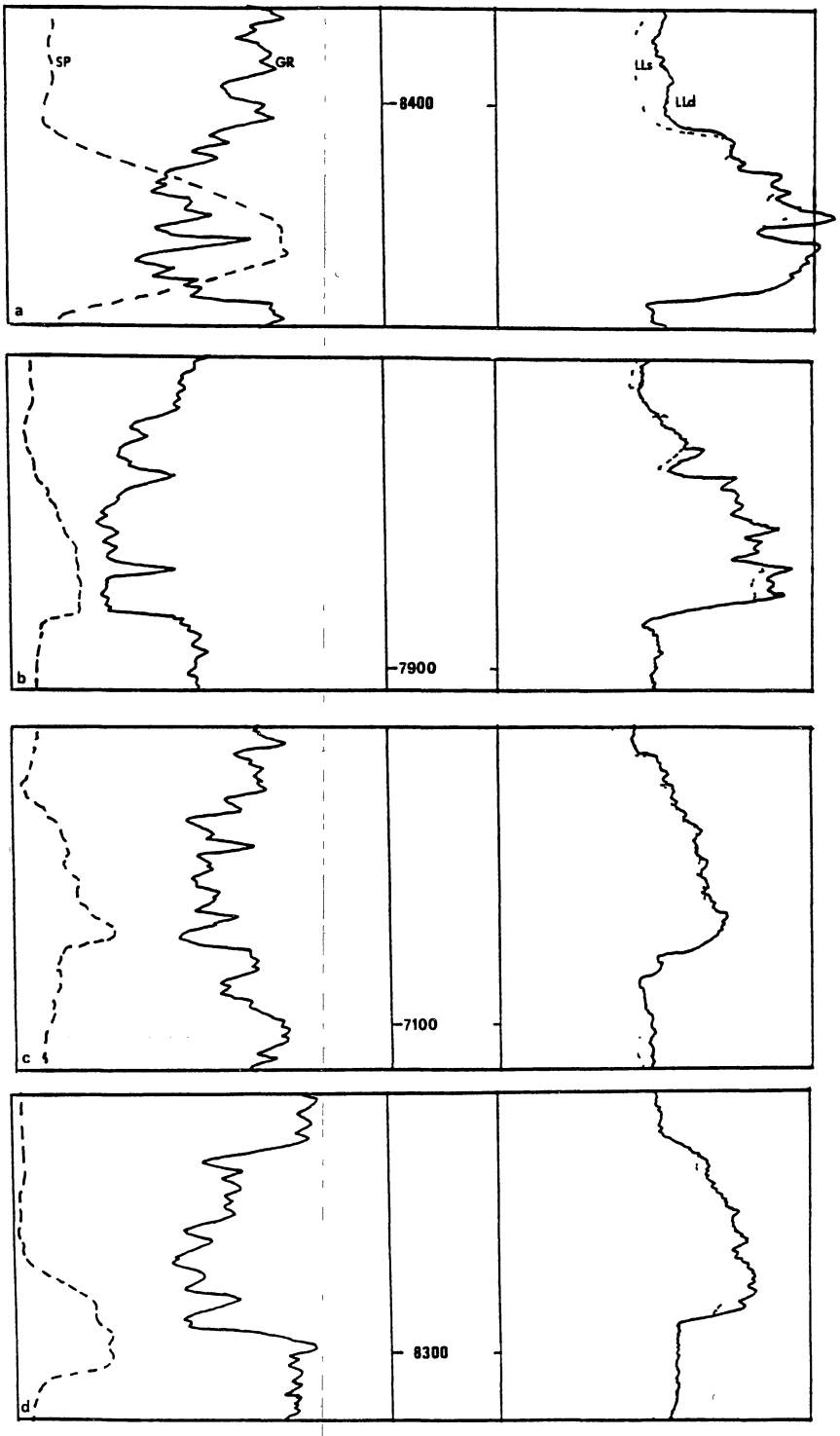

Figure 61. Bell-shaped SP Curves generated due to Fining-Upward sequences, a from Talih #2, b from Unity #2, c from Unity #10 and d from Unity #7 Wells.

system (Davis, 1983; Miall, 1980). The rippled sands, mottled siltstones and mud drapes observed topping the fining-upward sequences are commonly typical deposits found near the top of point bars (Miall, 1980). The thick intervals of claystone, multi-colored mudstone with occasional burrowing structures and plant material are believed to have been deposited on flood plains during stream overflooding.

The rocks of the Aradeiba Formation are, therefore, believed to have been deposited in channel, bank and flood basin environments within a meandering system (Figure 62). The presence of very fine sediments including calcareous mudstone and their very nature of fine rhythmic lamination, brings the possibility of a lacustrine environment of deposition in the picture. However the typical coarsening-upward sequences of the lacustrine system (Davis, 1983) are not dominant, and the occasional presence of such sequences is attributed to probable periods of uplift in the source area. Some of the minerals most abundant in the lacustrine sediments for instance zeolites (analcime) (Davis, 1983) have not been recorded. Therefore an open lacustrine environment is not favored. However deposition of these finely laminated sediments in a

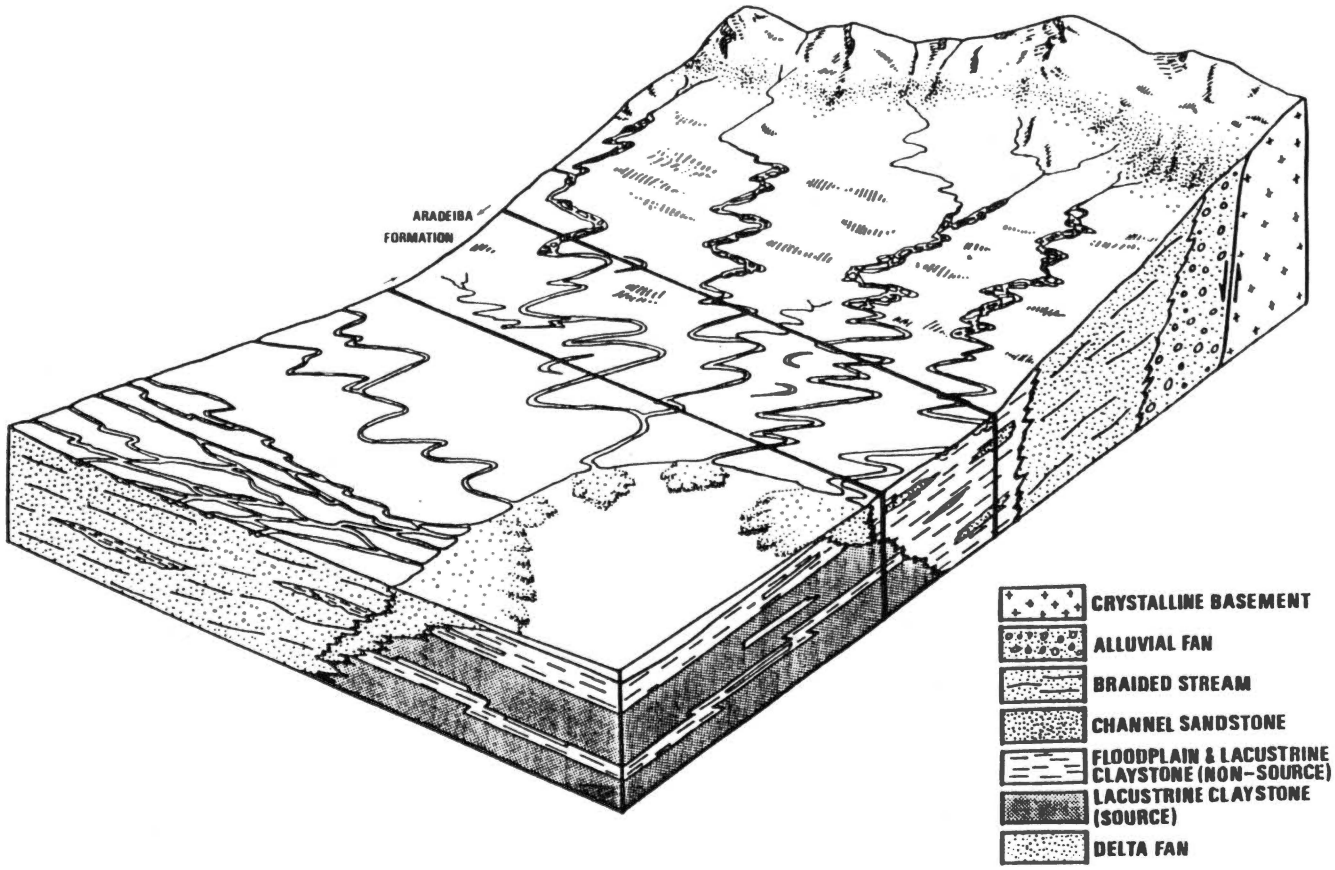

Figure 62. Schematic Diagram Showing the Environments of Deposition of the Aradeiba Formation. (After Schull, 1988.)

marginal lacustrine setting in the peripheries of graben-host lakes of the rift basin is not an intolerable interpretation.

CHAPTER VII

DIAGENESIS AND POROSITY

Introduction

In the first part of this chapter we will discuss the diagenetic phenomena that contributed actively in shaping and reshaping the fabric composition of the Aradeiba Formation sandstones. Reduction of the total rock volume, destruction of primary and (later on) secondary porosities by means of precipitation of newly formed diagenetic minerals, from solution or alteration of pre-existing minerals and creation of secondary porosity are major episodes in the diagenetic history of the Aradeiba Formation rocks. In the second part a sequential account of the various diagenetic products is thoroughly discussed and tabulated as a suggested paragenetic sequence generalized for the three sand members of the Aradeiba Formation. The third part of this chapter deals with the primary and the various types of secondary porosities. It also discusses the resultant reservoir quality.

Diagenesis

i. Compaction

During the early stages of deposition throughout the shallow subsurface, sediments underwent relatively rapid mechanical compaction, due to active supply of sediment weight dumped into the subsiding Abu Gabra basin, and the lack of abundant cementation. The total rock volume should have probably suffered a rapid shrinkage during that stage. The effects of that compactional stress are evident in a number of features. The more subtle grains were squeezed and aligned amongst the brittle framework grains (Figure 63). Fracturing and deformation of minerals (especially heavy minerals and feldspars) and undulose extinction witnessed near quartz grain contacts, which may have resulted from "solid-state ductile-grain deformation" (McBride, 1978) all indicate mechanical compaction. The clay mineral reactions are known to release significant amounts of free siliceous water (Hower et al, 1976). This would facilitate the compaction process in a chemical rather than a simple mechanical sense.

ii. Cementation

The alteration of pre-existing framework grains into

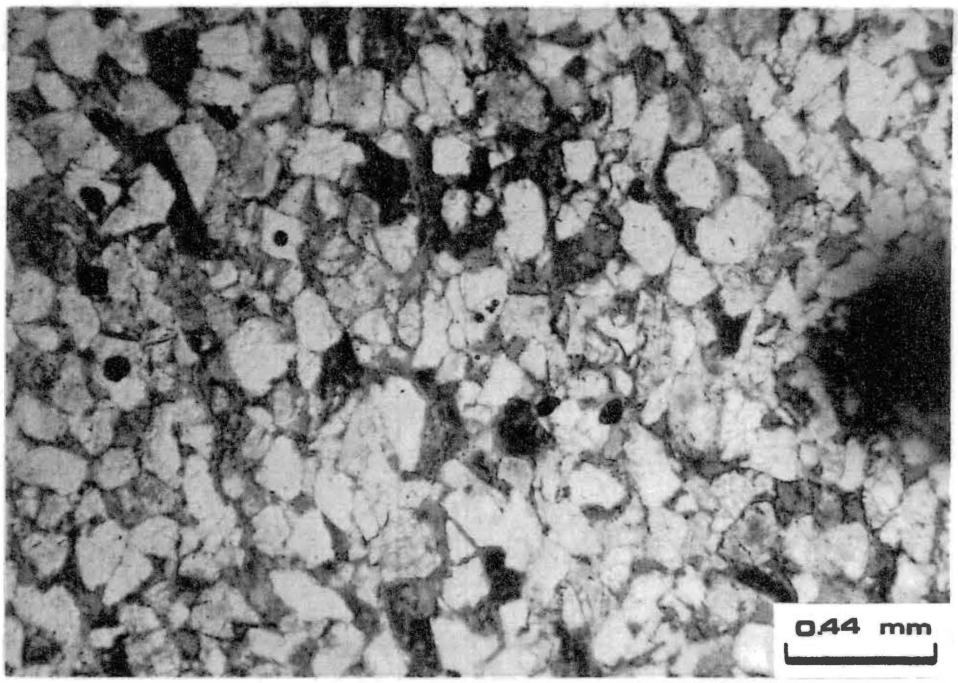

Figure 63. A Microphotograph showing the Effect of Compaction Diagenesis on the Rocks of the Aradeiba Formation. Notice the Alignment of the Ductile Grains amongst the Brittle ones; Plane Polarized.

different minerals, the precipitation from solutions and the mineral-overgrowths are the main processes responsible for cementing the sediments of the Aradeiba Formation. The cements include minor amounts of quartz and feldspar overgrowths, sparry calcite, pyrite, smectite, illite, chlorite and substantial amounts of kaolinite blocking a large number of pores. Significant cementation might have started within the time frame of effective compaction and it has, ever since, been an on-going process.

iii. Replacement

Many replacement relationships have been observed under the microscope, between various mineral constituents in the rocks of the Aradeiba Formation. The most abundant relationships are the replacement of K-feldspar by kaolinite, K-feldspar by calcite and less importantly kaolinite replaced by calcite (Figures 64, 65 and 66). In other occurrences the chloritization of mica and sericitization of plagioclases is very common. The presence of smectite and illite in the finer upper sands, makes the thought of smectite-illite transformation inescapable (Hower et al, 1976).

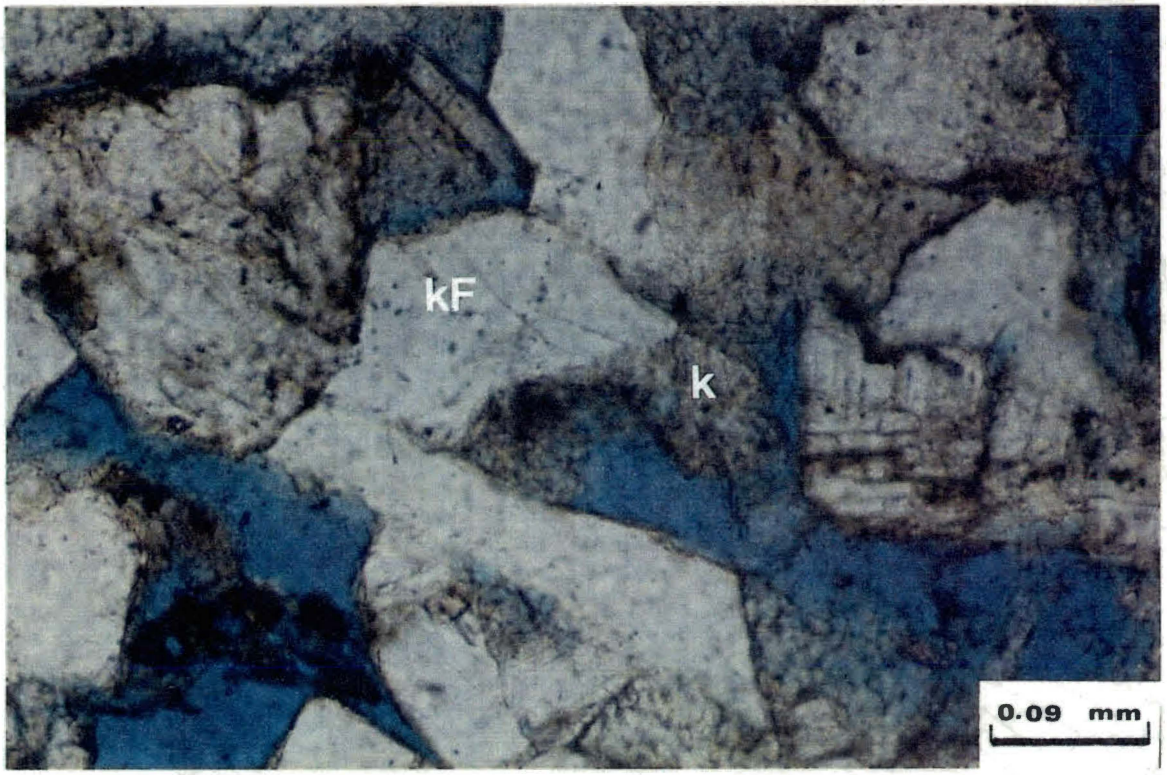

Figure 64. A Microphotograph showing the Replacement Relationship of Kaolinite (K) to K-Feldspar (KF); Plane Polarized.

Figure 65. A Microphotograph same as Figure 64 with the Polars Crossed.

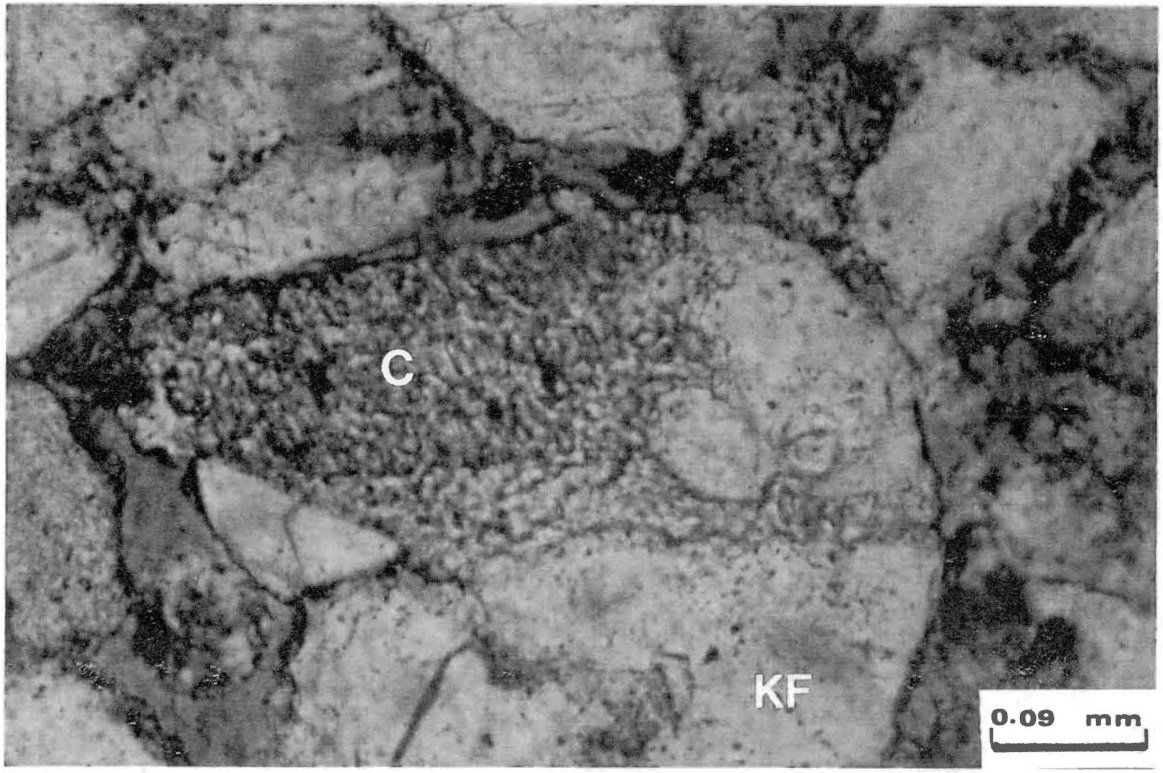

Figure 66. A Microphotograph showing the Replacement Relationship of Calcite (C) to K-Feldspar (KF); Plane Polarized.

iv. Dissolution

Partial and complete dissolution of both framework grains (overwhelmingly feldspars and less importantly rock fragments) and cement (mainly calcite) are remarkable features in the sandstone of the Aradeiba Formation. The dissolution episode was probably activated by water released from shale compaction during the active subsidence. For instance, the conversion of smectite-to-illite, one of the common shale reactions, releases water that facilitates the dissolution of framework grains like K-feldspars through hydrolysis reactions (Hans Fuchtbauer, edited by Parker and Sellwood, 1983). Moreover, the carbonic acid (H_2CO_3) formed during the catagenesis phase of the thermal maturation of organic matter in the sediments, is responsible for dissolving the calcite cement (Schmidt and McDonald, 1979).

Feldspar grains which constitute an average compositional percentage of 7.2% (probably a few percentages higher before dissolution and alteration) suffered the most of dissolution. However, the available completely unaltered feldspar grains have probably escaped dissolution due to the very low solubility of feldspar.[1] Therefore, saturation must have been attained with a small amount of dissolution (Knut Bjorlykke, edited by Parker and Sellwood, 1983). The following equations are given by AL-shaieb and Shelton 1981 to illustrate the dissolution of feldspars.

---

[1]The solubility of K-feldspar is 3x10-7 mole/litre and that of Na-feldspar is 6x10-7 mole/litre in pore water (Berner, 1978).

$$3KAlSi_3O_8 + 2H_2CO_{3aq} + 12H_2O \rightleftharpoons KAl_3Si_3O_{10}(OH)_2 + 2K^+_{aq} 6H_4SiO_{4aq} + 2HCO^-_{3aq}$$
K-Feldspar — Illite — Silicic acid

$$2KAl_3Si_3O_{10}(OH)_2 + 2H_2CO_{3aq} + 3H_2O_l \rightleftharpoons 3Al_2Si_2O_5(OH)_4 + 2K^+_{aq} + 2HCO^-_{3aq}$$
Illite — Kaolinite

$$2KAlSi_3O_8 + 2H_2CO_{3aq} + 9H_2O_l \rightleftharpoons Al_2Si_2O_5(OH)_4 + 2K^+_{aq} + 4H_4SiO_{4aq} + 2HCO^-_{3aq}$$
K-Feldspar — Kaolinite — Silicic acid

To a lesser degree, calcite, sedimentary and metamorphic rock fragments, heavy minerals have undergone various degrees of dissolution.

Diagenetic Sequence

Studying the paragenetic relationships between the various cementing minerals of the Aradeiba Formation rocks has not always been an easy task. Nevertheless, a good effort has been devoted utilizing the obvious replacement relationships together with the general rules of paragenesis (Fuchtbauer, edited by Parker and Sellwood, 1983) to construct a diagenetic sequence shown as Figure 67. Solid lines on Figure 67 indicate strong evidence from the thin sections, where discontinuous lines point to uncertainty and sound interpretation. The three members of the Aradeiba Formation display the same common diagenetic features and mineral-relationships. Therefore, this diagenetic sequence has been established as a representative for all three members.

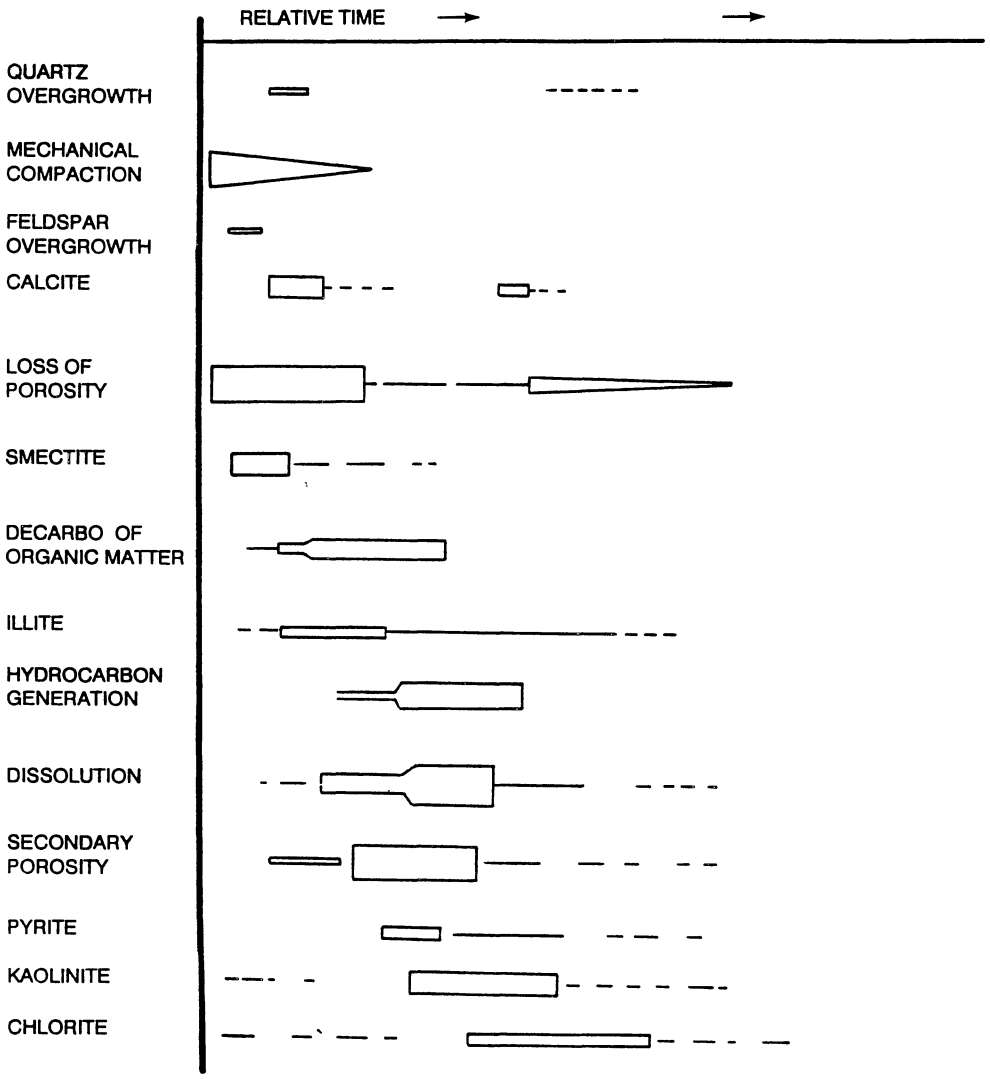

Figure 67. The Paragenetic Sequence of the Aradeiba Formation

Calcite

Calcite has been an early diagenetic cement in the sands of the Aradeiba Formation. Alteration of feldspars, biotite and heavy minerals to calcite seems to have occurred early during diagenesis. However, a second episode of calcite formation must have taken place probably during the late stages of diagenesis. That is evident from the occurrence of numerous occasions where kaolinite (a late diagenetic product) has been replaced by calcite.

Quartz Overgrowth

Silica is an insignificant cement in the Aradeiba Formation sands. Trace amounts are observed in some of the cores, however, five of the cores lack any observed quartz overgrowth as studied under the microscope, bearing in mind that quartz constitutes an average compositional percentage of 51%. There are different explanations for the absence of quartz overgrowth, Horn (1965) and Tillman and Almon (1979) indicated that clay mineral coating of the quartz grains inhibit silica cementation. The abundance of an extensive clay matrix and the presence of isopachous chlorite must have, therefore, hindered the syntaxial overgrowth of quartz in the Aradeiba Formation sandstones. Hayes (1979) stated that in quartz-poor

sandstones alkali and alkali-earth cations produced from the breakdown of feldspars and maphic minerals combine with dissolved silica to form authegenic clay minerals, not quartz overgrowth. According to Blatt (1979) quartz overgrowth cementation necessitates the presence of vertical subsurface circulation at shallow depths.

Pyrite

Pyrite cementation is related to the late stages of maturation of organic matter, when the sulfide ion was a dominant species in the subsurface solutions. It is observed to exist in stylolites in many occurrences.

Feldspar Overgrowth

Very few occurrences of feldspar overgowth have been observed (see Chapter V). The feldspar cementation is believed to have taken place during early diagenesis while sediment compaction was mostly effective causing the framework grains to undergo pressure solution.

Smectite

Authegenic smectite constitutes an extensive cement predominantly in the finer sands of the Aradeiba A-member. It is suggested that smectite was the first clay mineral to form diagenetically in the Aradeiba Formation. It has been postulated by Burns and Ethridge (1979) and

Galloway (1974) that smectite formation takes place early during diagenesis by " mechanical infiltration of colloidal clay-rich waters" or by alteration of feldspars. The lateritic soil known to cover extensive areas to the south of the Abu Gabra basin probably has contributed effectively to the formation of authegenic smectite.

Illite

Pore-filling and pore-lining illite is locally very abundant in the upper sands of the Aradeiba Formation (Figure 68). During the course of diagenesis with increasing temperature and pressure, hydrous clay minerals like smectite become unstable (60-100C) and transforms to illite (Hower et al, 1976). This transformation is explained by the following equations according to Hower et al, 1976.

$$\text{Smectite} + K^{+} + AL^{3+} \rightarrow \text{illite} + \text{quartz} + H^{+}$$

or

$$\text{Smectite} + \text{K-feldspar} \rightarrow \text{illite} + \text{chlorite} + \text{quartz}.$$

Bruce Velde (edited by Parker and Sellwood, 1983) stated that illite also forms from transformation of kaolinite when the temperature range is between 120 C and 150 C, as follows:

$$3AL_2Si_2O_5(OH)_4 + 2K^{+} \rightarrow 2KAL_3Si_3O_{10}(OH)_2 + 2H^{+} + 3H_2O$$

Kaolinite → Illite

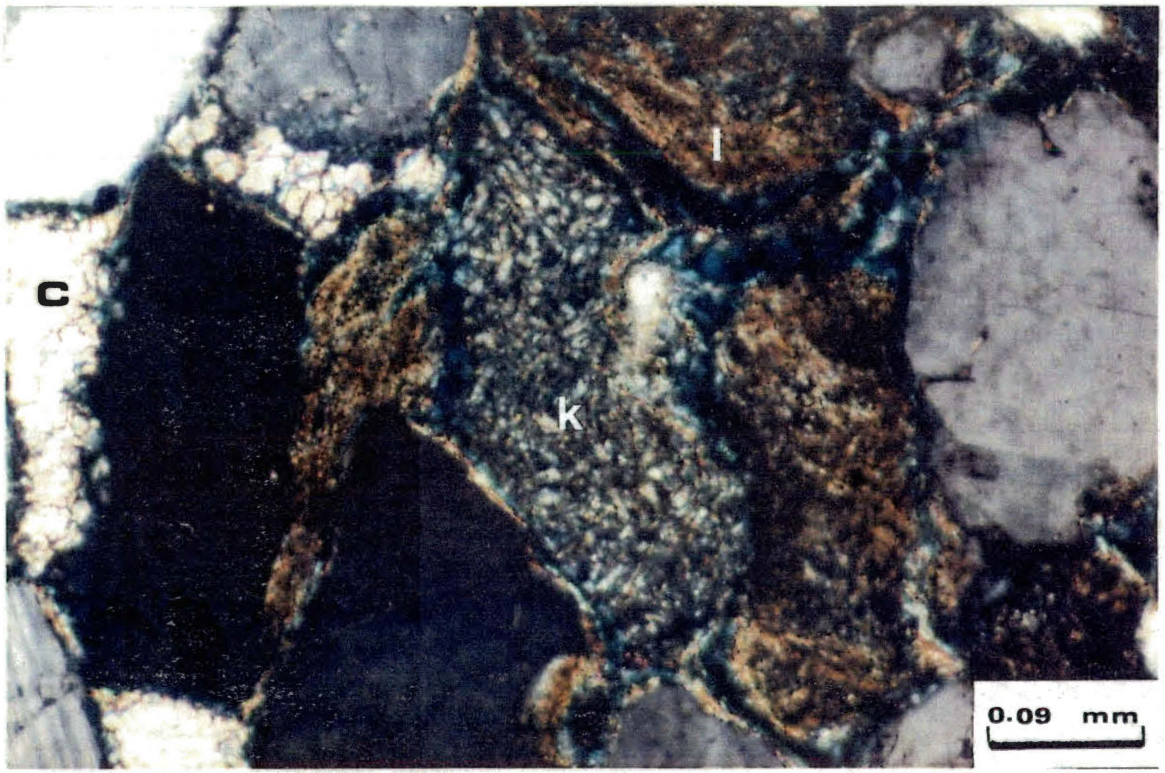

Figure 68. A Microphotograph showing Illite (I) Cement as Pore-Filling and Lining. Calcite (C); Kaolinite (K); Cross Polarized.

Chlorite

Chlorite is a lesser important cement as compared to the other clay minerals in the sands of the Aradeiba Formation. Two episodes of formation of chlorıte are believed to have taken place. Early diagenetic chlorite (namely, bertheirines or 7-Å chlorite) has probably formed in the sediments closer to the rift lakes (Bruce Velde, edited by Parker and Sellwood, 1983). The second episode of regular chlorite formation is believed to have occurred later on, when the temperature increased and more free Mg+ and Fe+ ions have been avaılable in the system (Bruce Velde, edited by Parker and Sellwoood, 1983).

Kaolinite

It is the most extensive type of authigenic clay mineral in the Aradeiba Formation readily observed on various parts of the core samples. Kaolinitization of feldspar dominated the three sandstone members giving rise to a discrete pore-filling cement.

Initial high permeability allowed more subsurface weathering which might have enhanced the kaolinitization process. The process of kaolinitization is believed to have been an on-going diagenetic phenomenon, however, it was mostly active after the extensive episode of dissolution. The reasons being more framework grains were dissolved (particularly feldspars) and the porosity and

permeability were enhanced by dissolution to allow more water circulation.

Porosity and Reservoir Quality

Introduction:

Water and wind-deposited sands are commonly known to possess initial porosities of the order of 35 to 40 percent and permeabilities of several darcys (Hayes 1979). These initially high petrophysical properties are continually reduced with increasing depth due to diagenetic processes such as compaction and cementation (Chepikov et al, 1959, 1961; Savkerich, 1969; Yermolova and Orlova, 1962; Schmidt et al, 1977, Hayes 1979). Ironically, other diagenetic phenomena are responsible for creating new porosity and enhancing the pre-existing intergranular porosity deep in the subsurface. Studying the porosities of the Aradeiba Formation rocks, clearly suggests a rather distinctive portrayal of the above sequence, reduction, destruction, creation, enhancement and even further reduction of porosity. The reservoir quality, due to the porosity modifications and the precipitation of extensive clay mineral cement was, therefore, clearly affected.

Porosity Types:

The overall average visual porosity is 15.17% varying from trace to 32%. The initial primary intergranular porosity was extremely reduced (especially in the C and B members) due to rapid compaction accompanied the subsidence of the Abu Gabra basin. Diagenetic dissolution of feldspars contributed a great deal to resurrect the porosity to its present levels. Less importantly is the contribution of cement dissolution (mainly calcite), quartz corrosion (Figure 69) and fracture porosity. Partial and complete feldspar dissolution (Figure 70) have been detected in the Aradeiba Formation sandstone indicating secondary porosity, together with oversized fabric-selective pores, elongate pores, inhomogeneity of packing and honeycomb structures (Figures 71, 72 and 73). Plotting the porosities of the Aradeiba Formation rocks versus depth (Figure 74) also provides an alternate supportive evidence of presence of secondary porosity, since the curve does not indicate a linear decrease in porosity with increasing depth as it is commonly accepted. It is worth noting that the log-derived porosities on Figure 74 are a few percentage degrees higher than those calculated from the thin sections (Appendix A), believed to be mainly caused by the extensive microporosity

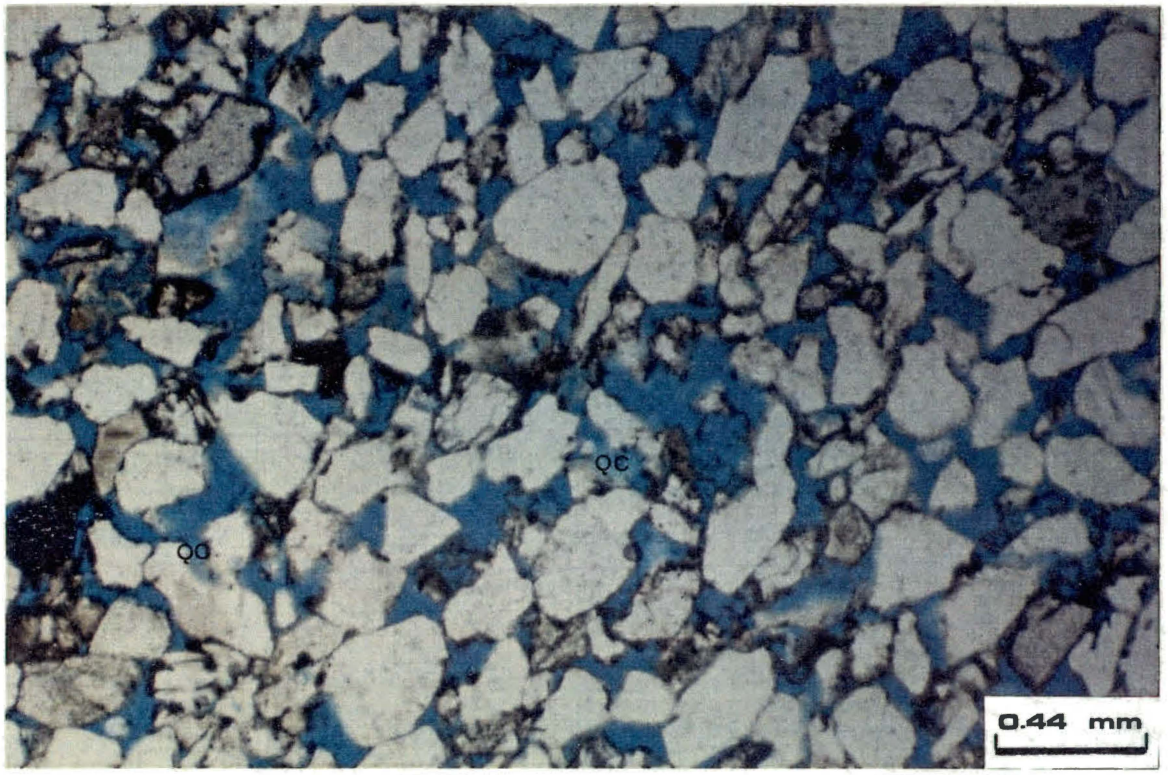

Figure 69. A Microphotograph showing Quartz Corrosion (QC) in the Sandstones of the Aradeiba Formation; Plane Polarized.

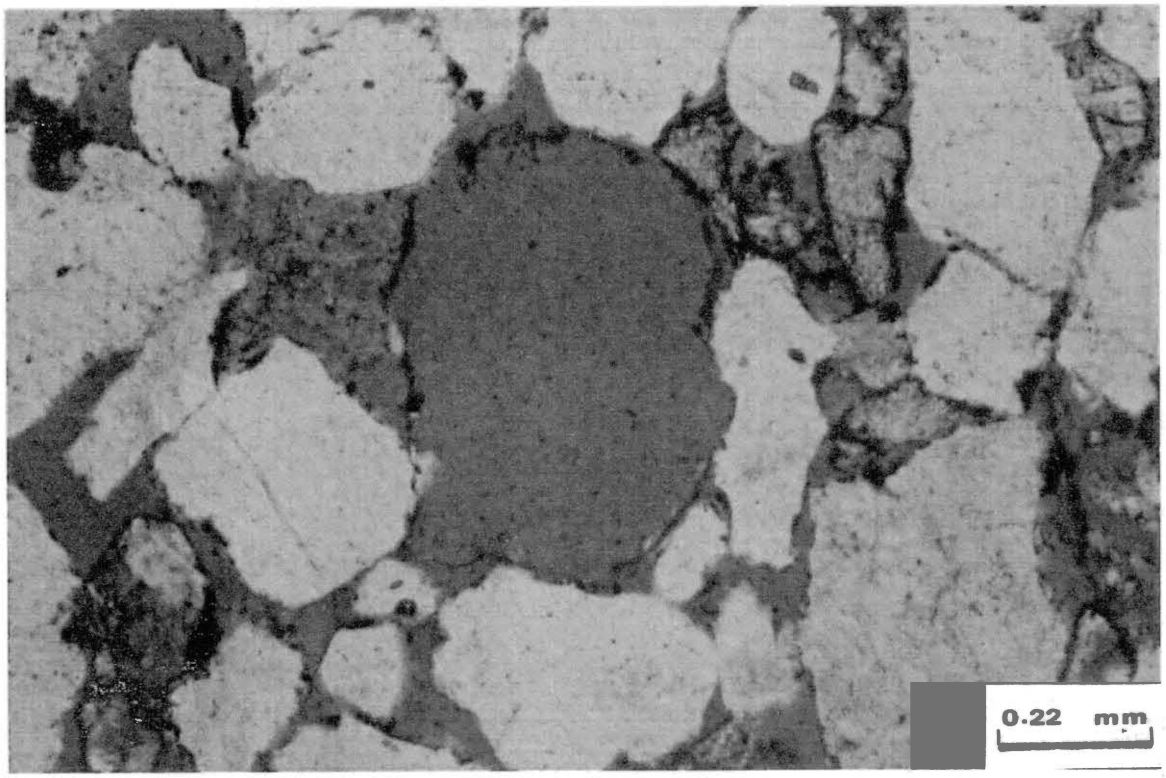

Figure 70. A Microphotograph showing Complete Moldic Dissolution of a Feldspar Grain; Plane Polarized.

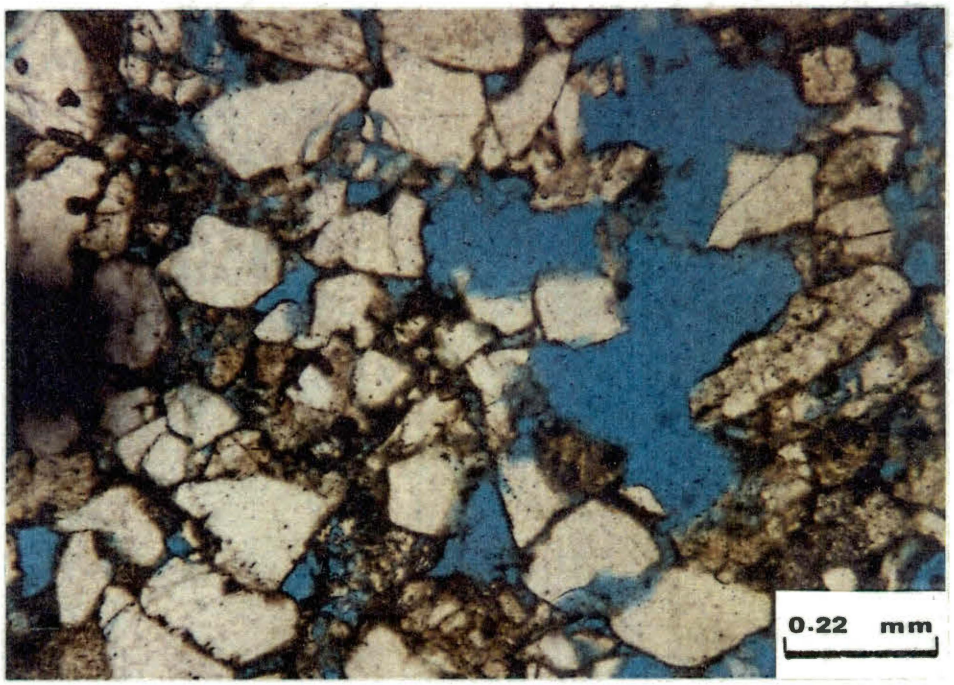

Figure 71. A Microphotograph showing Oversized Pore Spaces indicating Secondary nature of Porosity; Plane Polarized.

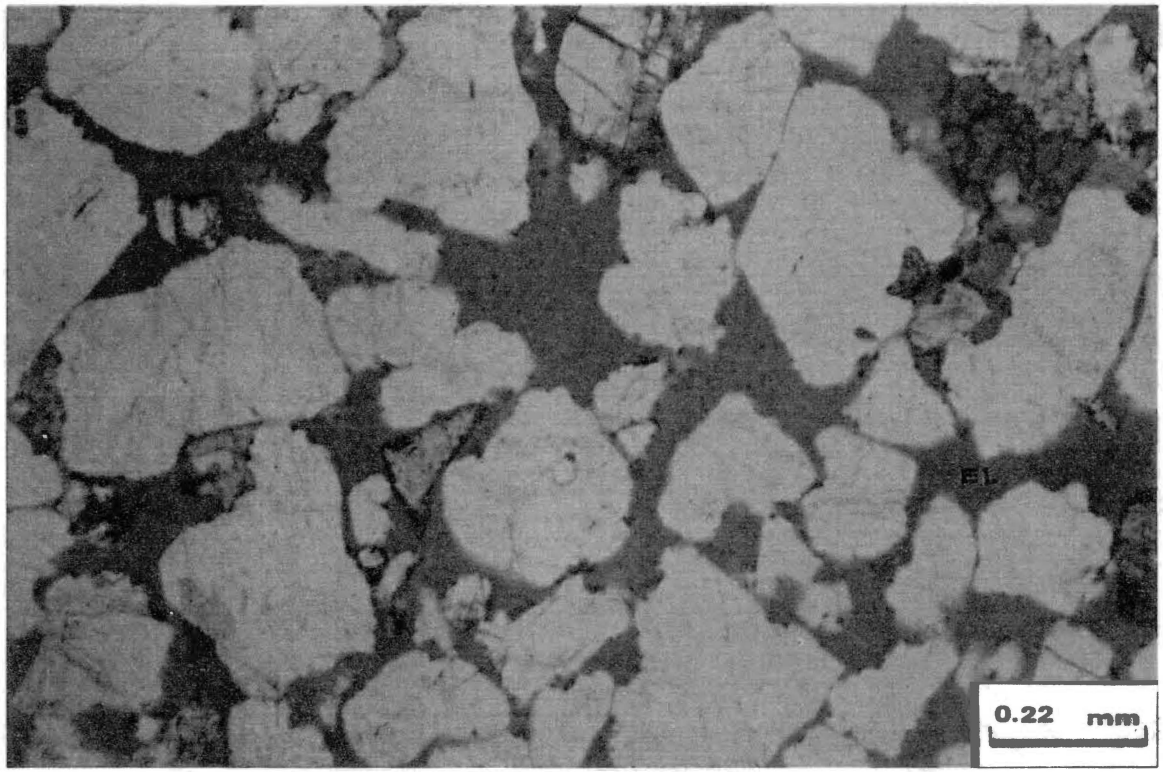

Figure 72. A Microphotograph showing Elongate Pore Spaces (EL) also indicating Secondary Porosity; Plane Polarized.

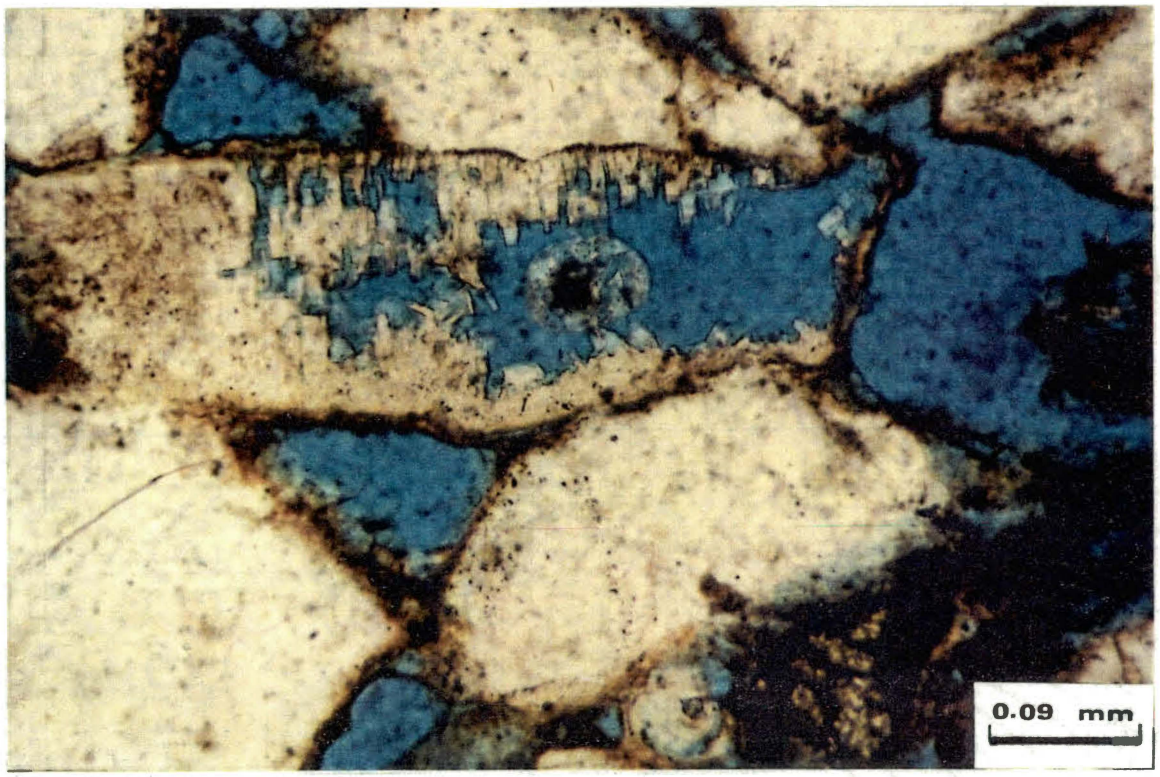

Figure 73. A Microphotograph showing Honeycomb Structure due to Partial Dissolution of Feldspar; Plane Polarized.

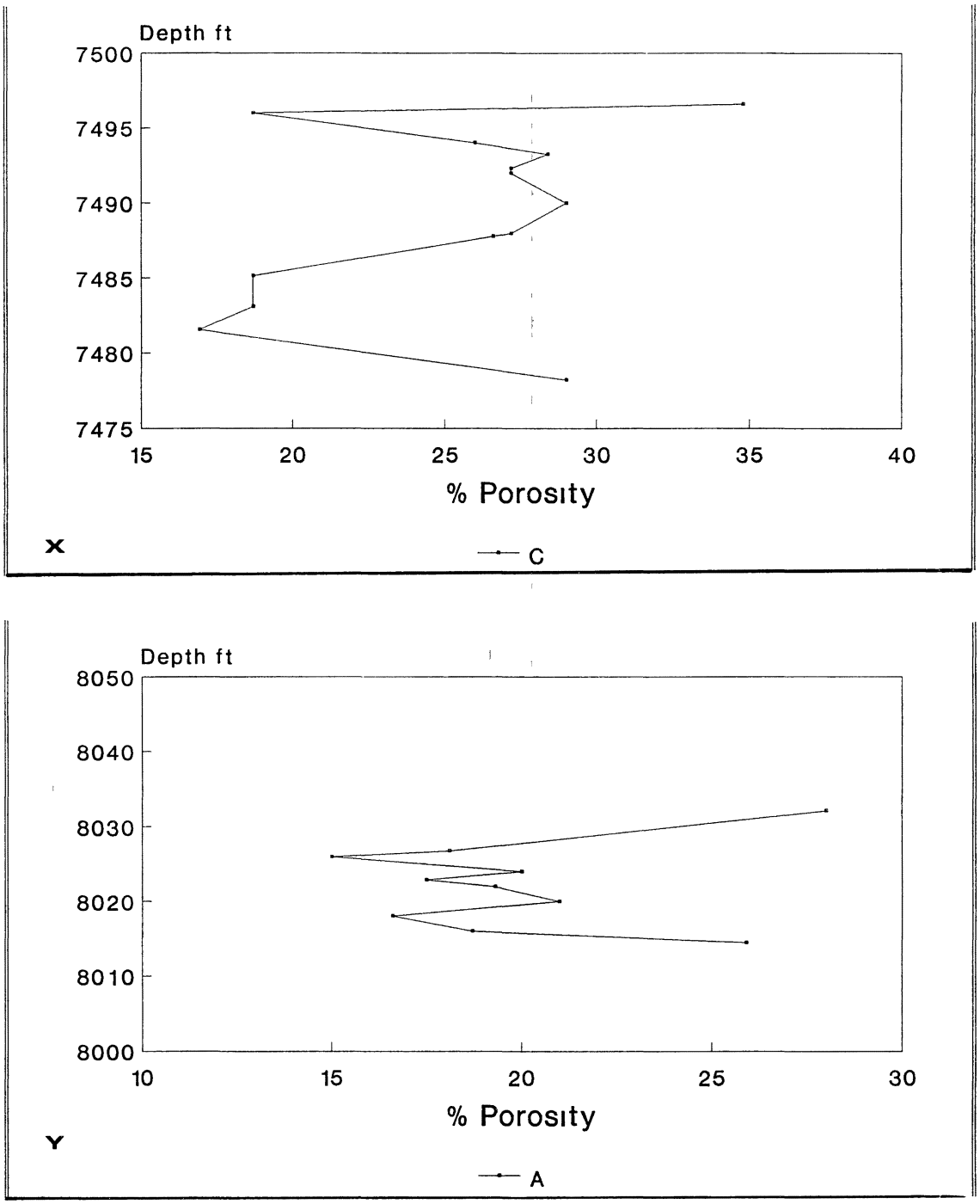

Figure 74. Plots of Porosity versus Depth, X for Aradeiba-C (Unity #11); Y for Aradeiba-A (Unity #9).

included in the authigenic clay mineral cements. The total average secondary porosity is estimated at 5.65% with a range varying from trace to 14%. Microphotograph restoration (Figures 75 and 76) gives a useful qualitative idea of the dissolution-related secondary porosity in the rocks of the Aradeiba Formation. Evidence from thin sections led the author to believe that the newly-formed secondary pores are locally occupied by kaolinite cement. However, this can be attributed to turbulent flow of the drilling fluid causing a "brushing effect" on the kaolinite cement.

Reservoir Quality:

The fact that diagenesis plays a very significant role in molding the petrophysical qualities of sedimentary reservoirs has been stated repeatedly in the literature. In the sediments of the Aradeiba Formation porosities and permeabilities have been rapidly reduced and, later on, developed and enhanced by various diagenetic phenomena. The initial composition of the sediments has, undoubtedly, been a major factor in deciding which diagenetic processes would dominate leaving greater impacts on the reservoir qualities. Naturally other elements such as the subsidence rate, the geothermal gradient, the depositional environments and the proximity from the source area are

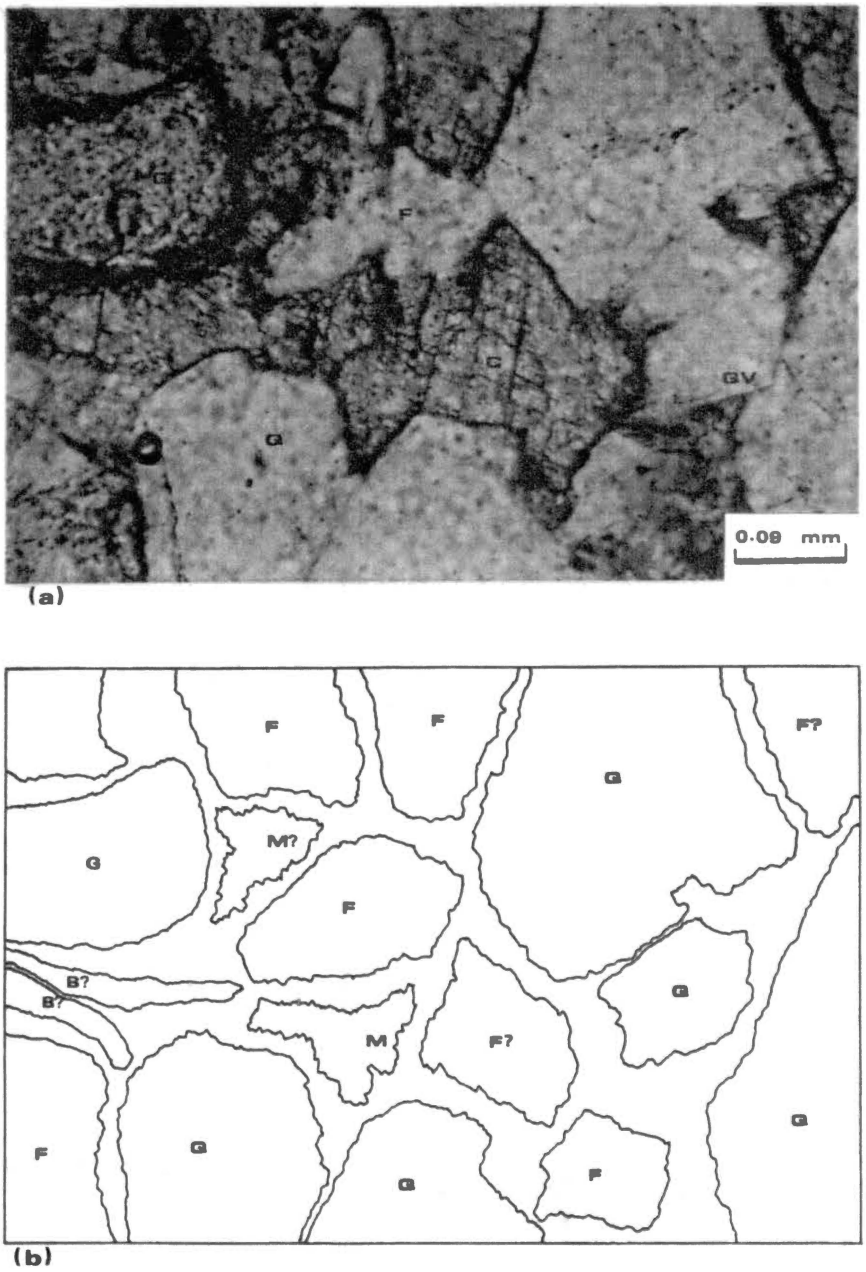

Figure 75. A Microphotograph (a) restored to the state of "No Diagenesis" (b) to illustrate the loss of Porosity resultant from various Diagenetic Processes. F = Feldspar; Q = Quartz; M? = Probably Matrix; G = Garnet; B? = Probably Biotite.

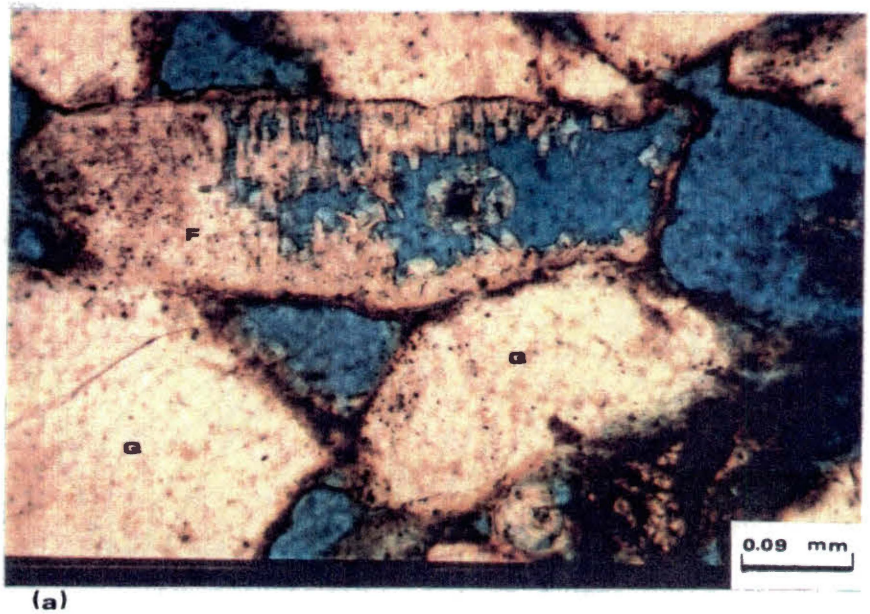

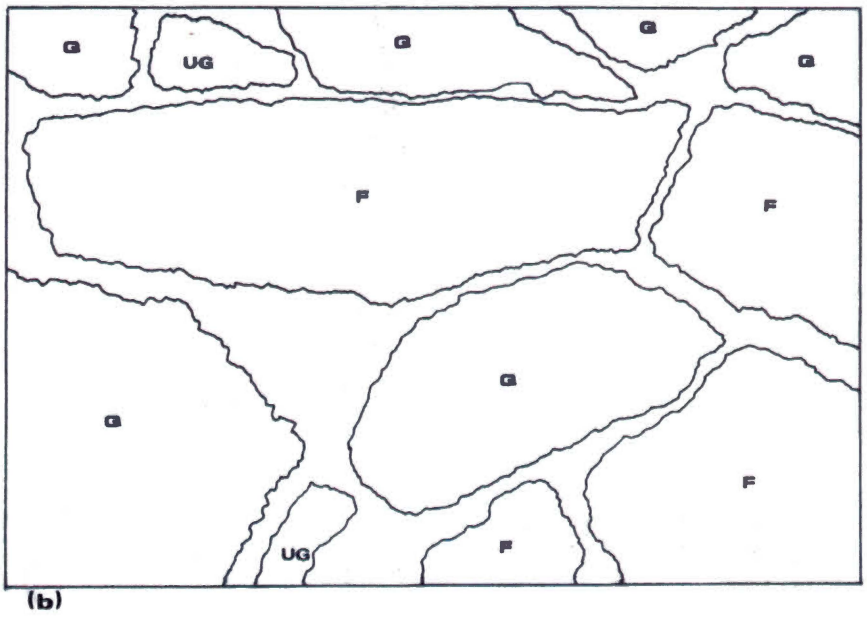

Figure 76. A Microphotograph (a) restored to the state of "No Diagenesis" (b) to demonstrate how Diagenetic Processes created Secondary Porosity. Q = Quartz; UG = Unidentified Grain; F = Feldspar.

quite significant. The majority of the samples studied, are subarkosic according to Folk's (1968) classification of sandstones (see Chapter V), obviously due to the high feldspar content. Figures 75 and 76 in which microphotographs are restored to the state of "no diagenesis" except for compaction, indicate that the initial sediment-composition must have had substantial amounts of feldspar grains and other subtle constituents with low chemical stabilities. This should give us a clearer idea about the loss of primary porosity and hence permeability caused by compaction. However, these feldspar grains were, later on, proved to be a vital source of secondary porosity caused by their dissolution. This phenomenon has been observed in all three members of the Aradeiba Formation. However, it is more noticeable in the sands of the Aradeiba C-member, which seems to have lost most of its primary porosity. The remarkable array of diagenetic cements, particularly authigenic clay minerals have a rather obvious impact on the reservoir quality. In the Aradeiba B and A members extensive amounts of smectite, illite and less chlorite and kaolinite have increased the surface area and created microporosity in the pores and pore-throats. This has accordingly increased the amount of irreducible water and decreased the effective intergranular macroporosity and

therefore, probably, lowered the permeability. However, the sands of the Aradeiba A-member possess substantially higher porosities (Appendix A) as compared to those of the B-member. The Aradeiba C-member which is relatively clean, contains appreciable amounts of kaolinite and some isopachous chlorite that also contributed to porosity and permeability damage. The tremendous moldic porosity in the Aradeiba C-member appears to be mostly isolated and therefore, one would probably expect relatively low permeability. According to Chevron Oil Company, oil has been recovered from all three members of the Aradeiba Formation. The Aradeiba A-member produces up to over 3600 B/D (for an individual well) with gravities range between 20 and 36 A.P.I. degrees. The poor quality B-member has a maximum productivitiy rate below 300 B/D with gravities in the range of 13 to 31 A.P.I. degrees. The cleaner C-member produced under 300 B/D of mostly lighter oil with 36 A.P.I. degrees.

CHAPTER VIII

REMARKS, CONCLUSIONS AND RECOMMENDATIONS

1. This huge basın in southcentral Sudan has been referred to as "The Muglad Block" or "The Muglad Basin" by Chevron after a small town on the northwestern portion of the basın. In this study it has been thought more appropriate to use the name "The Abu Gabra Basın," in mınd is the fact that the first published gravity work on the area (Browne and Fairhead, 1983) referred to the hosting rift as the Abu Gabra Rıft. Furthermore, the first discovery well drilled in the basin by Chevron ıs called Abu Gabra. For these reasons the name "Abu Gabra Basin" has been used throughout thıs investigatıon.

2. The Abu Gabra Basın is a rift basin situated on the eastern portıon of the Central African Rift.

3. The structural style of the basın and the study area is characterized by a complex layout of rift normal and normal lystric faults that locally exhibit a growth nature.

4. The notıon "Nubian Sandstone Formatıon" is not appropriate any further, after the drilling for oil has proved extensive thıckness, diversity ın rock facies and

sedimentary structures for the Mesozoic System in Sudan interior.

5. The Aradeiba Formation (Upper Cretaceous-Turonian) represents the lowermost member of the Darfur Group. It consists of thick intervals of fine flood-plain sediments interbedded with up to 80-feet-thick sandstone intervals, designated C, B, and A.

6. Eight lithofacies could be recognized in the rocks of the Aradeiba Formation, on the basis of variation in lithology and sedimentary structures.

7. The studied samples of the Aradeiba Formation sandstone mainly classify as subarkose according to the Folk's 1968 sandstone classification.

8. Quartz, feldspars and rock fragments are the major detrital constituents, with mica and heavy minerals, specially garnet, as minor elements in the composition of the Aradeiba rocks.

9. Clay minerals (smectite, illite, kaolinite, chlorite and 7 Å chlorite) and calcite are the prominent diagenetic products with other diagenetic cements including pyrite, silica and feldspar overgrowths which are of a lesser quantitative significance.

10. The Aradeiba Formation was deposited within a meandering system belt in channel and basin flood-plain environments. A marginal lacustrine environment is suggested for those very fine rhythmic sandstones, siltstones and the dark and very dark gray claystones.

11. Diagenesis has played a greater role in shaping and reshaping the fabric of the Aradeiba Formation sandstones. Compaction, precipitation, alteration, dissolution and replacement are major episodes in the diagenetic history of the Aradeiba Formation rocks.

12. Feldspar grains have suffered the most of diagenetic dissolution, both partial and complete. Calcite, rock fragments, and detrital matrix experienced a lesser degree of dissolution.

13. The noticeable lack of silica cement is attributed to several probable factors, such as the early clay mineral coating of the quartz grains or the absence of effective vertical fluid circulation. However, it should be noted that the localized occurrences of quartz overgrowths were interpreted as such, because of the clearly diagenetic sharp angles developed around the quartz grains. No typical dust-rims were observed. In this regard a thermoluminescence study will be worthwhile to estimate with more accuracy the actual amount of overgrowth.

14. The total present porosity average is 15.%.

15. Tremendous amount of secondary porosity has been created by dissolution of the fragile framework grains and cement.

16. Kaolinite cementation is continually destroying both primary and secondary porosity.

17. The A-sandstone member of the Aradeiba Formation possesses the best petrophysical properties, very high porosity (locally up to 32%) and hence probably excellent permeability and deliverability. This member, however, contains a considerable amount of finer grained sediments that possess extensive micropore spaces.

18. The quality of the B-sandstone member is noticeably poor and its sand-to-clay ratio is considerably low. This member deteriorates going to the east and west away from the axis of the Unity Field.

19. The C-sandstone member is the cleanest with an overall greater thickness compared to the upper members. However, it seems to have lost most of its primary porosity, and the vast secondary porosity created through moldic dissolution is mostly disconnected. Fracturing might be a good suggestion to better produce from this member of the Aradeiba Formation.

20. Pore-clogging, resulting from the migration of the extensive kaolinite cement, should be expected if turbulent flow is applied during the development drilling stages.

REFERENCES CITED

Almon, W.R., 1984, Sandstone Diagenesis: Applications to Exploration and Exploitation. Denver, Colorado, Anadarko Production Company, 97 p.

Al-Shaieb, Z., and J.W. Shelton, 1981, Migration of Hydrocarbons and Secondary Porosity in Sandstones: Amer. Assoc. Petroleum Geologists Bull., V. 65, No. 11, p. 2433-2436.

Asquith, G., 1982, Basic Well Log Analysis for Geologists: Methods in Exploration Series, AAPG, Tulsa, Oklahoma, 216 p.

Avbovbo, J.A., E.O. Ayoola, and G.A. Osahon, 1986, Depositional and Structural Styles in Chad Basin of Northeastern Nigeria; AAPG Bull., V. 70, p. 1787-1798.

Baker, B.H., and J. Wohlenberg, 1971, Structure and Evolution of the Kenya Rift Valley: Nature, V. 229, p. 538-542.

_____, P.A. Mohr, and Williams, L.A.J., 1972, Geology of the Eastern Rift System of Africa: Geological Society of America. Special Paper 136, 67 p.

Bermingham, P.M., J.D. Fairhead, and G.W. Stuart, 1983, Gravity Study of the Central African Rift System: A Model of Continental Disruption. 2. The Darfur Domal Uplift and Associated Cainozoic Volcanism, in P. Morgan, ed., Processes of Continental Rifting Tectonophysics, V. 94, p. 205-222.

Browne, S.E., and J.D. Fairhead, 1983, Gravity Study of the Central African Rift System: A Model of Continental Disruption. 1. The Ngaoundere and Abu Gabra Rifts: Tectonophysics, V. 94, p. 187-203.

Browne, S.E., J.D. Fairhead, and I.I. Mohamed, 1985, Gravity Study of the White Nile Rift, Sudan, and its Regional Tectonic Setting: Tectonophysics, 113(1-2), p. 123-137.

Burke, K. and J.F. Dewey, 1974, Two Plates in Africa During the Cretaceous? Nature, V. 249, p. 313-316.

_____ and J.T. Wilson, 1972, Is the African Plate Stationary? Nature, V. 239, p. 387-390.

Burst, J.F., 1969, Diagenesis of Gulf Coast Clayey Sediments and its possible relation to Petroleum Migration; AAPG Bull., V. 53, No. 1, p. 73-93.

Carroll, D., 1970, Clay minerals: a guide to their x-ray identification, The Geological Society of America, Boulder Colorado, Special Paper 126, 80 p.

Davis, R.J., Jr., 1983, Depositional Systems; a genetic approach to sedimentary geology: Prentice-Hall, Inc., New Jersey, 669 p.

Edwards, W.N., 1926, Fossil Plants from the Nubian Sandstone of Eastern Darfur. Q. J. Geol. Soc. London, V. 82: p. 94-100.

Folk, R.L., 1974, Petrology of Sedimentary Rocks: University of Texas, Hemphill Publ. Co., 182. p.

Galloway, W.E. and D.K. Hobday, 1983, Terrigenous Clastic Depositional Systems: Springer-Verlag, New York, p. 115-184.

Girdler, R.W., 1958, The Relationship of the Red Sea to the East African Rift System: Geol. Soc. London. Quart. Jour., V. 114, Pt. 1, No. 453, p. 79-105.

Girdler, R.W., J.D. Fairhead, R.C. Searle, and W.T. Sowerbutts, 1969, Evolution of Rifting in Africa: Nature, V. 224, p. 1178-1182.

Gordon, S.F., and Lee Suttner, 1986, Alluvial Fans and Fan Deltas: A Guide to Exploration for Oil and Gas. IHRDC, Publishers, Boston, MA, p. 1-66.

Hunt, J.M., 1979, Petroleum Geochemistry and Geology: A Series of Books in Geology, Editor: James Gilluly, W.H. Freeman and Company, San Francisco, 617 p.

Jonas, E.C., and E.F. McBride, 1977, Diagenesis of Sandstones and Shale: Application to Exploration for Hydrocarbons. Austin, Texas, Department of Geological Sciences, The University of Texas at Austin Continuing Education Program Publication No. 1, 164 p.

Krauskopf, K.B., 1979, Introduction to Geochemistry: McGraw Hill Book Co., New York, 617 p.

Lawyer, L.C. and B.V. Kay, 1984, The Challenge of the Sudan: Geophysics: The Leading Edge of Exploration. February, p. 26-28.

Louis, C. and G.H. Goudarzi, 1976, Stratigraphic and Tectonic Framework of Libya AAPG, Foreign Reprint Series No. 1, Amer. Assoc. Petr. Geol., Tulsa, Oklahoma, p. 5-16.

Lowell, J.D. and G.J. Genik, 1972, Sea Floor Spreading and Structural Evolution of Southern Red Sea: AAPG Bulletin, V. 56, p. 247-259.

Mahfouz, S.A., A.M. Abou-Khadrah, and B. Mabrouk, 1980, Petrographic, Mineralogical and Geochemical Studies on the Nubian Sandstone and the Umm Ruwaba Formation of East Kordofan, Sudan, part 1: Bull. of the Faculty of Science, Assiut Univ., V. 49, p. 341-365 (Arabic Sum.).

Markert, J.C., and Z. Al-Shaieb, 1984, Diagenesis and Evolution of Secondary Porosity in Upper Minnelusa Sandstones, Powder River Basin, Wyoming: p. 367-389.

McBride, E.F., and E.C. Jonas, 1977, Diagenesis of Sandstone and Shale: application to exploration for hydrocarbons, Department of Geological Sciences, The University of Texas at Austin, Austin, Texas, Continuing Education Program Publication No. 1, p. 10-22.

McDonald, David A., and Ronald C. Surdam, 1984, Clastic Diagenesis: AAPG Memoir 37. Tulsa, Oklahoma, The Amer. Assoc. Petr. Geol. 434 p.

McKenzie, D., 1978, Some Remarks on the Development of Sedimentary Basins. Earth Planet. Sci. Lett., V. 40; p. 25-32.

McKenzie, D.P., D. Davies, and P. Molnar, 1970, Plate Tectonics of the Red Sea and East Africa: Nature, V. 226, No. 5242, p. 243-248.

Medani, A.H., and J.R. Vail, 1974, Post Cretaceous Faulting in Sudan and its Relationship to the East African Rift System: Nature, V. 248, p. 133-135.

Nesse, W.D., 1986, Introduction to Optical Mineralogy, New Yourk, Oxford University Press, 325 p.

Parker, A., and B.W. Sellwood, 1983, Sediment Diagenesis. Boston, D. Reidel Publishing Company, p. 57-288.

Perry, E., and J. Hower, 1970, Burial Diagenesis in Gulf Coast Pelitic Sediments; Clays and Clay Minerals, V. 18, p. 165-177.

Pettijohn, F.J., and P.E. Potter, 1964, Atlas and Glossary of Primary Sedimentary Structures. Springer-Verlag, New York, Inc., 370 p.

Reading, H.G., 1986, Sedimentary Environments and Facies: (2nd ed.) Elsevier, New York, 613 p.

Roberts, D.G., 1969, Structural Evolution of the Rift Zones in the Middle East: Nature, V. 223, No. 5201, p. 55-57.

Schmidt, V., and D.A. McDonald, 1979, The Role of Secondary Porosity in the Course of Sandstone Diagenesis: in Aspects of Diagenesis, Soc. Econ. Paleon. and Min., Spec. Publ. No. 26, p. 175-207.

_____, and _____, 1979, Texture and Recognition of Secondary Porosity in Sandstones: in Aspects of Diagenesis, Soc. Econ. Paleon. and Min., Spec. Publ. No. 26, p. 208-226.

Scholle, P.A., and D. Spearing, 1982, Sandstone Depositional Environments: AAPG, Memoir 31, Amer. Assoc. Petr. Geol., Tulsa, Oklahoma, 410 p.

Scholle, P.A., and P.R. Schluger, 1979, Aspects of Diagenesis. Tulsa, Oklahoma, Soc. Econ. Paleo. Miner., p. 125-242.

Schull, T.J., 1988, Rift Basins of Interior Sudan: petroleum exploration and discovery. Amer. Assoc. Petr. Geol., Tulsa, Oklahoma. AAPG Bull., V. 72, N. 10 (October 1988), p. 1128-1142.

Whiteman, A.J., 1971, The Geology of the Sudan Republic: Clarendon Press, Oxford, 290 p.

Wilson, M.D., and E.D. Pittman, 1977, Authigenic Clays in Sandstones: Recognition and Influence on Reservoir Properties and Paleonvironmental Analysis: Jour. of Sed. Petr., V. 47, No. 1, p. 3-31.

APPENDICES

APPENDIX A

THIN SECTION DATA

Well Name	U #8	U #9	U #9	U #11	U #11	U #11	U #11	U #11	U #11
Depth	7374.1	8402.9	8409.75	7478 45	7481.55	7483 1	7485 15	7487.8	7492.3
Strat Unit	AR-C	AR-C	AR-C	AR-C	AR-C	AR-C	AR-C	AR-C	AR-C
DETRITAL									
CONSTITUENTS	66 0	63 0	72 0	83 5	81 0	70 0	86 0	78 0	83 0
Quartz	52.0	46.0	54 0	54.0	50 0	36 0	68 0	51.0	67.0
Monocrystalline	52.0	46 0	53 0	53.5	50.0	35 0	67 0	50 5	66.0
Polycrystalline	TR	TR	1.0	0 5	TR	1 0	1 0	0.5	1.0
Feldspar	4.0	11 0	9 0	11 0	14 0	21 0	10 0	11 0	8 0
K-Feldspar	3 5	8 5	7.0	9 0	12 0	16 0	9 0	9 5	5 0
Plagioclase	0 5	2 5	2 0	2 0	2 0	5 0	1 0	1 5	3 0
Rock Fragments	6 0	2 0	4 0	4 0	4 5	4 0	1 0	3 0	2 0
Chert	TR	TR	1 0	0 5	TR	0 5	TR	TR	TR
Siltstone	2 0	0 5	TR	TR	0 5	TR	TR	TR	-
Claystone	1 0	0 5	0.5	1 0	2.0	2 0	TR	2.0	1.5
Metamorphic	3 0	1 0	2 0	2 0	1 5	1 0	0 5	1 0	TR
Other Grains	4 0	3 0	2 0	4 0	1 5	2 0	2 0	4 0	1.0
Muscovite	1 0	0 5	TR	0 5	TR	TR	0 5	IR	TR
Biotite	2.0	1 5	TR	1 0	0.5	TR	1.0	1 0	TR
Garnet	1.0	1 0	0 5	TR	TR	TR	TR	2 0	TR
Chlorite	TR	TR	0 5	TR	TR	-	TR	TR	-
Zircon	-	TR	TR	0.5	-	TR	-	TR	-
Tourmaline	-	TR	TR	TR	TR	IR	TR	TR	TR
Plant Material	TR	TR	TR	1 0	-	1 0	TR	TR	-
Matrix	3.0	1 0	3.0	10 5	11 0	7.0	5 0	9.0	5.0
Clay Clasts	2 0	1 0	2 0	10 0	10 5	7 0	5 0	9 0	4.5
Chlorite	TR	TR	IR	-	TR	TR	-	-	TR
Silt	1	TR	0.5	TR	TR	TR	-	TR	TR
DIAGENETIC									
CONSTITUENTS	32 0	16 0	15 0	4 0	7 0	11 0	3 5	8 0	2 0
Cements	29 0	2 0	2 0	TR	1 0	1 0	TR	2 0	-
Silica	-	TR	TR	-	-	-	-	-	-
Feldspar	-	TR	TR	-	0 5	TR	-	-	-
Calcite	28 0	1 0	1.0	TR	TR	0 5	IR	1 5	-
Pyrite	1 0	0 5	0 5	TR	TR	TR	-	TR	-
Authegenic Clays	3 0	14 0	13 0	3 0	6 0	10 0	3 0	6 0	2 0
Kaolinite	TR	TR	-	2 5	5 0	6 0	3 0	5 5	1 5
Smectite	1.0	11 0	TR	-	-	3 0	-	-	-
Illite	TR	2 0	2 0	TR	0 5	IR	-	TR	IR
Chlorite	TR	IR	10 0	TR	TR	IR	-	TR	TR
Porosity	1 0	17 0	12 0	12 0	11 0	13 0	10 0	14 0	14 0
Primary	TR	9 0	5 0	7 0	7 0	8 0	4 0	8 0	5 0
Secondary	1 0	8 0	7 0	5 0	4 0	10 0	6 0	6 0	9 0

Well Name	U #11	U #11	T #2	U #9	U #11	U #11	U #2	U #2
Depth	7493 25	7496 6	8628 2	8236 4	7268 2	7274 15	7868 4	7869 0
Strat Unit	AR-C	AR-C	AR-C	AR-B	AR-B	AR-B	AR-A	AR-A
DETRITAL								
CONSTITUENTS	79.0	80 0	76 0	59 0	84 0	73 0	73 0	71 0
Quartz	61 0	55 0	53 0	34 0	54 5	51 0	56 0	54.0
Monocrystalline	59 0	53 0	53 0	34 0	55 5	50 5	55 0	54 0
Polycrystalline	2 0	2 0	TR	TR	0 5	0 5	1 0	-
Feldspar	12 0	13 0	8 0	5 0	5 0	6 0	3 0	5 0
K-Feldspar	10 0	12 0	6 0	4 0	3 0	5 5	2 5	3 0
Plagioclase	2 0	10 0	2 0	1 0	2 0	0 5	0 5	2 0
Rock Fragments	2 0	6 0	7 0	5 0	5 0	4 0	2 0	3 0
Chert	TR	0 5	1 0	TR	TR	TR	-	TR
Siltstone	TR	1 0	TR	1 0	1 0	TR	1 0	-
Claystone	1 0	2 0	3 0	2 0	3 0	1 0	0 5	1 0
Metamorphic	0 5	2 5	2 5	1 5	0 5	2 5	0 5	1.5
Other Grains	2 0	1 0	6 0	1 0	2 0	2 0	2 0	1.0
Muscovite	TR	TR	0 5	TR	0 5	TR	1 0	TR
Biotite	TR	TR	2 5	TR	1 0	0 5	TR	TR
Garnet	TR	TR	1 0	TR	TR	0 5	0.5	TR
Chlorite	-	-	TR	-	TR	TR	TR	-
Zircon	TR	TR	TR	TR	-	-	-	TR
Tourmaline	TR	-	TR	TR	TR	TR	-	TR
Plant Material	0.5	TR	TR	TR	TR	TR	-	TR
Matrix	2.0	5.0	2 0	14 0	17 0	10 0	10 0	8.0
Clay Clasts	2 0	5.0	2 0	13 0	16 0	9 0	8.0	7.0
Chlorite	-	-	-	-	TR	TR	TR	-
Silt	-	-	TR	1 0	TR	TR	1 5	1 0
DIAGENETIC								
CONSTITUENTS	8 5	7 0	10 0	27 0	6 5	4 0	5 5	9 5
Cements	TR	4.0	TR	4 0	TR	-	1 0	TR
Silica	-	-	TR	3 0	-	-	-	-
Feldspar	-	-	-	TR	-	-	-	-
Calcite	-	4 0	-	TR	-	-	1 0	TR
Pyrite	TR	TR	-	TR	TR	-	-	TR
Authegenic Clays	8 0	3 0	9.0	23 0	6.0	4 0	4 5	9.0
Kaolinite	6 5	2 5	3 0	17 5	5 0	3 5	4 0	7 0
Smectite	1 0	TR	-	2 0	-	-	TR	-
Illite	TR	TR	5 5	3 0	TR	TR	0 5	1 5
Chlorite	TR	TR	TR	TR	TR	TR	TR	TR
Porosity	12.0	13 0	14 0	14 0	9 5	23 0	18 0	19 5
Primary	5 0	10 0	6 0	10 0	7 5	20 0	8 0	16 0
Secondary	7.0	3 0	8 0	4 0	2 0	3.0	10.0	3.5

Well Name	U #2	U #2	U #2	U #2	U #2	U #2	U #9	U #9
Depth	7869 9	7870.8	7871 3	7872 7	7873 0	7873 1	8014 45	8022 9
Strat Unit	AR-A	AR-A	AR-A	AR-A	AR-A	AR-A	AR-A	AR-A
DETRITAL								
CONSTITUENTS	70 0	67 0	68 0	65 0	67 0	69 0	67 0	94 0
Quartz	50 0	56 0	48 0	53 0	54 0	52 0	53 0	36 0
Monocrystalline	50 0	54.0	48 0	52 0	53 0	51 0	51 0	35 0
Polycrystalline	TR	2.0	TR	1 0	1 0	1 0	2 0	1 0
Feldspar	3 0	4.0	5 0	2 0	4 0	4 0	6 0	8 0
K-Feldspar	3 0	3.0	3 0	2 0	3 0	3 0	4 0	6 5
Plagioclase	TR	1 0	2 0	-	1 0	1 0	2 0	1 5
Rock Fragments	4 0	1.0	5 0	3 0	3 0	2 0	3 0	3 0
Chert	TR	-	-	-	TR	-	TR	TR
Siltstone	1 0	0 5	1 0	TR	-	TR	-	TR
Claystone	1 0	-	3 0	1 0	1 0	TR	0 5	1 0
Metamorphic	2 0	0.5	1 0	2 0	2 0	1 5	2 0	1 5
Other Grains	2 0	TR	3 0	2 0	1 0	2 0	3 0	12 0
Muscovite	TR	-	TR	1 0	TR	TR	TR	2 0
Biotite	1 0	TR	TR	TR	TR	0 5	TR	3 0
Garnet	TR	-	1 0	TR	0 5	0 5	1 50	4 0
Chlorite	TR	-	TR	-	TR	TR	TR	TR
Zircon	-	-	TR	-	TR	TR	TR	TR
Tourmaline	-	-	TR	0 5	TR	-	TR	TR
Plant Material	TR	-	TR	TR	TR	TR	TR	2.0
Matrix	11 0	6 0	7 0	5 0	5 0	9 0	2 0	35 0
Clay Clasts	9 0	5 0	5 0	4 0	4 5	7 0	2 0	34.0
Chlorite	TR	-	TR	TR	TR	-	TR	TR
Silt	2 0	1 0	2 0	1 0	TR	2 0	TR	TR
DIAGENETIC								
CONSTITUENTS	17 0	9 0	12 0	8 0	11 0	10 0	20 0	0 5
Cements	3 0	4 0	4 5	2 0	3 0	3 0	1 0	TR
Silica	TR	TR	-	TR	-	-	-	-
Feldspar	TR	-	-	-	TR	-	-	-
Calcite	2 0	3 0	4 0	1 0	2 5	2 0	TR	TR
Pyrite	TR	TR	0 5	TR	TR	TR	TR	TR
Authegenic Clays	14 0	5 0	7 0	6 0	8 0	7 0	19.0	0 5
Kaolinite	10 0	4 0	6 0	3 0	7 0	5 0	TR	-
Smectite	3 0	TR	0 5	1 0	-	TR	-	-
Illite	1 0	TR	TR	1 0	TR	0.5	TR	TR
Chlorite	-	TR	TR	TR	TR	TR	18 0	TR
Porosity	12 0	18 0	20 0	20 0	22.0	18 0	13 0	5 0
Primary	4.0	12 0	12 0	15 0	19 5	12 0	9 0	2.0
Secondary	8 0	6 0	8 0	5 0	2 5	6.0	4 0	3.0

Well Name	U #9	U #9	U #11	U #11	U #11	U #11	U #11	U #11	T #3
Depth	8026 8	8032 1	7065 0	7067 0	7068 45	7073 6	7076 1	7080 1	8231 5
Strat Unit	AR-A	AR-A	AR-A	AR-A	AR-A	AR-A	AR-A	AR-A	AR-A
DETRITAL									
CONSTITUENTS	61 5	58 0	70 5	77 5	76 5	81 0	64 0	73 5	61 5
Quartz	50 0	48 0	52	56 0	65 0	67 0	48 0	58 0	43 0
Monocrystalline	48 0	46 0	50 5	56 0	64 5	65 0	48 0	57 0	42 5
Polycrystalline	2 0	2 0	0 5	TR	0 5	2 0	TR	1 0	0 5
Feldspar	6 0	5 0	7 0	8 0	6 0	10 0	9 0	7 0	8 0
K-Feldspar	4 0	3 5	6 0	7 0	5 0	9 0	8 5	6 5	5 0
Plagioclase	2 0	1 5	1 0	1 0	1 0	1 0	0 5	0 5	3 0
Rock Fragments	4 0	4 0	3 0	3 0	3 0	3 0	TR	3 0	2 0
Chert	TR	TR	-	TR	-	-	-	TR	-
Siltstone	1 0	1 0	TR	TR	TR	TR	-	TR	-
Claystone	1 0	0 5	2 0	1 0	2.0	2 5	-	1 0	1 0
Metamorphic	1 5	2 0	0 5	1 0	1 0	0 5	TR	1 5	1 0
Other Grains	1 0	0 5	8 0	10 0	2 0	1 0	6 0	5 0	8 0
Muscovite	-	-	0 5	2 0	TR	TR	2 0	1 0	1 0
Biotite	TR	TR	1 0	3 5	1 0	TR	3 0	3 0	3 0
Garnet	TR	TR	3 0	2 5	0 5	TR	TR	0 5	3 0
Chlorite	-	-	0 5	TR	TR	-	-	-	TR
Zircon	TR	-	TR	TR	TR	TR	-	TR	0 5
Tourmaline	TR	TR	0 5	TR	TR	TR	TR	TR	0 5
Plant Material	TR	TR	TR	-	TR	TR	TR	TR	-
Matrix	TR	0 5	TR	TR	-	-	TR	TR	TR
Clay Clasts	TR	TR	TR	TR	-	-	TR	TR	-
Chlorite	-	-	-	-	-	-	-	-	-
Silt	-	TR	-	-	-	-	-	-	TR
DIAGENETIC									
CONSTITUENTS	14 5	12 0	22 0	16 0	8 5	5 5	26 5	22 0	16 5
Cements	0 5	3 0	4 0	TR	TR	TR	TR	-	0 5
Silica	-	1 0	-	-	-	-	-	-	TR
Feldspar	-	Tr	-	-	-	-	-	-	-
Calcite	TR	-	4 0	-	-	-	-	-	-
Pyrite	TR	TR	TR	TR	TR	TR	TR	-	TR
Authegenic Clays	14 0	9 0	18 0	15 5	8 0	5 0	26 0	22 0	16 0
Kaolinite	8 0	7 0	-	-	-	-	-	-	13 0
Smectite	TR	TR	17 0	15 0	7 5	4 5	25 0	21 5	TR
Illite	5 5	1 5	TR	TR	TR	TR	0 5	TR	2 5
Chlorite	TR	TR	TR	TR	TR	TR	0 5	TR	TR
Porosity	24 0	30 0	8 5	6 5	15 0	13 5	9 5	4 5	22 0
Primary	12 0	16 0	3 5	4 0	9 0	6 5	4 5	3 0	10 0
Seconday	12 0	14 0	5 0	2 5	6 0	7 0	5.0	1 5	12 0

Well Name	T #2	T #2	T #2	T #2	T #2	T #2
Depth	8235 3	8237 4	8239 4	8241 5	8244 0	8245 0
Strat Unit	AR-A	AR-A	AR-A	AR-A	AR-A	AR-A
DETRITAL						
CONSTITUENTS	66 0	70 0	64 0	63 0	68 0	71 5
Quartz	58 0	46 0	48 0	53 0	56 0	58 0
Monocrystalline	57 0	45 0	48 0	52 0	55 5	56 0
Polycrystalline	1 0	1 0	TR	1 0	0 5	2 0
Feldspar	3 0	10 0	7 0	4 0	6 0	6 0
K-Feldspar	1 0	9 5	6 0	4 0	5 0	5 5
Plagioclase	2 0	0 5	1 0	TR	1 0	0 5
Rock Fragments	3 0	3 0	3 0	1 0	2 0	6 0
Chert	TR	TR	-	-	-	TR
Siltstone	TR	0 5	1 0	TR	TR	1 0
Claystone	1 5	1 0	1 0	0 5	1 0	3 0
Metamorphic	1 0	1 0	1 0	0 5	0 5	1 5
Other Grains	1 5	9 0	2 0	2 0	4 0	1 0
Muscovite	TR	2 0	TR	-	TR	-
Biotite	0 5	4 0	TR	TR	TR	TR
Garnet	0 5	2 0	TR	TR	2 0	0 5
Chlorite	TR	TR	-	-	TR	TR
Zircon	TR	TR	TR	-	0 5	TR
Tourmaline	-	TR	-	TR	TR	TR
Plant Material	-	TR	TR	TR	TR	-
Matrix	TR	2 0	4 0	3 0	-	TR
Clay Clasts	TR	2 0	2 0	1 0	-	TR
Chlorite	-	-	-	-	-	-
Silt	-	-	2 0	2 0	-	-
DIAGENETIC						
CONSTITUENTS	5 0	11 0	11 0	9 0	8 0	11 0
Cements	3 0	1 0	2 0	1 0	4 0	6 0
Silica	TR	TR	TR	TR	2 0	2 0
Feldspar	-	-	-	-	TR	-
Calcite	2 5	1 0	TR	TR	1 0	4 0
Pyrite	TR	-	TR	TR	TR	-
Authegenic Clays	2 0	10 0	9 0	7 0	4 0	5 0
Kaolinite	2 0	8 0	5 0	4 0	3 0	4 0
Smectite	-	-	3 0	1 0	-	-
Illite	-	1.5	1 0	1 5	0 5	0 5
Chlorite	TR	TR	-	TR	TR	TR
Porosity	29 0	19 0	26 0	28 0	24 0	17 5
Primary	19 0	13 0	14 0	20 0	13 0	15 0
Secondary	10 0	6 0	12 0	8 0	11 0	2 5

APPENDIX B

X-RAY DIFFRACTION

X-RAY DIFFRACTION

Four runs were conducted for each sample studied, using X-Ray Diffraction techniques. The Bulk-Run treats the whole sample with all of its mineral constituents. The other three runs (Natural, Glycolated and Heated) are conducted only for the clay extracted from the bulk samples.

Preparation of Samples

Bulk Run

The whole sample is crushed and reduced down to the finest grain size attainable. The resultant powder is then strained using a standard 400 U.S. Sieve. The final product is then used for X-Ray Diffraction.

Natural Run

The following procedure is followed to extract the clay from the bulk sample powder:

Removal of carbonates and soluble salts

1. Place 20g sample in a 250 ml centrifuge bottle.
2. Add 100 ml $\pm$ 5 ml NaOac (Sodium acetate) solution.
3. Stir well & heat bottle at 80° for at least 1/2 hour.
4. Stir several times, cool.

5. Centrifuge at 1500 rpm for 5 minutes & decant.
6. If carbonate is present it will fizz, then add more and leave overnight.
7. Give sample a final centrifuge-wash with 50 ± 5 ml of NaOac.
8. Wash off sample with distilled water, 3-4 times.

Oxidation of organic matter

1. Add 20 ml water to above centrifuged residue and heat at 80° C.
2. Add 1 ml of H_2O_2.
3. When frothing subsides add more until 25 ml has been added.
4. *CAUTION--H_2O_2 will cause severe burns--wash affected skin with water immediately!
5. Wash off sample with distilled water, 3-4 times.

Removal of iron oxide coatings

1. Remove from hot plate, add 10-15 ml of saturated NaCl solution.
2. Fill bottles (250 ml) 2/3 full with water, stir, centrifuge and decant.
3. Add 100 ± 5 ml citrate buffer to sample, stir, and place on hot plate.
4. At 75°-80° C, slowly add 1 teaspoon (4g) of Na dithionite (Sodium hydrosulfite) to the warm suspension.

5. Stir slowly at first, then vigorously.
6. After 10-15 minutes on hot plate, remove, cool to room temp., centrifuge and decant.
7. Centrifuge--wash with 50 ± 5 ml of citrate buffer.
8. Wash off buffer with distilled water, 3-4 times.

A sample from the final clay extract is used for X-Ray Diffraction, designated as the Natural Run.

Glycolated Run

To detect swelling clays, a sample of the clay extract is immersed in Glycol overnight, then exposed to the X-Ray Diffraction machine.

Heated Run

The same sample above is heated at 500°C for two hours before subjected to X-Rays.

ABBREVIATIONS USED ON X-RAY DIFFRACTION CHARTS

B-Run	=	Bulk Run
N-Run	=	Natural Run
G-Run	=	Glycolated Run
Ch-Run	=	Heated Run
S	=	Smectite
I	=	Illite
Chl.	=	Chlorite
7 Å Chl.	=	7 Å Chlorite

K	=	Kaolinite
Cr	=	Cristobalite
Q	=	Quartz
K-F	=	K-Feldspar
P	=	Plagioclase
Cal	=	Calcite

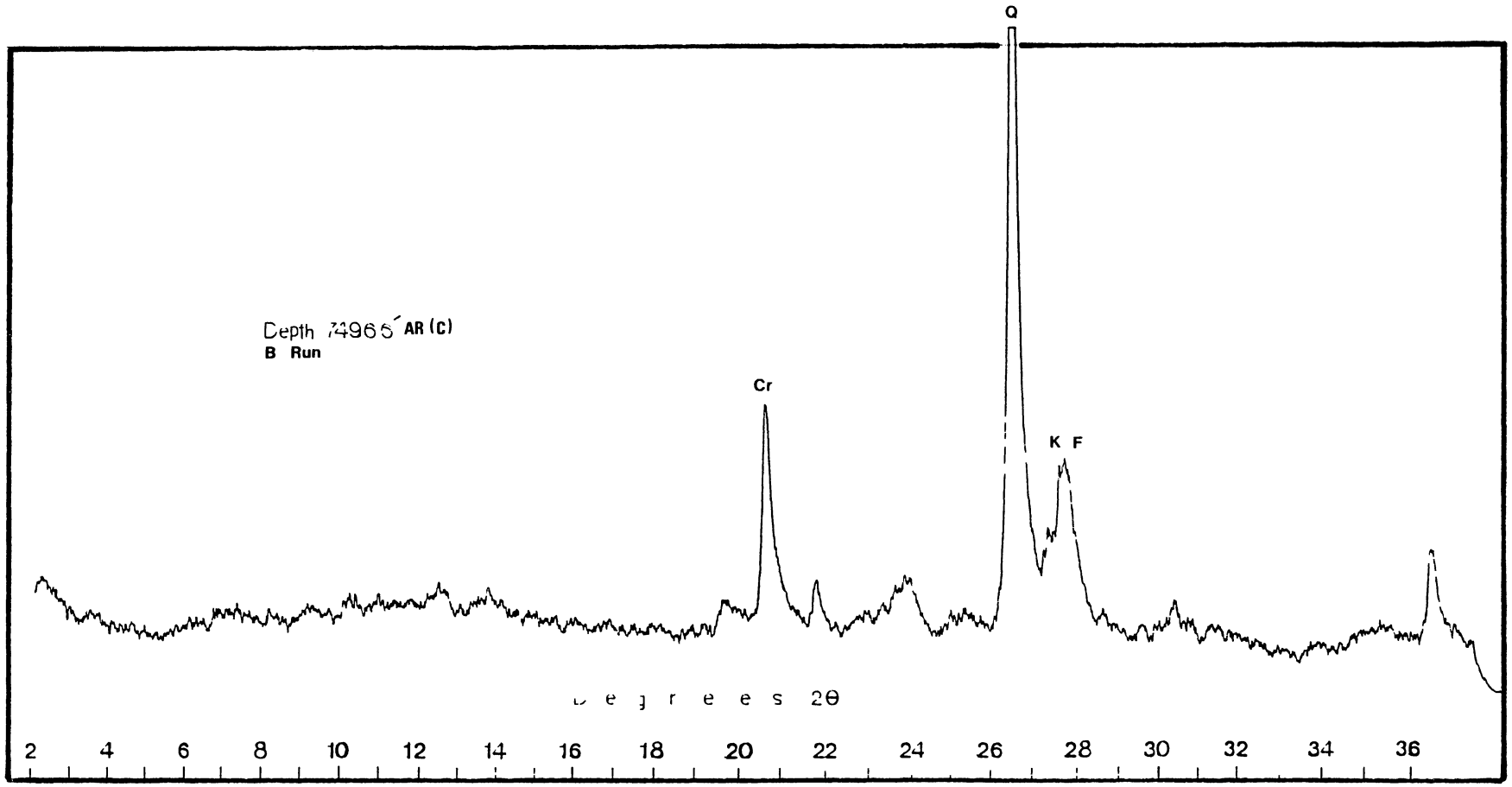
Q
Depth 4965' AR (C)
B Run
Cr
K F
Degrees 2θ
2
4
6
8
10
12
14
16
18
20
22
24
26
28
30
32
34
36

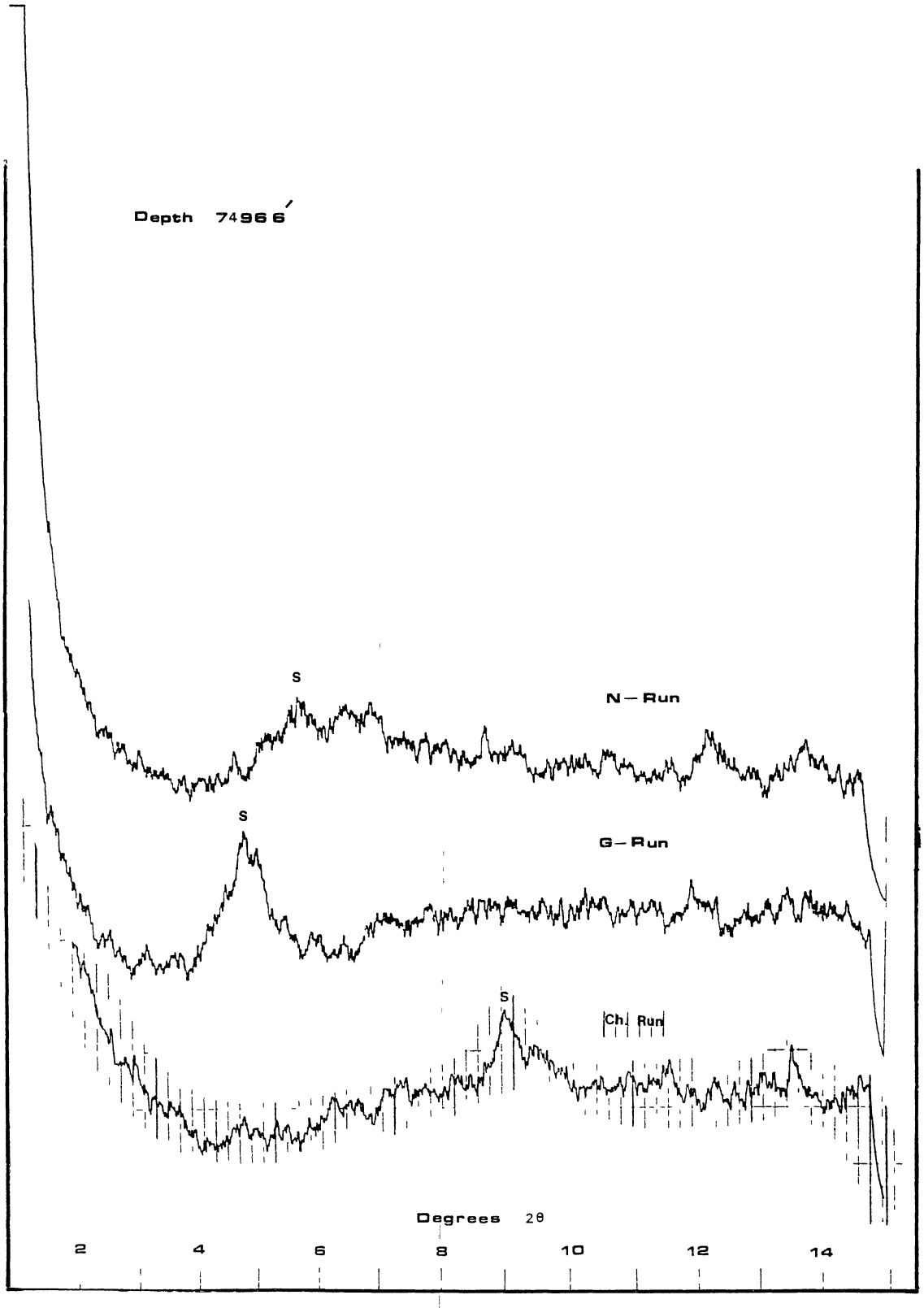
Depth 7496 6′
S
N—Run
S
G—Run
S
Ch Run
Degrees 2θ
2
4
6
8
10
12
14

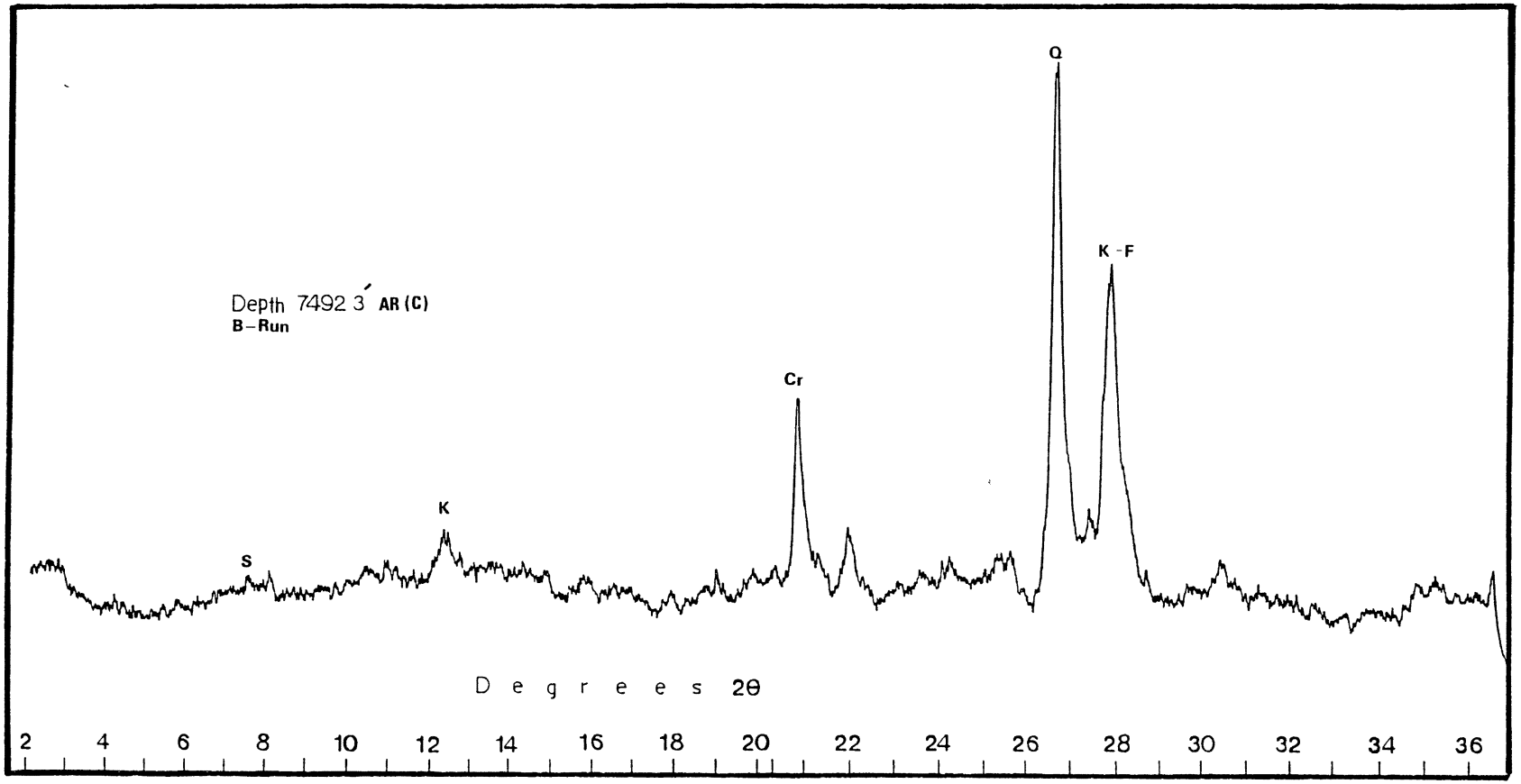
Depth 7492 3´ AR (C)
B–Run
Q
K-F
Cr
K
S
Degrees 2θ
2
4
6
8
10
12
14
16
18
20
22
24
26
28
30
32
34
36

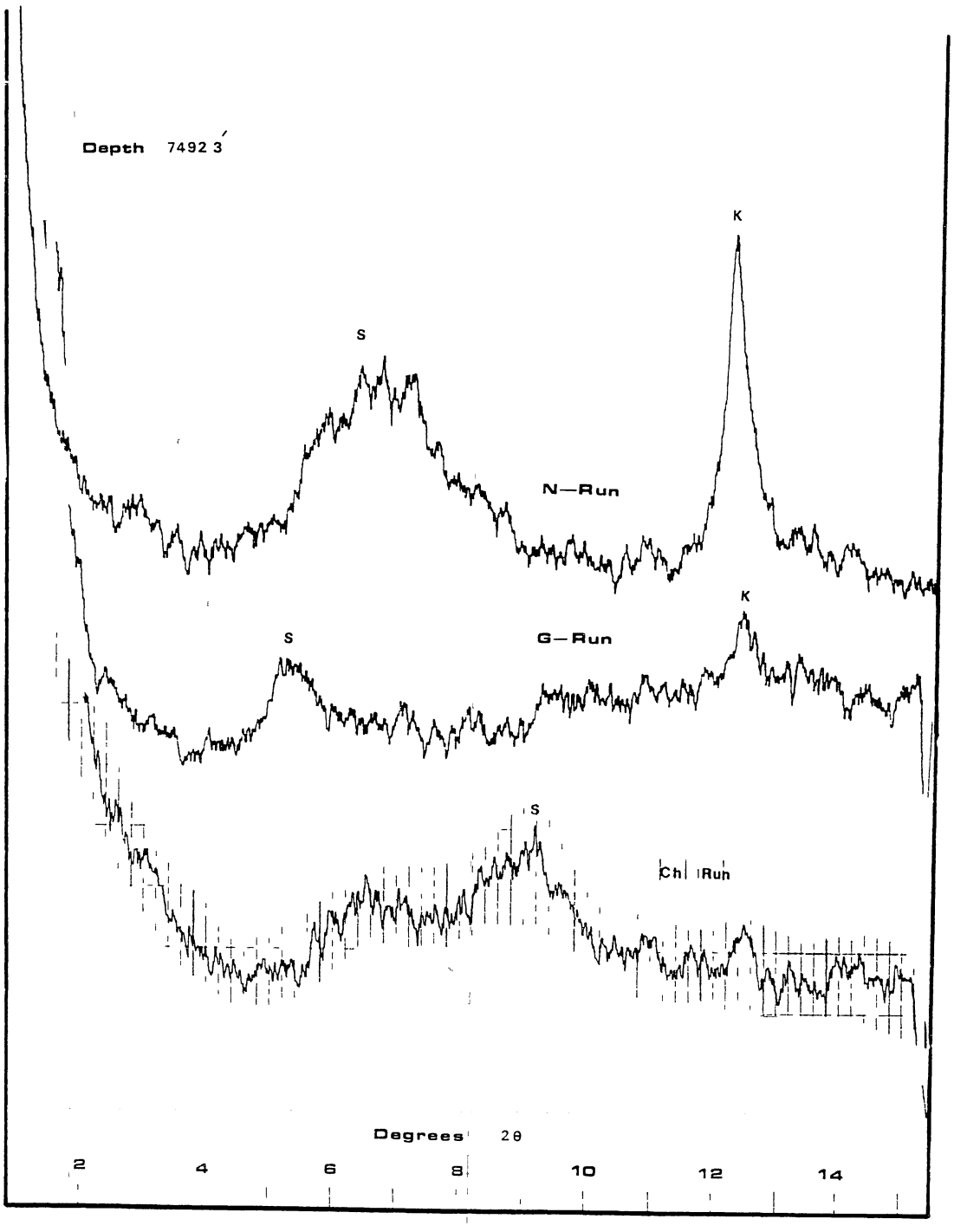
Depth 7492 3′
K
S
N—Run
K
S
G—Run
S
Chl Run
Degrees 2θ
2
4
6
8
10
12
14

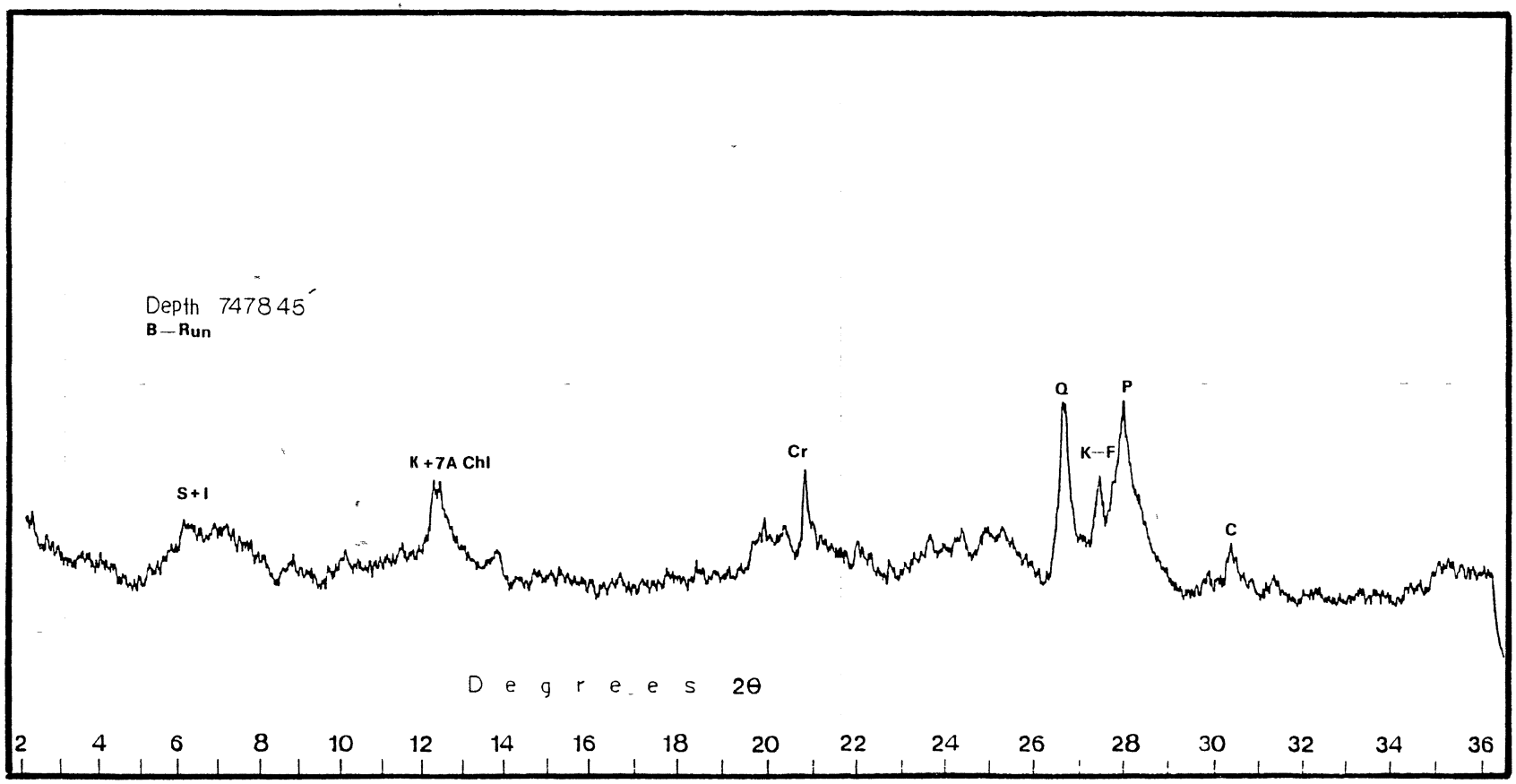
Depth 7478 45'
B—Run
S+I
K+7A Chl
Cr
Q
P
K—F
C
Degrees 2θ
2
4
6
8
10
12
14
16
18
20
22
24
26
28
30
32
34
36

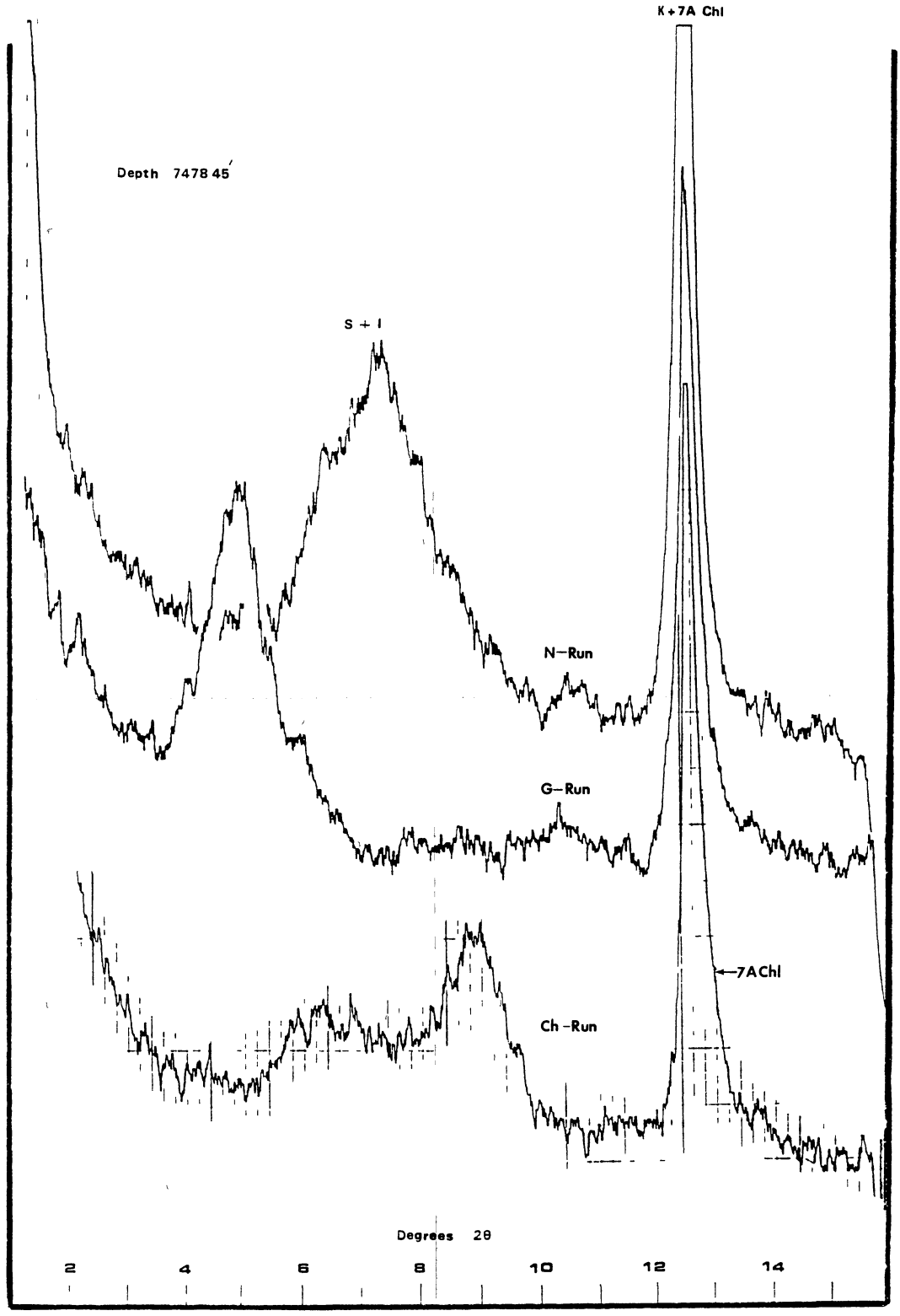
K+7A Chl
Depth 7478 45'
S + I
N–Run
G–Run
7AChl
Ch –Run
Degrees 2θ
2
4
6
8
10
12
14

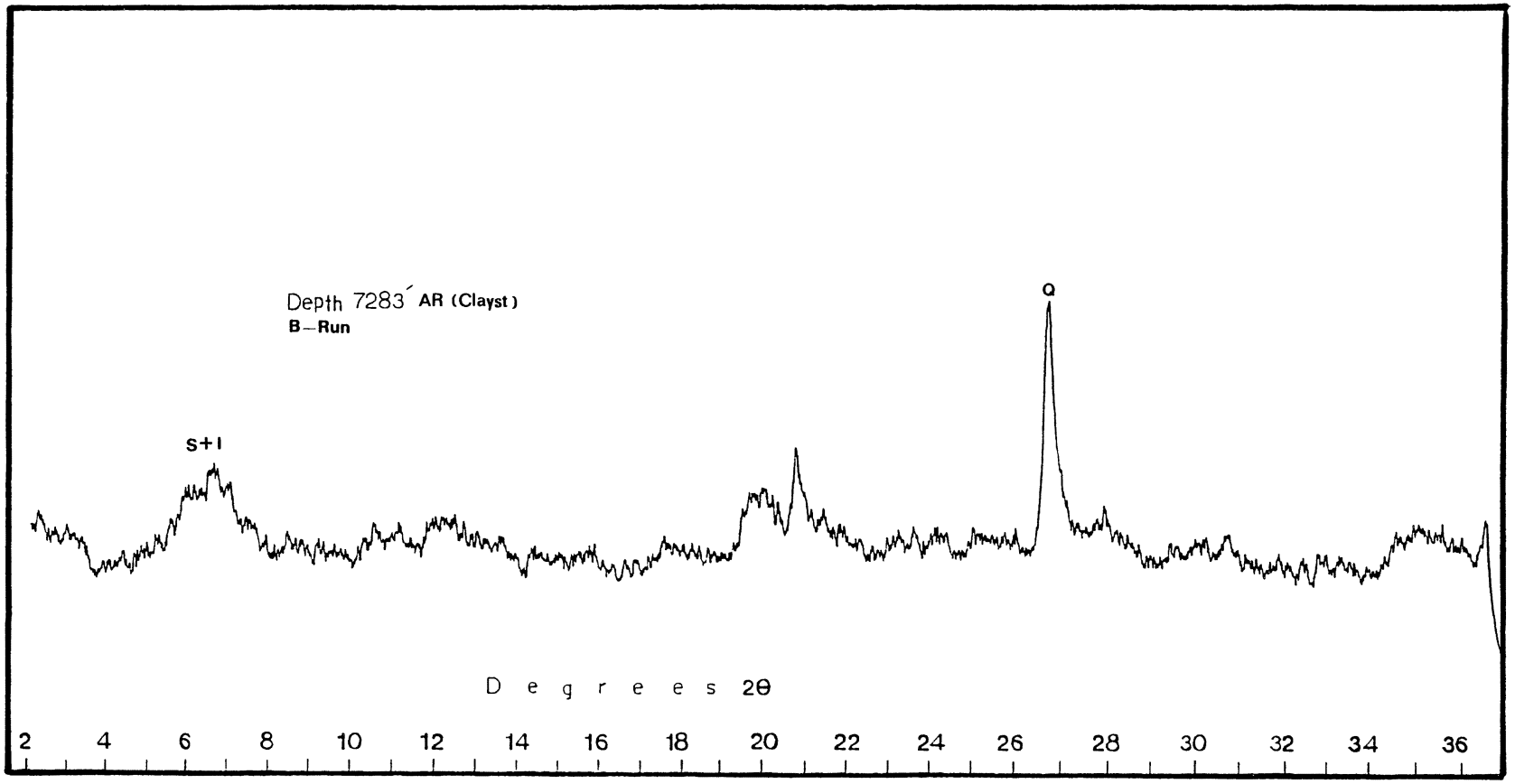
Depth 7283´ AR (Clayst)
B—Run
S+I
Q
D e g r e e s 2θ
2 4 6 8 10 12 14 16 18 20 22 24 26 28 30 32 34 36

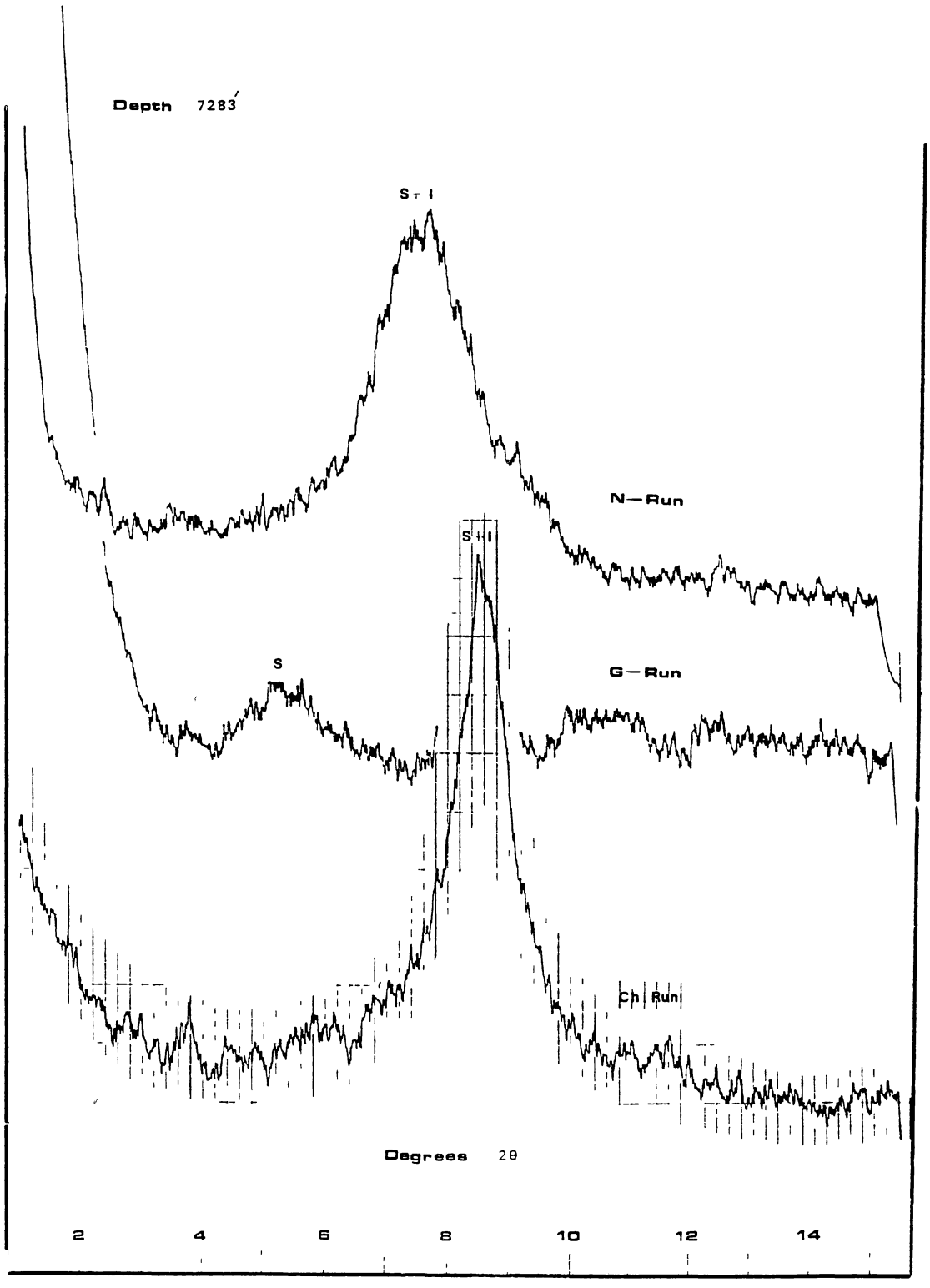
Depth 7283'
S + I
N—Run
S + I
S
G—Run
Ch Run
Degrees 2θ
2
4
6
8
10
12
14

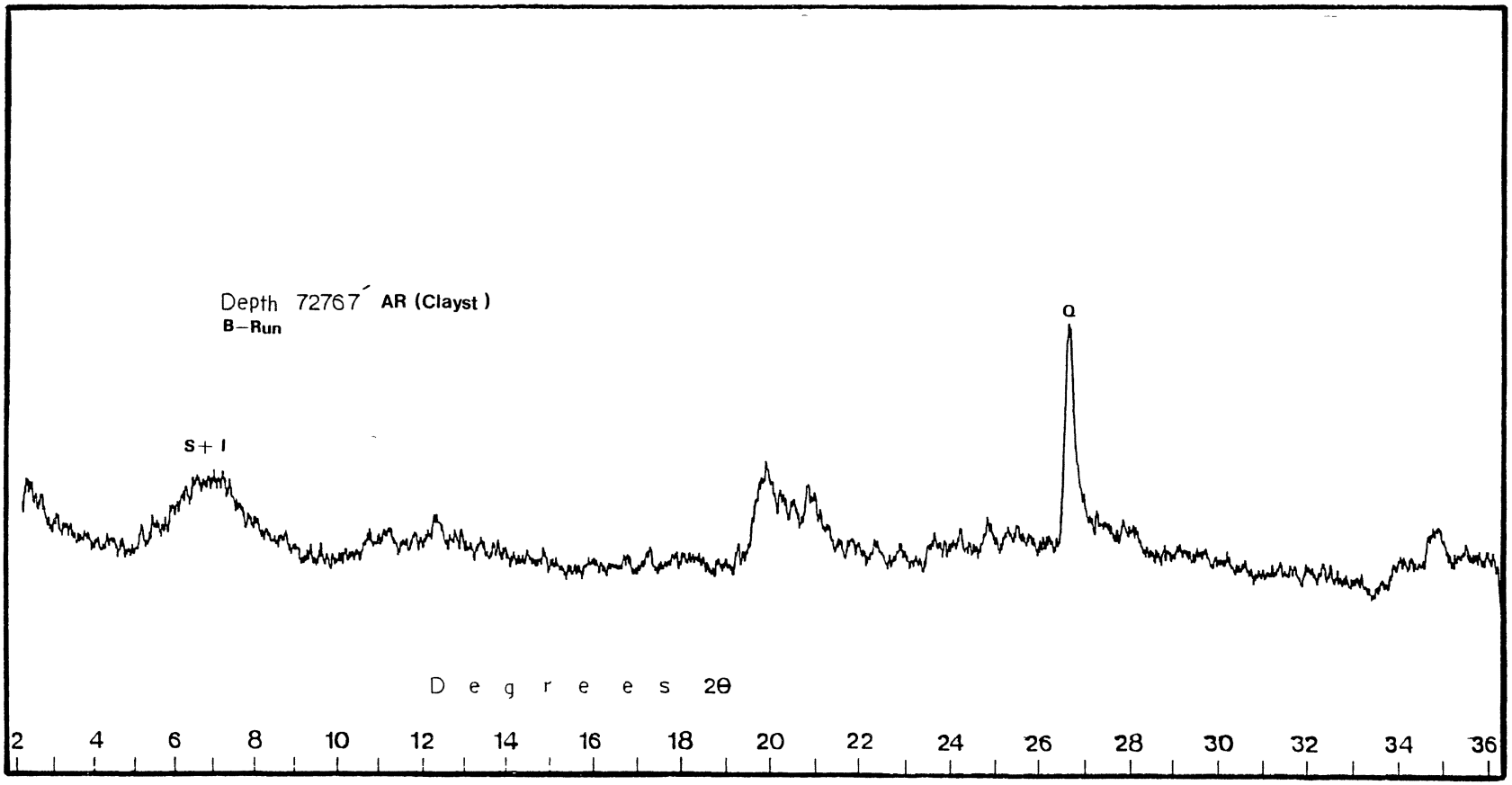
Depth 7276.7´ AR (Clayst)
B–Run
S+I
Q
D e g r e e s 2θ
2 4 6 8 10 12 14 16 18 20 22 24 26 28 30 32 34 36

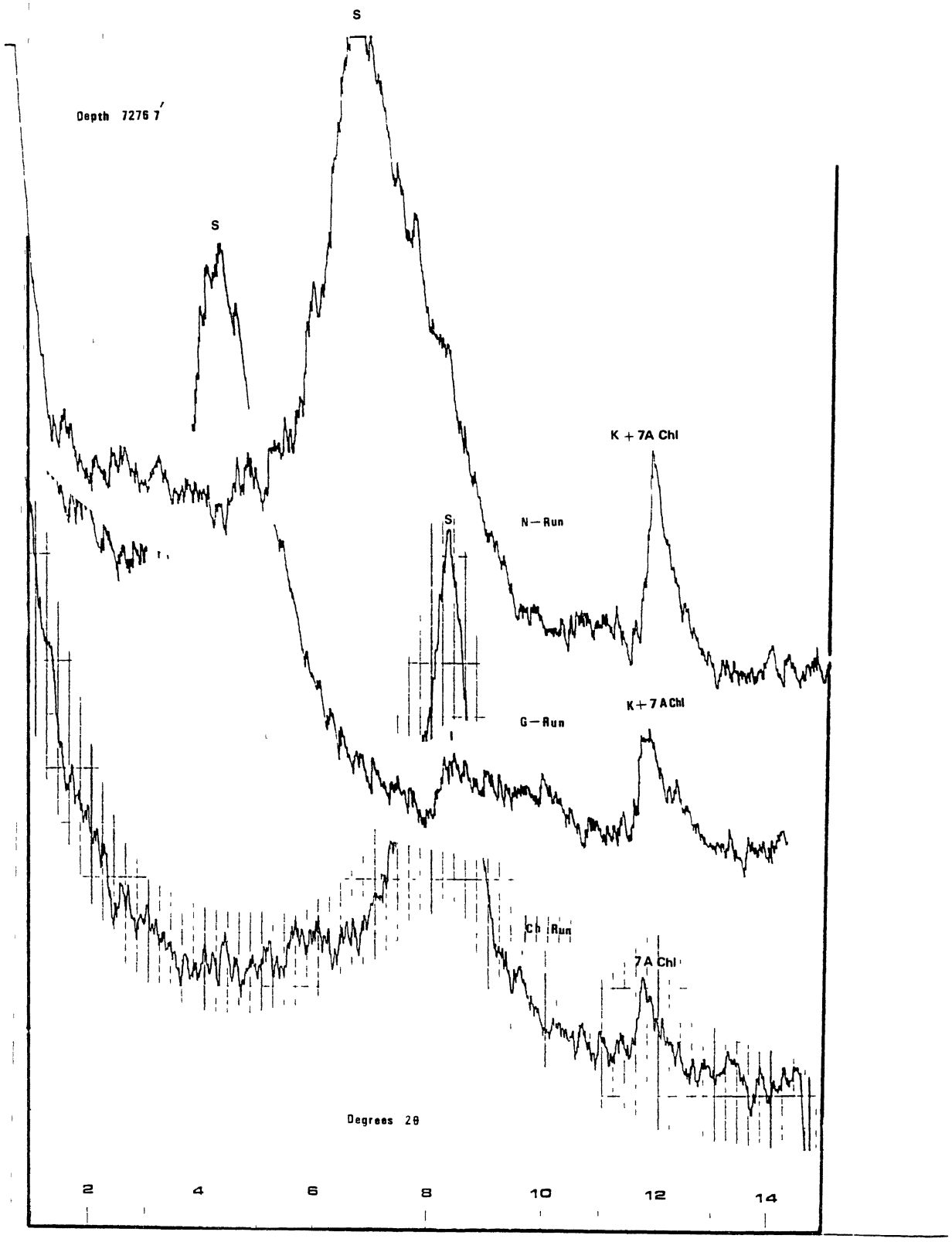
S
Depth 7276 7'
S
K + 7A Chl
N—Run
S
K+7AChl
G—Run
Cb Run
7A Chl
Degrees 2θ
2
4
6
8
10
12
14

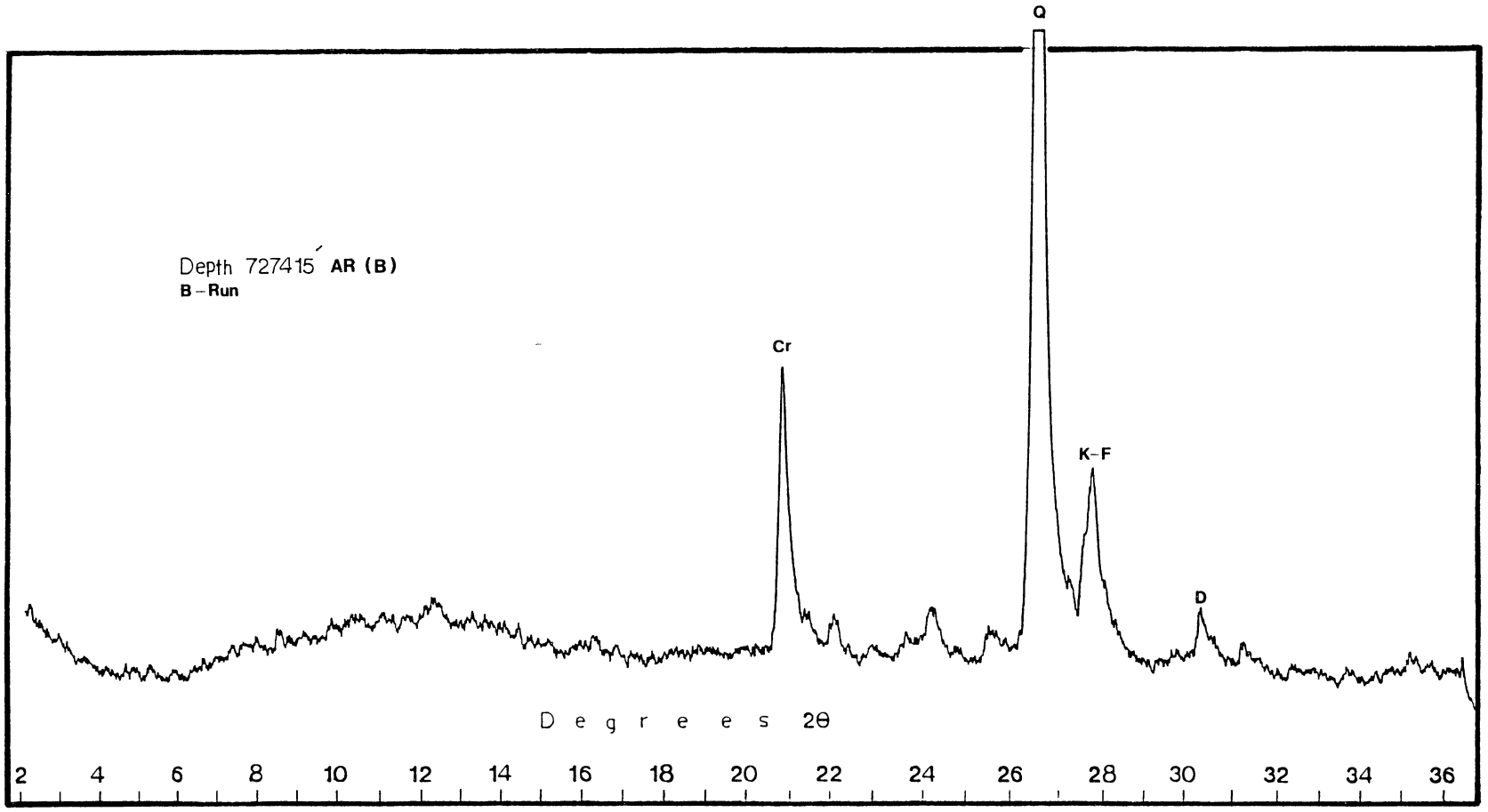
Q
Depth 727415´ AR (B)
B-Run
Cr
K-F
D
Degrees 2θ
2
4
6
8
10
12
14
16
18
20
22
24
26
28
30
32
34
36

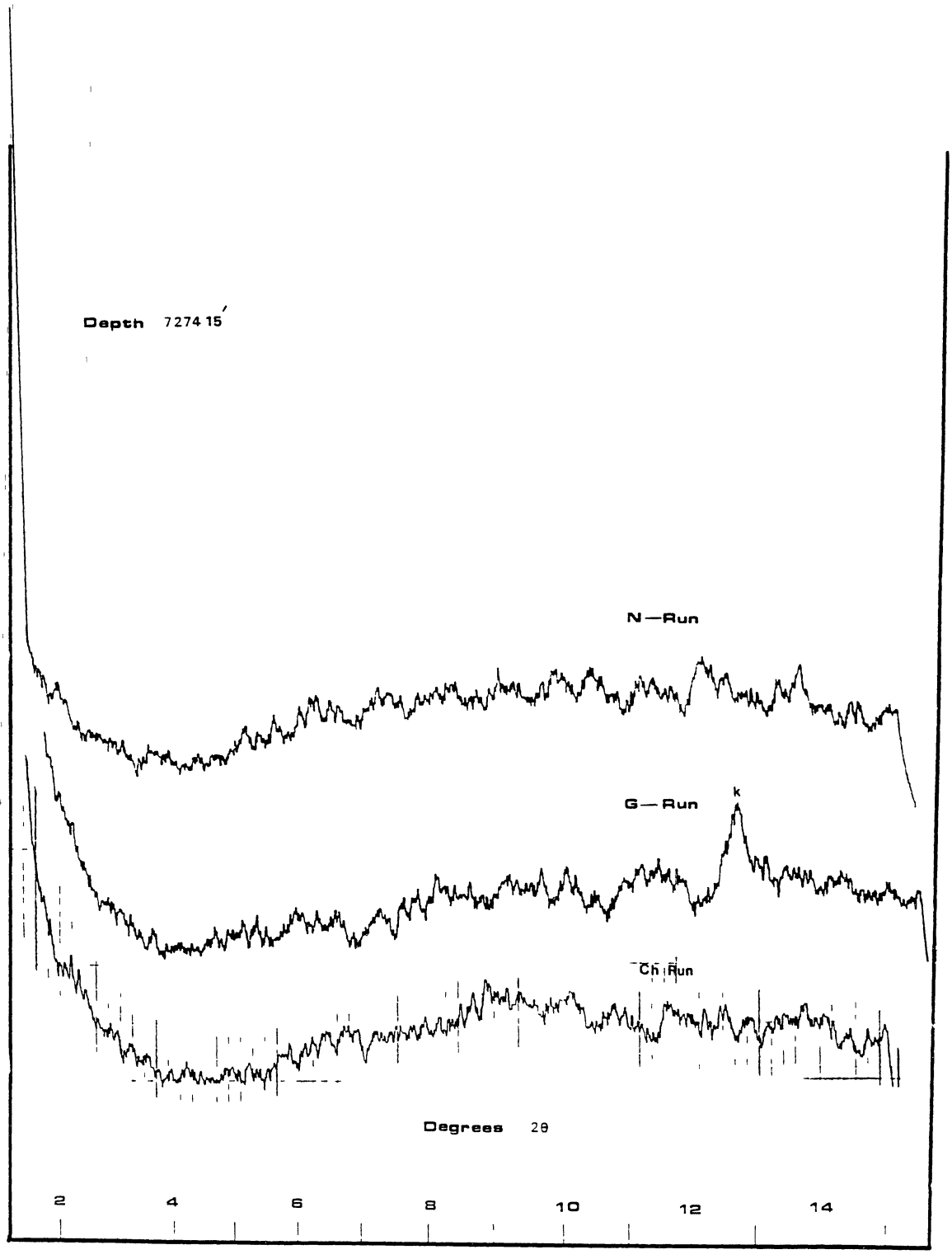
Depth 7274 15′
N—Run
G—Run
k
Ch Run
Degrees 2θ
2
4
6
8
10
12
14

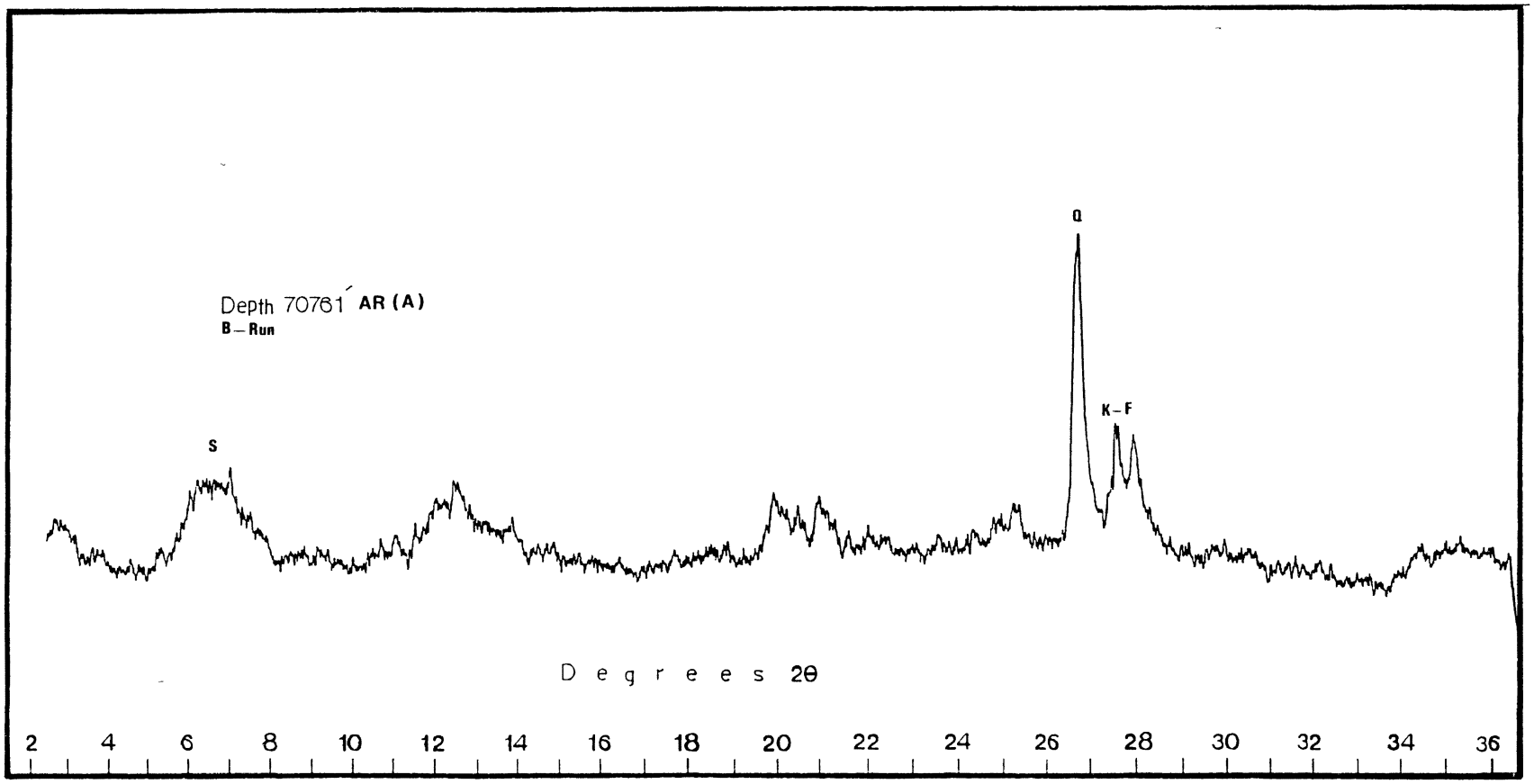
Depth 7076' AR (A)
B – Run
S
Q
K – F
Degrees 2θ
2
4
6
8
10
12
14
16
18
20
22
24
26
28
30
32
34
36

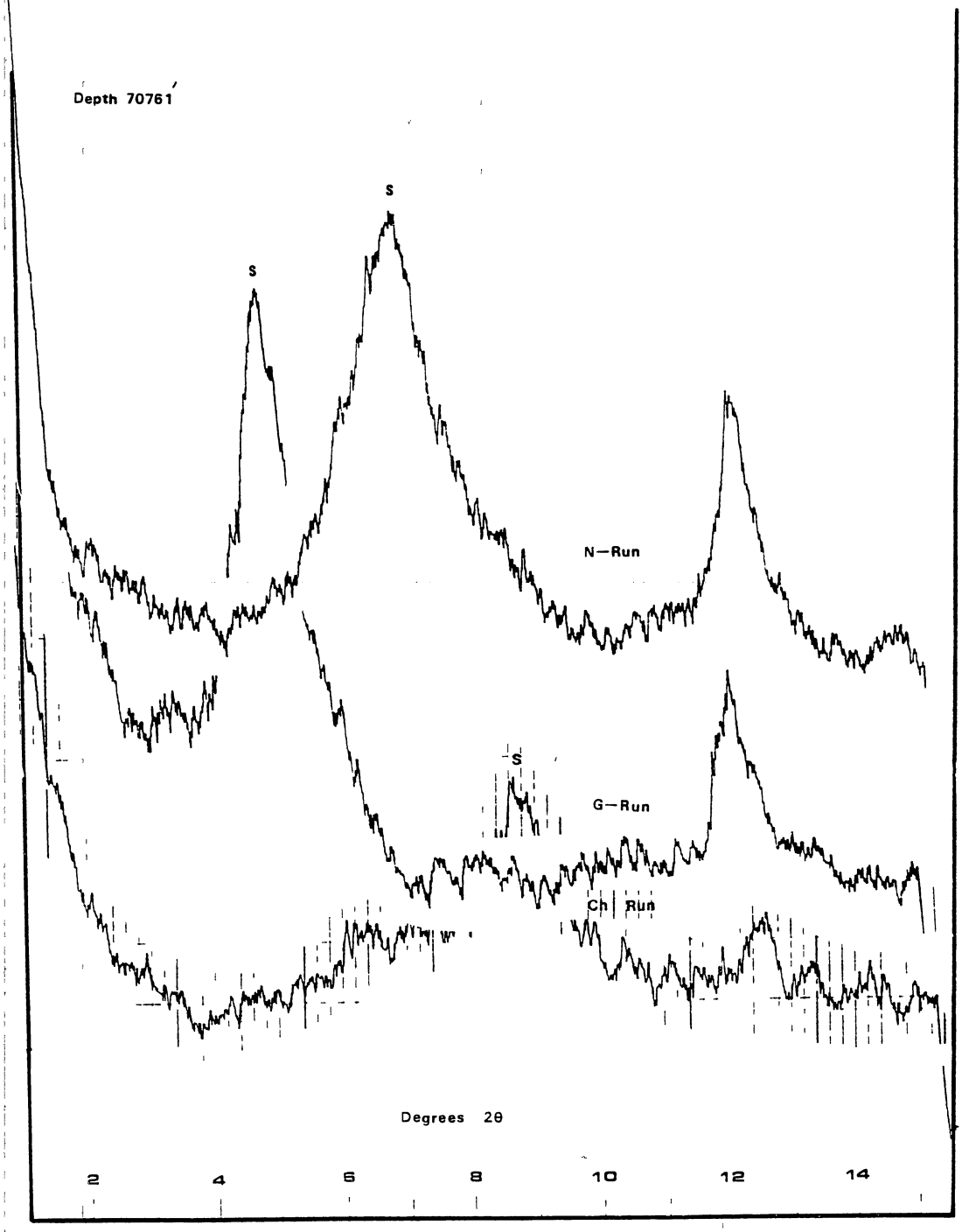
Depth 70761'
S
S
S
N—Run
G—Run
Ch | Run
Degrees 2θ
2
4
6
8
10
12
14

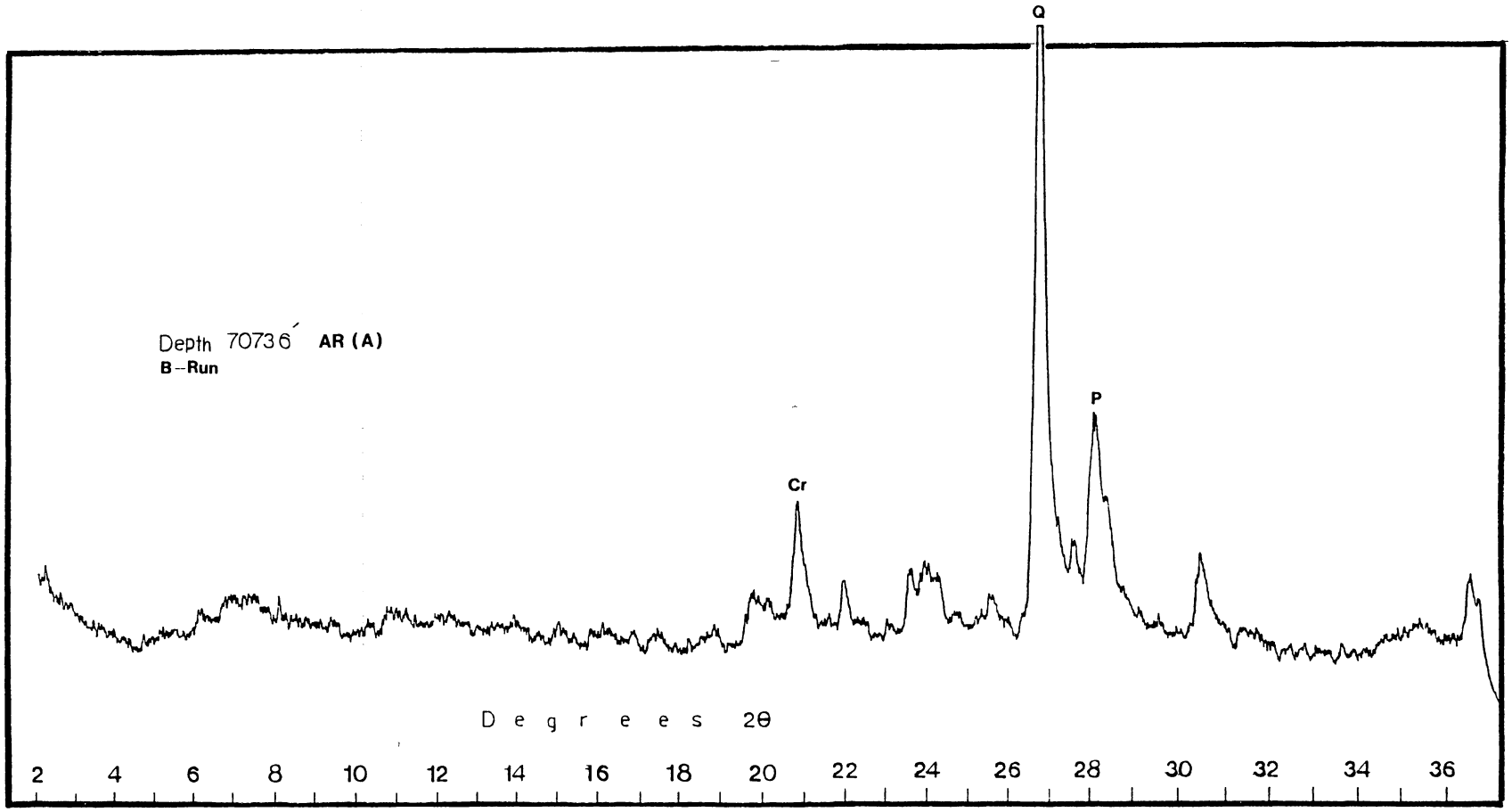
Q
Depth 7073.6´ AR (A)
B–Run
P
Cr
D e g r e e s 2θ
2 4 6 8 10 12 14 16 18 20 22 24 26 28 30 32 34 36

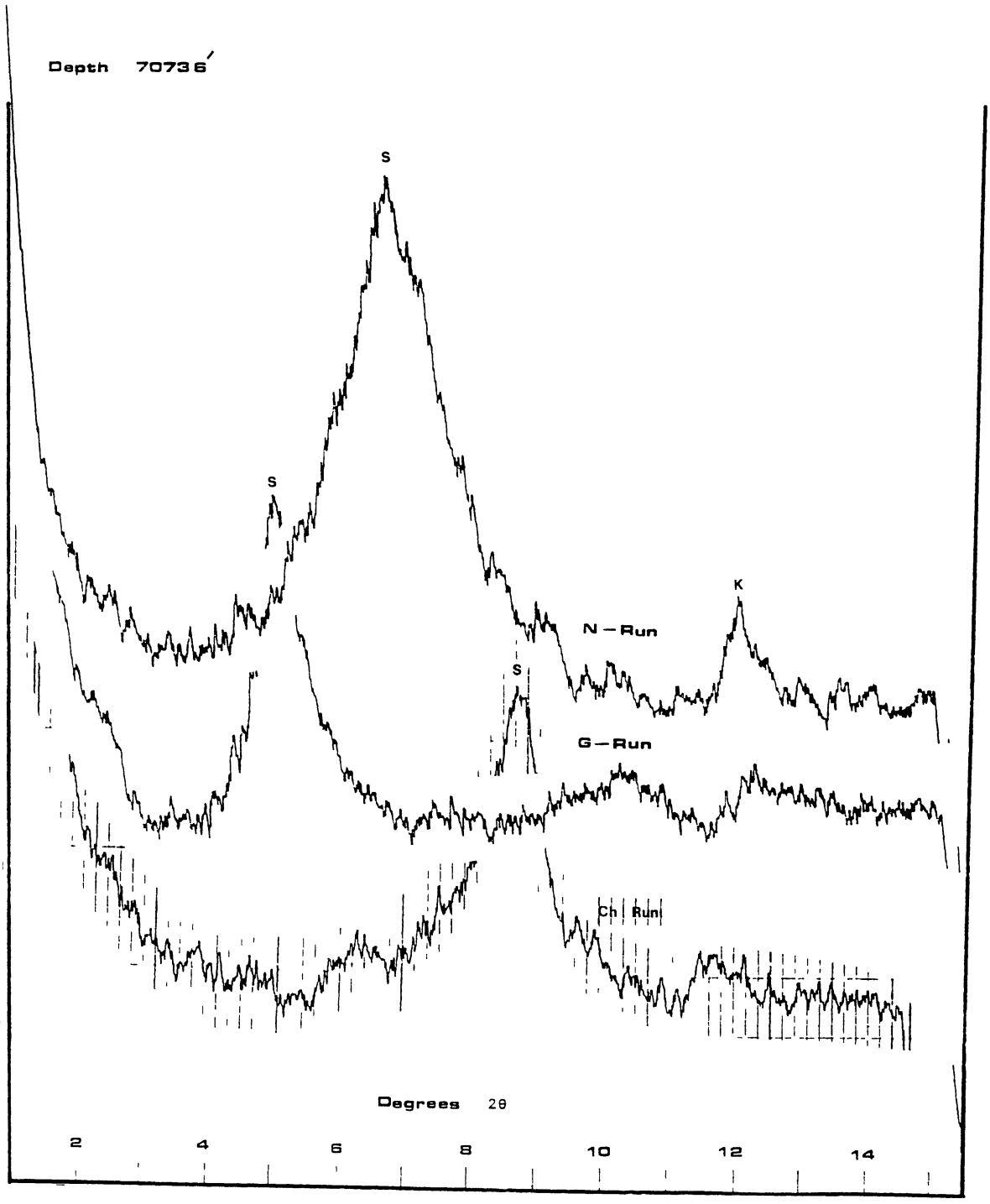
Depth 7073.6'
S
S
S
K
N – Run
G – Run
Ch 1 Run
Degrees 2θ
2
4
6
8
10
12
14

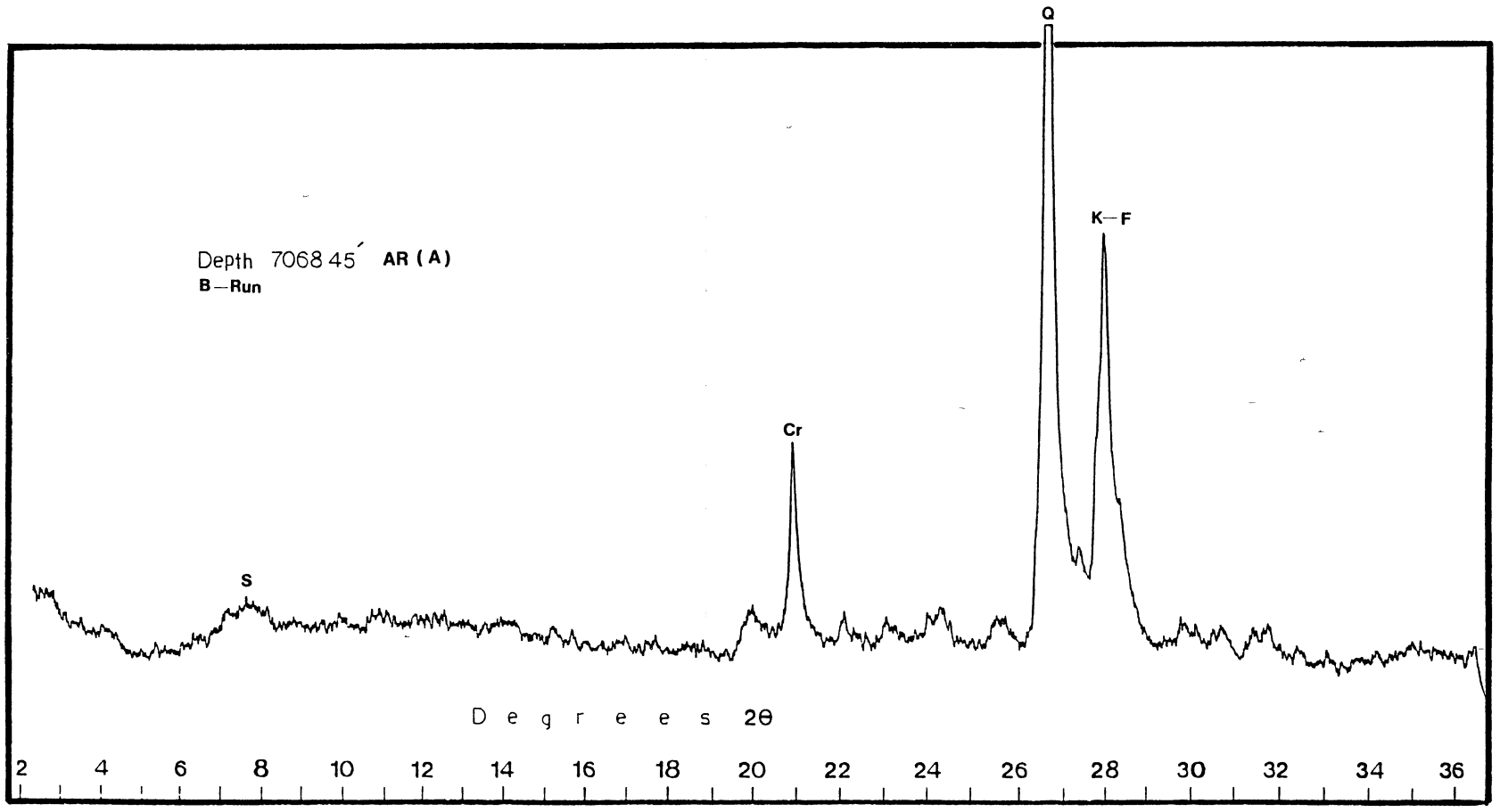
Q
K—F
Cr
S
Depth 7068 45´ AR (A)
B—Run
D e g r e e s 2θ
2 4 6 8 10 12 14 16 18 20 22 24 26 28 30 32 34 36

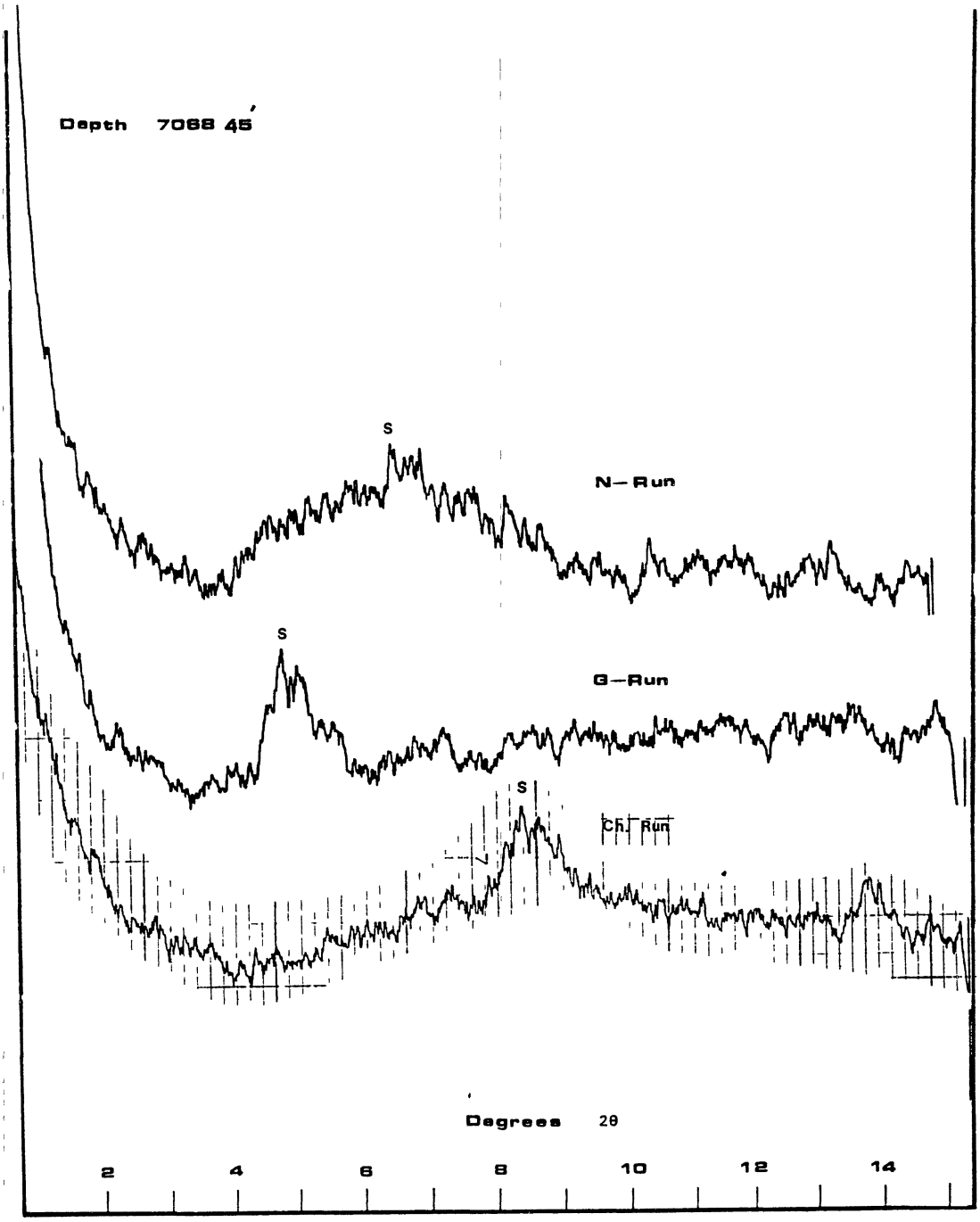
Depth 7068 45'
S
N—Run
S
G—Run
S
Ch. Run
Degrees 2θ
2
4
6
8
10
12
14

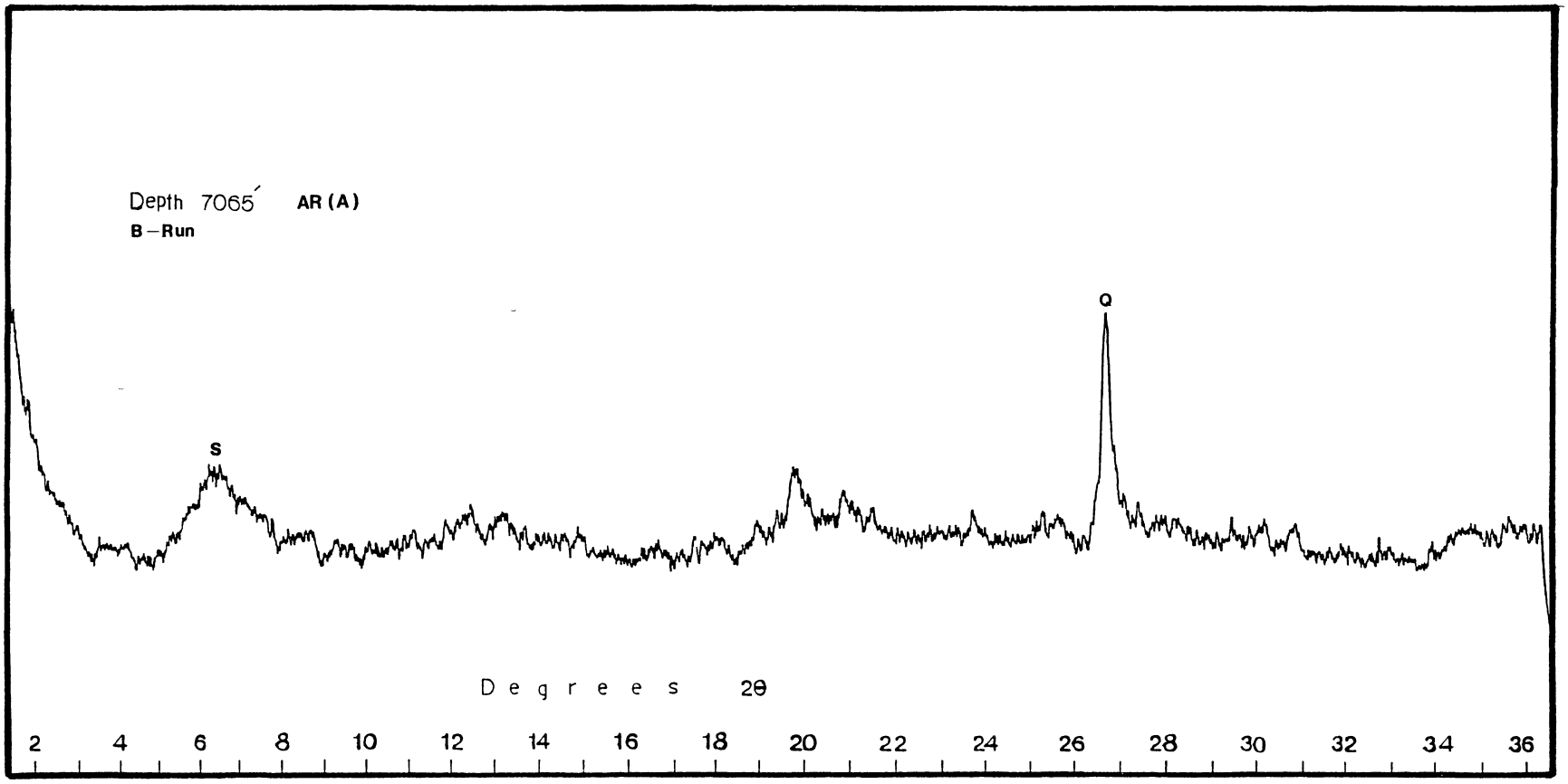
Depth 7065´
AR (A)
B – Run
S
Q
Degrees 2θ
2
4
6
8
10
12
14
16
18
20
22
24
26
28
30
32
34
36

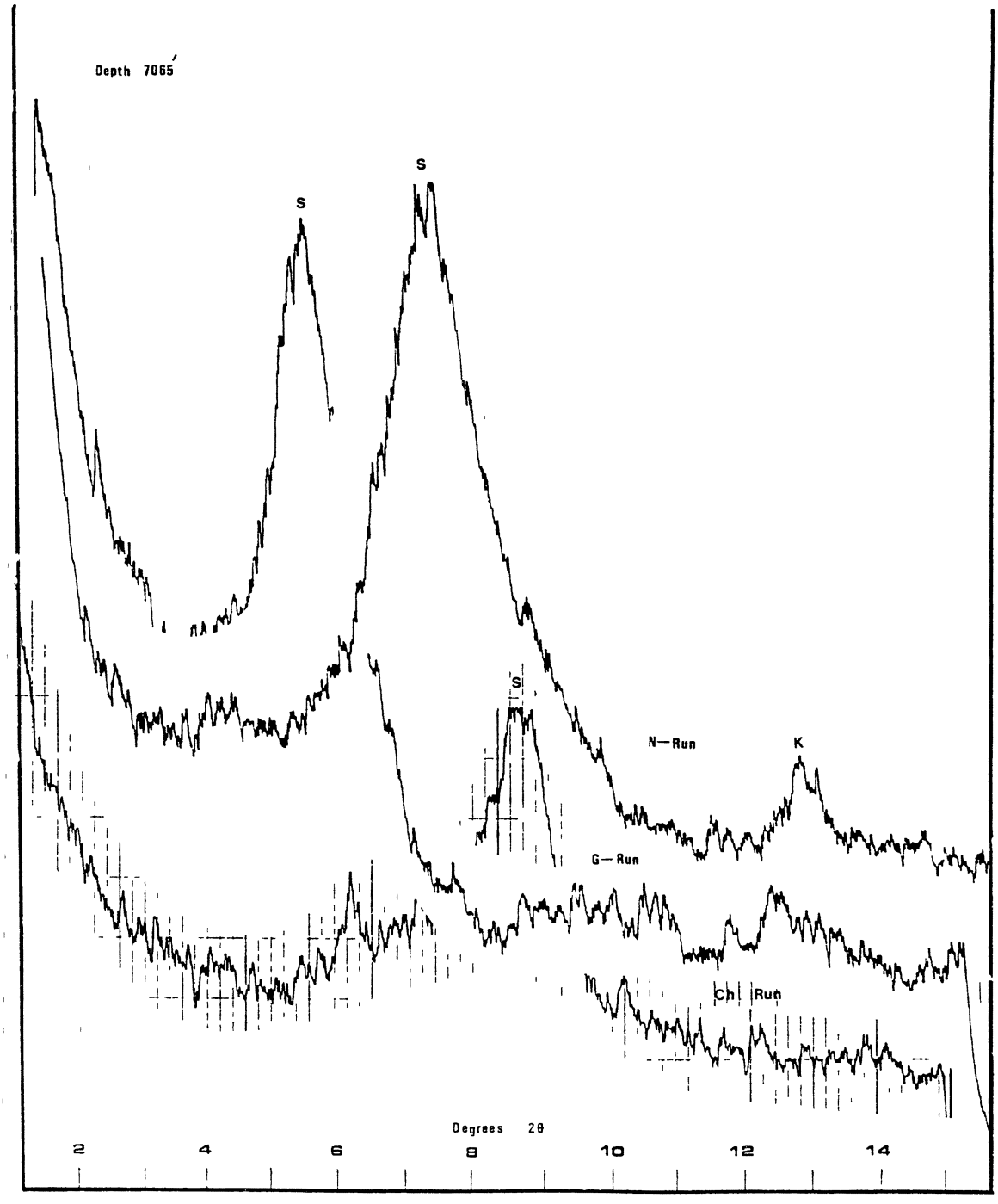
Depth 7065'
S
S
S
N—Run
K
G—Run
Ch Run
Degrees 2θ
2
4
6
8
10
12
14

APPENDIX C

WELL LOG DATA AND LOG ADJUSTMENTS

WELL LOG DATA AND LOG ADJUSTMENTS

This appendix contains the electric well log data utilized in the construction of the cross-sections and the sand-thickness maps attached to this thesis. Table I provides the following depths for each well, where available.

1. Top Aradeiba Formation (Aradeiba Claystone).
2. Top Aradeiba A-member.
3. Bottom Aradeiba A-member.
4. Top Aradeiba B-member.
5. Bottom Aradeiba B-member.
6. Top Aradeiba C-member.
7. Bottom Aradeiba C-member.
8. Bottom Aradeiba Formation.

Log-Core Depth Adjustments

Various depth discrepancies have been noticed between the core and the log depths. Table II gives the depth difference for each log and the corresponding core.

Table 1. - Electric Well-Log Data

Well Name	Location		Top Arad. Fm.	Top Arad. A-Member	Bott. Arad. A-Member	Top Arad. B-Member	Bott. Arad. B-Member	Top Arad. C-Member	Bott Arad C-Member	Bott. Arad. Fm.
	Lat. ° ' "	Long ° ' "								
Unity #1	9 34 36	29 38 54	6556	6855	6871	--	--	7202	7224	7494
Unity #2	9 28 11	29 40 35	7355	7828	7883	8053	8100	8268	8299	--
Unity #3	9 25 48	29 41 7	7582	7954	8003	8191	8214	8353	8381	8681
Unity #4	9 29 1	29 39 36	7635	8102	8132	8337	8348	8416	8533	8825
Unity #5	9 27 30	29 40 15	7722	8202	8255	8426	8477	8608	8679	--
Unity #6	9 26 40	29 40 33	7490	7968	8014	8041	8087	8166	8209	8564
Unity #7	9 29 33	29 39 48	7736	8222	8271	8335	8350	8427	8446	8579
Unity #8	9 30 14	29 39 37	6900	--	--	7124	7166	7339	7367	7714
Unity #9	9 28 48	29 40 9	7518	8003	8047	8229	8265	8388	8455	8814
Unity #10	9 30 46	29 40 30	6688	7033	7073	7247	7288	7401	7484	7798
Unity #11	9 30 18	29 40 21	6700	7054	7101	7266	7309	7431	7507	7848
Unity #12	9 31 10	29 40 12	6652	7010	7043	7226	7270	7392	7438	7748
Unity #13	9 27 52	29 40 17	7503	7941	8010	8170	8191	8327	8383	8700
Unity #14	9 27 51	29 39 48	7791	8057	8082	--	--	--	--	8494
Unity #15	9 28 9	29 40 19	7384	7837	7891	8058	8097	8218	8284	8575
Unity #16	9 27 53	29 40 28	7348	7824	7869	8040	8073	8200	8220	8570
Unity #17	9 28 16	29 39 50	7663	8192	8214	--	--	--	--	8395
Unity #18	9 28 39	29 40 44	6943	7285	7319	7382	7396	7500	7533	7943
Talih #1	9 32 31	29 38 48	7849	8220	8261	8420	8453	8554	8577	8810
Talih #2	9 33 4	29 38 24	7715	8217	8266	8413	8450	8605	8625	8883

A negative sign indicates that the log depth is shallower than the core depth by the number of feet indicated.

TABLE II

LOG-TO-CORE DEPTH ADJUSTMENTS

Well Name	Core	Adjustment
Unity #2	Aradeiba-A	-2.0
Unity #8	Aradeiba-C	-7.4
Unity #9	Aradeiba-C	-4.6
Unity #9	Aradeiba-B	-4.0
Unity #9	Aradeiba-A	-3.0
Unity #11	Aradeiba-C	-1.0
Unity #11	Aradeiba-B	5.2
Unity #11	Aradeiba-A	10.1
Talih #2	Aradeiba-C	-6.7
Talıh #2	Aradeiba-A	-4.0

Log Restoration

Some of the resistivity logs display an obvious offsetting noticed between the first track (Gamma Ray and SP Logs) and the tracks of the resistivity curves. This

phenomenon has been noticed on logs from the Unity No. 3, Unity No. 5, Unity No. 6 and Unity No. 7 wells. These offsets have been restored and the depths were maintained following the resistivity curves. Figure 1 is a sample illustrating the restoration procedure followed.

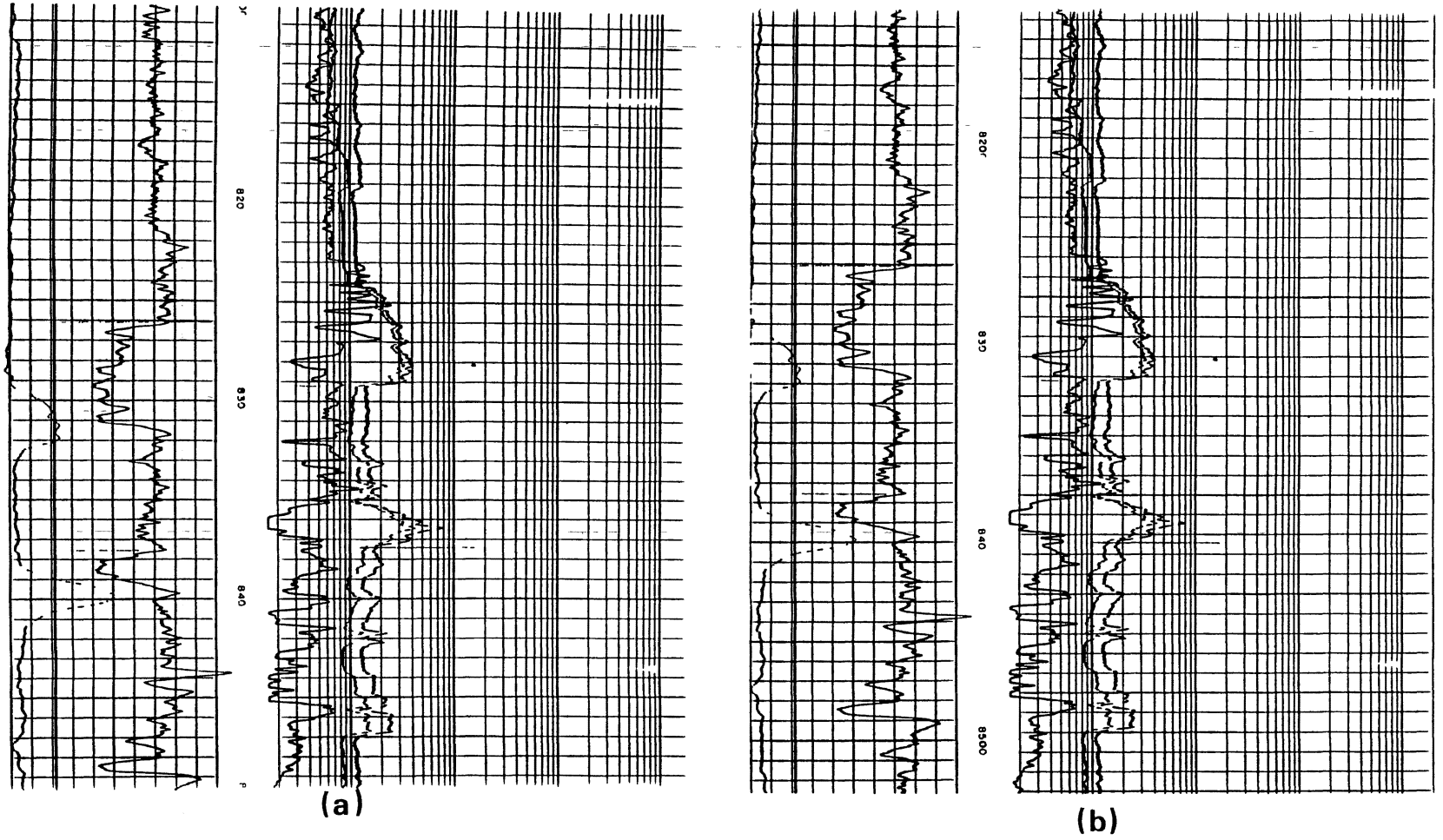

Figure 1. Electric-Log Tracks Adjustment (a) Original (b) Adjusted.

VITA

Azhari A. Abdalla

Candidate for the Degree of

Master of Science

Thesis: THE PETROGRAPHY, DIAGENESIS AND ENVIRONMENTS OF DEPOSITION OF THE ARADEIBA FORMATION IN THE UNITY AND TALIH FIELDS, ABU GABRA BASIN, SUDAN

Major Field: Geology

Biographical:

Personal Data: Born in Zalingie, Sudan, September 26, 1956, the son of Abdalgadir Abdalla and Batool Ibrahim.

Education: Graduated from Al-Fashir High School, Al-Fashir, Sudan, in May, 1975; received Bachelor of Science (Honors) Degree in Geology from Khartoum University in July, 1980; completed requirements for the Master of Science degree at Oklahoma State University in May, 1990.

Professional Experience: Joined the General Petroleum Corporation of Sudan in August 1980 as an exploration geologist to present.

A

A'

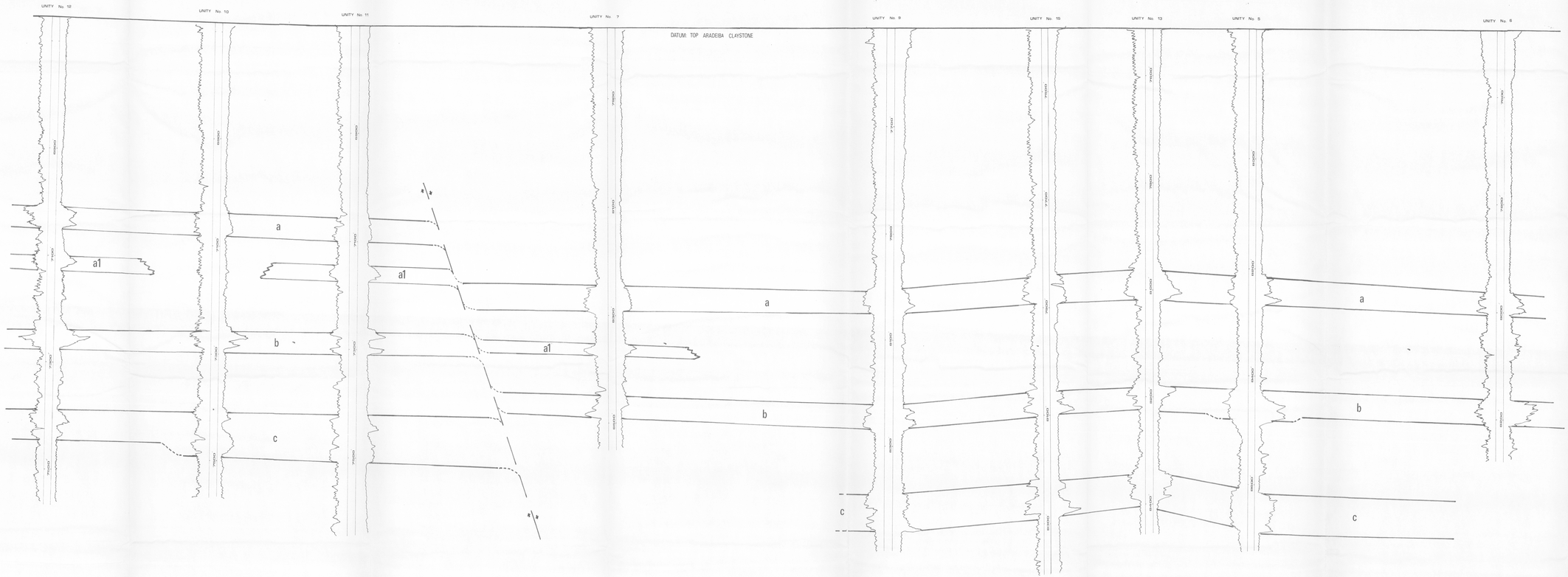

PLATE I

Oklahoma State University

REGIONAL NORTH-SOUTH STRATIGRAPHIC CROSS SECTION

VERTICAL SCALE	HORIZONTAL SCALE
1 = 65	1 = 500

Geologist: Azhari A. Abdalla (3/88)

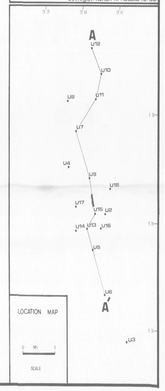

B

B´

UNITY No. 14

UNITY No. 13

UNITY No. 15

UNITY No. 2

UNITY No. 18

DATUM: TOP ARADEIBA CLAYSTONE

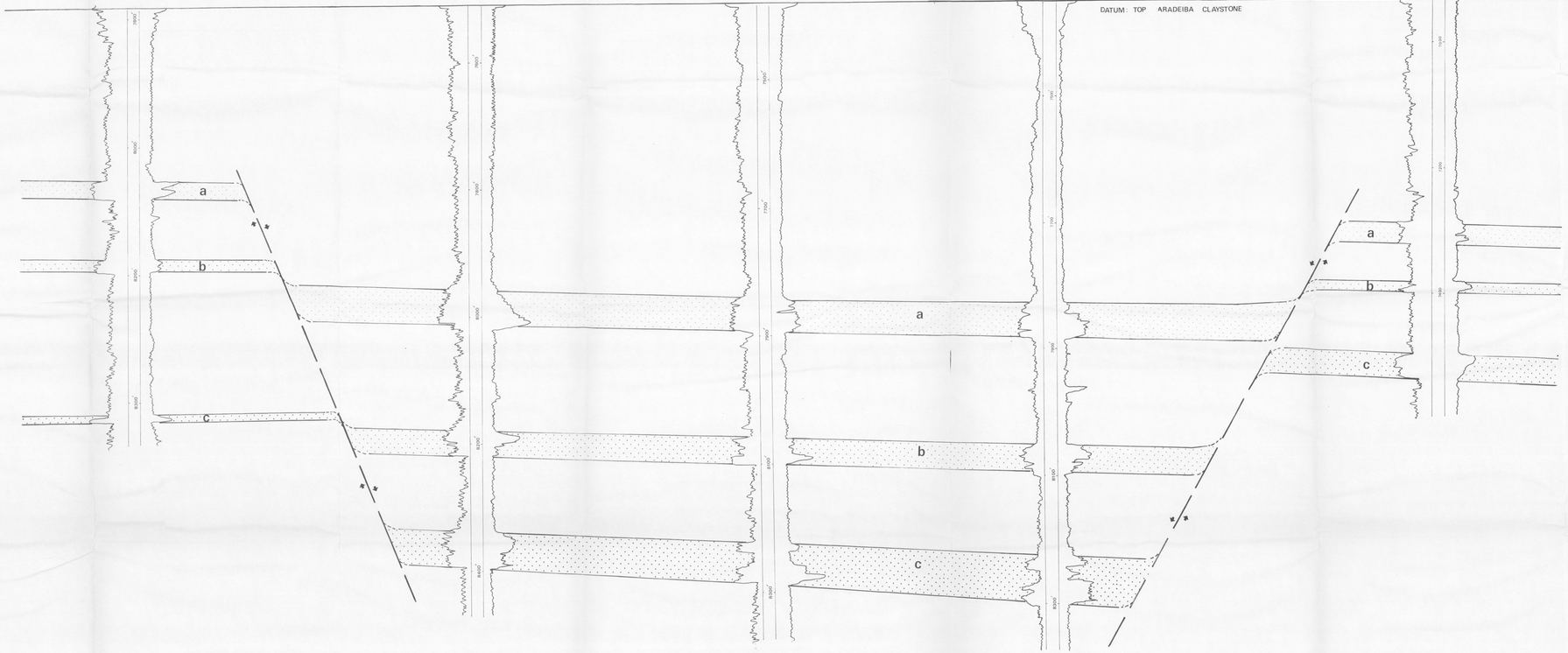

PLATE II

Oklahoma State University

REGIONAL WEST-EAST STRATIGRAPHIC CROSS SECTION

VERTICAL SCALE	HORIZONTAL SCALE
1 = 65	1 = 285

Geologist : Azhari A. Abdalla (3/88)

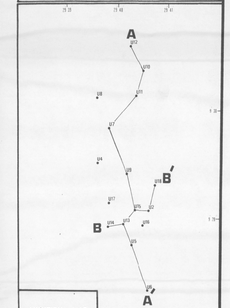

LOCATION MAP

0 Mi 1

SCALE

29° 38′ 29° 40′ 29° 42′

9° 36′ 9° 34′ 9° 32′ 9° 30′ 9° 28′ 9° 26′

U1 T2 T1 U U10 U8 U11 L7 U4 U9 U18 U17 U15 U2 U14 U13 U16 U5 U6 U3

10 20 30 40 30 20 10

60 50 40 20

PLATE III

Oklahoma State University

ARADEIBA-C NET-SANDSTONE ISOLITH MAP

SCALE

0 Mi 1

N

C.I. 10 Ft

U UNITY
T TALIH

GEOLOGIST AZHARI A. ABDALLA

29° 38′ 29° 40′ 29° 42′

9° 36′ 9° 34′ 9° 32′ 9° 30′ 9° 28′ 9° 26′

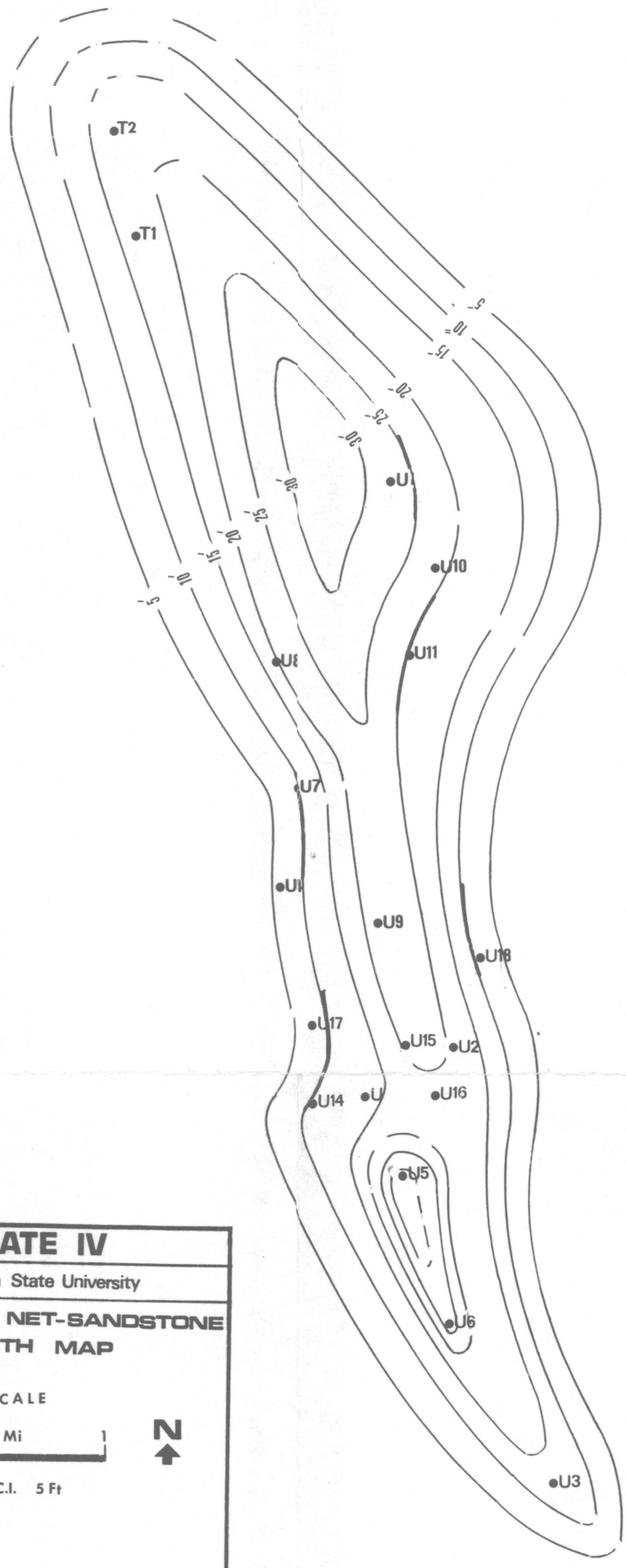

PLATE IV

Oklahoma State University

ARADEIBA-B NET-SANDSTONE ISOLITH MAP

SCALE

0 Mi 1

N

C.I. 5 Ft

GEOLOGIST AZHARI A. ABDALLA

29° 38′ 29° 40′ 29° 42′

9° 36′ 9° 34′ 9° 32′ 9° 30′ 9° 28′ 9° 26′

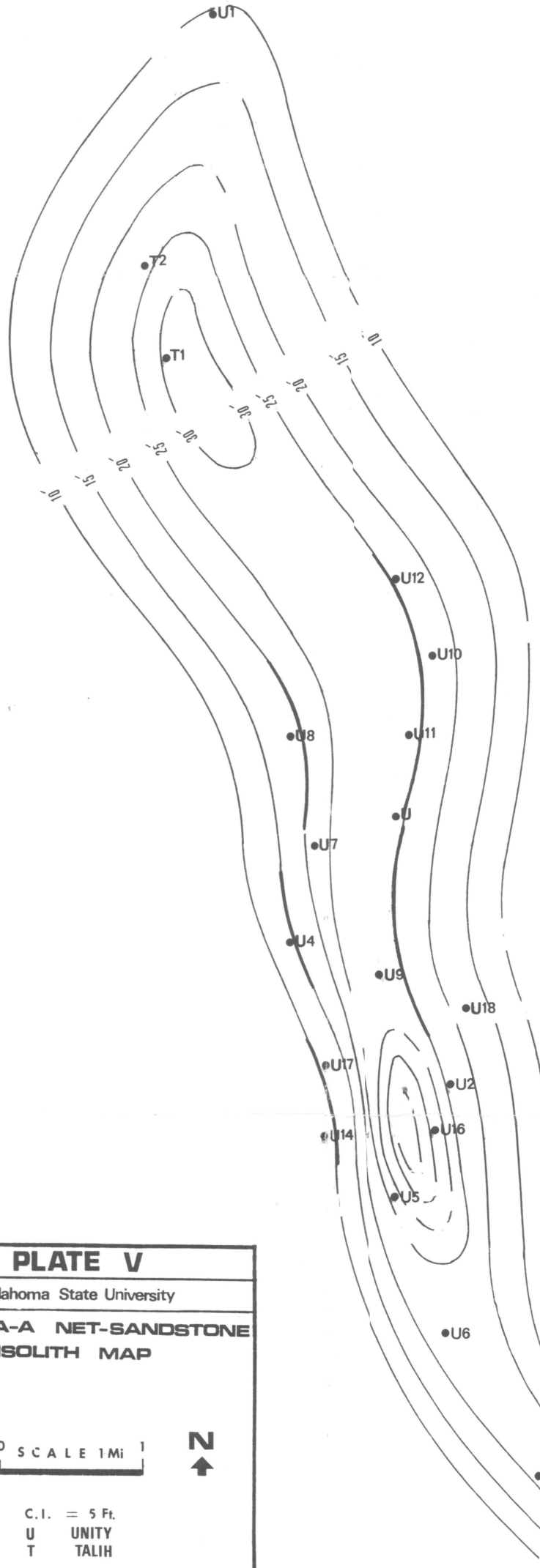

PLATE V

Oklahoma State University

ARADEIBA-A NET-SANDSTONE ISOLITH MAP

0 SCALE 1 Mi 1

N

C.I. = 5 Ft.
U UNITY
T TALIH

GEOLOGIST AZHARI A. ABDALLA